CELL WALLS AND COTTON FIBRE DEVELOPMENT

Mercedes Clara Hernandez-Gomez

Submitted in accordance with the requirements for the degree of Doctor of Philosophy (Ph.D.)

The University of Leeds

Faculty of Biological Sciences

June, 2015

To my gradma Ino, who used to say:

"el saber no ocupa lugar"

One can never know too much

The candidate confirms that the work submitted is his/her own, except where work which has formed part of jointly-authored publications has been included. The contribution of the candidate and the other authors to this work has been explicitly indicated below. The candidate confirms that appropriate credit has been given within the thesis where reference has been made to the work of others.

Cotton plants belonging to the PimaS7, China10, Krasnyj, 30834 and JFW15 cultivars were grown by Bayer Cropscience. All samples were collected and processed by the candidate and Jean-Luc Runavot during the candidate's PhD secondment to Bayer CropScience, Belgium from 20th April to 28th July 2013. FM966 "Batch 1" and "batch 2" FM966 plants were grown by the candidate at the University of Leeds.

In Chapter 3, Table 3-1, measurements of fibre quality and related parameters using the High Volume Instrument (HVI) method was done in CIRAD (French Agricultural Research Centre for International Development), France.

In Chapter 3, the monosaccharide composition and linkage experiments leading to Figure 3-2, Figure 3-3 and Figure 3-4 were performed by the candidate and Jean-Luc Runavot at Bayer Cropscience, Belgium during the candidate's PhD secondment to Bayer CropScience, Belgium for two cotton cultivars and by Jean-Luc alone for the rest of the cultivars.

In Chapter 3, the microarray experiment leading to the heatmap in Figure 3.9 was performed by Xiaoyuan Guo at the University of Copenhagen, Denmark.

Acknowledgements

I would like to thank my supervisor Prof. Paul Knox for being a great supervisor and giving me the opportunity to do this PhD. He was very supportive, available at any time and always with a very positive attitude towards my work. I have learnt much from him during this PhD, about cell walls and about dealing with the scientific world.

Thank you to all my lab members: Sue, our excellent lab technician who has helped me so efficiently with lots of lab and admin stuff and my lab PhD/postdoc mates: Valerie, Sara, Tomas T., Jie and Tom B. who guided me through some techniques on cotton fibres at the beginning of my project. Thanks to the electron microscopy facility technician Martin Fuller who helped with sectioning.

To Jean Luc Runavot in Bayer Cropscience (Gent, Belgium) who collected all samples with me during my stay in Bayer and showed me how to do the monosaccharide linkage and composition experiments and did many of the samples after I left. Thank you to Frank Mealewater for his supervision during my stay in Bayer and his help and support with the manuscript on cotton fibre heteromannan and heteroxylan polysaccharides.

Thank you to Walltrac and the Marie Curie funding that have made my life easy during these years. Harry Gilbert in the University of Newcastle for providing all the CBMs used in this work and for all his help on the CBM3a discussion in this thesis and all the work he did that is included in the CBM3a manuscript. Xiaoyuan Guo for performing the glycan microarray experiment at the University of Copenhagen. Thanks to all Walltrac fellows, our great manager Alex and all PIs for the good times during every Walltrac meeting.

I want to thank my parents and brothers that have always been there for me, I made it here thanks to them. Thanks to all my friends in Avila, Madrid and London for still being there. To all my friends in Leeds, for the great nights out and pub days. Special thanks to: my Leeds brother Rupesh for taking care of me, I shall not forget. To the HIJAS! Gloria, Kasia, Ambra, Rocio and Yoselin (and Jessica), I had the time of my life, I learnt so much from them. To Sean for all he does for me every day. This PhD would definitely have not been the same without these people.

Abstract

The developing cotton fibre is an excellent model to study cell wall biochemistry, structure and function as it is a single cell with an unusual capacity for cell elongation and cell wall synthesis. Mature cotton fibres are the purest form of cellulose in nature, nonetheless the primary and secondary cell walls contain non-cellulosic polysaccharides and glycoproteins that modulate fibre development and may ultimately determine fibre quality traits such as length, fineness and strength. A comparative analysis of the fibre cell wall changes during development was carried out on selected cultivars with distinct fibre properties from four domesticated species *G. hirsutum, G. barbadense, G. herbaceum* and *G. arboreum*. Significant differences were found between species regarding the developmental dynamics of non-cellulosic epitopes, the developmental pace in terms of cell wall adhesion and detachment through the cotton fibre middle lamella, the timing of the transition phase and the cellulose deposition rate. The analysis of monosaccharide linkage and composition, and polysaccharide epitope immunolocalization using monoclonal antibodies, evidenced for the first time the presence of the hemicellulosic polysaccharide mannan in the developing and mature cotton fibre. Moreover, high magnification images of the fibre cell wall showed novel localization of several non-cellulosic polysaccharides, such as the presence of arabinoxylan between cellulose layers in the secondary cell wall. In addition, very important developmental processes, such as degradation/modification of pectic galactan and highly methyl-esterified homogalacturonan were developmentally profiled. Finally, further analysis of fibre glycan biochemistry led to the discovery of the capacity of *Ct*CBM3a to bind to xyloglucan in addition to crystalline cellulose.

Table of Contents

List of Tables

List of Figures

List of abbreviations

+b: yellowness of fibre

Ab: antibody

AFM: atomic force microscopy

AGP: arabinogalactan protein

APC: AGP polysaccharide complex

AX: arabinoxylan

CESA: cellulose synthase A

CFML: cotton fibre middle lamella

CSC: cellulose synthase complex

CSCL: cellulose synthase complex-like

*Ct*CBM: carbohydrate binding module from *Clostridium thermocellum*

CW: cell wall

Dha: 3-deoxy-D-lyxo-heptulosaric acid

DP: degree of polymerization

DPA: days post anthesis

EC: enzyme commission

EDC: epitope detection chromatography

Elong: fibre elongation

ER: endoplasmic reticulum

EXP: expansin proteins

FLA: fasciclin-like arabinogalactan protein

FM966:   FibreMax® (966 line)

FTIR: Fourier Transform Infra-Red Spectroscopy

GalA: galacturonic acid

GAX: glucuronoarabinoxylan

GC: gas chromatography

GDP: guanidine di-phosphate

GFP: green fluorescent protein

GPI: glycosylphosphatidyl inositol

GX: glucuronoxylan

HG:	homogalacturonan
HPLC:	high pressure liquid chromatography
HRGP:	hydroxyproline-rich glycoprotein
ICAC:	international cotton advisory committee
JIM:	John Innes monoclonal
KDO:	3-Deoxy-d-*manno*-octulosonic
LM:	Leeds monoclonal
mAb:	monoclonal antibody
MALDI:	matrix-assisted laser desorption/ionization
MR:	maturity ratio
MS:	mass spectrometry
NMR:	nuclear magnetic resonance
o/n:	over night
PACE:	polysaccharide gel electrophoresis
PBS:	phosphate buffered saline
PEL or PL:	pectate lyase
PM:	plasma membrane
Rd:	reflectance degree
RGI:	rhamnogalacturonan I
RGII:	rhamnogalacturonan II
RT:	room temperature
SFI:	short fibre index
ST:	sialyltransferase
Syp61a:	syntaxin of plants 61
TGN:	trans Golgi network
UHML:	upper half mean length
UI:	uniformity index
XEH:	xyloglucan endohydrolase
XET:	xyloglucan endotransglycosylase
XG:	xyloglucan
XGA:	xylogalacturonan
XTH:	xyloglucan endotransglucosylase/hydrolase
YFP:	yellow fluorescent protein

Chapter I

1   Introduction

Plant cell wall biology is a broad area of knowledge that covers numerous topics. The content of this introductory chapter has been selected to provide a concise literature review relevant to this thesis project on plant cell walls and cotton fibre development. The first part describes the major features of cell wall components and cell wall architectures. The second part is dedicated to a more detailed analysis on the composition and structure of cotton fibre cell walls during development.

1.1   Biology and evolution of plant cell walls

Plant cell walls are complex and dynamic polysaccharide-rich composites that surround all plant cells. Cells walls are highly diverse in composition and architecture, evolved to fulfil a vast range of functions. Cellulose, non-cellulosic polysaccharides (pectins and hemicelluloses), glycoproteins, lignin and waxes are the main constituents of plant cell walls. The amount as well as the structure and distribution of these components vary across the plant kingdom, among tissues and even within a single cell. In fact, our understanding of the architectural diversity of these components in the cell wall is still limited.

The origin of the plant cell wall is believed to have occurred 3.5 billion years ago as a result of selective pressure to move from a heterotroph system to an autotroph system in which a cell wall was needed to control turgor pressure and allow higher intracellular osmolarities (Duchesne and Larson, 1989). Multicellularity, the colonization of land and the subsequent development of vascular tissues are major events in plant evolution that brought with them major changes in the cell wall composition and structure (Popper et al., 2011). Multicellularity required structural cell wall changes like the creation of a "sticky" middle lamella to hold neighbouring cells together after cell division and the development of plasmodesmatal connections (Raven, 1997) while terrestrialization required many stages of cell wall

specialization to permit growth on land for which the development of a specialized vascular tissue for efficient nutrient transport was one of the most imperative needs.

In higher plants, cells have a primary cell wall which may contain cellulose, pectin, hemicelluloses (those glycans that are not cellulose or pectin), proteins and glycoproteins, and in some tissues specialized cells develop a secondary cell wall that generally contains relatively increased amounts of cellulose and also lignin. Primary and secondary cell walls have different mechanical and biological properties. The primary cell wall is synthesized at cell division and during cell expansion and is adjacent to the middle lamella (intercellular region). The main mechanical property of the primary cell wall is its flexibility to allow cell expansion while still bearing internal osmotic and tensile forces preventing cell bursting. Plant cells communicate and interact with neighbouring cells and the environment through their primary walls, diffusing water, nutrients and hormones and generating outward and inward signals (Ridley et al., 2001; Mohnen, 2008) to respond and adapt to external changes. Some cells develop an inner secondary cell wall once cell growth has stopped. This is a more rigid structure that strengthens the cell against external forces preventing cell collapse. The secondary cell wall is highly insoluble due to the higher amounts of cellulose and lower branching ofIts noncellulosic polysaccharides . Additionally the presence of lignin in the secondary cell wall makes it highly hydrophobic (Doblin et al., 2010).

Although a simple models are usually used to depict the plant cell wall structure, it is obvious that the cell wall has substantial heterogeneity in composition and architecture (Burton et al., 2010). The most relevant information to introduce this thesis project regarding cell wall composition and architecture can be found in 1.1.2 and 1.1.3 respectively. The next chapter focuses on the current techniques to study this cell wall heterogeneity.

1.1.1 How do we study cell walls?

The polysaccharides found in cell walls are cellulose, callose, xyloglucan, heteroxylans, mixed-linkage glucans, heteromannans and pectins (homogalacturonan (HG), rhamnogalacturonan-I (RG-I), rhamnogalacturonan-II (RG-II) and substituted galacturonans). Studying the composition and architecture of these polysaccharides within the plant cell wall involves three different structural levels: the glycosyl residue and linkage composition of isolated polymers (primary structure), their intra and inter-molecular links (secondary structure) and the spatial disposition of intact polysaccharides within the cell wall (tertiary structure).

The primary structure of the glycan cell wall components, that is the monosaccharide composition and linkage is usually studied by a combination of several techniques and instrumentation. Briefly, polysaccharides are extracted and solubilised from the cell wall by enzymatic and chemical cleavage. Then, the formation of alditol acetates or TMS (trimethylsilyl) methyl glycosides are the most common approaches. The identification and quantification of each monosaccharide and the linkage composition analysis is usually done by coupling gas chromatography (GC) to mass spectroscopy (MS) equipment (GC/MS) (Albersheim et al., 1967; Pettolino et al., 2012). Details of the chemical structure of homopolymers like cellulose and callose are commonly studied by X-ray diffraction, Fourier Transform Infra-Red Spectroscopy (FTIR) and Nuclear Magnetic Resonance (NMR) (Atalla and Vanderhart, 1984; Him et al., 2001; Thomas et al., 2013).

In addition to these techniques, cocktails of selected enzymes with high specificity are used to degrade plant materials so that is possible to understand the secondary structure of cell wall polysaccharides. Chromatographic techniques such as high pressure liquid chromatography (HPLC) or polysaccharide gel electrophoresis (PACE) (Goubet et al., 2002) used in combination with known oligosaccharide standards allows the quick identification and isolation of mono- and oligosaccharides after sequential enzymatic cleavage.

Monoclonal antibodies (mAbs) and carbohydrate-binding modules (CBMs) are used to detect cell wall components *in-situ* by fluorescence imaging and electron microscopy. More recently, glycan probes can be used to profile the cell wall composition through high through-put techniques like glycan microarrays (Moller et al., 2008; Fangel et al., 2012). Glycan microarrays have been extremely useful so far to discover specific tissue localization of cell wall polymers (McCartney et al., 2003; Ordaz-Ortiz et al., 2009; Giannoutsou et al., 2013), and to compare cell wall compositions from multitudinous samples uncovering even plant evolutionary relationships (Leroux et al., 2015).

Thanks to these probes and associated techniques much has been discovered about the primary and secondary biochemical composition of cell walls, although our knowledge does not yet cover as many species, tissues, and developmental stages as it is wished. Even more difficult is to comprehend the final tertiary structure or architecture of polymers in the cell wall since most extraction methods tend to destroy some of the native polysaccharide interactions. Understanding glycan interactions is an important part of cell wall research as some key functional aspects as well as biosynthetic pathways may lay behind these interactions. In this regard, a newly developed highly sensitive technique, named epitope detection chromatography or EDC (Cornuault et al., 2014) can provide data on the glycan heterogeneity of a sample indicating subpopulations of a given epitope using mAbs and pointing to unique glycan interactions.

The use of matrix assisted laser desorption/ionization mass spectrometry imaging (MALDI MSI) to analyse the compositional variation in a tissue is worth mentioning. The advantage of using MALDI imaging over common immunolabelling techniques is that it can provide accurate data of the glycan composition and its spatial distribution in the cell walls of a given tissue at once (Veličković et al., 2014). However, for MALDI imaging to compete with immunolabelling procedures, high-through-put data analysis, with advanced libraries to optimise reproducibility between different equipment, and

improved resolution (at the moment between 50-500 µm) need to be achieved.

Another increasingly used technique in cell wall research is atomic-force microscopy (AFM). It has a very powerful resolution at the molecular level and can be used to reveal the mechanical properties of cell walls. For example softness or stiffness depending on the cell wall pectic composition has been shown to be directly related to developmental processes such as fruit ripening (Paniagua et al., 2014; Veličković et al., 2014) and organ formation (Braybrook et al., 2012). AFM has also proved very useful to understand the assembly of cell wall proteins like extensins (Cannon et al., 2008) and other cell wall polysaccharides (Alsteens et al., 2008; Zhang et al., 2014).

In-vivo imaging of cell walls is very challenging due to the glycan nature of the majority of the cell wall components. Glycan tagging approaches for visualization are very limited compared to protein based experiments, thus, most experimental procedures rely on fixed materials. One approach to tag glycans for *in-vivo* experiments is radiolabelling. This is a very useful technique to study the synthesis, secretion pathways and degradation of cell wall polysaccharides in living cells (Fry, 2011). More recently, bioorthogonal click chemistry (Baskin et al., 2007; Soriano Del Amo et al., 2010) has arisen as an innovative technique with an incredible potential for *in-vivo* imaging of cell wall processes such as pectin biosynthesis (Anderson and Wallace, 2012) or cell wall lignification (Tobimatsu et al., 2014).

1.1.2 Cell wall components: biochemistry and function

1.1.2.1 Cellulose

Cellulose is the most abundant polysaccharide in nature. It is produced by the most primitive living forms on Earth such as marine cyanobacteria, bacteria and green algae and it is the major polysaccharide in later evolved terrestrial plants. Even urochordates (or tunicates) animals can also produce cellulose, whose origin is believed to be in an early event of lateral gene transfer of cellulose syntheses from bacteria (Nakashima et al., 2004).

Cellulose is a homopolymer of β-1,4-linked glucosyl residues (Figure 1-1A). The number of glucose units or degree of polymerization (DP) is variable and cellulose chains of up to 8000 glucosyl residues can be found in the primary cell wall and up to 15000 units in the secondary cell wall (Brown, 2004). In a cellulose chain each glucose is rotated 180° on the chain axis relative to the previous residue. This rotation of the β-linked glucosyl residues allow cellulose chains to easily stack (unlike the α-1,4- glucose found in starch) and be organized into microfibrils (Figure 1-10) that can form crystalline cellulose via numerous intra- and intermolecular hydrogen bonds (Figure 1-1) and van der Waals interactions. Depending how these chains interact, cellulose can acquire several conformations named as type I, II, III and IV. Cellulose I and II are stable crystalline conformations and type I is the main naturally occurring structure in which all reducing ends are in the same tip of the microfibril, called parallel configuration (Brown, 2004). The other two cellulose types, III and IV, are not found in nature but obtained chemically or after heat treatment (Wada et al., 2004). The native cellulose I is a composite of two distinct crystalline phases named Iα and Iβ and first observed by Atalla and Vanderhart (1984) when the glucose carbon atoms C1, C4 and C6 of cellulose I chains generated resonance multiplicities in solid-state ^{13}C nuclear magnetic resonance (NMR). Cellulose Iα is defined by a triclinic unit cell and cellulose Iβ by a monoclinic unit cell (B). In the Iα structure there is an unidirectional axial shift of each subsequent sheet of cellulose molecules that generates different hydrogen bonding (compared to

the Iβ structure) between the repeating disaccharide cellobiose (Fleming et al., 2001). The preference for one group in the cell wall varies between organism, for example, cotton cellulose is mainly formed of Iβ chains whereas Iα chains are more commonly found in bacteria and green algae (Mihranyan, 2011). Nevertheless, this preference can be modified by adding other polymeric additives like xyloglucan to the bacterial media (Yamamoto and Horn, 1994; Uhlin et al., 1995) indicating that the way cellulose chains are packed in the microfibril is an important factor for cell wall assembly and architecture (Figure 1-10 A). In fact, the alternation of highly crystalline regions with less crystalline (or amorphous) affects the interaction with other cell wall polymers and the final cell wall physical properties (Park and Cosgrove, 2012).
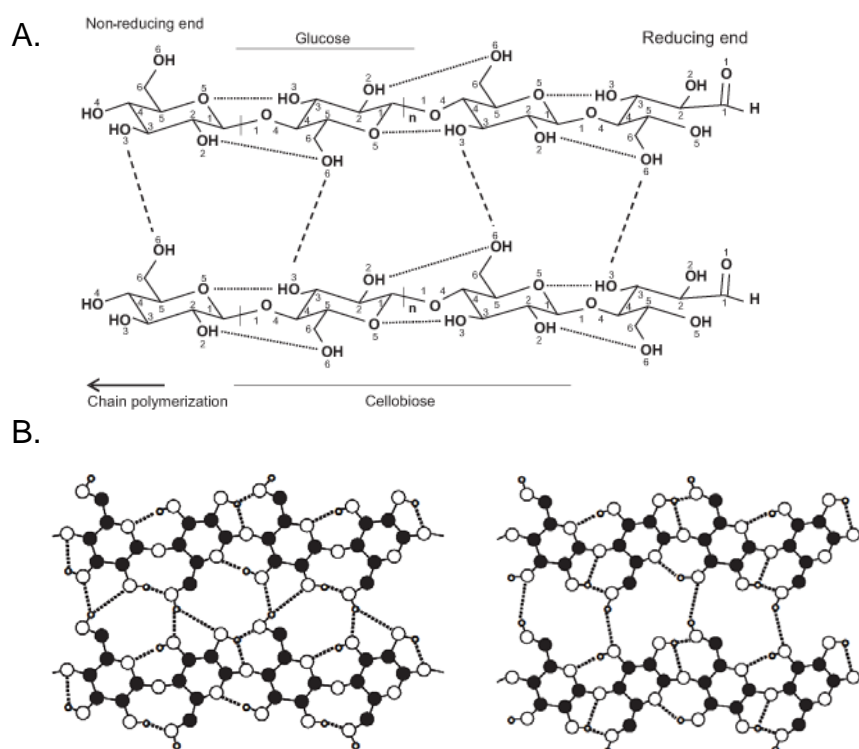
Figure 1-1. Structure and composition of cellulose. A. Cellulose I structure. Two cellulose chains of β-1,4-linked glucoses showing inter-chain hydrogen bonding (dashed lines) and intra-chain hydrogen bonding (dotted lines). B. Hydrogen-bonding patterns (dotted lines) in cellulose Iα (left) and Iβ (right) based on the crystal structures of Images taken from (Šturcová et al., 2004; Festucci-Buselli et al., 2007).

In the living cell the arrangement of cellulose chains into microfibrils and the interaction of these microfibrils with other polymers is a dynamic process that occurs through a complex combination of factors, from the biosynthesis of the glucan chains to enzyme-mediate cellulose interactions with other polymers. Cellulose microfibrils are deposited in the cell wall by the cellulose synthase A (CESA) complexes (CSC) placed at the plasma membrane. Each CSC is formed by six hexagonally arranged subunits called rosette with a diameter of 30 nm at the outer membrane surface (Lei et al., 2012). The first plant CESA protein was discovered by Pear et al. (1996) in cotton fibres. Since then several cellulose isoforms have been discovered in many more organisms. In Arabidopsis, CESA1, 3 are essential to synthesise cellulose in the primary cell wall and have been shown to also bind CESA 6 and its redundant isoforms CESA2, 5 and 9. CESA 4, 7 and 8 are involved in the synthesis of cellulose in the secondary cell wall. Turner and Somerville (1997); Arioli et al. (1998) produced some of the early work in the discovery of cellulose synthases and a full list of the Arabidopsis genes and mutations involved in cellulose synthesis can be found in a recent review by Li et al. (2014).

A 36-chain microfibril model (6x6 model) has been the most persistent in the literature, however recent publications created computational models of 24-chain and 18-chain microfibrils that actually fit better with experimental data from NMR and X-ray analysis (Fernandes et al., 2011; Newman et al., 2013; Thomas et al., 2013). These models imply that three CESA domains assemble into each one of the six rosette subunits (3x6 model) instead of the commonly accepted 6x6 model producing 36-chain microfibrils, however it has been shown that CESA proteins tend to form dimers, tetramers and hexamers but not the trimers that would be required for a 18-chain microfibril as reviewed by Kumar and Turner (2015). Cosgrove (2014) proposed another possibility with the existence of a CESA regulator that would turn on and off multiple CESA in the traditional 6x6 model synthesising microfibrils with less or more chains. This would explain to some extent the variation of the cellulose microfibril diameter between organisms from 3-10 nm in higher

plants to 10-25 nm in algae and bacteria. The orientation of cellulose microfibrils in cell walls is important during cell wall elongation as it confers to the wall the strength needed to bear external forces. During many years scientists have observed that the orientation of the cellulose microfibrils and CESA activity in the cell wall is closely related to cortical microtubules. More recently, it has been discovered the first link between CESAs and microtubules through the cellulose synthase interacting 1 (CSI1) protein, which could act as a docking port to guide cellulose synthases along microtubules (Bringmann et al., 2012; Li et al., 2012). Other factors that regulate CESAs cell wall movement are reviewed elsewhere (Bringmann et al., 2012; Li et al., 2014; McFarlane et al., 2014).

1.1.2.2 Callose

Callose is a chain of β-1,3-linked glucosyl residues (Figure 1-2) sometimes substituted with β-1,6-branches. Callose is synthesised at the plasma membrane by callose synthases and is involved in numerous biological processes (Chen and Kim, 2009). Plasmodesmatal gating is regulated by the synthesis and degradation of callose by specific β-1,3-glucanases at the plasmodemasta neck (Zavaliev et al., 2011) controlling very important biological processes like cotton fibre elongation (Ruan et al., 2001; Ruan et al., 2004) and lateral root development (Benitez-Alfonso et al., 2013).
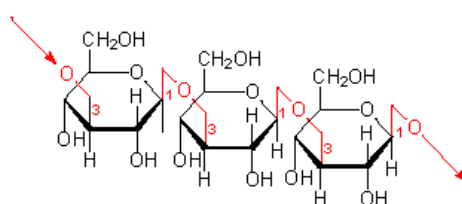
Figure 1-2. Structure and composition of callose. Callose is a chain of of β-1,3-linked glucoses.

Callose is involved in cell plate maturation during cytokinesis (Park et al., 2014) and also serves as essential physical barrier when synthesised between the membrane and the cell wall following pathogen attacks (Ellinger and Voigt, 2014). Callose deposition in the cell wall of the growing pollen tube is located between the membrane and an external pectin layer restricted to the distal part and no callose is observed at the growing tip (Chebli et al., 2012). This callose deposition around the pollen tube is thought to act as load bearing of mechanical forces controlling the diameter of the pollen tube, however this might not be the principal function of callose in the mature cell wall of pollen tubes (Parre and Geitmann, 2005). Interestingly, the amount of methyl-esterified pectin at the apical tip seems to somehow associate with callose digestion at the distal part (Parre and Geitmann, 2005).

1.1.2.3 Xyloglucan

The primary structure of xyloglucan (XG) varies depending on species and tissues. Many XG motifs have been characterized and classified into types, such as the XXXG- and XXGn- type whose single-letter nomenclature was described by Fry et al., 1993. The XG backbone is composed of a β-1,4-linked glucoses with side chains of α-D-xylosyl residues at C-6 of backbone β-D-glucosyl residues. β-D-galactosyl (partially O-acetylated) and α-L-fucosyl-1,2-β-D-galactosyl residues can be found at C-2 of the α-D-xylosyl residues and α-L-arabinosyl at C-2 of some of the backbone β-D-glucosyl residues or at C-3 of α-D-xylosyl residues (Figure 1-3).

Xyloglucan is thought to appear when plants conquered land as it is present in all land plants but not algae, however this is not yet clear as xyloglucan was detected using mAbs in the green alga *Chara coralline* (Domozych et al., 2009) and ancestral xyloglucan modifying enzymes like xyloglucan endotransglucosylase (XET) have also been found in the genus *Chara* (Van Sandt et al., 2007). In monocotyledon cell walls (type II) XG are less abundant than in dicotyledons plants (Carpita, 1996).
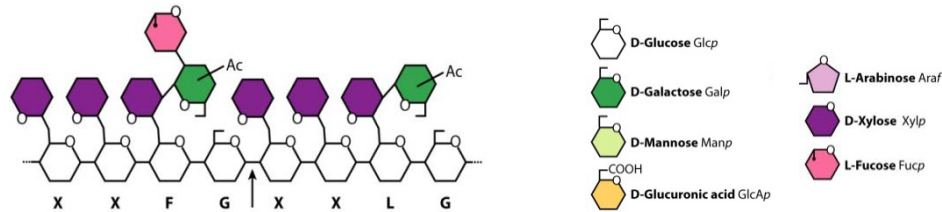
Figure 1-3. Structure and composition of xyloglucan. The xyloglucan backbone is a chain of β-1,4-linked glucoses. Side chains include: α-D-xylosyl residues at C-6 of the β-D-glucosyl backbone residues. β-D-galactosyl (partially O-acetylated) and α-L-fucosyl-(1→2)-β-D-galactosyl at C-2 of the α-D-xylosyl residues. α-L-arabinosyl at C-2 of some of the backbone β-D-glucosyl residues or at C-3 of α-D-xylosyl residues. Image modified from (Scheller and Ulvskov, 2010).

This structural complexity of linkages and residues requires several enzymes to generate a full xyloglucan motif. The gene family *CELLULOSE SYNTHASE-LIKE C* (CSLC4) are β-1,4-glucansynthases that produce the xyloglucan backbone. Several different xylosyl and galactosyltransferases are involved in the synthesis of the side chains that occurs in the Golgi in multiprotein complex (Zabotina, 2012). Two main xylosyltransferases are the XXT1 and XXT2 and a *xxt1 xxt2* double mutant in *Arabidopsis* failed to produce detectable xyloglucans (Cavalier et al., 2008). Traditionally, xyloglucans (XG) have been considered one of the major structural components of the primary cell wall of dicotyledon plants (type I cell wall) as they are believed to coat and link cellulose microfibrils that would be otherwise unconnected, creating a network of cellulose xyloglucan that can bear tension forces and is directly implicated in cell wall remodelling during growth and tissue development in response to hormones and via the activity of xyloglucan endotransglucosylase/hydrolases (XTH) (Hayashi and Kaida, 2011). However, the XG deficient *xxt1 xxt2* double mutant showed a surprisingly normal phenotype (Cavalier et al., 2008) which has called in to question the generally believed essential role of XG in the cell wall. The traditional cell wall model has been revisited recently and is discussed in section 1.1.3. XG is also known to be internalised by the cell during cytokinesis and accumulate at the cell plate as ready-to-go material into the

new forming cell wall and as part of the middle lamella together with pectic homogalacturonan in growing tissues like roots (Vaughn et al., 1996; Baluska et al., 2005). XG also accumulates in the middle lamella of cotton fibres, although it has to be noted that the cotton fibre middle lamella does not originate from cell division (Singh et al., 2009).

1.1.2.4 Heteroxylan

Xylan can be traced back in evolution to early organisms, such as green algae where homoxylans with a β-1,3-linked xylosyl residues replace cellulose and in some red seaweeds have mixed β-1,3/1,4-linked homoxylan polymers (Ebringerova and Heinze, 2000). In land plants, xylan structures differ between species and tissues. The heteroxylan backbone (Figure 1-4) is uniquely formed by β-1,4-linked xylosyl (partially O-acetylated at C-2) residues with single or double substitutions at C-2 or C-3 of the xylosyl backbone residues with α-arabinofuranosyl chains named arabinoxylans (AX) or α-glucosyluronic (can be methylesterified at C-2) named glucuronoxylans (GX) or both and thus named glucuronoarabinoxylans (GAX) (Hao and Mohnen, 2014).
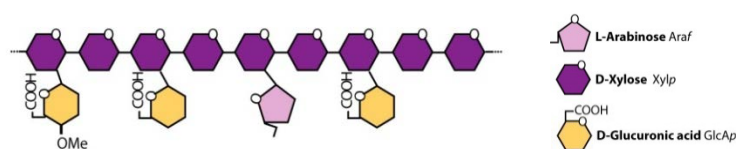
Figure 1-4. Structure and composition of heteroxylan. The heteroxylan backbone is formed by β-1,4-linked xylosyl (partially O-acetylated at C-2 of β-xylosyl residues). Side chains include: α-arabinofuranosyl, α-glucosyloronic acid and 4-methyl-α-D-glucosyluronic acid residues at C-2 or C-3 of the backbone β-xylosyl residues. Figure modified from (Scheller and Ulvskov, 2010).

In dicots, heteroxylan is less abundant (after xyloglucan) in the primary cell wall but the major hemicellulose in the secondary cell wall in the form of GX (Rennie and Scheller, 2014). Xylan, not xyloglucan, is the dominant

hemicellulosic component of the cell walls in monocots, where AX and GAX are very abundant. Up to 70% (w/w) in weight is AX (Ebringerová et al., 2005) while GAX can make up to 20-40% of primary cell walls and 40% of secondary cell walls in monocots (Scheller and Ulvskov, 2010). Dicot XG functions is mostly carried out by GAX and mixed-linkage glucans in monocots (Carpita, 1996). Many arabinofuranosyl units are cleaved from GAX and the xylosyl backbone acetylated when the monocot cell wall is assembled, so they can bind cellulose as XG does in dicots. This highly substituted GAX is usually found in association with the also less abundant pectic polysaccharides to create porosity and spacing in the monocot cell walls (Carpita, 1996).

A feature of the dicot plants but not grasses is the presence of a xylan reducing-end sequence (XRES) which is a terminal tetrasaccharide at the reducing end of GX [-4-β-D-Xyl-(1→4)-β-D-Xyl-(1→)-α-L-Rha-(1→2)-α-D-GalA-(1→4)-D-Xyl] that might act as an initiator or terminator of xylan backbone (York and O'Neill, 2008) during biosynthesisXylan is an essential component of the secondary cell wall in the xylem that helps cells to bear the negative pressure due to transpiration that allows water transport. Several studies on mutants with a collapse or "irregular xylem" (*irx* mutants) have been very useful in the understanding of xylan biosynthesis (Ebringerova and Heinze, 2000; Brown et al., 2007; Scheller and Ulvskov, 2010; Pauly et al., 2013; Hao and Mohnen, 2014; Rennie and Scheller, 2014). . Xylan biosynthesis and addition of side chains is thought to occur primarily in the Golgi. IRX9 (from the glycosyl transferases family GT43), IRX10 and IRX14 have been demonstrated to mediate the synthesis of the xylan backbone (Ren et al., 2014; Rennie and Scheller, 2014). Some of the enzymes involved in the synthesis of the xylan side chains have been characterised so far, for example, GUX1 and GUX2 transfer glucuronic acid to the C-2 position in the xylosyl backbone residue and XAX1 (from the GT61 family) has been shown to mediaof the enzyme that catalizes the addition of arabinofuranosyl residues to the xylan backbone has been demonstrated (Anders et al., 2012; Chiniquy et al., 2012).

1.1.2.5 Heteromannan

The mannan backbone can be formed by mannosyl residues solely (mannans) or by glucosyl and mannosyl residues (glucomannans), although they usually contain galactosyl residues as side chain (Figure 1-5) of the main backbone (galactomannans and galactoglucomannans) (Moreira and Filho, 2008).
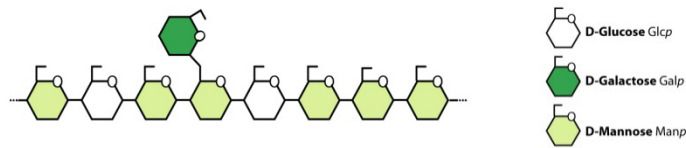
Figure 1-5. Structure and composition of heteromannan. The heteromannan backbone if formed of β-1,4-linked glucosyl/mannosyl (1:1 to 20:1 ratio) residues (partially O-acetylated at C-2 or C-3 of mannosyl residues). Side chains are made of α-D-galactosyl at C-6 of backbone mannosyl residues. Image modified from (Scheller and Ulvskov, 2010).

Heteromannans are highly conserved in plant evolution and are commonly found in the primary cell walls of charophytes and early land plants (bryophytes and lycophytes) but are less abundant in the later evolved gymnosperms and angiosperms (Nothnagel and Nothnagel, 2007). In the latter, other hemicelluloses seem to have replaced heteromannans in their structural roles (Scheller and Ulvskov, 2010). Nonetheless, heteromannan polysaccharides can be found in both primary and secondary cell walls of dicotyledonous plants. In *Arabidopsis,* mannans are abundant in the secondary cell walls of xylem cells and thickened epidermal walls (Handford et al., 2003) where they are proposed to be linkers of the hemicellulose-cellulose network (Schröder et al., 2009). Mannans, in particular galactomannans, are important for carbohydrate storage and very abundant in many plant seeds (Reid et al., 2003; Rodriguez-Gacio Mdel et al., 2012). Other mannan-associated functions include cell signalling during plant

growth (Liepman et al., 2007), zygotic embryogenesis (Goubet et al., 2009) and vascular cell differentiation (Beňová-Kákošová et al., 2006).

Regarding mannan biosynthesis, Dhugga et al. (2004) reported mannan synthase activity in the Golgi apparatus by cellulose synthase-like (CSL) proteins from the CSLA family and, more recently, it has been showed that the CSLD family is also involved in mannan synthesis and acts in a multimeric complex (Verhertbruggen et al., 2011; Yin et al., 2011).

1.1.2.6 Pectin

Pectins are a large family of galacturonic acid (GalA) rich molecules which are present in all land plants. They play major roles in cell and tissue morphology, plant growth and developmental processes which, is reflected in their structural heterogeneity and complexity. There are four major types of pectin domains covalently linked: homogalacturonan (HG), rhamnogalacturonan-I (RG-I), rhamnogalacturonan- II (RG-II) and substituted galacturonan known as apiogalacturonan and xylogalacturonan (Figure 1.1).

The composition, structure and relative abundance of pectin molecules varies between cell types, developmental stages and in specific cell wall locations within a single cell. Here some of the main features of each pectin domain and its biosynthesis relevant to the project are highlighted. A detailed review on pectin structure, function and biosynthesis is covered elsewhere (Caffall and Mohnen, 2009; Harholt et al., 2010; Yapo, 2011; Atmodjo et al., 2013).

1.1.2.6.1 Homogalacturonan (HG)

HG is a chain of α-1,4 galactosyluronic acid residues partially methyl esterified at C-6 (Figure 1-6). The pattern of methyl-esterification that occurs in the HG backbone is of major relevance as it confers different physical properties to the cell wall. A low degree of esterification in

homogalacturonan allows the formation of Ca^{2+} bridges between blocks of de-esterified galactosyluronic acid residues of two adjacent HG chains (Figure 1-10 B). The resulting structure of overlapping HG chains form gels that, inside the cell wall environment, modulate cell wall porosity and strength and contribute to intercellular adhesion (Willats et al., 2001).
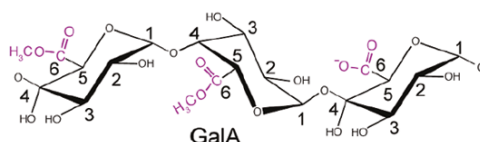
GalA

Figure 1-6. Structure and composition of homogalacturonan. Homogalacturonan is composed of a chain of α-1,4 galactosyluronic acid residues which can be partially methyl esterified. Image modified from (Dick-Perez et al., 2011).

Highly methyl-esterified HG is produced in the Golgi complex and released to the cell wall in an esterified form which is then de-esterified as needed *in-muro* by pectin methyl esterases (PMEs) subsequently rigidifying the cell wall as Ca^{2+} crosslinks blocks of newly de-esterified HG. Similarly to methyl esters, acetyl esters can prevent HG dimerization via calcium (Ralet et al., 2003) and overexpression of a de-acetylesterase in tobacco impaired cell elongation affecting cell extensibility (Gou et al., 2012). Acetylation of HG is not as common as HG methylation, in fact, acetyl-esterification is mostly found in the RGI backbone and only some plant species like sugar-beet are rich in acetyl-esterified HG.

1.1.2.6.2 Rhamnogalacturonan-I (RG-I)

The structural diversity of the RG-I molecules is very broad (Figure 1-7). The backbone is composed of the [→4)-α-D-GalpA-(1→2)-α-L-Rhap-(1→] disaccharide which can be partially O-acetylated at the C-3 of galactosyluronic acid. RG-I structural heterogeneity arises from its side chains which can be formed by α-1,4-galactosyl and α-1,5-arabinosyl at C-4

of the rhamnosyl backbone residues. The galactan side chains residues can also be double substituted at C3 and C6 with α-L-arabinosyl residues which can be linked to terminal α-L-fucosyl residues or with β-D-glucosyluronic acid residues (that can be methyl esterified at the C4 of the glucosyluronic acid). Arabinan chains branching from the galactan side chains can form connections with other arabinan chains forming hydrogen and di-ferulic bonds as in sugar beet root cell walls (Levigne et al., 2004).
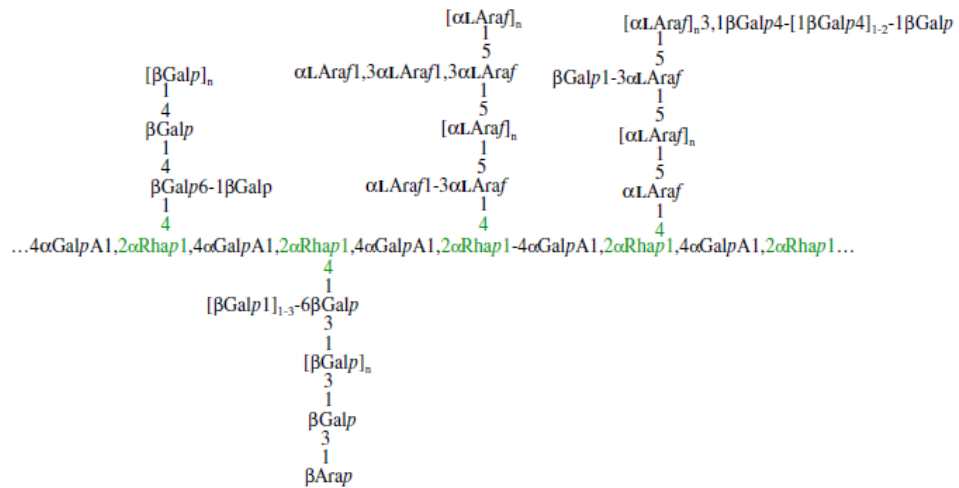
Figure 1-7. Structure and composition of RG-I. RG-I backbone is composed of →4)-α-d-GalpA-(1→2)-α-L-Rhap-(1→ disaccharide (partially O-acetylated at C-3 of galactosyluronic acid). Side chains include: α-D-galactosyl and α-L-arabinosyl at C-4 of backbone rhamnosyl residue, α-L-arabinosyl and terminal α-L-fucosyl, β-D-glucosyluronic acid and 4-O-methyl glucosyluronic acid at C-(3-6) of galactosyl residues. Image taken from (Caffall and Mohnen, 2009).

Seed mucilages are very rich in RG-I which is largely unbranched, while half of the rhamnose residues are substituted in the RG-I extracted from cell walls. The structure and composition of the RG-I side chains is very variable between species, tissues and cells and is spatially regulated (Jones et al., 1997; Willats et al., 1999; Orfila et al., 2001; McCartney et al., 2003). These variations modulate cell wall properties associated with cell expansion, cell to cell adhesion, developmental processes and cell signalling.

Detection of β-1,4-D-galactan with the LM5 antibody showed that galactan marks the transition zone near the onset of rapid cell elongation in Arabidopsis seedlings and slow root elongation mutants presented reduced amounts of β-1,4-D-galactan at the transition zone, indicating a role of galactan in the cell elongation processes (McCartney et al., 2003). On the other hand, cell wall stiffness has been correlated with higher galactan abundance in pea cotyledons after cell expansion has occurred (McCartney et al. 2000).

Depolymerization of pectin is needed for fruit ripening. Loss of galactan side chains was observed just before fruit maturation and softening, whereas selective loss of highly branched α-1,5-L-arabinans associated with fruit ripening and in over-ripened fruits correlated with a further significant loss of fruit firmness and compressive resistance possibly due to better accessibility of HG degrading enzymes after RG-I debranching (Peña and Carpita, 2004). Cell-cell adhesion in the colour-less non ripening (*Cnr*) tomato mutant is compromised (Thompson et al., 1999) showing a disrupted deposition of *α-1,5-L-arabinan* and low HG crosslinking in the middle lamella (Orfila et al., 2001).

1.1.2.6.3 Rhamnogalacturonan-II (RG-II)

RG-II is the most complex pectin molecule in composition as it is composed of α-1,4-linked galactosyluronic acid backbone with side chains at C-2 and C-3 substituted with up to 11 different glycosyl residues. The side chains are classified into A, B, C and D and composed of some unusual glycosyl residues like apiosyl (in the A and B chains), 3-Deoxy-d-*manno*-octulosonic or KDO (in chain C) and 3-deoxy-D-lyxo-heptulosaric acid or Dha (in the D chain) glycosyl residues (Figure 1-8). RG-II can be dimerized by a borate diester crosslink between two apiosyl residues of the side chain A (Figure 1-10 C). The negative effect of RG-II boron complex disruption in wall strength has been extensively documented by boron deficiency and Arabidopsis mutants (Caffall and Mohnen, 2009). The highly conserved

primary structure of RG-II among different plant taxons denotes a significant role of this polymer in the cell wall structure and pectin network, possibly more related to the general scaffolding of cell wall. The future development of a probe against RG-II would mean a significant advance that would help to study its specific localization *in-situ* and interactions with other cell wall glycans.
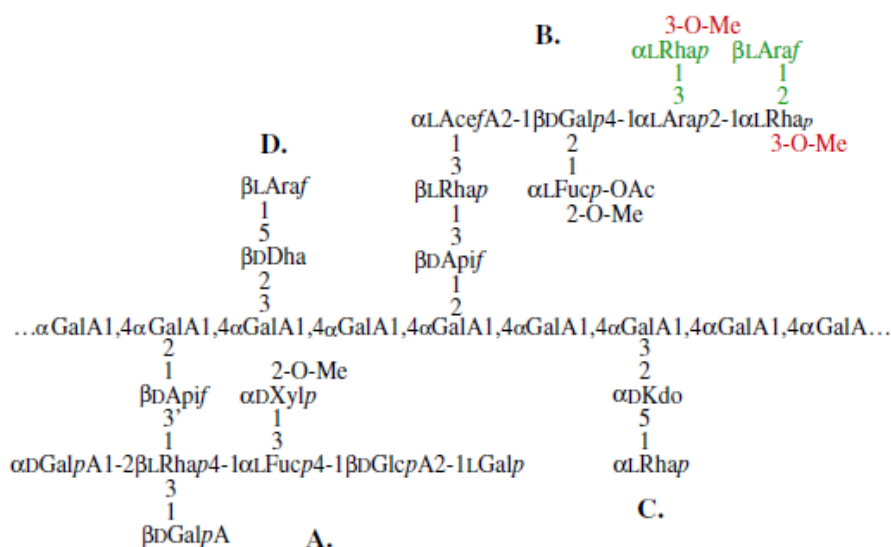
Figure 1-8. Structure and composition of RG-II. RG-II backbone is formed by α-1,4-linked galactosyluronic acid residues. Side chains are formed of up to 11 different glycosyl residues attached to apiosyl (A,B), KDO (C) and Dha (D) glycosyl residues at C-2 or C-3 of backbone galactosyluronic acid. Image taken from (Caffall and Mohnen, 2009).

1.1.2.6.4 Substituted galacturonans

Substituted galacturonans have a HG backbone of α-1,4-linked D-galactosyluronic acid substituted with two types of side chains. Type A has the apiobiose disaccharide D-Api-1,3'-D-Api at C-2 or C-3 of backbone galactosyluronic acid forming apiogalacturonan only found in some fresh- and salt- water hydrophytic monocots like sea grass and duckweed (Longland et al., 1989). Type B has monomeric or dimeric β-1,4-linked xylosyl residues at C-3 of backbone galactosyluronic acid forming xylogalacturonan (XGA) (Zandleven et al. 2007; Willats et al. 2004).
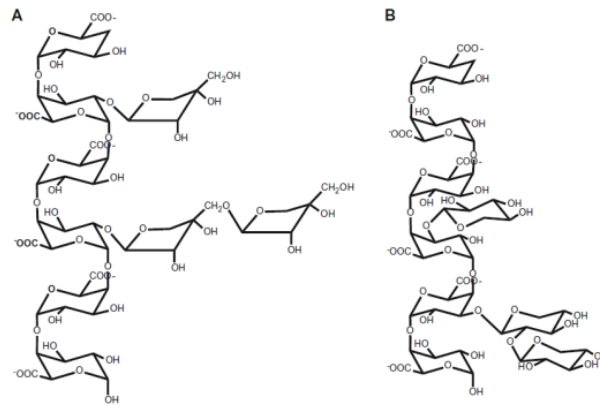
Figure 1-9. Structure and composition of substituted galacturonans.
The backbone consists of α-1,4-linked D-galactosyluronic acid and the side chains of D-Api-1,3'-D-Api (apiobiose disaccharide) at C-2 or C-3 of backbone galactosyluronic acid (A) and β-1,4-linked xylosyl residues at C-3 of backbone galactosyluronic acid (B). Image taken from (Caffall and Mohnen, 2009).

1.1.2.6.5 Pectin biosynthesis

Pectin is the most complex cell wall polysaccharide and certainly not much is known about its biosynthesis. Thanks to immunolocalization studies using tagged pectin biosynthetic proteins and pectin-directed probes, it has been established that at least a major part of pectin synthesis occurs inside the Golgi and it is modified as it is being transport towards the cell wall (Driouich et al., 2012). It is not known if pectin is synthesised in domains (HG and RG) that are later attached to each other in blocks (domain synthesis model) or if pectin is produced consecutively from the non-reducing end (consecutive glycosyltransferase model) in the Golgi (Atmodjo et al., 2013).

The membrane bound α-1,4-D-galacturonosyltransferase (HG:GalAT) elongates the HG chain by catalysing the transfer of D-GalA from UDP-D-GalA to the non-reducing end of HG chains, although it does not initiate the *novo* synthesis when isolated and tested *in-vitro* (Akita et al., 2002). Some of the core genes with proven HG:GalAT activity identified in Arabidopsis are the *GAUT1, GAUT7* genes (Atmodjo et al., 2011) and very recently two Arabidopsis orthologs of a protein found in the cotton fibre Golgi, named

Golgi-related 3 (CGR3) have been shown to be highly associated with HG methylesterification in the Golgi (Held et al., 2011; Kim et al., 2015) and adds to the previously reported putative methyltransferases QUA2 family (Mouille et al., 2007).

In the case of RG-I, the backbone is synthesised inside the Golgi by a GalAT and a rhamnosyltransferase (RhaT) (this last one still not identified) while the side chains need several glycosyltransferases. GALACTAN SYNTHASE 1 (GALS1) has been identified in Arabidopsis as a β-1,4-galactosyl transferase (GalT) involved in the synthesis of the RG-I galactan side chain. Knockout mutants of this gene resulted in less galactan and its β-1,4-GalT activity has been proven *in-vitro* (Liwanag et al., 2012). Putative α-1,5-arabinosyl transferases involved in the RG-I arabinan side chains are the ARABINAN DEFICIENT 1 and 2 (ARAD1, ARAD2) although its biochemical α-1,5-AraT activity has yet to be proven *in-vitro* (Harholt et al., 2006; Harholt et al., 2012).

RG-II requires at least 41 unique glycosyl transferases. A few genes have been identified to encode for putative RG-II:glycosyl transferases such as the GLUCURONOSYLTRANSFERASE1 (GUT1) β-1,4-glucuronosyl transferase of the chain A (Iwai et al., 2002) although this seems to contradict the work from where AtIRX10 homologs of the Nicotiana plumbaginifolia GUT1 appear to be involved in xylan biosynthesis and not RG-II (Brown et al., 2009). Another is the Kdo-transferase of the chain C (Seveno et al., 2010) and the RGXT1–4 α-1,3-xylosyl transferase which is the only one whose activity has been proved biochemically so far (Egelund et al., 2006).

1.1.2.7 Cell wall proteins

There are abundant cell wall proteins with very specific functions. Endogenous plant enzymes involved in cell wall polysaccharide turnover and cell wall remodelling such as specific glycanases (galactosidases, arabinosidases, pectate lyases, xyloglucanases, etc) are very important however only the cell wall proteins most relevant to this work are introduced below:

1.1.2.7.1 Hydroxyproline-rich glycoproteins (HRGPs)

One of the most relevant cell wall protein from the point of view of cell wall structure and expansion are the hydroxyproline-rich glycoproteins (HRGPs) families of extensins and arabinogalactan proteins (AGPs) which were first identified by Lamport and Northcote (1960). HRGPs are very ancient proteins that can be found in algae (Miller et al., 1972), although some plants, like grasses have evolved to rely less on structural HRGPs than other land plants (Kieliszewski and Lamport, 1987). HRGPs are very basic proteins that contain motifs of glycosylated hydroxyproline with arabinan, mainly in extensins, or arabinogalactan (AG), in AGPs (Seifert and Roberts, 2007; Lamport et al., 2011). HRGP families are sorted depending on the type of hydroxyproline (Hyp) repeats, based on the Hyp-contiguity hypothesis (Shpak et al., 2001). Extensins are cell wall located and rod-shaped proteins that contains contiguous Hyp residues in a hydrophilic motif that alternate with hydrophobic motifs sometimes containing tyrosine residues that allow them to self-assemble and form dendritic networks with pectin via acid-base interactions that could also implicate covalent cross-links (Lamport et al., 2011). On the other hand, other AGPs contain clustered non-contiguous Hyp residues and are associated with the plasma membrane and intercellular spaces (Seifert and Roberts, 2007). The glycan chains attached to the protein backbone are type II arabinogalactan (AG) made of β-1,3-galactan and β-1,6-linked galactan chains connected to each other by (1,3-1,6)-linked branch points and terminal arabinosyl residues at

O-3 and O-6 position or glucuronic acid at O-6 of the galactan resulting in an acidic side chain (Carpita and Gibeaut, 1993; Ellis et al., 2010).

There is a high degree of variation in the AGP protein backbone and its glycan composition and structure. This heterogeneity has been found between cells and tissues and evidence suggests that AGP composition reflects their functional role (Majewska-Sawka and Nothnagel, 2000). The classical AGP contains a single central domain rich in Pro, Ala, Ser and Thr and a GPI (glycosylphosphatidyl inositol) anchor signal sequence domain (lipid tail) to the cell membrane (Schultz et al., 2000) involved in cell signalling. Other AGPs contain one or two fasciclin-like domains, called fasciclin-like AGPs (FLA), a multifamily of cell adhesion proteins common to all kingdoms (Johnson et al., 2003) which in Arabidopsis has also been related to plant strength by affecting cell wall deposition (MacMillan et al., 2010). Some AGPs are thought to be released to the cell wall in parallel with cellulose synthase and bind cellulose as well as other polysaccharides like xyloglucans. It is suggested that they act as "plasticizers" that contribute to the general strength of the cell wall by modulating the action of cell wall remodelling enzymes (Seifert and Roberts, 2007; Ellis et al., 2010), on contrary to extensins that enhance cell wall rigidity at the end of cell expansion (Lamport et al., 2011). AGPs are also involved in pollen development (Nguema-Ona et al., 2012), hormonal interaction during root growth (Seifert et al., 2014), in somatic embryogenesis in cotton (Poon et al., 2012) and in cotton fibre initiation and elongation (Li et al., 2010). Other functions include signalling transduction pathways during development, pathogen defence or mechanical and environmental stresses (Pickard, 2013).

1.1.2.7.2 Pectin methyl esterases (PMEs)

Pectin esterification is known to be differentially regulated between tissues and developmental stages of a tissue (Knox et al., 1990) or even spatially at the cellular level, as in the well documented case of the elongating pollen tube (Bosch et al., 2005; Krichevsky et al., 2007). Pectic HG is synthesised

and deposited in a highly methylesterified form, which is then modified in varying degrees depending on finely regulated cellular localization of pectin methylesterases (PME) and pectin methylesterase inhibitors (PMEi) (Wolf et al., 2003; Wolf and Greiner, 2012). During pollen tube tip growth, a highly methyl-esterified pectin form is deposited in the cell wall at the tip while PMEs specifically act at the tip shoulders de-esterifying pectin chains which can then interlock through calcium ions creating a more rigid and less extensible cell wall at the tip sides. This avoids expansion of pollen tube diameter, thus favouring polar cell elongation. Another case of cell growth regulation by pectin methylesterification via PME/PMEi is hypocotyl elongation. Low esterification degree of pectin correlates with low hypocotyl elongation in overexpressing heterologous PMEs in Arabidopsis (Derbyshire et al., 2007). Similarly the elongation phase of the developing cotton fibre is correlated with the expression profiles of endogenous PMEs (see Liu et al. (2013) and section 1.2.1).

1.1.2.7.3 Xyloglucan endotransglycosidase/hydrolase (XTH) family

XTHs are one of the most important enzymatic remodelling cell wall proteins with two main catalytic activities: xyloglucan endotransglucosylase (XET) and xyloglucan endohydrolase (XEH). They were first discovered by both Fry et al. (1992); Nishitani and Tominaga (1992) and details of this family classification in the Enzyme Commission (EC) and nomenclature can be found in Rose et al. (2002). XTHs are evolutionary linked to bacterial lichenases that specifically cleave β1,3/β1,4-glucans (or mixed-linkage glucans) as recently postulated by Eklöf et al. (2013) upon discovery of a intermediate enzyme with action over both xyloglucan and mixed-linkage glucan from *Populus trichocarpa.*

The combined action of XG endohydrolases and XG endotransglycosidases cleaves donor xyloglucan chains and paste the end to the non-reducing terminal residue of another xyloglucan chain, xyloglucan oligosaccharide or water. XTHs cleave and rearrange xyloglucan chains which drastically impacts cell wall strength through the modification of load-bearing tethers between cellulose and xyloglucan and allows cell elongation by promoting

cell wall loosening (Nishitani and Tominaga, 1992; Rose et al., 2002). *In-vivo* co-localization of XET activity and xyloglucan oligosaccharide substrates was observed in the elongating zone of Arabidopsis roots (Vissenberg et al., 2000) and the association of XTH activity with cell elongation has been commonly reported in many developing tissues including the cotton fibre (Michailidis et al., 2009; Lee et al., 2010; Shao et al., 2011). Peaks of XET activity were also observed after cessation of growth such as maize leaves (Palmer and Davies, 1996) and lignifying tissues in asparagus (O'Donoghue et al., 2001) suggesting a role of XET in cell wall strengthening. Later on, XG and XTHs enzymes were localized in the secondary cell wall of tension wood fibres in poplar where XET is thought to incorporate XG into the developing secondary cell wall and create reinforcing links between the primary and the S1 cell wall layers (Bourquin et al., 2002) and also in the gelatinous (G) with outer cellulose layers in tension wood to allow stem bending (Nishikubo et al., 2007). A XTH (XTH31) has also been recently involved in aluminium resistance by modulating the amount of aluminium binding to hemicellulose (Yang et al., 2011) since its content in knockout mutants of XTH31 and its interactor XTH17 was significantly reduced (Zhu et al., 2012; Zhu et al., 2014).

1.1.2.7.4 Expansin (EXP) superfamily

Expansins are cell wall located proteins that are thought to act by non-covalent interactions with cellulose microfibrils, and between cellulose and other polysaccharides, inducing cell wall loosening without hydrolysis in a pH dependent manner (Cosgrove, 2000; Cosgrove et al., 2002) often due to hormonal response (Zhao et al., 2012). Plant expansins are encoded by many genes that are divided into 4 subfamilies: the classical α- and β-expansins and their truncated versions expansin-like A and expansin-like B (Sampedro and Cosgrove, 2005) formerly called γ-and δ-expansins (Li et al., 2003). The analysis of α- and β- expansins sequences of different plant origins suggested that α-expansins are more related to cell wall loosening in dicots while β-expansins, which are highly abundant in grass pollen (Tabuchi et al., 2011), are thought to be an evolutionary response to the higher

arabinoxylan content in grasses and thus able to more specifically act on grasses cell walls (Sampedro et al., 2015). Expansins are present in bacteria and fungi and plant expansins are thought to have an ancestral common origin possibly before land colonization as expansin-like sequences have been identified in amoebae (Li et al., 2002) although it has been recently suggested that bacterial and fungi expansins genes appeared due to the rare event of horizontal gene transfer from plants to bacteria and fungi (Nikolaidis et al., 2014). Swollenins are a fungal type of expansin known to swell cellulose rich materials like cotton fibres without increasing the amount of reducing sugars (Saloheimo et al., 2002) to facilitate the action of glucanases over cellulose. Similarly to bacterial (Bunterngsook et al., 2015) and fungal expansins, plant expansins have been found to act synergistically with glucanases to enhance crystalline cellulose degradation (Seki et al., 2015). Thus, expansins induce cell wall extension in many tissues and organs that require cell wall softening such as during fruit ripening (Rose et al., 1997) or root hair formation (ZhiMing et al., 2011). In cells undergoing high elongation processes like in the cotton fibres six fibre-specific α-expansins have been identified (Harmer et al., 2002) with essential roles during cell elongation (Ruan et al., 2001).

1.1.3 Cell wall architecture

How all these polysaccharides and proteins assemble together to form the 3D structure of the cell wall is not clear. Traditionally, it has been considered that the primary cell wall architecture is formed by two independent networks: the cellulose-hemicellulose network (1) and the pectin network (2). In the cellulose-hemicellulose network, cellulose microfibrils are crosslinked by hemicelluloses like xyloglucan in a "tethered network" (Somerville et al., 2004). XG-cellulose interactions in this tethered network would confer different mechanical properties to cell walls necessary for the cell to expand, resist compressive and tensile forces via XTH modifications (Cosgrove, 2005; Albersheim et al., 2011). Following the results from Cavalier et al. (2008) in which plant materials from the *xxt1 xxt2* double mutant of Arabidopsis produced no detectable XG, it has been demonstrated that XG, apart from strengthening the cell wall, are also very important during cell wall loosening by α-expansins to allow the cell wall to extend (Park and Cosgrove, 2012). This might account for the smaller phenotype of the *xxt1 xxt2* double mutant, however it is difficult to reconcile the general assumption of an essential role of XG in the tethered network model with the otherwise normal phenotype of the *xxt1 xxt2* double mutant. Moreover, the mechanical properties of the cell wall (in cucumber and Arabidopsis) after specific endoglucanase restriction of XG do not correspond with the predictions derived from the tethered network model (Park and Cosgrove, 2012) (Figure 1-10 D). These findings support the idea that cellulose microfibrils are not separated from each other as usually depicted but in contact, and that XG mediates this non-covalent binding in a domain of restricted enzymatic access (Figure 1-10 D). These domains have been called biomechanical hotspots and AFM visualizations of never-dried onion epidermal cells support this idea (Zhang et al., 2014). These biomechanical hotspots could be formed by two cellulose microfibrils coming in close contact, possibly just linked by a monolayer of xyloglucan binding to the hydrophilic surfaces of both microfibrils (Cosgrove, 2014; Park and Cosgrove, 2015).

On the other hand, it is known that pectins can also bind cellulose *in vitro* (Zykwinska et al., 2005) and, by enzymatic digestion, pectic side chains have been detected to connect cellulose microfibrils (Zykwinska et al., 2007). Moreover, recent work based on *in vivo*-like approach using NMR has shown that the xyloglucan-cellulose connections are not as abundant as initially thought and that pectins show numerous interactions with the surface of cellulose microfibrils (Dick-Perez et al., 2011). Moreover, pectin HG, RG-I, RG-II and substituted galacturonan domains form complex intramolecular configurations. All these domains can be covalently linked although it is not yet clear how. The most recent model proposed by Yapo (2011) suggests a RG-I core with two unbranched HG chains covalently linked to both ends of the RG-I backbone and other HG chains as side chains that would finish in RG-II dimer structures (see Figure 1-10 E). The pectin network is very complicated as all pectin domains could possibly be covalently linked to other polysaccharides. Thompson and Fry (2000) reported xyloglucan/pectin covalent interaction in suspension-cultured rose cells where 30% to 50% of the total cell wall xyloglucan might be synthesised from a pectin primer (Popper and Fry, 2008), although this might be somehow a feature of cultured cells only (Park and Cosgrove, 2015). Moreover, it has been recently shown that pectic RG-I can be part of a glycoprotein complex of arabinoxylan covalently linked to an arabinogalactan protein (Tan et al., 2013).

In conclusion, cell wall are extraordinary complex composites (Figure 1-10 F) with high diversity of polysaccharide interactions and fine regulation of the cell wall composition and architecture. Much is still to be discovered in this exciting field. This thesis research project focuses on the study of cotton fibre cell walls during development. This model was chosen because cotton fibres are an excellent single-cell model to study cell wall synthesis and cell expansion as they have an extraordinary capacity for cell elongation (independent of cell division) and secondary cell wall synthesis. The main features regarding the fibre cell wall development are described in the following section 1.2.
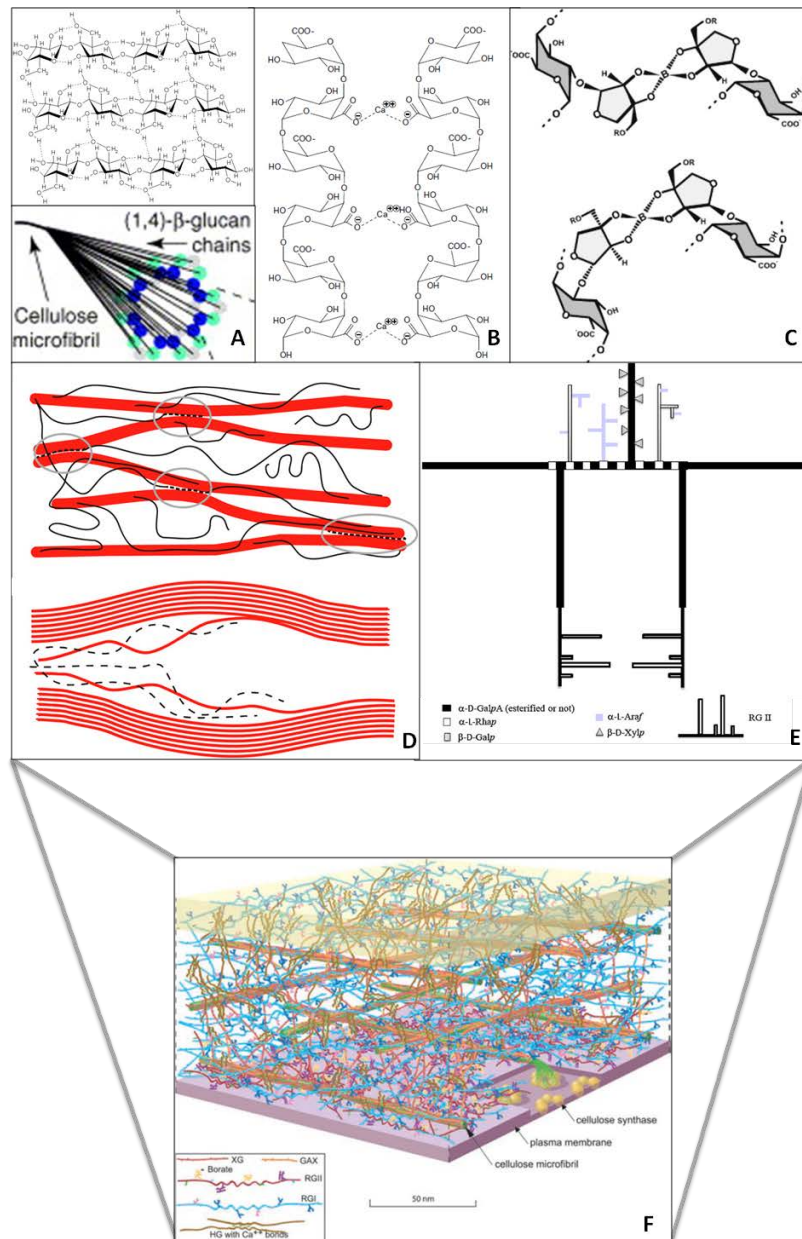
Figure 1-10. Secondary and tertiary structure of cell wall components.
A. Intra and inter molecular hydrogen bonds (dashed lines) in cellulose chains (upper image) form cellulose microfibrils (lower image). Adapted from (Scheible and Pauly, 2004). B. Calcium crosslinking of homogalacturonan chains. Taken from (Caffall and Mohnen, 2009) C. Two possible structures for the borate ester crosslink and the apiosyl residues in RG-II. Taken from Caffall and Mohnen, 2009. D. Xyloglucan-cellulose network proposed model. Taken from Park and Cosgrove, 2012b. E. Model of the macromolecular pectin structure. Adapted from Yapo, 2011. F. Primary cell wall model from *Arabidopsis* leaf. Taken from Somerville et al., 2004.

1.2 Cotton fibres

Cotton is one of the most important textile fibres with around 25 million metric tonnes produced each year (International Cotton Advisory Committee, ICAC). The genus Gossypium spp. includes approximately 50 species and four of them (*G. barbadense, G. hirsutum, G. arboreum and G. herbaceum*) have been domesticated for cotton fibre production. Two of these cultivated species - *G. hirsutum and G. barbadense* - are allotetraploids (AADD) resulting from the natural hybridization of two parental diploid lineages (the A and D genome groups) that probably occurred during the Cretaceous period (Wendel and Cronn, 2002). Efforts are being made towards the full sequencing of the cotton genome and the D genome from *G. raimondii* (Wang et al., 2012) and the A genome from *G. arboreum* (Li et al., 2014) have been recently completed.

The *G. hirsutum* Upland cotton variety by itself accounts for 90% of the world cotton production. The second species in importance is *G. barbadense*, whose Egyptian, Sea Island and Pima varieties are known for their fineness and their extraordinary length and tensile strength. This species provides around 8% of the total production (Harzallah and Drean, 2011). During the 2013/14 season the worldwide cotton production reached 24.05 million metric tons (approximately 110.46 million bales in the US system) (International cotton advisory committee, ICAC). China is the largest producer and consumer followed by India and USA and just the three of them account for the 60% of the total production (ICAC). In March 2011 the price of cotton hit a record at 103.9 U.S cents/kg, while the average price since 2012 has been 41.3 U.S cents/kg (IndexMundi) and the projection for 2015 is estimated around 31.7 U.S cents/kg (ICAC). The recent lower prices have caused cotton production to fall and it is predicted that consumption may surpass production in 2015/2016 (ICAC). The volatility of this market is partially due to the high demand of China, which has pushed up other world markets in the past years and the uncertainty about the Chinese government cotton stock policy in the near future.

Several environmental issues are associated with the cultivation of cotton. On one hand cotton plants require profuse irrigation using much of a region water resources, on the other, cotton is very supceptible crop to several phatogens like pink bollworm which requires the extensive use of pestides that contaminates groundwater and affect other non-target species. In 1996, BtCotton started to be commercialized by Monsanto with the aim to increase cotton production. This transgenic cotton was resistant to most of the major cotton pests (such as tobacco budworms, cotton bullworm, pink bullworms). The technology was based on the *B. thuringiensis* ability to produce the insecticidal crystal proteins. The use of Bt cotton has remained controversial ever since due to Monsanto commercialization politics and the recently discovered resistance of bullworms to Bt cotton after farmers have been cultivating crosses of Bt cotton with non-Bt cotton (Tabashnik et al., 2013).

The cotton industry is vast and the use of cotton fibres span from all sorts of textiles to paper currency, cosmetics, sanitary products, furniture upholstery and many more. Therefore the study of the biology behind the distinctive fibre properties and quality has become of interest to the agro business sector and crop science institutions. But cotton fibres are not only important for textile and derivative industries, they also represent an exceptional single-cell model to study cell wall synthesis and cell elongation (Haigler et al., 2012).

1.2.1   Cotton fibre cell wall development

The first floral buds are detectable 50 days after seed germination, flowering (anthesis) occurs between 61 and 67 days after germination and cotton boll opening usually takes place during day 80 to 90, although this is highly influenced by temperature and other environmental factors (Munger et al., 1998). The flower ovary encloses 4/5 carpels (locules) which normally contain 8 seeds (ovules) and each ovule generates approximately 14,500 lint (long) fibres (Bowman et al., 2001).

Cotton fibres start elongating at the day of anthesis and fibre growth lasts between 50 and 60 days depending on environmental conditions and germplasm. Fibre development is a finely regulated process usually divided into five sequential and overlapping events: initiation, elongation, transition, secondary cell wall synthesis and desiccation (often misleadingly referred as maturation) (Figure 1-11). A mature fibre is composed of nearly 95% cellulose, however, cellulose only accounts for approximately 35-50% of the primary cell wall of expanding fibres (Tokumoto et al., 2002) and therefore, other matrix polysaccharides are the major components of the cell wall. These are pectins, non-cellulosic glycans and glycoproteins.

These cell wall polymers and glycoproteins undergo active synthesis, modification and turnover during fibre development. The coordinated function of these polymers and glycoproteins is essential for proper fibre development and is a determinant in the final fibre properties.
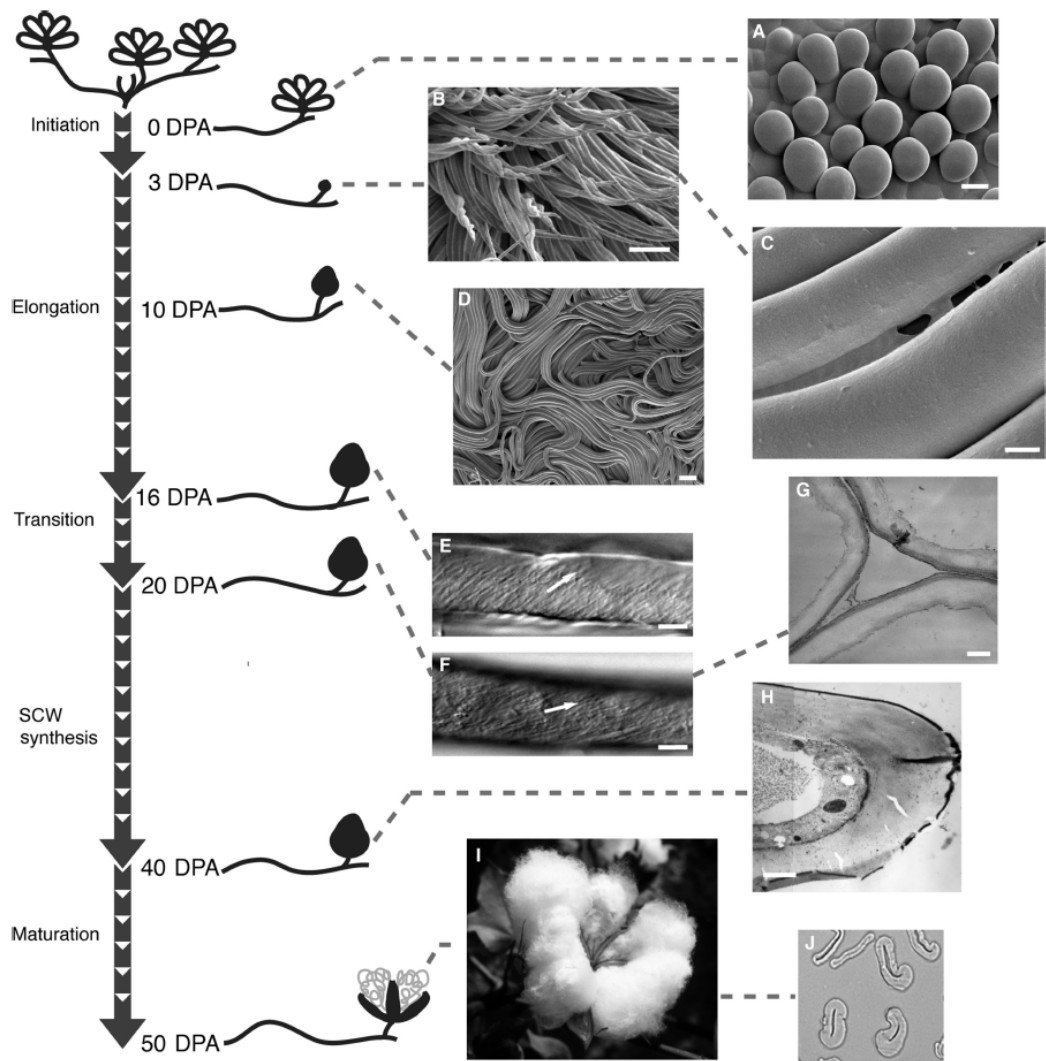
Figure 1-11. Cotton fibre developmental stages. A. Cryo-field-emission SEM of fibre initials on the ovule surface (bar=10µm). B. 3 days post anthesis (dpa) fibres (bar=100µm). C. CFML stretched between two 3 dpa fibres (bar=4µm). D. Ordered bundles of fibres inside the boll (bar=100µm). E, F. Differential interference contrast micrographs indicating microfibril angle (as highlighted by arrows) in fibre at 16 dpa (E) and 20 dpa (F) (bars=10 µm). G, H. TEM fibre cross-section show early stage of secondary wall thickening (G) (bar=300nm) and a more advanced stage of secondary wall deposition (bar=1 µm) (H). I. Mature cotton boll. J. Cross-section of mature fibre viewed in the light microscope. SCW, secondary cell wall. Taken from (Haigler et al., 2012), original from The Cotton Foundation (http://www.cotton.org/foundation/index.cfm).

The timing of these developmental events and the final fibre qualities vary between germplasms and are also largely influenced by temperature cycles during fibre growth (Thaker et al., 1989; Roberts et al., 1992; Liakatas et al., 1998). The features of fibre development are usually defined by dpa and for the commercial *G. hirsutum* line are as follows:

Fibre initiation takes place from 0 to 5 dpa when selected epidermal cells emerge from the seed surface forming the fibre initials (Figure 1-11 A). Fibre density can be up to 1,300 fibres/mm2 (Paiziev and Krakhmalev, 2004) and the fibre initials: total epidermal cells ratio is 1:3.7 at anthesis (Stewart, 1975). The fibre diameter is determined during this stage and it usually ranges between 11 and 22 µm (Paiziev and Krakhmalev, 2004; Wilkins and Arpat, 2005).

Vaughn and Turley (1999) found two distinctive electron opaque layers in the primary cotton cell wall of 2 dpa fibres. Using anti-PGA (de-esterified pectin) and anti-xyloglucan antibodies, they showed that only the de-esterified pectin antibody bound to the outer layer whereas xyloglucans were only found in the inner layer (Vaughn and Turley, 1999). A more detailed analysis on polysaccharide and glycoprotein distribution with a broader set of antibodies during fibre initiation has been recently carried out (Bowling et al., 2011). This work corroborated the presence of a pectin sheath pointed out by Vaughn and Turley (1999) and also showed a change in the pectin and AGP components in the primary cell wall of cotton fibres up to 3 dpa. No presence of homogalacturonan with low degree of esterification (JIM5) was detected in any cell of the epidermal layer; however the JIM5 epitope was recognized in fibres at 2 dpa. The 1$\rightarrow$5 arabinan side chain on RG-I was detected by LM6 all over the ovule epidermis, but recognition by LM5 of the 1$\rightarrow$4 galactan side chain only appears in cotton fibre at 2 dpa, suggesting an important role of galactan in fibre elongation. Interestingly, AGP detection (CCRC-M7 antibody) is observed in 1 dpa epidermal cell but is no longer present in 2 dpa fibres (Bowling et al., 2011).

Fibre elongation starts at around 3 dpa and can last for 15 days. Cotton fibres acquire a conical tip shape and start elongating in groups in a spiral-

like manner gathered in bundles by the cotton fibre middle lamella (CFML). Although cotton fibres were thought as independent cells during the elongation process, Singh et al. (2009) suggested the existence of a specialized outer layer of the primary cell wall that can join several fibres together into a tissue-like bundle (Figure 1-11 C). The cotton fibre is a tissue with connectivity between cells by the CFML but it is not a tissue during all its development. The middle lamella in the cotton fibre does not originate from the cell plate formed after cytokinesis since each fibre elongates from one epidermal seed cell and no cell division occurs. Thus, the CFML originates upon cell contact at the beginning of cell elongation and it is degraded after elongation. This middle lamella contained xyloglucans (CCRC-M1 antibody) and was enriched with de-esterified HG (JIM5 antibody) (Singh et al., 2009). The functions of the CFML include to optimise the space inside the very packed environment of the locule facilitating elongation inside the boll and probably the maintenance of the high turgor pressure needed for rapid cell elongation (Paiziev and Krakhmalev, 2004; Singh et al., 2009). As fibres grow, they turn and fold over themselves thanks to the CFML (Figure 1-11 D) until the secondary cell wall deposition starts; it is only then that the CFML is degraded.

It is not clear how cotton fibres elongate as they share and lack characteristics of both the tip and the diffuse growth mode (Qin and Zhu, 2011). Elongating cotton fibres share the transversal orientation of cortical microtubules with respect to the direction of elongation observed in the diffuse growth (Seagull, 1992), but lack the organelle concentration at the tip of the cell that occurs in tip growing cells such as pollen tubes (Ruan, 2007). On the other hand, a Ca^{2+} gradient was found at the tip of elongating fibres (Huang et al., 2008) and an increase of reactive oxygen species (ROS) and enzymes involved in ROS metabolism were important during the elongation process (Mei et al., 2009) similar to that observed in the tip growth.

By 17-20 dpa, the transition phase occurs and it is defined as the end of elongation and the beginning of secondary cell wall deposition. Fibres do not stop elongating abruptly, elongation slows down around 17 dpa but goes on

for several days simultaneously with secondary cell wall deposition (Schubert et al., 1976) and this final elongation is believed to be achieved through tip growth since the rest of the fibre cell wall is locked in place when the secondary cell wall starts to be deposited (Haigler, 2010). Haigler (2010) also suggested that fibres end elongation by somehow sensing fibre weight as cultured fibres grown at lower temperature delay their secondary cell wall deposition until they achieve their full length potential (Haigler et al., 1991).

The transition phase is characterized by an abrupt increase in the rate of cellulose synthesis (Meinert and Delmer, 1977) and the formation of the winding layer (similar to the S1 layer in xylem vessels) which is the first of the secondary cell wall layers to be deposited. The cellulose microfibrils in the winding layer are orientated to an angle of 20-30° (Figure 1-11 E) to the elongation axis and in opposite helical gyre to the next secondary cell wall layer where cellulose microfibrils are placed at a 70° angle (Figure 1-11 F) to the elongation axis (Flint, 1950). The winding layer confers a significant degree of the final fibre strength (Stiff and Haigler, 2012). More layers of cellulose are formed during the secondary cell wall deposition stage (Figure 1-11 H), each one with a steeper helical gyre compared to the previous outer layer. A peculiar feature of cotton fibres is the change of direction of cellulose microfibrils called reversals (Flint, 1950; Yatsu and Jacks, 1981; Seagull, 1986), which happens several times along the fibre.

Extensive cell wall remodelling takes place during fibre development. Changes in terms of monosaccharide composition, degree of polymerization of cellulose and changes in the molecular weight of pectic fractions and xyloglucan have been reported (Meinert and Delmer, 1977; Timpa and Triplett, 1993; Tokumoto et al., 2002).

The changes in the primary structure of cell wall polysaccharides are associated with the variation in molecular weight (MW) and degree of polymerization (DP) throughout fibre differentiation. In general, it has been observed that the primary cell wall during the first developmental stages is composed of polymers with lower molecular weights (MW) (ca. 140,000 Da) than those present in the mature fibre (ca.2,250,000 Da) (Timpa and Triplett,

1993). This represents the overall tendency, which is highly biased by cellulose polymerization, indeed a more dynamic trend is observed when looking at particular polysaccharides:

The amount of cellulose increases continuously during development and the cellulose production rate is remarkably higher after the elongation stage is finished. Cellulose molecules with high DP is found in 8 dpa fibres; however the range of cellulose DP during this initial stage is rather broad (Tokumoto et al., 2002). During the secondary wall formation this wide DP range of cellulose polymers is narrowed and in mature fibres most cellulose molecules reach a high degree of polymerization (DP=10,650) (Timpa and Triplett, 1993; Tokumoto et al., 2002). Callose (β-1,3-glucans) increases alongside with fibre elongation and decrease thereafter (Tokumoto et al., 2002), which is in accordance with the findings of Ruan et al. 2001 about callose deposition and its possible role in elongation through plasmodesmata closure.

Tokumoto et al. (2002) also showed that the amount of xyloglucan increases early in development and decrease after cessation of elongation. Moreover, the amount of xyloglucan drops off after elongation whereas the overall xyloglucans molecular weight decreases from 12 to 17 dpa in first place to then increase after fibre elongation (between 17-28 dpa). This variation in the xyloglucan structure has been correlated to cell wall loosening that would allow rapid fibre growth.

The presence of heteroxylan has not been explore in detail. Glycan microarray analysis indicated small quantities of the LM10 and LM11 xylan epitopes in an alkali extract of developing fibre cell walls (Singh et al., 2009; Avci et al., 2013) and only cotton linters xylan has been analysed by NMR (Kim and Ralph, 2014).

Little information can be found about heteromannan in cotton fibres. The monosaccharide mannose was long ago detected in cotton fibres (Meinert and Delmer, 1977), and incorporation of radioactivity from GDP-Man was shown to be correlated with that from GDP-Glc in particle fractions at the

primary cell wall stage (Buchala and Meier, 1985). However, the analysis of these radioactive products was not explicitly related to heteromannan polysaccharide and no direct evidence of its presence in the cotton fibre cell wall has been reported so far.

The amount of galacturonic and rhamnose containing sugars increased during elongation and decreases during secondary cell wall formation. Conversely, the molecular mass in the pectic fraction increased throughout development, particularly during the secondary wall thickening phase (Tokumoto et al., 2002). These sugars are the backbone components of pectin suggesting a general enlargement of the pectic macromolecule. On the other hand, the amount of arabinan and galactose sugars (main components of RG-I side chains) is considerably higher in the early elongation stages than during the transition phase (between 17 to 28 dpa); and their MW decrease during elongation (Tokumoto et al., 2002). This correlates with the data from Singh et al. (2009), in which the RG-I galactan probe disappeared at the transition phase, suggesting again that galactan RG-I side chain plays a key role during fibre elongation and that RG-I turnover is related to cessation of elongation.

The degree of HG esterification is of major importance during elongation. A lower pattern of pectin esterification in cotton fibres when compared to other plant cell walls is noticeable (Mort et al., 1993). Low pectin esterification has been related to cell wall loosening and fibre elongation as it is needed by cotton pectate lyase to degrade pectin. Pectin degradation would loosen the cell wall promoting cell elongation. In fact, maximum transcription rate of the pectate lyase gene was found at 10 dpa, when the highest elongation rate takes place (Wang et al., 2010). Moreover, antisense *GhPEL* transgenic lines were deficient in pectin degradation which impaired cell wall loosening and consequently reduced fibre elongation (Wang et al., 2010).

Cell wall proteins like AGPs and expansins also modulate fibre elongation. Although β-Yariv reagents do not affect cell wall extensibility directly (Seifert and Roberts, 2007), suppression of the FLA gene *GhAGP4* by RNAi inhibits elongation and affects cytoskeleton polymerization and cellulose distribution

(Li et al., 2010). Six different α-expansins from *G. hirsutum* have been characterised and *GhExp1* is highly expressed only in elongating fibres, evidencing a significant role of expansins during elongation (Harmer et al., 2002). Recently, the expansin *GbEXPATR* (truncated homolog of *GbEXP2*) has been reported to be specific of *G. hirsutum* whose overexpression results in longer fibres and had a drastic effect on cell wall reorganization (Li et al., 2015).

Cell wall loosening is crucial for cell wall expansion, but other factors, like high turgor pressure and cytoskeleton rearrangements, are also indispensable during this phase. Plasmodesmata connect the epidermal ovule cells with the fibres at the cell base. Previous studies have suggested that plasmodesmata closure during the elongation phase greatly influences the final length of cotton fibres (Ruan et al., 2001). Callose is known to be deposited around plasmodesmata to regulate their aperture (Zavaliev et al., 2011). Cell turgor during elongation is maintained by the enhanced expression of membrane transporters genes observed by Ruan *et al.* (2001) that promotes the uptake of osmotically active solutes, while plasmodesmata closure avoids water loss. Moreover, callose has been detected by immunolabelling at the fibre base around plasmodesmata closed pores, evidencing yet again a direct implication of callose in plasmodesmata closure and consequently in the elongation process (Ruan et al., 2004). With this regard, the callose degrading enzyme, callose glucanase, would be an interesting target in future studies for genetic quality improvement.

Sucrose synthase (SUS) enzyme also plays an important role during elongation, as it releases glucose monomers that will form polysaccharides during cell wall synthesis. In fact, a recent study has shown that overexpression of a potato sucrose synthase in cotton improved fibre length (Xu et al., 2012). Similar effects to those of the sucrose synthase have been found for the vacuolar invertase in cotton (Wang et al., 2010), opening new doors for genetic cotton improvement. Many efforts have been directed to reveal differential expressed genes during cotton fibre development (Samuel Yang et al., 2006; Lee et al., 2007; Iqbal et al., 2008) and their effect on cell

elongation and secondary wall formation (Gou et al., 2007). These studies have provided helpful genetic information to create transgenic cotton lines aiming to improve fibre quality and properties (Arioli, 2005; Haigler et al., 2005; Al-Ghazi et al., 2009).

Around 55 days after flowering the boll opens, <u>fibres desiccate</u> and become suitable for harvest (Figure 1-11 I). Over 95% of the mature cotton fibre dry weight is cellulose and they can reach 3-5 cm long and they acquire a twisted conformation when they desiccate, an essential feature of fibres so that they can be spun into yarns. This conformation is due to the way the cellulose is deposited in secondary cell wall as this polymer accumulates in layers with different deposition angles that cause the fibre to twist. At the final stage the secondary cell wall can be around 4 µm thick (Kim and Triplett, 2001). The remaining outer primary cell wall that surrounds the secondary wall is a thin layer of approximately 200 nm (Singh et al., 2009) and a cross section of a fibre has the appearance of a horse shoe (Figure 1-11 J). During this final stage the boll opens and cotton fibres are finally exposed to air and desiccate (transition from mobile to highly hydrogen-bonded structure) it is then when fibres are collected and the industrial process takes places to convert them in all sorts of items.

1.2.2 Textile manufacturing process – from fibres to clothes

Cotton manufacturing processes consists of four principal steps: yarn formation, fabric formation, wet processing and finishing. To produce cotton yarn, seeds are removed in a process called ginning and fibres are organized into slivers and prepared for spinning. Fibre spinning is carried out in one of these common systems: the traditional ring spindle, a rotor spinner or the modern an air-jet spinner (Basra, 2000; Gordon and Hsieh, 2006). Yarns are then interlaced into fabric by weaving or knitting depending on the final application (Gordon and Hsieh, 2006). The ability of a fibre to produce a good yarn depends on the fibre characteristics, for example a finer fibre would produce a stronger yarn than coarser fibres as more fibres will fit in a given yarn section. Also, stronger fibres but not too rigid would obviously

produce stronger yarns, a feature that is very desirable to the textile industry as fibre can be then processed in very high–speed spinning rotors and can withstand harsh anti-wrinkle treatments (Stewart et al., 2010).

The wet processing or finishing consists on chemical treatments that adds value to the raw fabric to meet specific product requirements. The most common finishing treatments are scouring where the fabric is boiled in an alkali solution to remove impurities, bleaching with an oxidazing agent to remove natural cotton pigmentation or just increase whitening, mercerizing which is an alkali bath that swells cotton fibres and increases dyeability by lowering the cellulose crystallinity order (Stewart et al., 2010) and dyeing and printing (Gordon and Hsieh, 2006; Babu et al., 2007). The efficiency of these treatments to generate better end products also depends on the initial fibre characteristics. For example, a fibre with thicker secondary cell wall has increased dyeability as there is more cellulose per unit area for the dye to bind as far as the fineness of the fibre is not compromised. Several strategies have been followed to obtain cotton fibres with improved dyeability (Blackburn and Burkinshaw, 2003; Blackburn and Harvey, 2004; Ceylan et al., 2013) as this is one of the most costly and environmentally harmful steps of textile manufacturing since it requires the use of vast amounts of water and the need to treat dyeing effluents (Blackburn, 2004; Babu et al., 2007).

In summary, the suitability of a fibre for industrial use is determined by its quality which depends on mature fibre characteristics such as fineness, strength and secondary cell wall thickness.

1.2.3 Fibre quality

Fibre quality is an ambiguous term since not only depends on germplasm but also on environmental conditions that affect fibre development and the final fibre characteristics (see 1.2.4). Fibre quality is commonly denoted as the fibre fitness for textile processing. From the point of view of a physiologist fibre quality comes from the potential of a germplasm to cope with adverse environmental conditions, which then links to the cotton farmers and manufacturers idea of better fibre quality which means

reduction in production costs. In any case, fibre quality is defined based on a system of standardised measurements established in the U.S by the USDA-AMS.

The most widely used method to measure cotton fibre characteristics is the high volume instrument (HVI) developed in 1969 by the USDA (U.S. Department of Agriculture) which can determine fibre quality indexes such as the fibre quality index (FQI) and spinning consistency index (SCI), used to define the industrial value of a cotton sample and, in the long term, to direct cotton breading or direct genetic engineering fibre (Suh and Sasser, 1996; Majumdar et al., 2005). Another instrument developed in the 80s to obtain fibre quality measurements is the Advanced Fibre Information System (AFIS). The main difference with the HVI method is that AFIS provides individual fibre measurements and gives more detailed data such as fibre length distributions in a given sample. Although no significant difference was found as to generate useful information for fibre quality improvement with the final conclusion that either method might be used for that purpose (Kelly et al., 2012).

Only the fibre properties of micronaire, length, length uniformity, short fibre content, strength, elongation, reflectance degree and yellowness using the HVI method has been studied in this project. A brief explanation of the fibre characteristics taken into account and their impact on fibre quality is included here as a summary from several articles published on cotton/textile specific journals and books (Suh and Sasser, 1996; Montalvo, 2005; Incorporated, 2013; Rieter, 2015).

1.2.3.1 Micronaire

The micronaire value is obtained by measuring the resistance to an airflow of a mass of cotton when it is compressed to a fixed volume and depends on the fibre fineness and maturity (Montalvo, 2005; Montalvo et al., 2006). The finer the fibre, the lower the micronaire for a given fibre maturity (cell wall thickness) since the resistance to the airflow will be higher due to a higher surface area of the sample. Breeders and cotton manufacturers select fibres

with a micronaire between 3.8 and 4.5, as fibres that do not fall in this range cause problems for spinning and dyeing.

1.2.3.2 Length

Before measuring fibre length by an optical device, a weight of fibres are held, combed and brushed to unclamp, and smooth fibres in a parallel disposition (Suh and Sasser, 1996). Several length measurements are acquired with the HVI method. Upper half mean length (UHML) is the average length of the longest half when divided by weight and mean length is the average length that can be expressed by weight or by fibre length. Length uniformity index (UI) is the ratio of the mean length divided by the upper half mean length usually expressed as a percentage. Short fibre content (SFC) is directly related to length uniformity and is express as the percentage by weight of fibres in the sample that are less than 12.7 mm in length. More measurements are obtained with HVI and are reviewed elsewhere (Suh and Sasser, 1996). Fibre length and fibre length uniformity affect yarn strength and how fine a yarn can be made as well as the efficiency of the spinning process.

1.2.3.3 Bundle strength

HVI determines fibre strength by measuring the force required to break a fibre bundle in two and is expressed as grams-force (g/tex). A tex unit is the weight in grams of 100 meters of material. Fibres can be very strong (31 g/tex and over), strong (29–30), average (26–28), intermediate (24–25), or weak (23 and below). Bundle strength correlates with yarn strength and this is a desirable quality so that fibres can endure manufacturing process with minimal breakage.

1.2.3.4 Elongation

Fibre elongation is related to fibre strength and corresponds to the maximum stretch that can be attained by a fibre bundle before breaking. It is usually indicated as the percentage of the starting length and for cotton fibres is class as very low (below 5.0%), low (5.0-5.8%), average (5.9-6.7%), high (6.8-7.6%) or very high (above 7.6%). Fibre elongation is a very important

quality as it accounts for the elasticity of the end textile product which is directly related to textile creasing, however, high elongation also makes the spinning process more complicated.

1.2.3.5 Reflectance degree (Rd) and yellowness of fibre (+b)

HVI systems can also measure the colour of a given sample with a colorimeter in which a pressed fibre sample is illuminated and the light reflected through a yellow and blue filter is measured. The light from the blue filter measures the reflectance degree (Rd) or in other words, the brightness or greyness of the sample. The yellowness of the fibre (or degree of pigmentation) is computed from the amount of light that passes through the blue and yellow filter. Although the fibre colour is less relevant to the manufacturing processing, it has been observed that deterioration of fibre colour either environmentally during growth or by storage conditions can affect dying efficiency (Hughs et al., 2011).

In summary, good fibre length, strength and micronaire values are essential in a high quality fibre and are desirable characteristics to target in programmes for cotton quality improvement either by selective breeding or direct genetic intervention. Nonetheless, cotton fibres that do not meet textile standards find their niche market in applications other than clothing, like cosmetics, paper and construction materials.

Examples of excellent fibre quality is the Pima variety from the *G. barbadense* species, also known as Egyptian cotton. Another example of excellent fibre is FiberMax (FM) (*G. hirsutum*), important variety of the commonly named Upland cotton, and produced by Bayer CropScience under the FiberMax® brand name. FibreMax is commercialized worldwide as not only produces high quality fibres but also has very good yields and disease resistance. In this work, six different cultivars have been studied PimaS7 and China10 (*G. barbadense*), FM966 (*G. hirsutum*), Krasnyj (*G. herbaceum*), 30834 and JFW15 (*G. arboreum*).

1.2.4   Factors influencing fibre quality

The fibre physiology is mostly determined by genotype but the developmental process is regulated by hormones and other environmental factors that might result in lower or higher quality fibres. In particular gibberellic acid and auxin are vital for fibre development and successful fibre initiation in unfertilized ovules depends on the presence of these hormones (Gialvalis and Seagull, 2001) and a precise balance of these and other hormones is indispensable for appropriate fibre development. The effects of hormonal treatments in the correct development of cotton fibres in cultured cotton have been extensively studied in the 70s and 80s (Beasley and Ting, 1973; Dhindsa, 1978) and are reviewed in Kosmidou-Dimitropoulou and Board (1986) and more recently (Stiff and Haigler, 2012). New targets to improve cotton quality are being explored, such as the expression of the auxin gene iaaM that increases fibre lint yield in more than 15% and improved fibre fineness (Zhang et al., 2011). Targeting hormonal regulation is an example of alternatives to conventional breeding that are not fully exploited yet.

Environmental variations during plant growth might modulate fibre development not allowing the fibre to fully develop its genetic potential. Temperature, water availability, mineral nutrition and pests have a significant effect on the final fibre length, strength and maturity (reviewed by Bradow and Davidonis (2000); Bradow and Davidonis (2010)). Temperature is one of the major environmental factors influencing fibre development. Lower temperatures decrease the elongation rate while increasing the time in the elongation phase (Gipson, 1986). *G. hirsutum* plants grown at different day/night temperatures showed that fibre length increased with temperature up to 22°C to decline afterwards, while micronaire and uniformity increased up to 26° and strength increased linearly with temperature (Lokhande and Reddy, 2014). The thickness of the secondary cell wall is largely affected by temperature. Cool night temperatures slow down cellulose deposition during secondary cell wall phase which can be observed as rings in cross sections

of swelled fibre due to the lower rate of cellulose deposition between day and night in cultured ovules (Haigler et al., 1991).

Other factors like the retention of bolls and the plant canopy architecture (associated with irrigation and light conditions) have an effect on the production and distribution of metabolic resources and are linked to variations in fibre micronaire and strength (Pettigrew, 2001).

In a more subtle way, fibre characteristics such as length and maturity can also vary depending on the seed location with respect to the boll and locule as well as the boll position in the same plant. Fibres from seeds at the apical or basal ends are shorter that the middle ones and seed at the apex produce less mature fibres than those at the basal end (Bradow and Davidonis, 2000). Similarly, fibres from bolls located at lower and higher nodes usually have reduced quality fibres than those in the middle part (Bradow and Davidonis, 2010). Moreover, harvest and post-harvest methods can also influence fibre quality, for example increasing the short fibre content with the use of machinery during the harvesting, ginning and lint cleaning (Bradow and Davidonis, 2000).

The success of breeding programmes looking for better quality fibres relies on the understanding of how a newly obtained genotype can perform in a selected environment. However many are the factors to take into account and the use of specific software developed to simulate and predict the effect environmental variation on fibre quality at even the fruit boll level is becoming very useful (Gu et al., 2014; Wang et al., 2014).

1.3 Summary and thesis aims

Cotton fibres are single cells that start elongating at the day of anthesis from selected seed epidermal cells. During fibre development four main sequential events occur: fibre initiation, elongation, transition to secondary cell wall thickening and cellulose deposition. In *G. hirsutum* fibre elongation lasts for up to 20 (dpa) and the fibres can reach 3 cm long. At approximately 20 dpa fibre elongation deceases and cellulose deposition in the secondary wall begins. The cotton fibre has an extraordinary capacity for cell elongation and secondary cell wall synthesis. Cellulose is the major component in mature fibres, however the amount and structure of other non-cellulosic polysaccharides in the primary and secondary cell wall of expanding fibres is finely regulated during development. The aims of this thesis project are:

- To clarify whether specific changes of the non-cellulosic are likely to differ between cotton lines and species and whether this changes make mature fibres more or less suitable for manufacturing processes (thesis objectives 1 and 2 below)
- Identify and describe the specific biochemical changes in the non-cellulosic glycan composition of developing cotton fibres from several cultivars and correlate their abundance and immunolocalization to fibre quality (thesis objectives 3 and 4 below).

1.4 Thesis objectives

The main objective of this thesis was to describe the genotypic variance of the non-cellulosic polysaccharides in the cotton fibre cell wall during development by comparing:

1. The developmental pace followed by six different cotton cultivars grown in equal environmental conditions based on cell adherence, secondary cell wall thickness and fibre detachment.
2. The monosaccharide and linkage composition of fibres during development in these cultivars.

48

3. The relative abundances of non-cellulosic glycan epitopes using mAbs and CBMs during fibre development in these cultivars and the correlation of the glycan epitope dynamics and fibre quality during the elongation and secondary cell wall thickening phases.

4. The *in-situ* localization of non-cellulosic glycan epitopes in developing fibres and functional relationships in regard to developmental stage and germplasm.

Further objectives that arose during the project included the study of potential interactions between cell wall polymers and the binding specificity of glycan-directed probes.

Chapter II

2 Materials and methods

2.1 Plant materials

Plant materials used in experiments included in Chapter 3 and 4 are cotton fibres from FM966-FibreMax® cotton plants sown in soil compost and grown in greenhouses at University of Leeds. The sowing was done in three batches where the greenhouse temperature was set at 20-25°C ("Batch 1") and 28-32°C ("Batch 2") both with a 18 h photoperiod. Cotton fibres from six domesticated inbred cotton lines (FM966-FibreMax®, JFW15 and 30834, Krasnyj, China10 and PimaS7) belonging to four different *Gossypium* species (*G. hirsutum, G. arboreum, G. herbaceum, G. barbadense*) and a mutant cotton line overexpressing cellulose synthase-like (CSLC4) and a xyloglucan 6-xylosyltransferase (XXT1) from *Arabidopsis thaliana* under the control of a fibre specific promoter in a Cooker (*G. hirsutum*) background. Seeds were sown in soil compost to which 30 g of Osmocote® 11N+11P+18K+ 2MgO +TE (working duration 5-6 months) was added to each pot and grown at Bayer Cropscience, Ghent. The settings for the day temperature were 24-26°C and temperature increased with warm weather up to 30-35°C with a 16 h photoperiod, except when outside light was >15 klux. Biological agents to control cotton insect pests included: *Aphidius colemani* against aphids, *Amblyseius Swirskii and Orius spp.* against thrips and *Amblyseius californicus* against spider mite. All cotton flowers were tagged on the day of anthesis so that bolls could be harvested at the desired dpa. Immunolabelling experiments of tobacco seeds overexpressing ST-YFP and Syp61-YFP included in Chapter 5 were grown in 2-(N-morpholino)ethanesulfonic acid (MES) media for 4 and 5 days at 26°C in agitation before fixation of whole seedlings in 4% (v/v) formaldehyde.

2.2   Preparation of cell wall materials

For the study of cell wall components by glycan microarrays, GC and GC/MS analysis, cotton bolls were frozen in liquid nitrogen immediately after collection and fibres from at least three different plants were detached from the seeds, pooled and boiled in 70% (v/v) ethanol for 30 min, air-dried and powdered using a nitrogen-cooled crusher (SPEX Sample Prep Freezer/mill 6870).

Alternatively, fibres stored at -80°C were freeze-dried before pulverization. 10 mg (dry weight) of each sample were lysed following the manufacturer's protocol in a TissueLyser LT (Qiagen) using 2 ml sample tubes RB (Qiagen) and 5 mm diameter stainless steel beads (Qiagen). For developing fibres up to 21 dpa 6 min at 50 Hz was enough to obtain a fine powder, for 30 DPA fibres 15 min were needed.

2.3   Preparation of cotton fibre exudate

The pericarp layers of 7 and 10 dpa cotton bolls were peeled and undisrupted seeds as found in each locule were placed into a tube containing water or phosphate buffer saline (PBS) and incubated for 3 h or overnight in a rotor. All seeds and fibres from one boll were incubated in 10 ml of water or PBS. After incubation seeds were removed and the liquid briefly spun to eliminate detached fibres pieces. The water or PBS liquid, named as fibre exudate, was aliquoted and snap-frozen in liquid nitrogen and stored until further use. 50 µl of the exudate were directly used in magnetic bead-assisted immunoprecipitation and 25 µl were injected for EDC experiments.

2.4   Cell wall extractions

Cell wall material from pulverized fibres (10 mg) was extracted sequentially with dH2O at room temperature (RT) for 2 h on a rocker followed by centrifugation at 12,000 g for 10 min. The supernatant was recovered and

stored at -20°C and the pellet re-suspended in 50 mM cyclohexanediamine tetraacetic acid (CDTA) for pectin extraction following the same procedure. A final cell wall polysaccharide extraction was done with 4 M NaOH + 1% (w/v) NaBH4 and the supernatant was neutralized with 80% acetic acid (all extraction volumes were 1 ml). Cell wall extracts were aliquoted and stored at -20°C

2.5 Monoclonal antibodies (mAbs) and carbohydrate-binding modules (CBMs)

Both resin sections and intact mature fibres were used for light microscopy detection of cell wall epitopes using a range of monoclonal antibodies and carbohydrate binding molecules (CBMs) that are described in Table 2-1.

Table 2-1. List of monoclonal antibodies and CBMs used		
mAb	Epitope	Reference
Anti-callose		
BS400-2 or LAMP2H12H7	(1→3)-β-glucan	(Meikle et al., 1991)
Anti-mannan		
LM21	Galacto-gluco-mannan	(Marcus et al., 2010)
LM22	Galacto-gluco-mannan	(Marcus et al., 2010)
BS400-4 or BGM C6	Galacto-gluco-mannan	(Pettolino et al., 2001)
Anti-xyloglucan		
LM15	XXXG motif of xyloglucan	(Marcus et al., 2008)
LM24	XXLG	(Pedersen et al., 2012)
LM25	XXXG/XLLG	(Pedersen et al., 2012)
CCRC-M1	Fucose containing xyloglucan	(Puhlmann et al., 1994)
Anti-xylan		
LM10	(1→4)-β-D-xylan	(McCartney et al., 2005)
LM11	(1→4)-β-D-xylan/arabinoxylans	(McCartney et al., 2005)
INRA-AX1	Arabinoxylan	(Guillon et al., 2004)
INRA-UX1	Glucuronoxylan	(Koutaniemi et al., 2012)
Anti-HG		
LM18	Partially Me-HG/no ester	(Verhertbruggen et al., 2009)
LM19	Partially Me-HG/no ester	(Verhertbruggen et al., 2009)
LM20	Partially Me-HG	(Verhertbruggen et al., 2009)
JIM5	Partially Me-HG/no ester	(Willats et al., 2000; Clausen et al., 2003; Manfield et al., 2004)

JIM7	Partially Me-HG	(Willats et al., 2000; Clausen et al., 2003; Manfield et al., 2004)
Anti-RG-I		
LM5	(1→4)-β-D-galactan	(Jones et al., 1997; Willats and Knox, 1999)
LM6	(1→5)-α-L-arabinan	(Jones et al., 1997; Willats et al., 1998; Willats and Knox, 1999)
LM13	Linearised (1→5)-α-L-arabinan	(Moller et al., 2008; Verhertbruggen et al., 2009)
LM16	Processed arabinan	(Verhertbruggen et al., 2009)
LM17	(1→5)-α-L-arabinan	(Verhertbruggen et al., 2009)
INRA-RU1	Unbranched RG-I backbone	(Ralet et al., 2010)
INRA-RU2	Unbranched RG-I	(Ralet et al., 2010)
BS400-3 or BG1	(1→3)(1→4)-β-glucan	(Meikle et al., 1994)
Anti-AGP		
LM14	AGP glycan	(Moller et al., 2008)
LM2	B-linked-GlcA in AGP glycan	(Smallwood et al., 1996; Yates et al., 1996)
JIM13	AGP glycan	(Yates et al., 1996)
Anti-extensin		
JIM20	Extensin	(Smallwood et al., 1994; Smallwood et al., 1995)
Others		
LM4	Pea amine oxidase, cell walls	(Laurenzi et al., 2001)
anti-PttXET16A	Xyloglucan endotransglycosylase	(Bourquin et al., 2002)
GFP	Green fluorescent protein	
CBM	Epitope	Reference
CBM3a	Crystalline cellulose	(Blake et al., 2006)
CBM2a	Crystalline cellulose	(McLean et al., 2000)
CBM4-1	Amorphouse cellulose	(Zverlov et al., 2001)
CBM28	Amorphouse cellulose	(Boraston et al., 2002)
CBM27	Mannan	(Boraston et al., 2003)
CBM61	β-1,4-galactan	(Cid et al., 2010)
CBM2b-1-2	Xylan	(Herve et al., 2009)
CBM22	Xylan	(Herve et al., 2009)

2.6   Determination of fibre characteristics

Fibre characteristics of length (mm), fibre uniformity (% length), strength (g/tex), elongation (%) and micronaire were determined with the High Volume Instrument (HVI) (Suh and Sasser, 1996) at the Agricultural

Research for Development-CIRAD (France) from 5 g of mature cotton of each line.

2.7 Secondary cell wall measurements

Thicknesses of secondary cell walls were measured in ImageJ using high magnification Calcofluor-White-stained cross sections of 10, 17, 25 dpa and mature fibres from PimaS7, FM966, Kranyj and JFW15 lines.

2.8 Glycan microarrays

Microarray analyses were carried essentially as described by Moller et al. (2007) but with minor modifications. Cotton fibre cell wall polymers were extracted sequentially in two solvents: 50 mM CDTA and 4 M NaOH with 1% (v/v) NaBH$_4$. For each of three replicates of each fibre at each dpa, 10 mg fibre was extracted in 300 µL of solvents. The supernatant from each extraction was printed in four replicates and four dilutions (1:2, 1:6, 1:18 and 1:54 [v/v] dilutions), giving a total of 48 spots representing each developmental stage for each solvent. Three independent prints were used for each antibody. This work was performed by Xiaoyuan Guo at the University of Copenhagen, Denmark.

2.9 Preparation of alditol acetates, partial methylation and GC acquisition parameters

Monosaccharide derivatization and partial methylation were based in the method used by Runavot et al. (2014) described below. This work was done in collaboration with Jean Luc Runavot at Bayer Cropscience in Ghent, Belgium.

2.9.1 Alditol acetates preparation

Monosaccharide derivatization was carried out based on several alditol acetate protocols (Albersheim et al., 1967; Blakeney et al., 1983; Pettolino et al., 2012). Briefly, 20 to 30 mg powdered samples, to which 250 µg of

internal standard (myo-inositol) was added, were hydrolyzed in 1 mL of 2 M trifluoroacetic (TFA) for 2 h at 120°C. Hydrolyzed samples were dried and reduced in 100 µL of 50 mg/mL sodium borohydride in 3 M ammonia for 1 h at 40°C. Excess borohydride was neutralized with 2 times 50 µL acetic acid and acetates were produced by adding 2 mL of anhydride acetic and 200 µL of 1-methylimidazole at room temperature for 20 min. The reaction was stopped by adding 5 mL of water and partitioning by the addition of 2 mL of chloroform. After washing of the chloroform phase with 5 mL of water the chloroform was transferred to a vial for injection on gas chromatography (GC).

2.9.2 Partial methylation for linkage analysis

Partial methylation was based on Ciucanu (Ciucanu and Kerek, 1984) and Pettolino (Pettolino et al., 2012) protocols with adaptations due to the high amount of cellulose in the samples: prior to the DMSO solubilisation, 20 to 30 mg of sample was boiled in water and precipitated in 70% ethanol and then dried to improve solubility of polysaccharides embedded in cellulose fibres. Finely powdered NaOH (40-50 mg) was added to the sample and stirred for 1 h. Iodomethane was added in 3 steps (respectively 150 µL, 150 µL and 200 µL) and excess iodine was removed by adding 1 mL of 0.1 M sodium thiosulfate (Allen et al., 2013). Partially methylated carbohydrates were recovered in 1 mL of chloroform and washed with 1 mL of water before being dried to continue with the monosaccharide analysis protocol at the hydrolysis step in 2.9.1.

Crystalline cellulose is very resistant polysaccharide to acid hydrolysis with 2 M TFA and therefore is only partly analysed by the methods used in this study, this particularly affects the results for older dpa. The results always refer to the extractible/accessible/hydrolysable polysaccharides that we considered as representative of the cotton fibres at these different developmental stages. These analyses detected neutral sugars only.

2.9.3 GC/MS settings

Sugars were injected using the on-column mode of injection on a Trace GC ultra with an ISQ single quadrupole GC-MS (Thermo Scientific, Belgium) and a flame ionization detector (FID) associated with a medium polarity, bonded phase DB-225 capillary column 30 m×0.25 mm×0.25 µm (Agilent, USA) using hydrogen as the carrier gas with a flow rate of 4 ml.min^{-1}. The MS transfer line was set at 240°C with 70eV electron impact ionization mode and the data from 41 to 450 m/z was acquired. The alditol acetates were separated by setting the oven to an initial temperature of 170°C, held for 0.5 min, and then ramped at 120°C.min^{-1} to 210°C, then ramped at 5°C.min^{-1} to 220°C, then ramped at 120°C.min^{-1} to 230°C, then ramped at 2°C.min^{-1} to 240°C and held for 0.5 min. The partially methylated alditol acetates were separated by setting the oven to an initial temperature of 150°C, held for 1 min, and then ramped at 120°C.min^{-1} to 180°C, then ramped at 5°C.min^{-1} to 220°C, then ramped at 120°C.min^{-1} to 240°C and held for 5.5 min.

2.10 Ovule culture

Cotton ovaries were harvested at 1 dpa or 2 dpa. Ovaries were sterilized in 70% ethanol for 5 min and washed with sterile water. All ovules of same ovary were transferred to 1 Petri dish under sterile conditions in a flow hood. Each Petri dish contained 12 ml of media Table 2-2. Ovules were culture in the dark at 28°C and media was changed every 3-5 days.

Table 2-2. Cotton ovule culture media recipe	
Microelements	M.S.medium 4 (M0238)
Macroelements	50 mM KNO3 as unique nitrogen source
	2 mM KH2PO4
	2 mM MGSO4
Vitamins	4 µM nicotinic acid
	4 µM pyridoxine-HCl
	4 µM thiamine-HCl
	1 µM myo-inositol

pH	5.0
Carbon source	100 mM glucose + 20 mM fructose
Hormones	10 µM IAA
	0.5 µM GA3

2.11 Immunochemistry and *in situ* fluorescence imaging

2.11.1   Resin embedding

Immediately after collection, small regions of fibre tissues were carefully dissected from cotton bolls, causing minimal tissue disruption, and submerged in 4% (v/v) paraformaldehyde in PEM (0.1 M PIPES pH 6.95, 2 mM EGTA, 1 mM MgSO4) buffer (Lee and Knox, 2014) for immunochemistry analysis. Fixed developing fibres were dehydrated, resin-embedded and sectioned as described previously (Lee and Knox, 2014). For whole mount surface labelling, developing fibres were teased apart and washed in PBS after fixation.

2.11.2   Mature fibre dewaxing

Mature fibres were neither fixed nor dehydrated but dewaxed before resin embedding: fibres were compressed to minimize air capture and placed inside glass jars. Solvents were used in a 75:1 ratio (v/w) and samples were vacuum infiltrated. Cotton fibres were treated with absolute ethanol for 90 min two times, followed by acetone for 60 min and ether for 60 min. Samples were left to air dry overnight. All steps were carried out under a fume hood at room temperature.

2.11.3   Enzymatic treatments

Samples were treated chemically and enzymatically prior to labelling when needed. Pre-treatments included:

- Pectin removal: 0.1 M sodium carbonate for 2 h at room temperature for removal of pectic polysaccharide methyl esters and recombinant pectate lyase from *Cellvibrio japonicus* (Megazyme) at 10 µg/ml in a 2 mM CaCl$_2$, 50mM CAPS (3-(Cyclohexylamino)-1-aminopropane

sulfonic acid) buffer, pH 10.0, for 2 h at room temperature with shaking for removal of pectic homogalacturonan Treatment with sodium carbonate de-esterified all pectins facilitating the action of the pectate lyase to remove pectin from fibre primary cell walls.

- Mannan removal: 10 μg/ml of recombinant beta(1,4)-mannanase from *Thermotoga maritima* (E-BMATM Megazyme) in 50 mM 3-(N-morpholino)propansulfonic acid (MOPS) pH 7.0 or buffer alone for 2 h at 37°C for heteromannan removal.

- Xyloglucan removal: 10 μg/ml of recombinant xyloglucanase (GH5) from *Paenibacillus* sp. (E-XEGP Megazyme) in 0.1 M sodium acetate pH 5.5 or buffer alone for 2 h at 37°C. Pectin removal was performed prior to xyloglucan when needed.

2.11.4   Standard immunochemistry procedure

Resin sections and whole mount fixed fibres were used for light microscopy detection of cell wall epitopes. PBS with 5% (w/v) milk protein was added for 30 min at room temperature to prevent non-specific binding. Primary antibodies were used at a 1:5 dilution (except for LAMP2H12H7, BGM-C6 and XET antibodies that were as specified by manufacturers) and CBMs were used at 20 μg/ml concentration in 5% milk/PBS in 5% milk/PBS for 1.5 h. Goat anti-rat, anti-mouse or ant-rat IgG Alexa Fluor488 (Life Technologies) were used as secondary antibodies in a 1:100 dilution in 5% milk/PBS and samples were incubated for 1 h. A three step labelling was carried out when using his-tagged CBMs. H1029 anti-his mouse antibody (Sigma-Aldrich) in a 1:1000 dilution in 5% milk/PBS for 1 h was used as secondary antibody and anti-mouse IgG Alexa Fluor488 (Life Technologies) in a 1:100 dilution in 5% milk/PBS for 1 h as tertiary antibody. Calcofluor White (Sigma–Aldrich) was used at 0.02 mg/ml in PBS for 5 min for visualization of cell walls. Anti-fade reagent Citifluor glycerol/PBS (Agar Scientific) was added before placing a coverslip.

Immunofluorescence imaging was performed using an Olympus BX61 microscope (http://www.olympus-global.com/) equipped with epifluorescence irradiation. Micrographs were obtained with a Hamamatsu ORCA285

camera (Hamamastu, http://www.hamamatsu.com) and PerkinElmer Volocity software. All related and comparative micrographs were captured using equivalent settings, and relevant micrographs were processed in equivalent ways for the generation of datasets.

2.11.5   Dual-labelling

Purified antibodies (see 2.14) were covalently coupled to fluorochrome using a Lightning-Link kit (Innova Biosciences) and following the manufacturer's protocol.

2.12 *In-vitro* analysis of antibody binding

2.12.1   Immunodot assay

1 µl of each samples was spotted on a nitrocellulose membrane and left to air dry. Membranes were blocked in 5% milk/PBS at RT for 1h. Immunoassay was carried out on a rocking platform. Primary antibodies were used at 1:10 dilution and CBMs at 20 µg/ml for 1 h. Anti-rat-IgG-peroxidase (A9037 Sigma-Aldrich) and anti-his-peroxidase (A7058 Sigma-Aldrich) were used as secondary antibodies at 1:1000 dilution in 5% milk/PBS for 1 h at RT. The enzyme substrate solution contained 1 mg/ml chloronaphthol and 6% (v/v) hydrogen peroxide. The reaction led to purple colour and was stopped after 10 min.

2.12.2   Enzyme-linked immunosorbent assay (ELISA)

Microtitre plates (Nunc, Fisher Scientific, Denmark) were coated overnight with 100 µl sample diluted as needed in phosphate-buffered saline (PBS). For heteromannan enzyme digestion on immobilized material, 100 µl of 10 µg/ml of recombinant beta(1,4)-mannanase from *Thermotoga maritima* (E-BMATM Megazyme) in 50 mM 3-(N-morpholino)propansulfonic acid (MOPS) pH 7.0 or buffer alone were added to each ELISA plate well and left for 2 h at 37°C. Plates were washed in tap water and blocked with 5% milk/PBS at RT for 2 h wrapped in tin foil. ELISA was performed as in (McCartney et al., 2005). Antibodies were used at 1:10 dilution or 10 µg/ml and CBMs at 20

µg/ml in 5% milk/PBS. Secondary rat mouse or his HRP were used at 1:1000 dilution in 5% milk/PBS. To reveal antibody binding, 100 µl of substrate was added (0.1 M sodium acetate buffer pH 6, 1% (v/v) tetramethyl benzidene, 0.006% (v/v) H_2O_2). The reaction was stopped by addition of 50 µl of 2.5 M H_2SO_4 to each well. Absorbance was read at 450 nm on a microtitre plate reader.

2.12.3   Quantitative *in-vitro* analyses of xyloglucan recognition for *Ct*CBM3a studies

For antibody/CBM capture ELISAs, 10-fold serial dilutions of 100 µg/ml tamarind xyloglucan (Megazyme) in PBS were coated (100 µl) on to microtitre plates. LM15 was used at 1:10 dilution of hybridoma cell culture supernatant in MP/PBS. For competitive-inhibition assessment of recognition of xyloglucan oligosaccharides microtitre plates were coated with 0.5 µg/ml xyloglucan to act as immobilised antigen. After blocking with MP/PBS and washing, six ten-fold serial dilutions from 50 µg/m of xyloglucan from tamarind seeds (P-XYGLN Megazyme), xyloglucan heptasaccharide (O-X3G4 Megazyme), guar galactomannan medium viscosity (P-GGMMV Megazyme) and cellohexaose (O-CHE Megazyme) haptens were prepared and 50 µl added to microtritre plate wells. Immediately after, 50 µl of 1:50 dilution of LM15 antibody or CBMs at 20 µg/ml were added to equivalent sets of microtitre plate wells containing soluble xyloglucan or oligosaccharide haptens and incubated for 1.5 h. Probe binding was determined as described above.

2.13   Sodium dodecyl sulfate polyacrylamide gel electrophoresis (SDS-PAGE) and immunoblotting.

Extracted cell wall polysaccharides and glycoproteins were analyzed by SDS-PAGE in 10% (w/v) acrylamide separating gels. Samples were diluted in 1:1 dilution with loading buffer (BioRad) and boiled for 5 min at 95°C. Gels were loaded with 30 µl (450 µg fibre) per well and run at 90V in a gel tank containing running buffer (25 mM Tris, 192 mM glycine, 0.1% SDS). SDS-

gels were transferred to nitrocellulose membranes for immunoblotting analysis of the polysaccharides and glycoproteins present in cell wall extractions across different developmental stages. BioRad blotting cassettes were placed into tanks containing transfer buffer (25 mM Tris, 192 mM glycine, 0.1% ethanol) and gels were transferred at 90V for 1.5 h. Nitrocellulose membranes were washed in PBS immunoblotting was performed as previously described for immunodot assays.

2.14 Euglobulin precipitation

To purify antibodies, 50 ml of hybridroma cell culture supernatant was dialysed in 2 mM sodium phosphate buffer pH 6 at 4°C for 4 days using a dialysis membrane of 24.5mm diameter and 12-14000 Da (Medicell Membranes) previously boiled in 2% sodium bicarbonate with 0.5 M EDTA at 80°C for 30 min. The buffer was changed once a day. These conditions induced the precipitation of the antibody which was collected by centrifugation. The antibody was resuspended in PBS, aliquoted and stored at -20°C until use.

2.15 Magnetic bead-assisted immunoprecipitation of cell wall epitopes

Epoxy magnetic beads (Dynabeads M-270, Life technologies) were coupled to purified antibodies following manufacturer's guidelines and protocol with a few modifications.

2.15.1 Antibody coupling to Dynabeads

In a 2 ml Eppendorf tube, 20 mg of beads were washed in buffer A (Table Table 2-3). Beads binding capacity is 5-10 µg antibody per mg of beads so 150-200 µg of purified antibody was added to the beads as follows:

(1000 µl Buffer A – vol. Ab) + 1000 µl Buffer B = 2000 µl total volume

The final concentration of ammonium sulphate was 1 M. To optimise antibody coupling to beads it was incubated o/n at 37°C on slow rotor.

Beads were placed on magnet for 1 min and supernatant collected in a new tube by pipetting. Beads were washed in 1.5 ml Buffer E or F three times using magnet and pipetting supernatant out. All supernatants were collected in new tube by pipetting in a new tube to check antibody binding efficiency by SDS-page. Beads were stored in 1ml buffer F at 4°C.

Table 2-3. Buffers used for magnetic based-assisted immuneprecipitation	
Buffer A	0.1 M sodium phosphate pH 7.4
Buffer B	2 M ammonium sulphate
Buffer C	PBS
Buffer D	PBS with 0.1% BSA
Buffer E	1 M glycine pH 2.8
Buffer F	0.1 M citric acid pH 3.1
Buffer G	2 M NaI

2.15.2 Isolation of polysaccharide molecules carrying antibody epitopes

Beads were washed one time in 1.5 ml PBS, tube was placed in magnet for 1 min, supernatant was discarded and 1 ml of sample added (diluted as needed in PBS). Beads and sample were incubated at RT on a rotor for 1 h. Beads were then washed 4 times 5 min each on a rotor with 1.5 ml PBS using magnet and all supernatant were collected in a new tube. Elution was done in two steps: 300 µl of buffers E, F or G to beads and incubated for 10 min on rotor, then another 300 µl of selected elution buffer was added and incubated for additional 15 min.

To check sample binding, efficient washing of remaining sample and elution of isolated polysaccharide, sample before and after binding, washes and elute were screened by ELISA. Further studies of the elute polysaccharide involved epitope detection chromatography analysis.

2.16 Epitope detection chromatography (EDC)

Cotton fibre cell wall extracts with water, CDTA and NaOH at different dpa were analysed by epitope detection chromatography as in Cornuault et al. (2014) with some modifications. Briefly, cell wall extractions, exudate or immunoprecipitated elutes were diluted in 1 ml dH_2O as appropriate and injected in the BioLogic low pressure chromatography system (BioRad). A 1 ml Hi-Trap ANX FF, 17-5163 (Ge, Healthcare) column was used. The chromatography salt gradients and buffers used are as follow:

Table 2-4. Chromatography settings Low pressure anion exchange chromatography salt gradients and flow rate.

Linear gradient: 48 fractions collected (1 fraction/min)		
Time (min)	**Buffer**	**Flow (ml/min)**
0.00-34.00	0-100%B	1
34.00-48.00	Buffer B	1
2-step gradient: 48 fractions collected (1 fraction/min)		
Time (min)	**Buffer**	**Flow (ml/min)**
0.00-20.00	0-50%B	1
20.00-35.00	50-100%B	1
35.00-48.00	Buffer B	1

Table 2-5. Buffers used for EDC.	
Buffer A	50 mM sodium acetate pH 4.5
Buffer B	50 mM sodium acetate 0.6 M NaCl pH 4.5
Buffer C	0.1 N NaOH
Buffer D	1 M Na_2CO_3

After the end of each run the column was washed with 5 ml of buffer C and then the injection loop was flushed with 5 ml of buffer A before the injection of the next sample. Fractions were automatically collected with a BioFrac fraction collector (BioRad) on a 96 well (2 ml capacity) plate box. pH was raised by the addition of 100 µl of buffer D to each well before manually transferring fractions to 96 microtitre plates. Coated plates were incubated overnight at 4°C before proceeding with the standard ELISA method as described in 2.12.2.

Chapter III

3 Cotton fibre development varies between cotton lines with different properties

3.1 Introduction

Fibre quality denotes the suitability of mature cotton fibre for industrial processing and can be described by standardized and measurable physical parameters. Some key parameters are fibre length, bundle strength and fineness, which are decisive factors during the dry processing (yarn spinning, weaving and knitting), and fibre maturity which is very important for the wet processing (scouring, dyeing and finishing) (Basra, 2000). A complete description of each fibre quality parameter taken into account here can be found in the general introduction (1.2.2 and 1.2.3).

Fibre quality improvement is pursued by manufacturers looking for less costly processing such as fibre dyeing or new downstream applications such as that used for in insulating clothing (John and Keller, 1996). It is well stablished which are the desirable parameters of mature fibres for particular manufacturing requests, nevertheless, fibre quality cannot be found in wild cotton and so it has been developed over time by selective breeding and, more recently, by direct genetic intervention.

Germplasm and growing conditions such us temperature are the biggest determinants of fibre quality (Tian et al., 2014). Genetic studies based on fibre transcriptome analysis are very useful to discover important genetic modulators and genes that can be targeted to achieve better fibre quality. Another approach is to study the biochemical nature of growing fibres since mature fibres are cell walls whose physical properties have to be rooted in the biochemical structure of its components. Understanding how the fibre cell wall develops from a structural/biochemical point of view is a worthwhile approach, not yet fully explored. Such an approach could lead to the identification of important changes that influence final fibre quality. The aim of this work was to generate useful information regarding fibre cell wall

polysaccharide biochemistry that can be taken into consideration for future functional studies and genetic improvement.

This chapter compares fibre cell wall development in several cotton cultivars belonging to the most commonly cultivated species: *G. barbadense, G. hirsutum, G. herbaceum* and *G. arboreum.* The cotton lines were selected based on their mature mechanical properties and suitability for industrial processing. The first part of this chapter describes the mature fibre properties of the selected lines, followed by a comparative analysis of their cell wall monosaccharide and sugar linkage compositions. In the third part, the fibre tissue morphology is described for each cultivar concerning cell wall adhesion and detachment, the cotton fibre middle lamella (CFML) and the degree of secondary cell wall deposition. In the four and fifth part the relative abundances of glycan epitopes during development in each cotton line are described and glycan profiles are correlated to fibre properties. In addition, the dynamics and abundances of the heteromannan, never described before in cotton, are analysed here. Discussion of the presence of this polysaccharide is not addressed in this chapter but in Chapter 4 (4.3.3) together with additional results regarding heteromannan immunolocalization in cotton fibres.

3.2 Results

3.2.1 Comparison of the physical quality parameters in mature fibres from six cotton cultivars

Six domesticated cotton cultivars with contrasting mature fibre properties were selected in order to compare fibre and cell wall development. These cultivars belonged to the *G. barbadense* (PimaS7 and China10), *G. hirsutum* (FM966), *G. herbaceum* (Krasnyj) and *G. arboreum* (30834 and JFW15) species. Seed fibres from each cultivar were carefully extended avoiding detachment from the seed surface and a representative fibre image from each cultivar is shown in Figure 3-1. Differences in fibre length, texture and puffiness of these cotton lines were observed. PimaS7, China10 and FM966 are long fibres with a softer aspect than Krasnyj and 30834 fibres and JFW15 had very short fibres with a coarser texture. In addition, several parameters related to fibre quality were measured by the High Volume Instrument (HVI) method (Suh and Sasser, 1996) in mature fibres from these cultivars (Table 3-1 below).

Table 3-1. HVI fibre quality standards measurements						
	PimaS7	China10	FM966	Krasnyj	30834	JFW15
	(*G. barbadense*)		(*G. hirsutum*)	(*G. herbaceum*)	(*G. arboreum*)	
Micronaire	4.12	3.77	4.15	3.88	5.26	7.69
UHML (mm)	32.26	33.04	28.76	21.86	22.31	16.42
UI (%)	85.5	85	84.9	77.8	79.8	71.7
SFI (%)	6.7	6.7	6.6	11.5	9.4	27.7
Strength (g/tex)	44.4	40.3	35	24	28.4	20
Elong (%)	5.5	6.4	5.6	6.5	6.4	8.7
Rd (%)	70.8	81.3	82.8	78.2	80.4	82.6
+b*	11.2	8.3	7	8.6	6.8	7
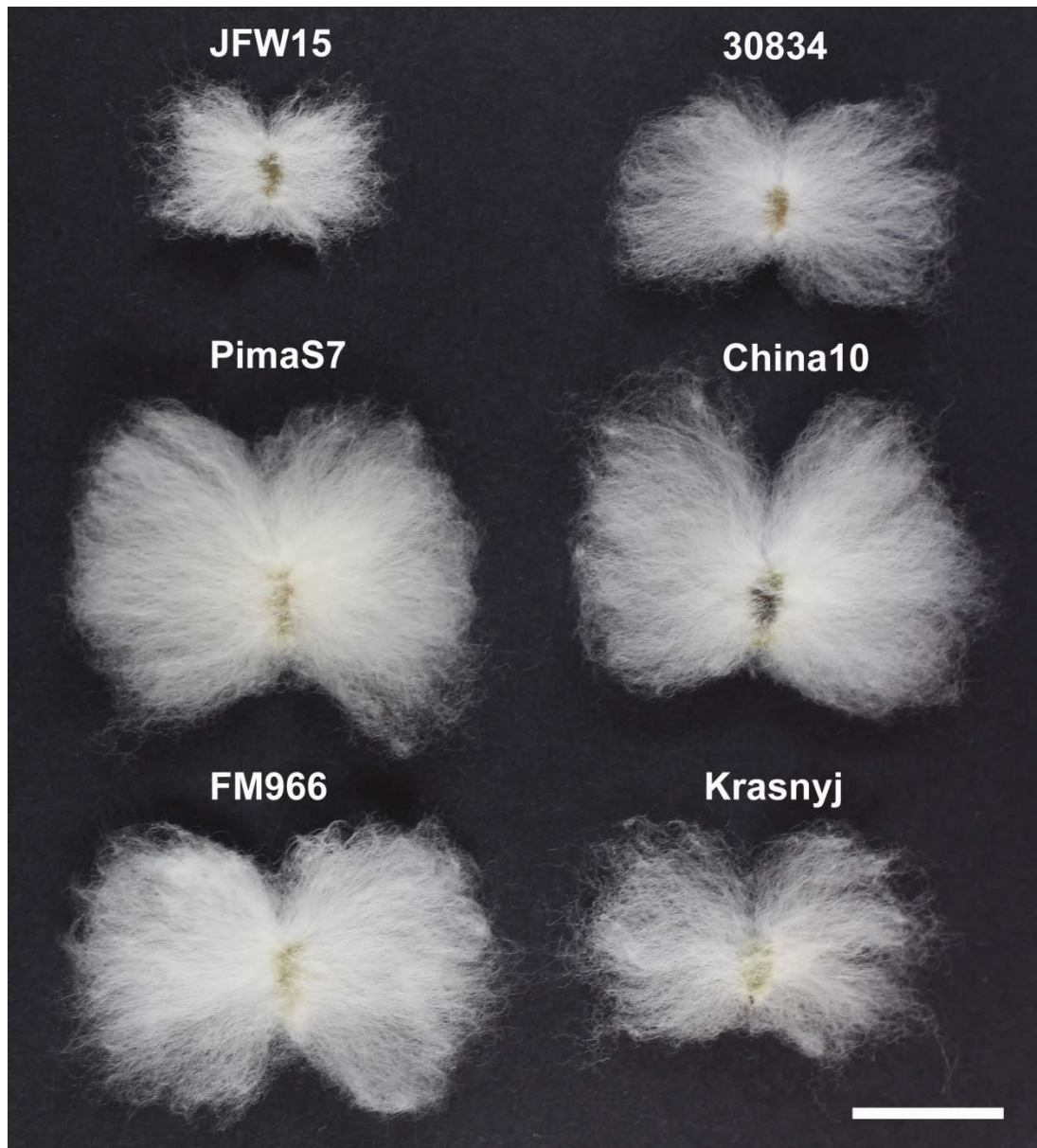
Figure 3-1. Cotton fibres from six cotton cultivars. JFW15 and 30834 (*G. arboreum*), PimaS7 and China10 (*G. barbadense*), FM966 (*G. hirsutum*), Krasnyj (*G. herbaceum*). Bar: 2 cm

PimaS7 and China10 (*G. barbadense*) showed the highest values of fibre length (32.26 and 33.04 mm respectively for the upper half fibre mean length), uniformity index (85.5 and 80%) and bundle strength 44.4 and 40.3 g/tex). PimaS7 and China10 were selected as representative lines of a very high quality cultivar with extraordinary long and strong fibres used in top class products. FM966 (*G. hirsutum*) fibres were also long (28.8 mm), highly uniform in length (84.9 %) and just slightly less strong (35 g/tex) than the *G. barbadense* lines. FM966 was selected as it is a high quality fibre sold worldwide under the brand name FibreMax® by Bayer CropScience. Krasnyj (*G. herbaceum*) and 30834 (*G. arboreum*) have much less satisfactory quality values of fibre length (21.86 and 22.31 mm) and uniformity (77.8 and 79.8%), with a high short fibre content (11.5 and 9.4%) and low strength (24 and 28.4 g/tex) compared to the *G. barbadense* and *G. hirsutum* lines.

Krasnyj and 30834 lines were selected as poor quality fibres belonging to two different species. Among all lines, JFW15 (*G. arboreum)* had the largest differences in its physical properties. JFW15 has poor fibre length (16.4 mm), low length uniformity (72%), bundle strength (20 g/tex), very high sort fibre content (27.7%) and extremely high micronaire (7.7). The JFW15 fibre elongation is much higher than for any of the other lines (8.7%). This line was selected as an example of a poor quality fibre which produces a non-spinnable fibre that is not suitable for textile processing. The colour of cotton fibres is measured by the degree of reflectance (Rd) and the yellowness of the fibre (b+). Only non-coloured fibres were chosen to facilitate imaging experiments performed in Chapter 4.

All these parameters showed clear differences in the six cultivars selected for this study as shown in Table 3-1. To shed some light on how fibre cell wall development may influence these mature physical characteristics, cell wall glycan profiles, and monosaccharide and sugar linkage compositions were determined for each line.

3.2.2 Monosaccharide and sugar linkage composition varies between cotton cultivars at equivalent time points

For a better understanding of the biochemistry of fibre cell wall polysaccharides, the monosaccharide and linkage compositions were analysed for each cotton line at several developmental stages.

The analysis of the alditol acetates by GC showed that the same monosaccharides (Figure 3-2) and linkages (Figure 3-3) were found in all cotton species and glucose was the more abundant monosaccharide in cotton fibres. Glucose is the only monosaccharide that showed increasing quantities during fibre growth and, in general, glucose amounts were doubled (from 6-11 mg to 12-22 mg per 100 mg fibre) between 8 dpa and 17 dpa in PimaS7, China10 and FM966 and from 8 to 15 dpa in the other three lines, Krasnyj, 30834 and JFW15. Interestingly, the other monosaccharides only showed a significant increase at 17 dpa in PimaS7 and China10 and to a less extent in FM966, Krasnyj and 30834. This points to an important compositional shift in the cell walls of the *G. barbadense* cultivars at 17 dpa possibly correlated with the end of fibre growth and the start of cellulose deposition. Glucose levels decreased from 17 to 25 dpa in most lines suggesting that glucose is only partially extractable in the thickening secondary cell walls.

Arabinose and galactose were the second and third most abundant monosaccharides in cotton fibres whose quantities ranged between 2 and 5 mg per 100 mg of fibre from 8 to 17 dpa in the PimaS7 and China10 lines (*G. barbadense*), 1 and 4 mg in Krasnyj (*G. herbaceum*), 30834 and JFW15 (*G. arboreum*) and 1 and 3 mg in FM966 (*G. hirsutum*). FM966 was the only line whose galactose levels surpass arabinose (at 13 dpa). Total arabinose and galactose quantities decreased over development in all lines, however this decrease was much faster in the *G. arboreum* JFW15 line that showed 1 mg of arabinose and galactose per 100 mg of fibre by 13 dpa (same levels were reached at 25 dpa in PimaS7 and China10).

In contrast, the amount of xylose, rhamnose, mannose and fucose per mg of extracted fibre was significantly lower in all cultivars. Interestingly, the amount of xylose in the *G. arboreum* and *G. arboreum* cultivas (Krasnyj, 30834 and JFW15) showed higher levels of xylose compared to the *G. barbadense* and *G. hirsutum* cultivars (PimaS7, China10 and FM966). Interestingly, the total amount of other monosaccharides other than glucose was reduced in the FM966 cultivar compared to the rest. Moreover, these experiments confirmed the presence of mannose in all lines up to a maximum of 0.5 mg per 100 mg of fibre in the PimaS7 cultivar.

The analysis of the sugar linkage composition (Figure 3-3) showed that the cellulose-derived 1,4-glucosyl linkage was highly abundant in cotton fibres increasing rapidly from ca. 40% of the molecular weight (in PimaS7, Krasnyj, 30834 and JFW15) or 60% (in China10 and FM966) at 8 dpa to over 90% at 25 dpa, correlating well with the increasing amounts of glucose in the monosaccharide analysis that becomes part of cellulose. The second major linkage was 1,5-linked arabinose, that accounted for 31% of the total linkages in PimaS7, 18% in China10, 15% in FM966, 24% in Krasnyj, 27% in 30834 and 23% in JFW15. The amount of 1,5-linked arabinose decreased more gradually in the *G. barbadense* PimaS7 and China10 lines than in the rest of the lines. This correlates well with the previous findings regarding the amount of arabinose at different developmental stages. The callose 1,3-linked glucose linkage appeared in cotton fibres only after 15 dpa in Krasnyj, 30834 and JFW15 and after 17 dpa in PimaS7 and China10, suggesting a role of callose in the transition phase. It is worth noting that the relative amount of the non-cellulosic linkages is significantly lower compared to that of cellulose in FM966 compared to the rest of the cultivars, this also correlates with the previous monosaccharide analysis where FM966 showed much lower amounts of any monosaccharide other than glucose.

A close up view of minor linkages is included in Figure 3-4. The terminal glucose linkage (xGlc1) was the most abundant of the minor linkages, followed by terminal arabinose (xAra1) and terminal xylose (xXyl1). The relative amount of these linkages decreased as fibre development continued

and detection was negligible after 25 dpa in most lines except for the xGlc1 linkage that persisted at low levels during later stages of development. Further evidence of the presence of a mannan polysaccharide in cotton fibre cell walls was observed as 1,4-linked mannose was detected at low levels. At 8 dpa, the mannan backbone linkage accounted for ca. 1 mol % of the total extracted linkages for most of the lines, and PimaS7 and China10 showed a higher occurrence of this linkage than the rest of the lines.

These results demonstrated that all cultivars were composed of the same monosaccharides and linkages, however, they showed different relative abundances at equivalent developmental time points (dpa) between cultivars suggesting a cultivar-dependent developmental pace. In addition, these data confirm the presence of a mannan polysaccharide in cotton fibres.
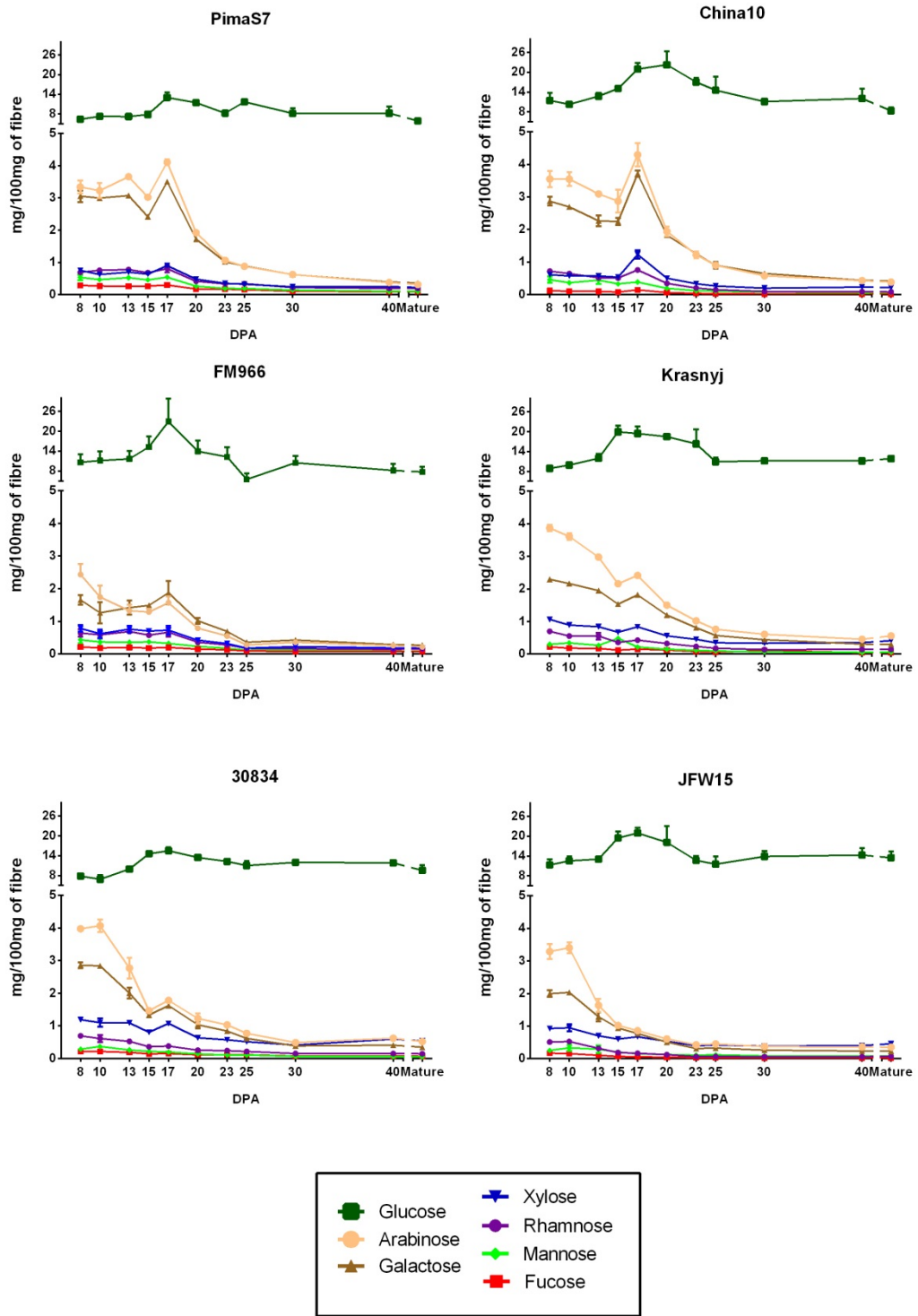
Figure 3-2. Monosaccharide composition of six different cotton species at 11 developmental stages. DPA: days post anthesis. Error bars: SD (n=6).
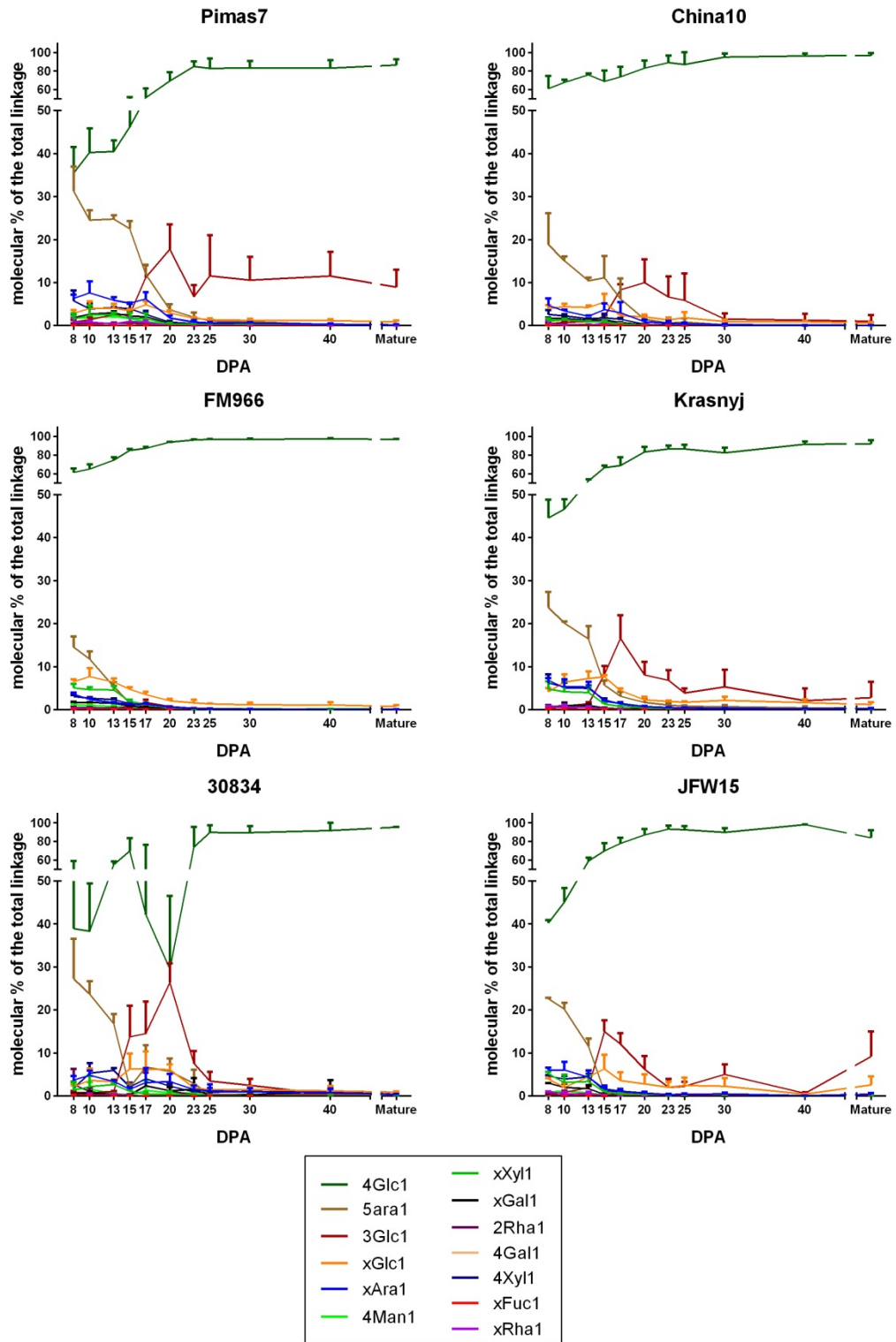
Figure 3-3. Total sugar linkage analysis from six different cotton species at 11 developmental stages. For clarity only upper error bars are shown: SD (n=6).
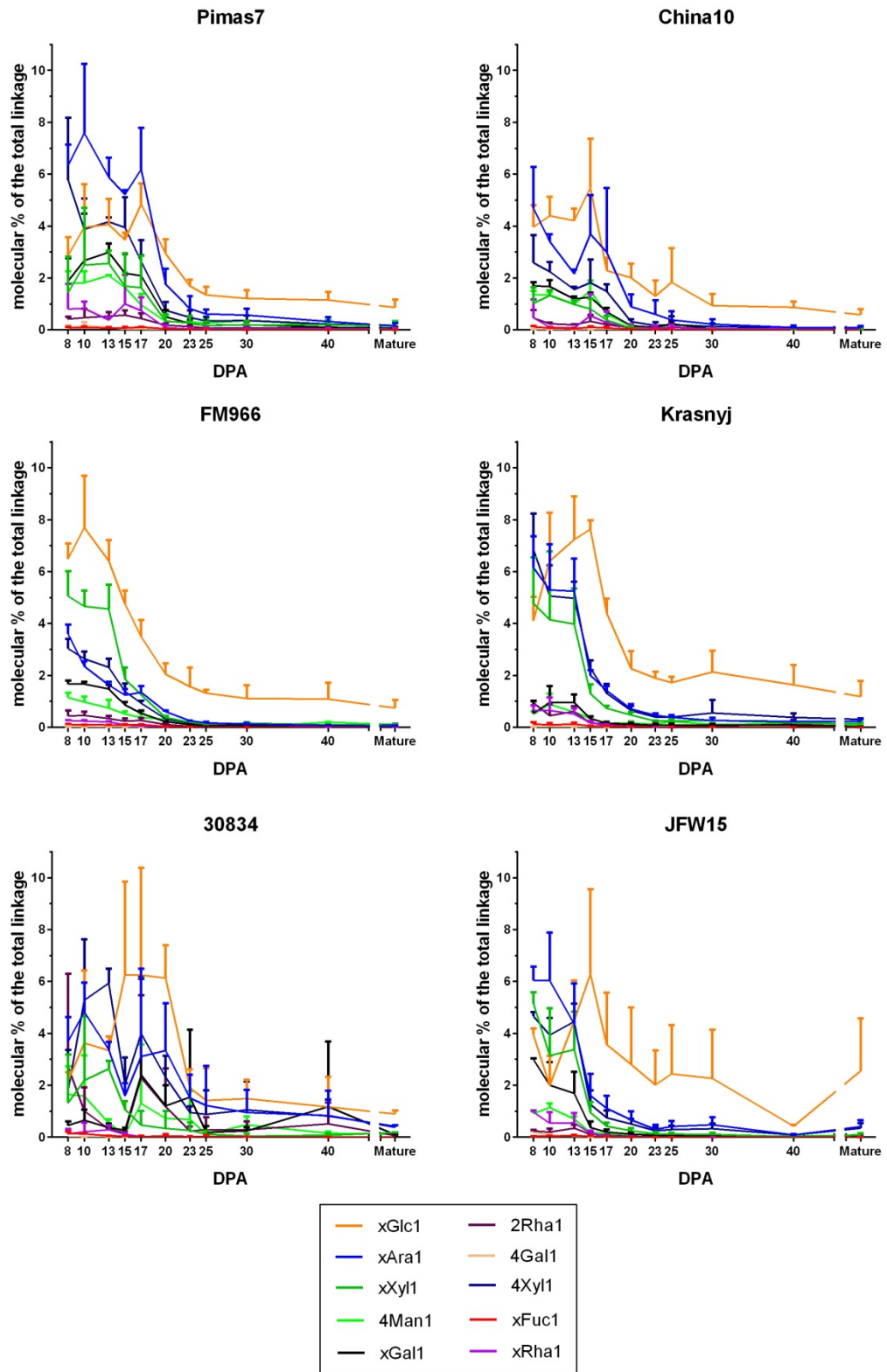
Figure 3-4. Close up view of minor glycosyl linkages. For clarity only upper error bars are shown: SD (n=6).

3.2.3 Three developmental features relevant to fibre developmental pace are determined by genotype and growth temperature

To study further the previously suggested differential developmental pace between cultivars, as well as the morphology of the fibre tissue and its cell walls during development, resin-embedded cross sections of fibre tissues from PimaS7 (*G. barbadense*), China10 (*G. barbadense*), FM966 (*G. hirsutum*), Krasnyj (*G. herbaceum*) and JFW15 (*G. arboreum*) were stained with Calcofluor White (Figure 3-5). This dye stains a wide range of β-glucans and is commonly used in plant tissues to reveal cell wall structures.

Figure 3-5 shows the remarkable differences found in the pace of fibre development in these lines at five sequential days post anthesis (5, 10, 17 and 25 dpa and mature fibres).

The term developmental pace is used here to indicate the speed at which common developmental features appeared in different cotton lines. The features considered here were cell wall adhesion and detachment, CFML synthesis and degradation and secondary cell wall deposition. Fibre cell adhesion was obvious by 5 dpa in China10 and FM966 only and enlarged regions of the CFML were already observed in the fibre tissue of these lines (see arrowheads 5 dpa top panels) whereas cell adhesion at the same dpa was incomplete in PimaS7, Krasnyj and JFW15 and no CFML was observed at this time-point. At 10 dpa all lines showed complete cell adhesion and enlarged regions of the CFML filled with material were widely spread throughout the tissue, except for the JFW15 fibre tissue which showed much fewer of these CFML structures. At 17 dpa, the start of cell wall detachment was visible in China10, Krasnyj and JFW15, however fibres in PimaS7 and FM966 were still highly adhered at 17 dpa. FM966 showed a peculiar characteristic of the CFML referred to as paired CFML bulges (arrows in 17dpa FM966 panel). These bulges were observed in pairs between two neighbouring cell walls and were present throughout the fibre tissue. CFML bulges became apparent at 10 dpa in the FM966 line (arrow in 10 dpa FM966 panel) and were also observed at later developmental stages (arrow
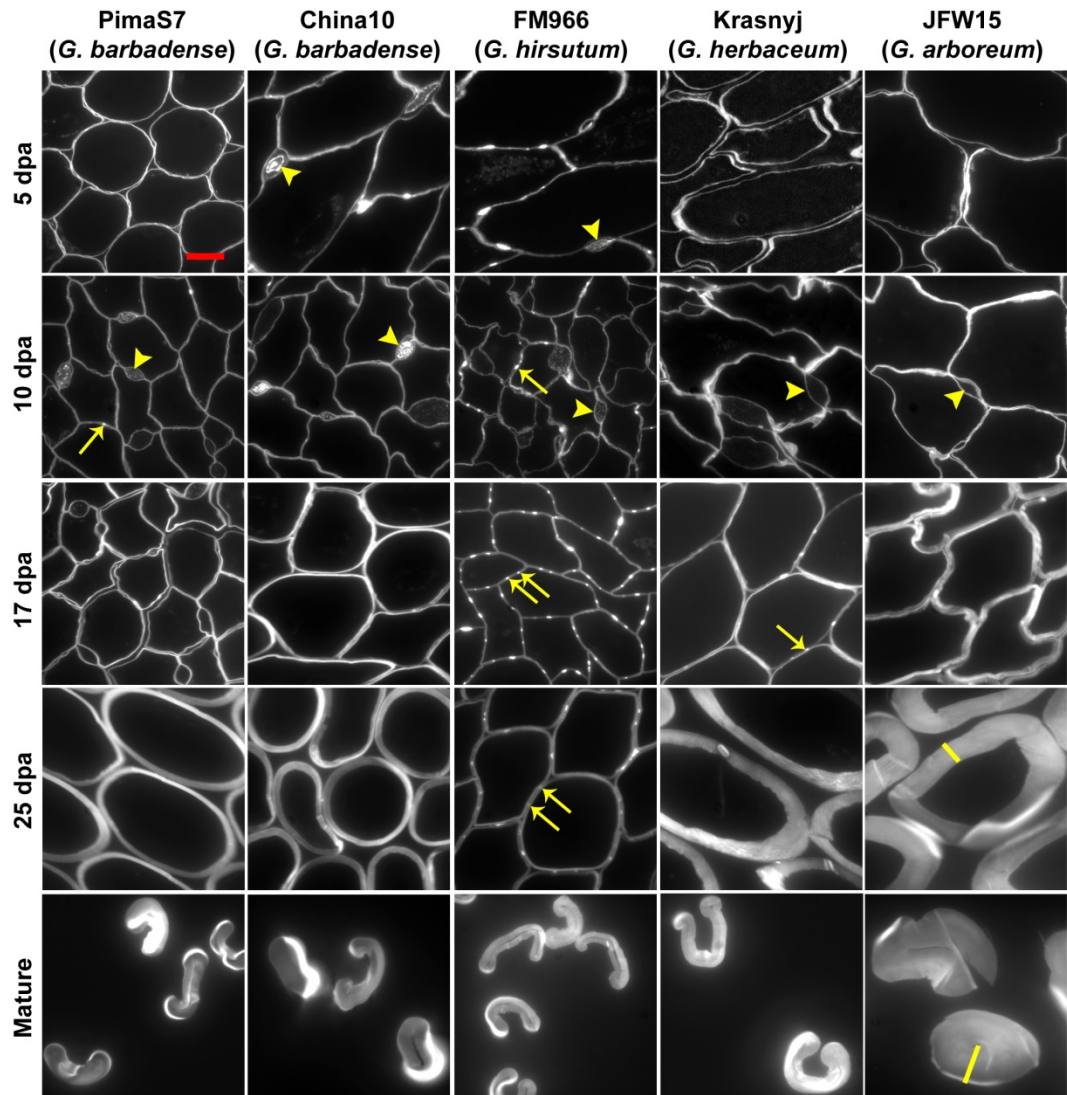
Figure 3-5. Cotton fibres throughout development. Calcofluor staining of cross sections of developing and mature cotton fibres of PimaS7 and China10 (*G. barbadense*), FM966 (*G. hirsutum*), Krasnyj (G. *herbaceum*) and JFW15 (G*. arboreum*). Arrowheads point at enlarged regions of the CFML, arrows points to a particular CFML feature consistent of a repetitive paired pattern of CFML bulges between two neighbouring cells which was mainly present in the *G. hirsutum* species. Yellow lines in 25 dpa and mature JFW15 panels show the extensively thickened secondary cell walls of this line. Scale bar in red (top left panel): 10 μm.

in 25 dpa FM966 panel). Others lines also showed paired CFML bulges but not as obvious and structured as in the FM966 line (arrow in 10dpa PimaS7 panel and in 17 dpa Krasnyj panel).

Cell wall detachment was delayed in the FM966 line compared to the other lines that seem to start fibre detachment by 17 dpa. Similar cell wall detachment is observed in FM966 only at 25 dpa. Moreover, clear differences in the start and rate of secondary cell wall deposition were also observed. Higher cellulose deposition was observed in the JFW15 line at 17 dpa and, while FM966 fibres showed thinner cell walls compared to any other line at 25 dpa, JFW15 and Krasnyj depicted extra-thickened cell walls. The higher rate of cellulose deposition in the JFW15 line was very evident at maturation.

In summary, while the *G. arboreum* (JFW15) and *G. herbaceum* (Krasnyj) cultivars showed early start secondary cell wall thickening and higher cellulose deposition rates, the *G. hirsutum* FM966 cultivar showed prolonged cell attachment and specific CFML patterns with lower cellulose deposition rate than even the *G. barbadense* lines (China10 and PimaS7). These immunohistochemical analysis showed that there are three cell wall-related features particularly relevant depending on the fibre developmental pace: cell adhesion and CFML, the timing of the transition phase and the cellulose deposition rate. These features appeared to be determined by genotype.

Apart from genotype, temperature is also an important factor that determines the final fibre quality of cotton fibres from the same cultivar. To study the impact of growth temperature on the previously described developmental features, cotton plants from the same cultivar - FM966 (*G. hirsutum*) - were grown in two batches where greenhouse diurnal temperature was set at 20-25°C ("Batch 1"), and 28-32°C ("Batch 2"). Fibres were collected at several days post anthesis. Cotton fibres were fixed and resin-embedded and transverse sections stained with Calcofluor White are shown in Figure 3-6.
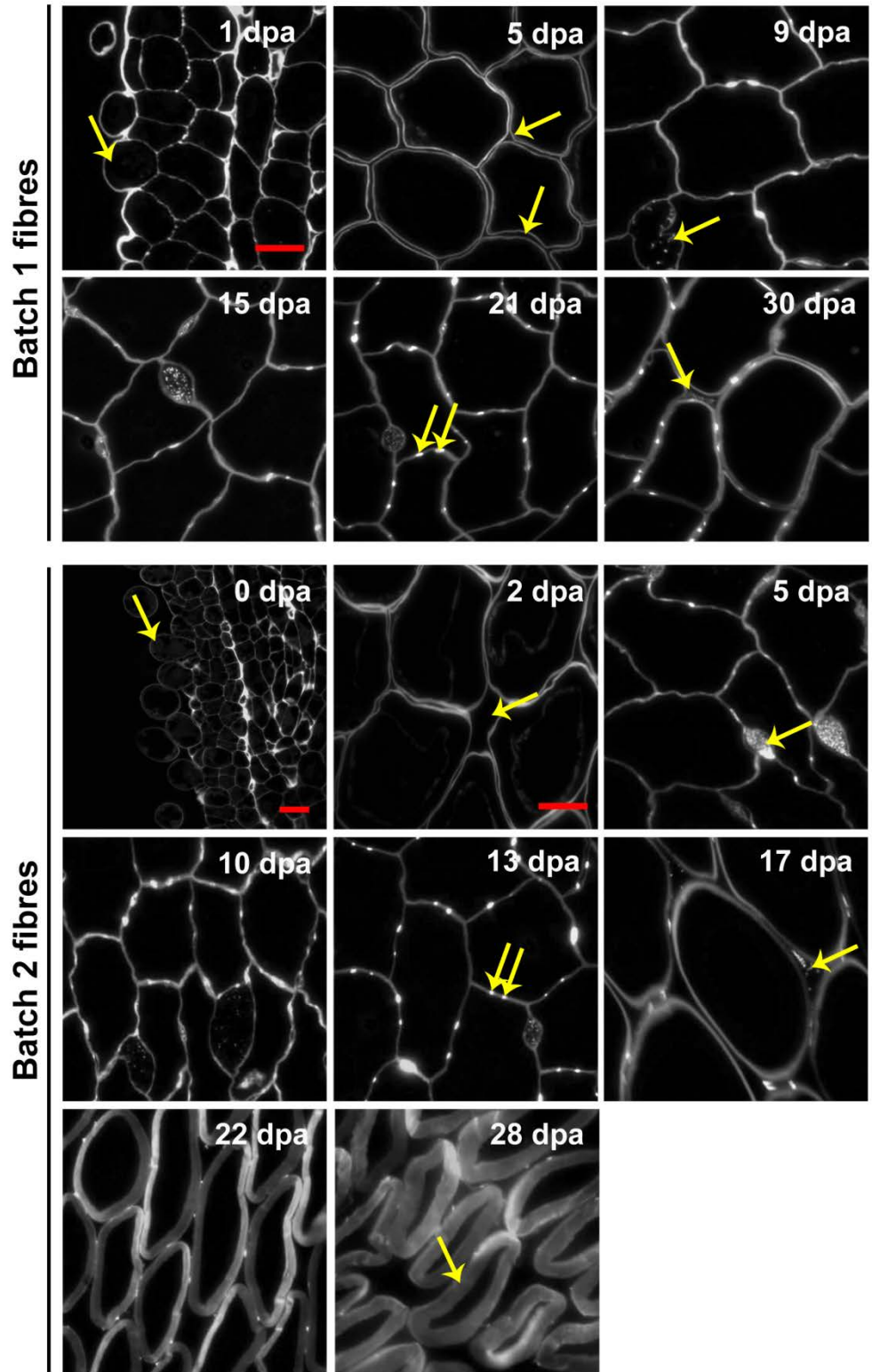
Figure 3-6. Calcofluor White images of transverse sections of FM966 fibres. Batch 1 fibres were grown at 20-25°C and Batch 2 fibres at 28-32°C. Scale bars: 10 μm (smaller scale bar is unique to 0 dpa Batch 2 fibres).

Figure 3-6 indicate that even though fibre tissue morphology in both batches underwent the same developmental feature changes, they differed in the timing of each developmental phase. The transition phase, marked by the degradation of enlarged CFML regions and the start of secondary cell wall deposition occurred earlier in fibres growing at higher temperatures. Fibres grown at higher diurnal temperatures (Batch 2) started elongating on the day of anthesis (0 dpa) and by day 2 showed a similar morphology to batch 1 at 5 dpa in which cells are still not completely adhered. Batch 2 fibres at 5 dpa displayed enlarged regions of CFML and were forming paired CFML bulges corresponding to fibres at 9 dpa in Batch 1. Paired CFML bulges were highly abundant at 17 dpa in Batch 2 and this was only matched at 21 dpa by Batch 1 fibres. The CFML was degraded around 30 dpa in Batch 1, however this was achieved at 17 dpa in Batch 2. While cellulose deposition started at 30 dpa in Batch 1, thicker secondary cell walls were observed earlier (22 and 28 dpa) in Batch 2 fibres.

These experiments showed that all the three features describing fibre developmental pace are also environmentally controlled, so that they can be altered within the same cotton cultivar depending on growing conditions such as temperature.

3.2.4 Secondary cell wall deposition ratio is significantly higher in the JFW15 cultivar

To corroborate the higher maturity of the JFW15 cultivar, the cell wall thickness was measured in Calcofluor-White-stained cross sections of 10, 17, 25 dpa and mature fibres of PimaS7, FM966, Krasnyj and JFW15 (Figure 3-7). Striking differences were found in the thickness of the JFW15 (*G. arboreum*) cell walls compared to those of FM966 (*G. hirsutum*). At 17 dpa, JFW15 fibres cell walls are thicker (1.1 µm) than in FM966 (0.3 µm) and the secondary cell wall of JFW15 at 25 dpa (5 µm) is thicker than that of mature FM966 fibres. Cell walls of mature JFW15 fibres appeared four times thicker (8 µm) than in FM966 (2 µm). These data indicate that JFW15 has a higher secondary cell wall deposition rate and produces an extra-thickened secondary cell wall whose synthesis starts at an earlier dpa than in the other lines, as JFW15 fibre cell walls at 17 dpa are significantly thicker compared to FM966. The extra-thick cell walls of JFW15 are associated with this line having shorter, weaker fibres. Krasnyj secondary cell wall thickening follows a similar trend compared to JFW15, however, mature Krasnyj fibres do not differ significantly from those of FM966 suggesting that secondary cell wall deposition ratio slows down at later stages and is comparable to FM966. Comparable cell wall thickness was observed at 17 dpa in PimaS7 and FM966 fibres however, PimaS7 produced more secondary cell wall from 17 to 25 dpa than FM966 suggesting a higher deposition ratio of cellulose in PimaS7 compare to FM966.
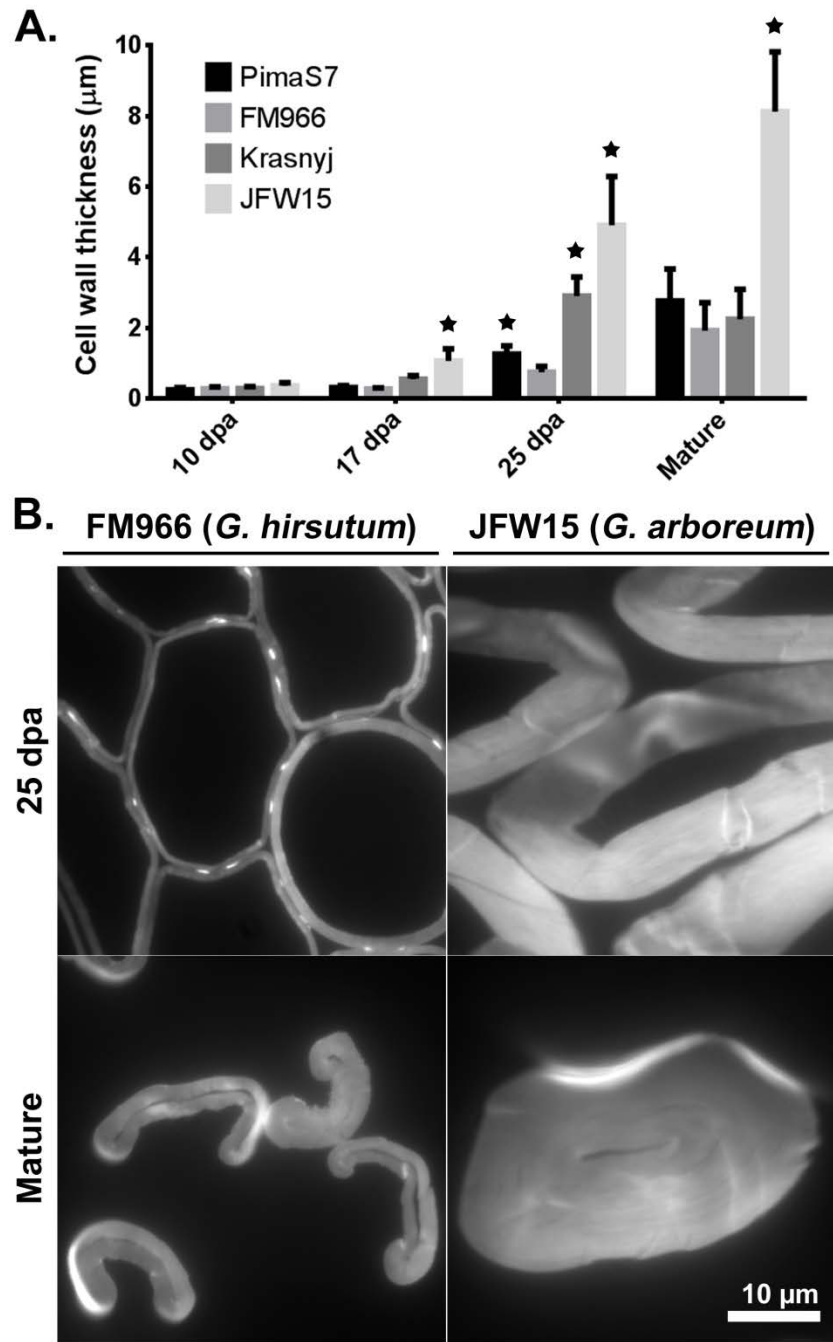
Figure 3-7. Difference in cotton fibre cell wall thickness. A. Measurements of cell wall thickness of 10, 17, 25 and mature fibres from four lines (PimaS7, FM966, Krasnyj and JFW15). Error bars: SD (n≥25). Asterisk: Student t-test p value <0.001 compared to FM966. B. High magnification micrographs of representative Calcofluor White-stained cross sections of 25 dpa and mature fibres from FM966 and JFW15.

3.2.5 Developmental profiles of detected glycan epitopes are also genotype-determined

In order to study the relative abundance of glycan epitopes in developing and mature cotton fibres and to understand the potential roles of specific cell wall polysaccharides in developmental events, fibre cell walls screened by glycan microarrays providing semi-quantitative data (Moller et al., 2007).

Before extracting fibre cell wall polysaccharides, cotton fibres were detached from seeds and boiled in 70% ethanol for 20 minutes to deactivate enzymes. A screening of the ethanol soluble epitopes along with a water and CDTA extractions of 8 dpa FM966 fibres can be found in Figure 3-8. The arabinan LM6, AGPs JIM13, xyloglucan LM15 and extensins JIM20 epitopes were very soluble in ethanol and consequently partially lost in the glycan array analysis as the ethanol residue was discarded. This technique limitation is addressed in the discussion (3.3.4).

Pulverized fibres were sequentially extracted with CDTA and NaOH. CDTA is used to extract cell wall pectins as it chelates calcium ions needed for pectin crosslinking while NaOH is used at high molarities to extract more recalcitrant cell wall polysaccharides deeply embedded and hydrogen bonded to the cellulose microfibrils such as, for example, xylan. CDTA and NaOH extractions from the selected six cultivars PimaS7 and China10 (*G. barbadense*), FM966 (*G. hirsutum*), Krasnyj (*G. herbaceum*) and 30834 and JFW15 (*G. arboreum*) fibres at 11 different developmental stages allowing for the identification of a total of 23 cell wall-related glycan epitopes (Figure 3-9). A detailed list of all the probes and their characterized epitopes can be found Table 2-1.

The pectic epitopes found in the CDTA extraction in order of relative abundance over time were de-esterified HG (LM19 and JIM5), highly esterified HG (LM20 and JIM7), RG-I-related arabinan (LM6), RG-I-related galactan (LM5), RG-I-related linear arabinan (LM13) and RG-I backbone (RU-II). Other non-pectic cell wall epitopes released in this extraction were AGP (JIM13), extensin (JIM20) and low amounts of callose (BS400-2),

xyloglucan (LM25, LM15) and glucuronoxylan (LM28) when compared to the NaOH extraction.

The epitopes found in the NaOH extraction in order of polymer abundance throughout fibre development were: xyloglucan (LM25, LM15, LM24), callose (BS400-2), glucuronoxylan (LM28), heteromannan (LM21, BS400-4 and CBM27), arabinoxylan (AX1 and LM11) and lower amounts of the pectic de-esterified HG LM19 epitope. Interestingly, higher relative amounts of LM5, LM6, LM13 were extracted with NaOH rather than in CDTA. As expected, highly methyl esterified HG epitopes such as LM20 and JIM7 were absent in the NaOH extraction due the de-esterification of pectins at high pH. AGPs (JIM13) and extensins (JIM20) were also abundant in the NaOH extraction. Other polymers like mixed-linkage glucan (BS400-3) and processed arabinan (LM16) were not found in the cotton fibre cell wall.
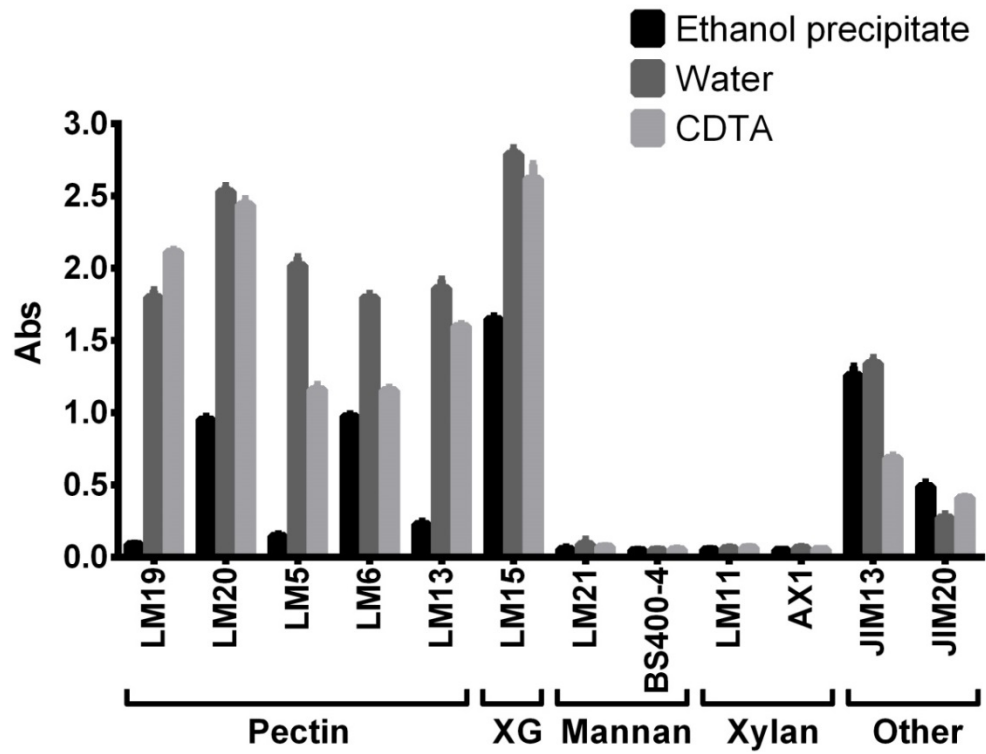
Figure 3-8. Analysis of soluble glycan epitopes. Glycan epitopes present in the ethanol soluble, water fibre extraction and CDTA fibre extraction of 8 dpa FM966 fibres.

Extraction: CDTA

Species	Cultivar	DPA	LM19	JIM5	LM20	JIM7	LM5	LM6	LM13	LM16	RU2	LM24	LM15	LM25	CBM3a	LM21	CBM27	LM10	LM11	LM28	AX1	BS400-2	JIM13	JIM20	BS400-3
G. barbadense	PimaS7	8	16	0	0	38	45	38	0	0	6	0	22	44	10	0	0	0	0	0	0	9	46	8	0
		10	39	13	15	42	30	34	0	0	7	0	25	42	14	0	0	0	0	0	0	16	41	5	0
		13	62	19	24	52	21	33	11	0	12	0	6	24	0	0	0	0	0	7	0	26	48	0	0
		15	61	21	21	48	18	32	14	0	13	0	6	21	0	0	0	0	0	16	0	25	44	10	0
		17	78	33	22	53	37	40	18	0	18	0	5	20	5	0	0	0	0	21	6	30	53	52	0
		20	66	25	0	24	9	18	6	0	10	0	0	0	0	0	0	0	0	5	0	18	45	30	0
		23	62	23	0	20	0	10	0	0	8	0	0	0	0	0	0	0	0	6	0	7	31	20	0
		25	54	17	0	16	0	7	0	0	6	0	0	0	0	0	0	0	0	0	0	8	28	22	0
		30	21	0	0	0	0	0	0	0	0	0	0	0	0	0	0	0	0	0	0	0	13	8	0
		40	25	6	0	0	0	0	0	0	0	0	0	0	0	0	0	0	0	0	0	0	8	0	0
		60	37	8	0	0	0	0	0	0	0	0	0	0	0	0	0	0	0	0	0	0	8	0	0
G. barbadense	China 10	8	23	0	6	39	47	43	6	0	0	0	34	52	16	0	0	0	0	0	0	8	48	9	0
		10	64	15	21	45	18	32	14	0	8	0	8	21	0	0	0	0	0	0	0	6	18	43	0
		13	95	40	38	65	42	48	33	0	24	0	8	28	8	0	0	0	5	50	6	39	68	73	0
		15	75	23	27	55	22	41	26	0	14	0	10	28	0	0	0	0	0	20	0	29	43	12	0
		17	84	26	36	65	29	37	14	0	6	0	77	73	54	0	0	0	0	0	0	12	40	10	0
		20	59	25	7	26	8	16	7	0	12	0	0	6	0	0	0	0	0	9	0	15	47	42	0
		23	52	19	0	19	0	10	0	0	7	0	0	0	0	0	0	0	0	0	0	15	42	37	0
		25	45	15	0	15	0	7	0	0	5	0	0	0	0	0	0	0	0	0	0	10	33	29	0
		30	43	10	0	10	0	0	0	0	0	0	0	0	0	0	0	0	0	0	0	7	27	18	0
		40	24	0	0	0	0	0	0	0	0	0	0	0	0	0	0	0	0	0	0	0	14	0	0
		60	26	0	0	0	0	0	0	0	0	0	0	0	0	0	0	0	0	0	0	0	10	0	0
G. hirsutum	FM966	8	52	10	33	59	20	32	7	0	0	0	23	46	9	0	0	0	0	0	0	18	50	0	0
		10	59	14	36	58	18	35	11	0	10	0	9	22	0	0	0	0	0	0	0	15	52	8	0
		13	70	27	36	61	15	29	6	0	15	0	6	17	0	0	0	0	0	15	6	23	53	7	0
		15	45	14	10	31	10	23	0	0	10	0	0	13	0	0	0	0	0	14	7	50	51	6	0
		17	78	40	18	37	8	16	0	0	19	0	0	10	0	0	0	0	0	8	0	28	70	46	0
		20	74	33	14	32	0	6	0	0	13	0	0	7	0	0	0	0	0	0	0	15	60	32	0
		23	55	19	8	17	0	0	0	0	6	0	0	5	0	0	0	0	0	0	0	11	49	25	0
		25	51	18	6	16	0	0	0	0	0	0	0	0	0	0	0	0	0	0	0	6	39	21	0
		30	19	0	0	0	0	0	0	0	0	0	0	0	0	0	0	0	0	0	0	6	23	9	0
		40	19	0	0	0	0	0	0	0	0	0	0	0	0	0	0	0	0	0	0	0	9	0	0
		60	25	0	0	0	0	0	0	0	0	0	0	0	0	0	0	0	0	0	0	0	6	0	0
G. herbaceum	Krasnyj	8	77	23	43	75	29	37	14	0	0	0	37	66	16	0	0	0	0	0	0	16	53	20	0
		10	56	11	23	50	17	29	6	0	0	0	11	32	0	0	0	0	0	0	0	18	62	7	0
		13	55	14	14	41	12	28	8	0	0	0	9	29	0	0	0	0	0	15	0	32	62	9	0
		15	58	20	11	36	6	20	8	0	0	0	0	11	0	0	0	0	0	0	9	52	47	13	0
		17	75	32	14	38	5	16	8	0	0	0	0	8	0	0	0	0	0	6	0	17	49	61	0
		20	66	26	11	32	0	16	6	0	0	0	0	8	0	0	0	0	0	12	0	15	41	51	0
		23	45	16	0	16	0	9	0	0	0	0	0	0	0	0	0	0	0	0	0	7	26	28	0
		25	55	19	0	21	0	10	0	0	0	0	0	0	0	0	0	0	0	0	0	6	26	30	0
		30	30	6	0	6	0	5	0	0	0	0	0	0	0	0	0	0	0	0	0	0	14	15	0
		40	36	8	0	7	0	0	0	0	0	0	0	0	0	0	0	0	0	0	0	0	5	8	0
		60	20	0	0	0	0	0	0	0	0	0	0	0	0	0	0	0	0	0	0	0	0	0	0
G. arboreum	30384	8	39	9	6	50	30	38	0	0	0	0	23	56	7	0	0	0	0	0	0	15	47	8	0
		10	36	10	0	39	22	28	0	0	0	0	8	39	0	0	0	0	0	0	0	22	52	6	0
		13	53	20	9	40	14	27	6	0	0	0	7	28	0	0	0	0	13	29	0	26	44	0	0
		15	51	20	0	23	9	18	0	0	0	0	0	7	0	0	0	0	0	28	5	51	42	7	0
		17	58	28	0	24	11	14	0	0	0	0	0	8	0	0	0	0	0	38	0	16	54	38	0
		20	33	12	0	7	0	7	0	0	0	0	0	0	0	0	0	0	0	10	0	10	37	21	0
		23	33	18	0	7	0	8	0	0	0	0	0	0	0	0	0	0	0	8	0	8	37	19	0
		25	34	13	0	6	0	9	0	0	0	0	0	0	0	0	0	0	0	11	0	5	30	17	0
		30	25	10	0	0	0	0	0	0	0	0	0	0	0	0	0	0	0	14	0	0	17	9	0
		40	34	17	0	0	0	0	0	0	0	0	0	0	0	0	0	0	0	13	0	0	13	7	0
		60	13	0	0	0	0	0	0	0	0	0	0	0	0	0	0	0	0	7	0	0	6	0	0
G. arboreum	JFW15	8	17	0	0	38	26	46	0	0	0	0	11	50	0	0	0	0	0	0	0	7	40	13	0
		10	43	7	0	49	21	39	10	0	0	0	10	42	0	0	0	0	0	0	6	18	47	7	0
		13	54	13	0	36	14	34	6	0	0	0	8	20	0	0	0	0	0	19	0	30	58	7	0
		15	36	11	0	13	0	12	0	0	0	0	0	0	0	0	0	0	0	13	7	59	42	8	0
		17	15	9	0	0	0	0	0	0	0	0	0	0	0	0	0	0	0	0	0	11	31	24	0
		20	25	16	0	6	0	0	0	0	0	0	0	0	0	0	0	0	0	7	0	6	26	15	0
		23	17	10	0	0	0	0	0	0	0	0	0	0	0	0	0	0	0	6	0	0	19	10	0
		25	8	0	0	0	0	0	0	0	0	0	0	0	0	0	0	0	0	0	0	0	18	9	0
		30	15	8	0	0	0	0	0	0	0	0	0	0	0	0	0	0	0	0	0	0	13	7	0
		40	6	0	0	0	0	0	0	0	0	0	0	0	0	0	0	0	0	0	0	0	8	0	0
		60	17	9	0	0	0	0	0	0	0	0	0	0	0	0	0	0	0	6	0	0	7	5	0

Extraction	Species	Cultivar	DPA	LM19	JIM5	LM20	JIM7	LM5	LM6	LM13	LM16	RU2	LM24	LM15	LM25	CBM3a	LM21	CBM27	LM10	LM11	LM28	AX1	BS400-2	JIM13	JIM20	BS400-3
NaOH	*G. barbadense*	PimaS7	8	35	0	0	0	59	61	35	0	24	11	72	78	53	32	0	0	0	20	0	32	37	5	0
			10	36	0	0	0	64	59	39	0	24	22	84	84	65	57	10	0	0	24	10	51	37	11	0
			13	33	0	0	0	56	50	42	0	22	23	81	82	62	60	12	0	0	25	12	58	31	18	0
			15	36	0	0	0	50	53	46	0	24	25	77	79	58	53	10	0	6	29	15	60	30	18	0
			17	26	0	0	0	35	43	37	0	13	21	62	73	50	45	10	0	7	28	25	80	30	24	0
			20	0	0	0	0	0	13	0	0	0	11	43	54	41	32	7	0	6	24	25	79	18	16	0
			23	0	0	0	0	0	10	0	0	0	10	55	59	43	43	10	0	0	21	21	71	17	13	0
			25	0	0	0	0	0	9	0	0	0	10	48	54	40	32	7	0	0	20	19	69	15	13	0
			30	0	0	0	0	0	6	0	0	0	7	16	35	33	5	0	0	0	16	13	59	10	10	0
			40	0	0	0	0	0	6	0	0	0	8	33	42	34	12	0	0	0	15	9	49	11	10	0
			60	0	0	0	0	0	12	0	0	0	24	47	53	39	24	0	0	0	15	0	25	17	10	0
	G. barbadense	China10	8	27	0	0	0	48	57	34	0	22	9	69	75	49	27	0	0	0	20	0	27	32	7	0
			10	20	0	0	0	38	43	37	0	16	16	71	71	51	34	7	0	6	21	10	42	27	16	0
			13	23	0	0	0	31	47	43	0	14	22	70	74	53	56	11	18	34	45	34	88	37	29	0
			15	32	0	0	0	51	59	56	0	20	31	76	76	59	59	12	0	10	33	17	63	32	22	0
			17	14	0	0	0	37	37	25	0	7	11	84	79	63	50	10	0	7	19	9	35	32	23	0
			20	0	0	0	0	0	17	0	0	0	10	40	49	37	29	5	0	8	27	29	83	23	20	0
			23	0	0	0	0	0	14	0	0	0	10	35	45	34	26	0	0	10	25	27	76	18	17	0
			25	0	0	0	0	0	9	0	0	0	9	32	42	32	22	0	0	0	23	21	69	16	16	0
			30	0	0	0	0	0	6	0	0	0	10	34	42	32	23	0	0	7	21	15	58	11	14	0
			40	0	0	0	0	0	6	0	0	0	8	29	39	30	11	0	0	0	18	9	42	13	13	0
			60	0	0	0	0	0	0	0	0	0	10	29	42	28	6	0	0	0	15	0	18	15	12	0
	G. hirsutum	FM966	8	19	0	0	0	32	31	18	0	11	7	92	86	73	50	10	0	0	15	5	29	35	13	0
			10	19	0	0	0	34	32	25	0	11	9	90	84	72	49	10	0	0	17	11	45	34	15	0
			13	21	0	0	0	29	32	18	0	6	14	91	85	73	48	8	0	10	21	18	58	36	26	0
			15	17	0	0	0	20	27	6	0	8	15	73	73	54	33	7	6	13	23	25	74	29	9	0
			17	0	0	0	0	0	9	0	0	0	7	62	67	51	30	6	0	6	18	35	93	31	25	0
			20	0	0	0	0	0	6	0	0	0	9	64	63	48	37	7	0	10	21	27	81	25	17	0
			23	0	0	0	0	0	0	0	0	0	7	45	51	38	22	0	0	7	19	22	72	21	15	0
			25	0	0	0	0	0	0	0	0	0	6	49	48	35	27	0	0	7	14	16	59	10	9	0
			30	0	0	0	0	0	12	0	0	0	7	23	38	29	6	0	0	0	12	13	58	11	7	0
			40	0	0	0	0	0	0	0	0	0	7	28	40	31	0	0	0	0	12	10	47	9	8	0
			60	0	0	0	0	0	0	0	0	0	7	30	39	29	0	0	0	0	10	0	20	9	9	0
	G. herbaceum	Krasnyj	8	36	0	0	0	53	48	41	0	14	23	90	85	66	48	7	0	8	23	9	40	48	29	0
			10	35	0	0	0	55	40	32	0	9	26	86	82	63	49	9	0	9	24	10	45	57	19	0
			13	48	0	0	0	52	45	39	0	9	38	74	75	53	41	5	5	20	35	17	52	60	29	0
			15	31	0	0	0	29	29	25	0	0	24	65	67	46	30	0	9	18	28	21	65	40	25	0
			17	10	0	0	0	8	18	8	0	0	15	60	64	44	21	0	10	21	25	28	80	28	32	0
			20	8	0	0	0	0	18	0	0	0	16	56	59	43	22	0	0	6	23	25	76	24	24	0
			23	0	0	0	0	0	9	0	0	0	10	38	45	36	11	0	0	5	18	21	70	15	21	0
			25	0	0	0	0	0	8	0	0	0	11	38	44	32	12	0	0	0	18	18	63	13	19	0
			30	0	0	0	0	0	8	0	0	0	9	24	34	28	7	0	0	0	17	12	50	11	17	0
			40	0	0	0	0	0	0	0	0	0	13	38	43	34	9	0	0	0	22	0	11	10	18	0
			60	0	0	0	0	0	5	0	0	0	9	23	37	30	0	0	0	0	23	0	9	8	14	0
	G. arboreum	30384	8	35	0	0	0	64	57	27	0	11	23	100	94	77	48	7	11	16	30	12	29	46	23	0
			10	49	0	0	0	70	53	23	0	11	30	96	91	74	49	7	10	16	32	13	33	50	23	0
			13	61	0	0	0	67	48	30	0	9	44	89	85	65	32	0	17	30	42	21	49	43	28	0
			15	33	0	0	0	36	23	10	0	0	25	70	70	49	13	0	10	17	34	25	72	25	16	0
			17	27	0	0	0	25	24	10	0	0	18	58	66	48	16	0	0	9	35	27	81	30	25	0
			20	12	0	0	0	7	10	0	0	0	14	37	49	36	8	0	0	0	28	23	73	16	20	0
			23	8	0	0	0	0	9	0	0	0	12	34	47	35	7	0	0	0	27	19	67	17	20	0
			25	9	0	0	0	0	9	0	0	0	13	39	46	35	8	0	8	15	29	22	63	14	19	0
			30	5	0	0	0	0	6	0	0	0	12	36	38	31	6	0	0	0	25	12	48	10	14	0
			40	0	0	0	0	0	7	0	0	0	11	40	40	30	0	0	0	9	29	10	19	12	15	0
			60	0	0	0	0	0	5	0	0	0	9	27	37	28	0	0	0	0	27	0	20	10	10	0
	G. arboreum	JFW15	8	40	0	0	0	58	62	39	0	14	17	92	90	69	48	8	6	10	23	8	15	26	11	0
			10	59	0	0	0	63	54	39	0	14	21	85	85	63	52	8	0	11	27	9	23	34	25	0
			13	60	6	0	0	45	45	31	0	8	21	73	75	52	33	0	0	8	35	12	45	27	16	0
			15	23	0	0	0	6	9	0	0	0	11	52	54	37	12	0	0	5	21	16	59	11	10	0
			17	0	0	0	0	0	8	0	0	0	7	20	37	32	0	0	0	0	25	20	72	14	24	0
			20	8	0	0	0	0	7	0	0	0	8	28	38	34	7	0	0	0	27	15	61	13	20	0
			23	0	0	0	0	0	0	0	0	0	8	23	32	29	0	0	0	0	24	9	47	10	15	0
			25	0	0	0	0	0	0	0	0	0	8	19	30	28	0	0	0	0	26	9	45	11	15	0
			30	0	0	0	0	0	0	0	0	0	8	24	35	31	5	0	0	0	27	9	42	10	14	0
			40	0	0	0	0	0	6	0	0	0	8	21	32	29	0	0	0	0	22	0	20	9	11	0
			60	9	0	0	0	0	0	0	0	0	8	29	36	30	5	0	0	0	30	0	11	9	11	0

Figure 3-9. Glycan microarray. CDTA and NaOH extractions of cotton fibres at 11 different developmental stages from six different cotton species. DPA: days post anthesis. Mat: mature. Values are means of 9 technical replicates scaled to one maximum value of 100 for all antibodies.

A comparative analysis of these epitope during development and between lines revealed interesting time- and cultivar-dependent profiles as described below.

3.2.5.1 Pectin

Fibre cell walls from all cultivars were generally rich in de-esterified HG (LM19) throughout development. In the CDTA extraction, the LM19 signal increased from 8 to 17 dpa and decreased thereafter for most of the lines. A similar trend was observed with the JIM5 probe which detects a wider range of HG esterification. *G. barbadense* lines PimaS7 and China10 had low amounts of the LM19 and JIM5 epitopes at 8 dpa, whereas the other lines presented a more steady increase from an higher initial amount. This suggests a later de-esterified pectin synthesis or later de-esterification of available esterified pectin (JIM7 and LM20) in the *G. barbadense* lines. On the contrary, the *G. arboreum* JFW15 line showed the lowest relative abundance and an earlier decrease of the LM19 epitope. LM19 and JIM5 epitope dynamics seem to have cultivar-dependent profiles where the generation of de-esterified pectin is slightly delayed in the *G. barbadense* lines.

In addition, highly esterified HG (JIM7) disappearance occurred at earlier stages in the *G. arboreum* lines 30834 and JFW15 (17 and 15 dpa respectively) than in the other lines (25 dpa). Moreover, the LM20 epitope, which binds to HG with a higher degree of esterification than JIM7 could not be detected at 8 dpa and after 17 dpa in the *G. barbadense,* whereas is FM966 and Krasnyj lines this epitope remained at 20 dpa. More interestingly, LM20 is absent in the *G. arboreum* lines at the dpa studied here. This points again at a cultivar-dependent profile of the highly methyl-esterified JIM7 and LM20 epitopes where pectin de-esterification in the *G. arboreum* lines occurs earlier than in other lines which correlates with earlier end of elongation by cell wall stiffening and, therefore, shorter fibre elongation phase associated with shorter fibres.

Similarly to the HG probes, the RG-I-related epitopes LM5, LM6, LM13 and RU2 were more abundant and more persistent throughout development in

the *G. barbadense* lines than in the rest of the lines and the *G. arboreum* JFW15 line showed faster disappearance of these epitopes than any other line. The LM5 and LM6 epitopes were extracted by CDTA as well as by NaOH, suggesting that these epitopes are part of two different glycan environments in the cell wall. On the other hand, the LM13 epitope was mostly found in the NaOH extraction suggesting that this epitope needs harsher conditions than the LM6 epitope to be extracted and might not be necessarily related to it. The HG backbone INRA-RU2 epitope was only present in the CDTA extraction for PimaS7 and China10 and FM966 lines and followed a similar trend to the LM19 HG epitope with lower relative abundance. This suggest a possible positive correlation between the persistence of RG-I side chains in the *G. barbadense* lines and their longer fibres.

3.2.5.2 Xyloglucan

A small proportion of xyloglucan was extracted by CDTA. The xyloglucan LM25 epitope in this extraction was found from 8 to 17 dpa in all lines, except for the JFW15 line (from 8 to 13 dpa only). China10 showed a particularly strong LM15/LM25 signals at 17 dpa, with no obvious trend otherwise. Xyloglucans were mostly obtained in the NaOH and they were abundant throughout development for all lines at early developmental stages decreasing with time. The *G. arboreum* lines 30834 and JFW15 lines showed a faster decrease of this epitope during development. A 50% signal decrease is rapidly reached at 15 dpa by JFW15 fibres and 17 dpa by 30834, whereas xyloglucan content in the PimaS7, China10 and Krasnyj fibres halved at 20 dpa or only at 23 dpa in FM966. Xyloglucans as pectins also showed a cultivar-dependent profile.

CBM3a binding profile is very similar to the LM15 and LM25 epitopes so it has been positioned next to the xyloglucan probes. CBM3a is commonly considered a probe for crystalline cellulose, nevertheless, the glycan binding capacity of this probe is rather peculiar and it is shown in this study to bind efficiently to xyloglucan as well as crystalline cellulose. This is studied and discussed in more detail in Chapter 5 (section 5.2.1).

3.2.5.3 Heteromannan

The heteromannan LM21 epitope was present in all cotton species and peaked at early developmental stages (8 to 10 dpa) except for the *G. barbadense* lines PimaS7 and China10 which showed a slightly delayed occurrence peaking between 13 and 15 dpa. The persistence of the LM21 epitope throughout fibre development has clear cultivar-dependent patterns. In JFW15 (*G. arboreum*), the LM21 signal drops between 10 and 15 dpa whereas in FM966 (*G. hirsutum*) and PimaS7 (*G. barbadense*) similar low levels are only reached at 30 dpa. The *G. herbaceum* line Krasnyj and the *G. arboreum* line 30834 showed a trend in between JFW15 and the other two species. The CBM27 probe could not recognize heteromannans in cotton to the same extent as LM21 suggesting that these two probes might recognize different epitopes of the cotton heteromannan molecule. These experiments added further evidence to demonstrate the presence of heteromannans in the cotton fibre. Analysis of FM966 and JFW15 fibres using ELISA corroborated the dynamics found in the glycan microarray and also demonstrated that LM21 binding was sensitive to the action a recombinant mannanase (Figure 3-10).

3.2.5.4 Heteroxylan

The amount of the xylan LM10 and LM11 epitopes found in cotton fibres was very low and only the glucuronoxylan LM28 and the arabinoxylan AX1 were taken into consideration. Low relative amounts of the glucuronoxylan LM28 epitope could be extracted with CDTA only from 13 to 17 dpa for all lines, whereas in the NaOH extraction the LM28 epitope was present at very similar levels throughout development in all lines. On the other hand, the arabinoxylan AX1 signal increased during the primary cell wall stage reaching a maximum at 17 dpa for all cotton species, except China10, and decreasing later during development with the levels in mature fibre being below the detection limit. JFW15 (*G. arboreum*) had the lowest relative amounts of the AX1 epitope.
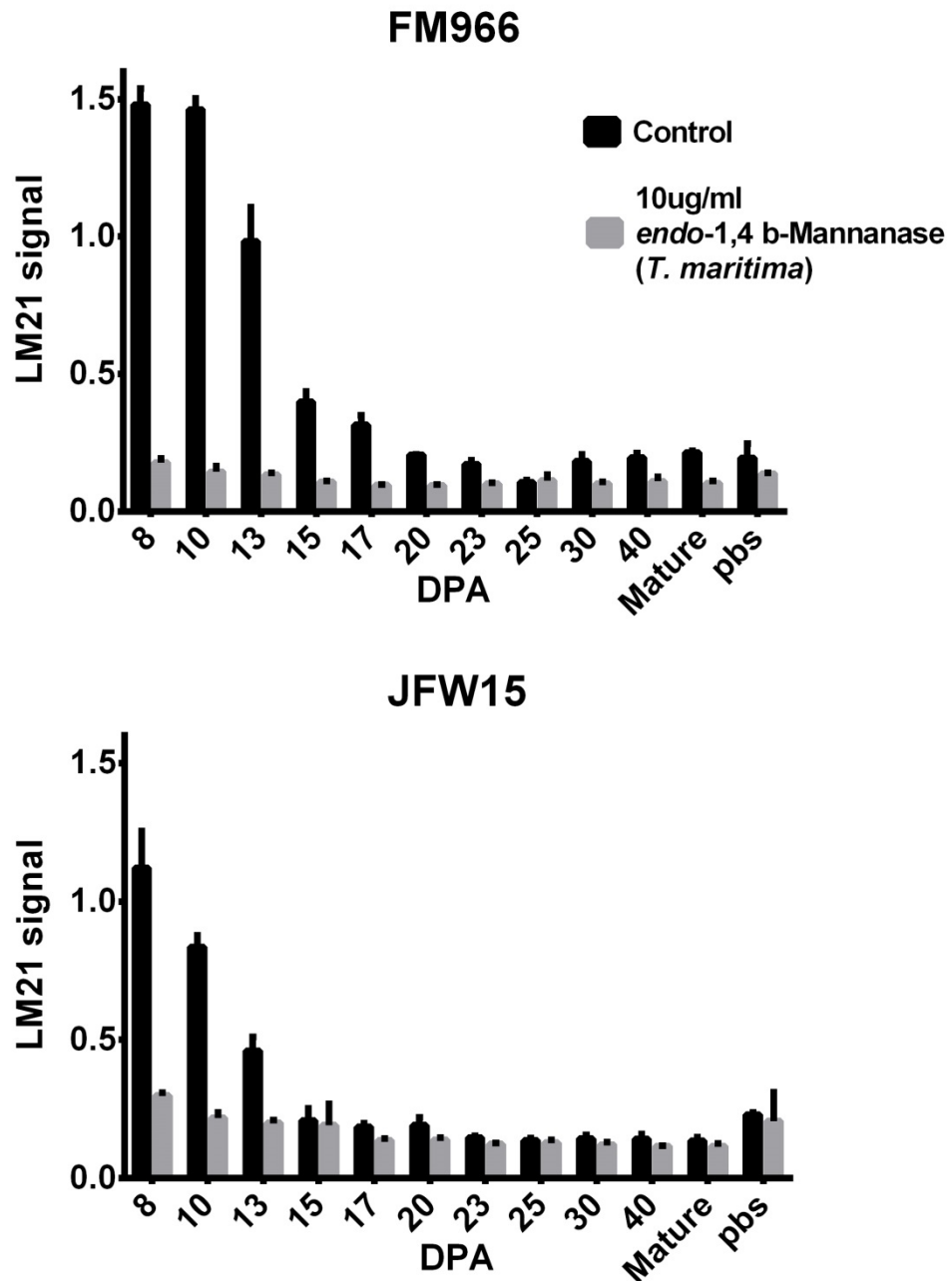
Figure 3-10. Enzymatic digestion of the LM21 mannan epitope in cell wall extracts of FM966 and JFW15 fibres at 11 time points. ELISA plates coated with equivalent amounts of NaOH cell wall extract of developing cotton fibres from FM966 (left) and JFW15 (right) were treated with endo-1,4 β-mannanase (from *T. maritima*). Control refers to LM21 signal with no enzyme and buffer only (50 mM MOPS pH. 7.0).

These results suggest that xylan-related epitopes such as the glucuronoxylan LM28 and the heteroxylan AX1 epitopes must be synthesized later in development than other polysaccharides described so far and that they less obvious cultivar-dependent profile in favour of a time-dependent profile.

Nevertheless, the China10 profile appears particularly contradictory to this suggestion, since the AX1 epitope showed two signal peaks, one at 13 dpa and another at 20 dpa, whereas signal is extremely low at 15 and 17 dpa. An experimental artefact is possible although other probes such as the pectin related ones were not affected at 17 dpa or even showed a significant strong signal at this stage as in the case of the xyloglucan probes.

3.2.5.5 Callose

Callose (BS400-2) was partially extracted in CDTA between 8 and 25 dpa but mostly found in the NaOH extraction showing a similar trend to the AX1 xylan epitope. The callose signal peaked at 17 dpa for all lines (except in China10) suggesting a possible time-dependent profile for the callose epitope.

3.2.5.6 Arabinogalactan-proteins and extensins

The AGP JIM13 epitope was abundant in the CDTA extraction and its signal decreased steadily from 8 to 30 dpa in all lines with no significant differences among lines. The same trend was observed in the NaOH extraction although the *G. arboreum* JFW15 line showed relatively lower levels of this epitope.

The JIM20 probe identifies specific arabinosylation patterns of cell wall extensins, and its signal was primarily detected in the CDTA extraction only after 17 dpa for all lines suggesting that extensin might be correlated to the end of fibre elongation. Lower relative amounts were found in the NaOH extraction and slightly higher signals were observed between 13 and 20 dpa in the PimaS7 and China10 *G. barbadense* lines and between 8 to 20 dpa for the rest of the lines.

In summary, these data suggest that the relative abundance of mainly many pectic and some hemicellulosic glycan epitopes in developing fibres is cultivar-dependent and suggest a possible correlation to fibre quality.

3.2.6 Correlation analysis between fibre quality parameters and glycan epitope developmental profiles

A basic correlation study between physical properties and the abundance of each glycan epitope during fibre development of all lines was carried out to recapitulate data in 3.2.1 and 3.2.2 in a visual, simpler way and as tentative study on how fibre polysaccharide developmental profiles may associate with fibre qualities. BS400-3, LM16 and LM10 probes were not present in cotton fibres and were excluded from this analysis.

As correlations for each time point (dpa) cannot render statistical biological significance, correlations were studied in two developmental phases: fibre elongation (8 to 17 dpa) and secondary cell wall deposition (17 to 60 dpa). To condense several data points into relevant information from each of these two phases, one value for each of these two developmental phases was extracted by calculating the approximation to the integral (area under a curve or Riemann Sums) between the time points limits 8-17 and 17-60. These areas represent the accumulation of epitope signal quantities at the elongation phase and at the secondary cell wall deposition phase.

An example for the JIM7 epitope can be found in Figure 3-11. The area (approximated by rectangles) under the curve between 8 at 17 dpa is the cumulative JIM7 signal value for a cotton cultivar during the elongation phase, and between 17 and 60 dpa during the secondary cell wall deposition phase. All the cumulative values of each epitope can be found in Table 3-2.

These values were correlated to fibre micronaire, elongation, short fibre content, length, length uniformity and strength values and correlation coefficients (Pearson's r) are represented in Figure 3-12.

The aim of this exploratory analysis was to point at high positive and negative correlations ($r =0.8$ has been marked as an indicative threshold) between fibre quality and glycan epitopes at these two stages.
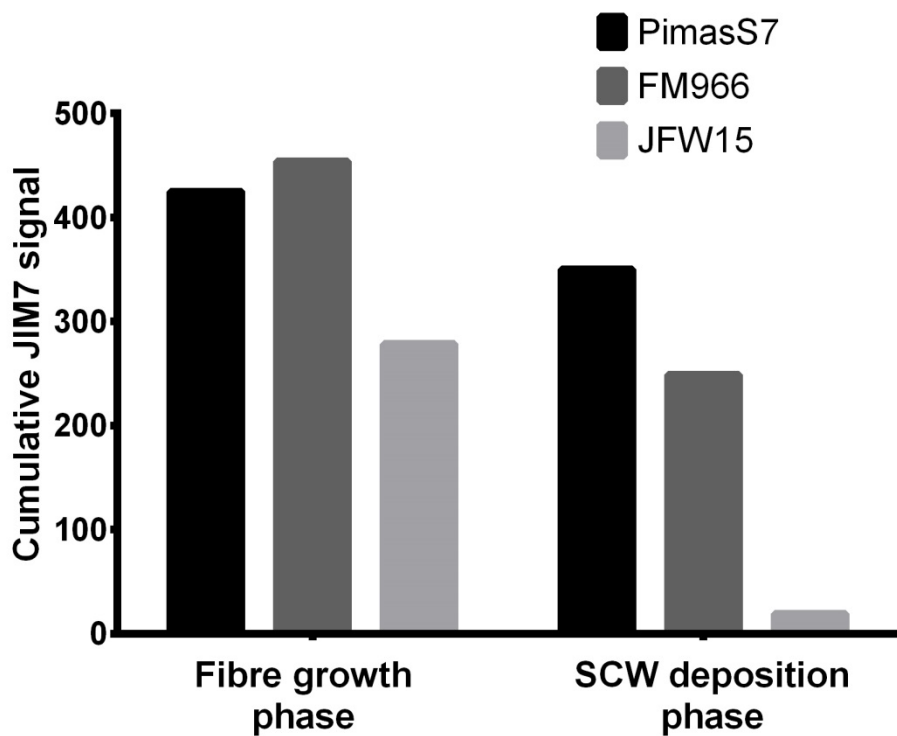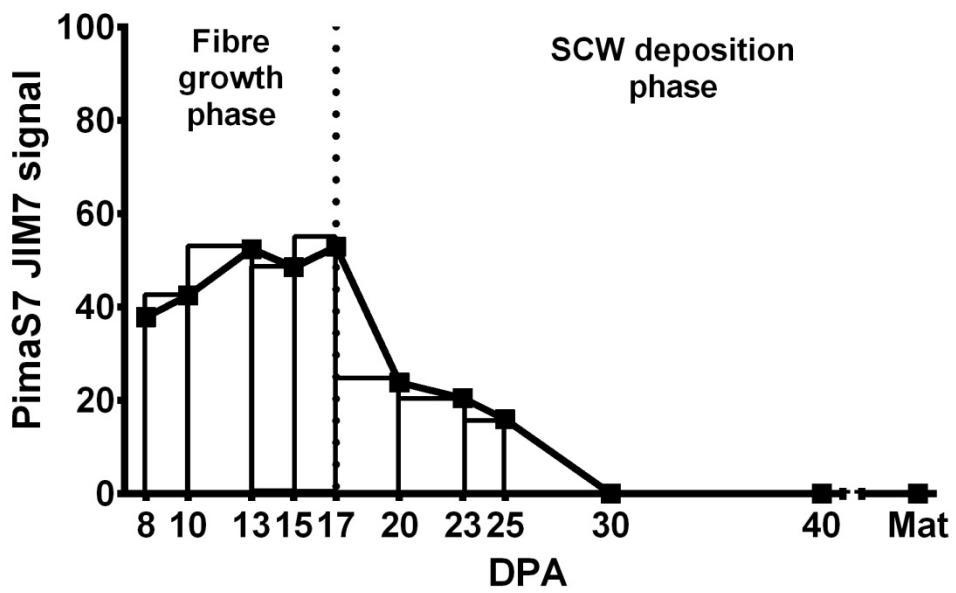
Figure 3-11. Example of integration for the JIM7 epitope in three cotton cultivars. A. Graphic representation of the Riemann Sum for the JIM7 signal epitope in PimaS7. B. JIM7 cumulative values used in the correlation analysis for each developmental phase in PimaS7, FM966 and JFW15.

Table 3-2. Cumulative values during fibre growth and SCW deposition phase per epitope in each cotton cultivar

Cumulative epitope signal in the CDTA extraction

Elongation phase

	LM19	JIM5	LM20	JIM7	RU2	LM5	LM6	LM13	LM15	LM25	LM21	CBM27	LM11	PDT5	AX1	BS-400-2	JIM13	JIM20
30384	421.9	153.1	29.2	320.2	0.0	148.4	225.3	15.7	61.8	245.3	0.0	0.0	32.8	166.7	10.2	251.2	425.8	75.3
China 10	653.1	209.2	245.4	487.3	113.4	269.5	362.3	189.3	169.6	302.6	0.0	0.0	13.0	180.9	15.4	221.6	453.2	224.3
FM 966	544.0	179.3	249.9	453.8	101.3	131.3	252.3	50.0	58.8	179.4	0.0	0.0	0.0	73.6	29.4	240.8	486.4	94.5
JFW 15	347.5	81.8	0.0	278.3	0.0	113.3	251.6	40.3	53.3	204.5	0.0	0.0	0.0	88.7	13.2	242.7	419.9	86.7
Krasnyj	547.8	158.6	171.9	414.3	0.0	118.6	235.6	71.9	85.0	247.8	0.0	0.0	0.0	42.3	17.3	260.8	503.9	146.0
PimaS 7	470.6	154.4	162.8	424.9	97.9	247.1	309.3	74.7	118.8	272.5	0.0	0.0	0.0	71.8	6.1	195.0	408.8	92.5

Secondary cell wall deposition phase

	LM19	JIM5	LM20	JIM7	RU2	LM5	LM6	LM13	LM15	LM25	LM21	CBM27	LM11	PDT5	AX1	BS-400-2	JIM13	JIM20
30384	1215.8	496.4	0.0	98.2	0.0	16.0	92.9	0.0	0.0	12.0	0.0	0.0	0.0	514.1	0.0	93.7	774.6	395.1
China 10	1525.6	291.6	74.1	349.9	81.1	67.1	152.3	42.6	115.3	127.2	0.0	0.0	0.0	27.1	0.0	212.5	928.6	471.4
FM 966	1336.1	269.8	108.3	248.8	82.6	12.2	43.2	0.0	0.0	48.4	0.0	0.0	0.0	11.9	0.0	177.9	903.2	370.4
JFW 15	539.4	240.6	0.0	19.1	0.0	0.0	0.0	0.0	0.0	0.0	0.0	0.0	0.0	95.1	0.0	34.6	512.3	241.0
Krasnyj	1583.5	399.6	54.9	413.0	0.0	8.2	168.6	28.5	0.0	35.5	0.0	0.0	0.0	44.2	0.0	107.5	536.1	649.5
PimaS 7	1553.0	409.5	33.0	257.6	96.0	81.5	161.9	46.2	7.9	29.7	0.0	0.0	0.0	61.4	9.2	144.4	688.1	355.7

Cumulative epitope signal in the NaOH extraction

Elongation phase

	LM19	JIM5	LM20	JIM7	RU2	LM5	LM6	LM13	LM15	LM25	LM21	CBM27	LM11	PDT5	AX1	BS-400-2	JIM13	JIM20
30384	169.9	0.0	0.0	0.0	0.0	60.1	317.6	14.7	1556.2	1776.9	142.5	0.0	318.3	1200.0	469.4	1584.0	542.9	637.7
China 10	21.1	0.0	0.0	0.0	10.5	55.5	310.9	37.4	1415.8	1834.9	691.9	15.6	112.1	826.7	482.4	1974.5	642.3	610.3
FM 966	0.0	0.0	0.0	0.0	0.0	0.0	124.5	0.0	1458.9	1850.8	349.5	30.4	79.0	554.6	492.9	2113.9	514.0	420.6
JFW 15	114.3	0.0	0.0	0.0	0.0	0.0	121.3	0.0	1019.2	1451.9	116.0	0.0	0.0	1097.0	197.3	1285.6	419.8	565.3
Krasnyj	40.6	0.0	0.0	0.0	0.0	12.6	336.0	12.5	1460.2	1805.3	355.7	0.0	63.6	904.4	318.6	1383.1	504.4	767.5
PimaS 7	39.0	0.0	0.0	0.0	19.6	52.4	352.3	55.2	1617.7	2026.2	839.8	87.6	29.0	736.4	468.0	2191.9	611.7	482.3

Secondary cell wall deposition phase

	LM19	JIM5	LM20	JIM7	RU2	LM5	LM6	LM13	LM15	LM25	LM21	CBM27	LM11	PDT5	AX1	BS-400-2	JIM13	JIM20
30384	401.9	0.0	0.0	0.0	62.5	503.2	378.0	190.4	759.8	741.8	293.2	24.2	176.4	318.8	171.6	458.6	360.3	205.5
China 10	211.6	0.0	0.0	0.0	144.0	359.1	437.2	371.3	659.4	668.9	418.3	66.4	127.2	270.3	155.1	514.1	288.7	186.1
FM 966	154.4	0.0	0.0	0.0	68.5	229.5	254.3	137.8	752.3	719.9	387.5	72.3	55.5	173.5	163.1	529.2	299.6	157.2
JFW 15	381.8	14.6	0.0	0.0	71.3	341.3	335.3	214.0	611.7	635.5	284.1	27.5	66.2	246.7	111.2	374.8	212.1	157.6
Krasnyj	314.4	0.0	0.0	0.0	58.7	390.0	336.7	277.7	679.0	676.5	355.2	42.1	135.5	251.2	146.9	489.9	449.5	231.9
PimaS 7	305.1	0.0	0.0	0.0	198.9	495.5	483.0	366.3	699.6	725.2	474.9	85.0	19.1	226.4	110.2	504.4	297.2	137.7

In general, most glycan epitopes tend to correlate positively with fibre length, strength and uniformity and negatively with fibre micronaire, elongation and short fibre content.

Most epitopes correlate positively with fibre quality. However, some epitopes show opposite correlations to the rest of the epitopes. For example, the glucuronoxylan LM28 epitope, the extensin JIM20 epitope and the NaOH extracted de-esterified HG epitopes (LM19 and JIM5), have a negative influence on fibre quality. In addition, pectic and heteromannan epitopes tend to be more significant during the fibre elongation phase and xyloglucans and xylans during the secondary cell wall phase.

During fibre growth, higher amounts of the pectic HG epitopes LM19, JIM5, LM20 and JIM7 were associated with higher fibre uniformity and length but not to strength, and with lower micronaire and short fibre content but not with lower fibre elongation. The RG-I related RU2 and LM5 epitopes only showed significant positive correlation with fibre length and strength to which mostly the CDTA extraction contributed in the case of LM5. Also, the heteromannan LM21 and CBM27 epitopes were correlated with longer, stronger and more uniform fibres.

During secondary cell wall deposition, xyloglucans appear to be highly associated with all quality fibre parameters, whereas the heteromannan LM21 epitope is only positively correlated with fibre length and strength. The arabinoxylan AX1 epitope does not show any important correlation during fibre elongation but it is significantly related to all fibre characteristics, except fibre micronaire, during secondary cell wall deposition. Similarly, the AGP JIM13 epitope was associated to length, strength and uniformity during secondary cell wall deposition but not during fibre growth. Although the glucuronoxylan LM28 epitope does not have a strong connection with any fibre characteristic, it showed opposite tendency to the rest of epitopes as previously mentioned. Together with the LM28, the extensin JIM20 epitope were the two epitopes negatively correlated to fibre length, strength, elongation and uniformity. Unlike LM28, the JIM20 epitope is also negatively associated with fibre micronaire and short fibre content.

Length 8-17 dpa

Length 17-60 dpa

Strength 8-17 dpa

Strength 17-60 dpa

Length uniformity 8-17 dpa

Length uniformity 17-60 dpa
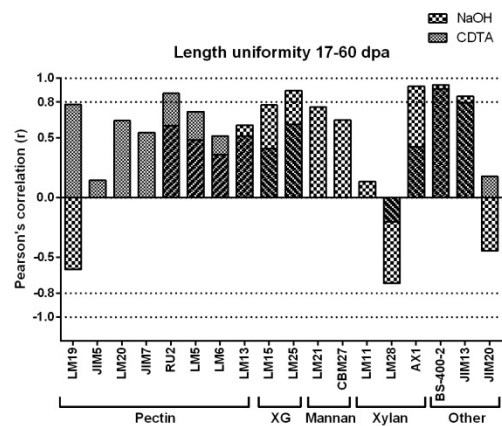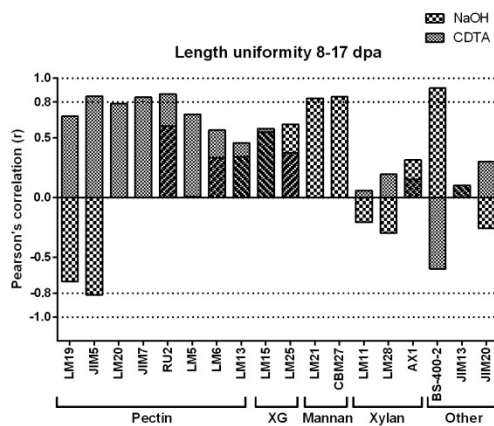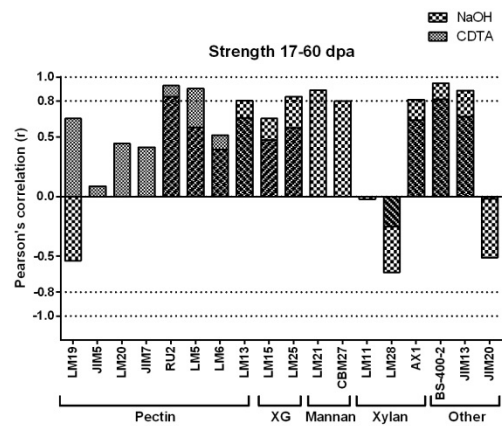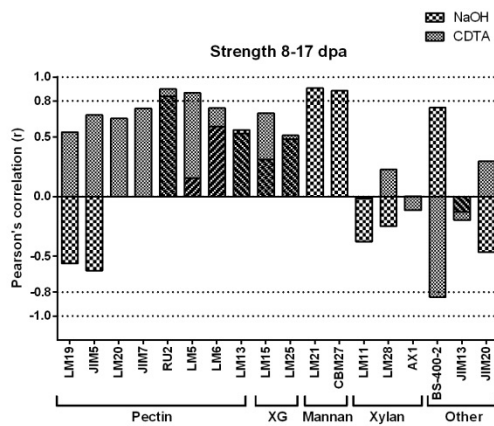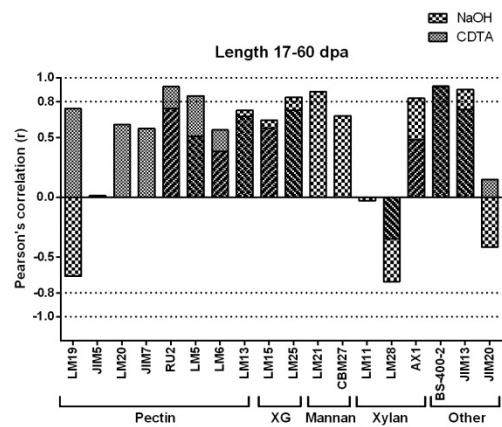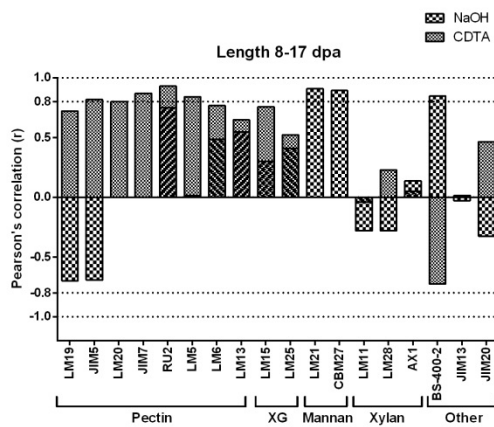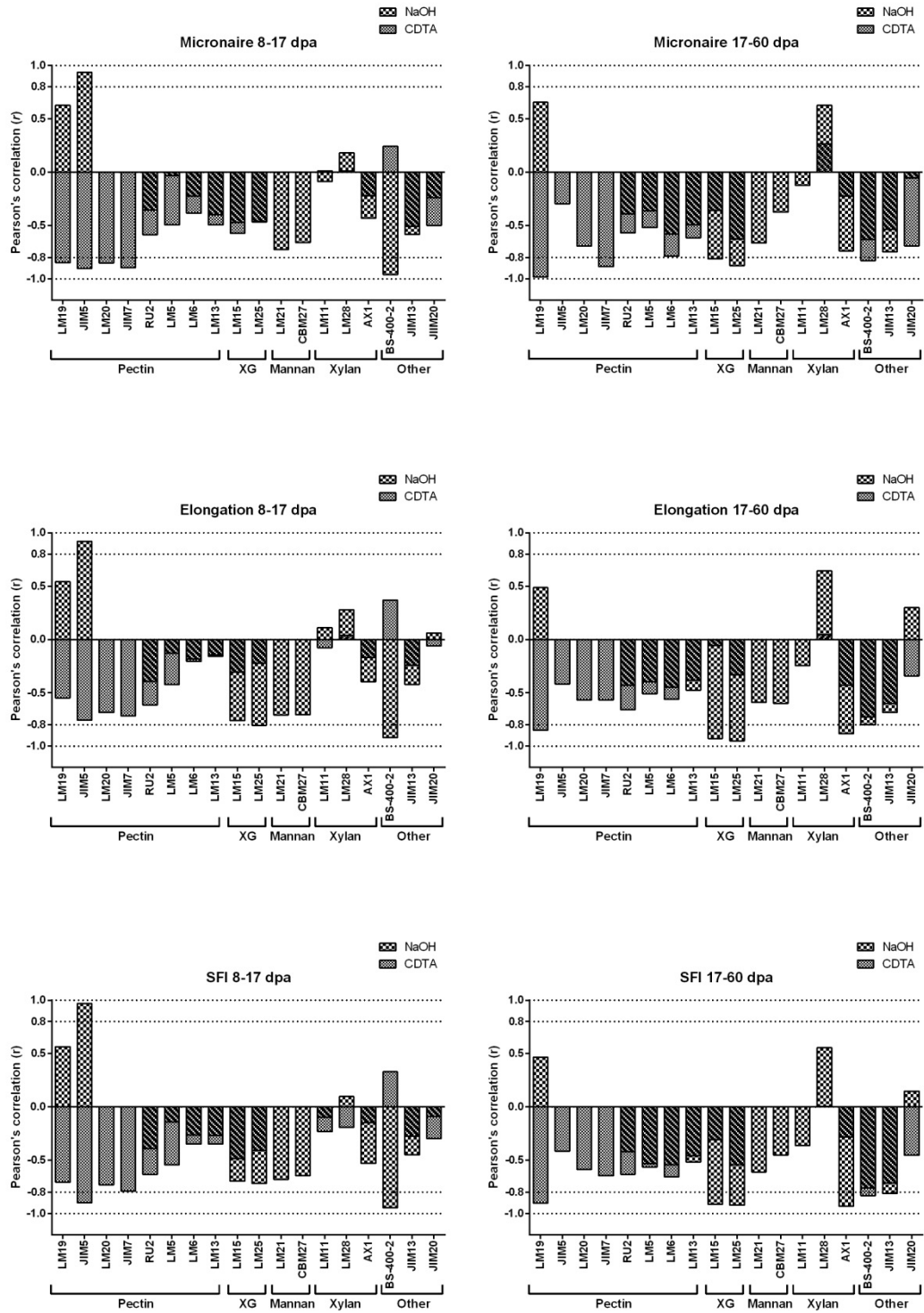
Figure 3-12. Correlation coefficient values. Pearson's *r* correlation values between epitopes and the fibre quality characteristics at the elongation (left column) and secondary cell wall deposition (right column) phases. Dotted line: indicative threshold of *r* =0.8. XG: xyloglucan. SFI: short fibre content.

100

3.3 Discussion

3.3.1 The JFW15 cultivar undergoes fast fibre development which correlates with its poor fibre quality.

JFW15 (*G. arboreum*) is not suitable for textile processing due to its high micronaire and poor fibre length and strength. These results demonstrated clear differences in the pace of development followed by JFW15. When compared to a commercial line such as FM966, JFW15 shows an earlier start (before 17 dpa) of secondary cell wall deposition and a thicker secondary cell wall at equivalent days post anthesis. These results suggest that the shorter and extra-thickened fibres of this line are associated with a shorter elongation phase and an extensive secondary cell wall phase with a higher cellulose deposition rate.

In addition to JFW15, Krasnyj (*G. herbaceum*) also showed significantly higher rate of cellulose deposition with much thicker cell walls at equivalent dpa compared to *G. barbadense* and *G. hirsutum*. Nonetheless, the secondary cell wall thickness of mature Krasnyj fibres did not differ significantly from those of FM966 indicating that Krasnyj cellulose deposition rate eventually slows down. This suggests that the cellular mechanisms that control the rate of cellulose deposition (Lei et al., 2012) are severely compromised in the JFW15 line and that aspects of this mechanism can be uncoupled. Several transcription factors have been identified as regulators of secondary cell wall synthesis, such some MYB and NAC domain transcription factors (Zhong et al., 2008; Wang et al., 2014; Zhong and Ye, 2014). Upstream regulatory steps of cellulose deposition lay in the control of transport, assembly and activity of the cellulose synthase complex through multiple pathways from direct phosphorylation (Chen et al., 2010) to endocytosis (Bashline et al., 2013) and microtubule cytoskeleton regulators (Lei et al., 2013). It is possible that the JFW15 cultivar is affected at any of these secondary cell wall deposition steps and further comparative studies at the transcriptome level (at several stages during secondary cell wall deposition) might help to elucidate this.

The JFW15 fibre has an extra-thick secondary cell wall and yet is very weak compared to fibres from other lines. The reason for this apparent contradiction may lay in the cell wall reversals. Reversals have been proposed as localised areas of cell expansion after the secondary cell wall is deposited and their frequency along the fibre depends on germplasm and developmental stage (Wakeham and Spicer, 1951). Reversals have been traditionally considered as weak points prone to breakage (Raes et al., 1968; Seagull, 1986) however, bundle strength can vary depending on the type of reversal and their frequency (Gould and Seagull, 2002). In fact, it is known that *G. arboreum* lines with thicker secondary cell walls have fewer reversals than any *G. hirsutum* line and improved *G. arboreum* lines with thicker cell walls but higher reversal frequency have been achieved (Chandra and Sreenivasan, 2011).

Furthermore, very few CFML regions between cells in the JFW15 line were observed and those present were filled with less material. A deficiency of CFML would negatively affect fibre adhesion and therefore fibre ability to achieve parallel lengths contributing to the lower length uniformity in the JFW15 line.

3.3.2 A delayed transition phase associates with high quality fibres

Extra-long high quality fibres belonging to the tetraploid species *G. barbadense* showed a time-extended presence of pectic, xyloglucan and heteromannan epitopes compared to other lines, suggesting a positive correlation of these polysaccharides with an extended fibre elongation phase (or a delayed transition phase) and thus longer fibres. However, *G. barbadense* cell wall cross sections showed significant cellulose deposition at 17 dpa compared to *G. hirsutum,* indicating an earlier start of secondary cell wall deposition in *G. barbadense.* Higher fibre length in *G. barbadense* could be due to a more efficient elongation rate even during a shorter period than in *G. hirsutum,* however this cannot not be confirmed unless fibre lengths measurements at developmental stages are performed. Based on previous literature where the fibre length of *G. barbadense* and *G. hirsutum*

lines and the rate of elongation was measured during development (Seagull et al., 2000; Chen et al., 2012), *G. barbadense* seemed to pass *G. hirsutum* cultivars in length only during the start of secondary cell wall formation, which has been explained by late fibre elongation through tip growth (Meinert and Delmer, 1977; Stewart et al., 2010; Stiff and Haigler, 2012) and it is possible that *G. barbadense* fibres use this system to increase significantly their final length.

3.3.3 Glycan epitopes can be used as markers of the end of cell wall elongation

While pectin, xyloglucan and heteromannan epitopes showed a line-dependent profile, other epitopes such as the callose BS400-2, extensin JIM20, arabinoxylan AX1 and glucuronoxylan LM28 showed a very specific time-dependent profile with no obvious influence depending on cotton cultivar/species.

The extensin JIM20 epitope appeared in cotton fibres after 17 dpa (20 dpa in the *G. barbadense* China10 line only) suggesting the association of extensins with the end of elongation. High extensin levels and cessation of cell elongation have been frequently reported. Accumulation of extensins is observed when growth is reduced in pea epicotyls (Sadava and Chrispeels, 1973) and small Arabidopsis inflorescence length associated with increased extensin levels (Roberts and Shirsat, 2006). More recently, overexpression of a cotton fibre-specific gene GhPRP5, encoding a lightly glycosylated proline-rich protein, in Arabidopsis plants reduced cell growth while knockdowns by RNA interference in cotton enhanced fibre elongation (Xu et al., 2013). Extensins are proteins that can crosslink via acid-base interactions or possibly via covalent links to other polysaccharides such as pectin, locking them into place and contributing to the end of cell wall expansion (Wilson and Fry, 1986; Lamport et al., 2011).

Callose (showed both by the BS400-2 probe and linkage analysis) also showed a prominent time-dependent profile of higher abundance at 17 dpa, suggesting a time specific regulation of callose synthesis and an uncoupling

of callose production and secondary cell wall deposition in the JWF15 line is difficult to explain.

Similarly to the extensin JIM20 and callose epitopes, the heteroxylan AX1 epitope also showed a peak at 17 dpa for all lines suggesting a later synthesis of this epitope compared to other hemicelluloses such as xyloglucans or heteromannans and points to a role of this polysaccharide during cellulose deposition.

Further discussion on the glycan arrays profiles compared to an extended immunohistochemical analysis using these same probes on cotton sections follows in Chapter 5.

3.3.4 Relationship between days post anthesis and fibre development events

After comparing fibre tissue morphologies in six cotton lines at several days post anthesis, it was observed that the timing of cell adherence through the CFML and the transition phase, as well as the speed at which cellulose is deposited in the secondary cell wall were the main morphological variables in fibre development.

The timing of fibre development have been traditionally defined in days post anthesis (dpa). In the case of the worldwide cultivated cultivars from *G. hirsutum* species, it is well established that fibre initiation occurs from 0 to 3 dpa, fibre elongation continues until 17 dpa, transition from fibre elongation to secondary cell wall thickening occurs from 17 to 20 dpa and secondary cell wall deposition carries on until 50-55 dpa (Basra, 2000; Stiff and Haigler, 2012). Here, it is shown that fibre developmental pace differs between cultivars from different species when grown at the same time in equivalent conditions. The relationship between dpa and developmental events in JFW15 differed significantly from the other lines analysed here. Moreover, fibre development can vary within the same cotton line when grown at different temperature as shown in 3.2.5. This means that choosing days post anthesis as the system to standardise studies in cotton fibre development can strongly confuse cross referencing between studies and the

interpretation of results. Perhaps glycan profiling would serve as a more suitable tool to describe fibre development.

3.3.5 Limits of the semi-quantitative techniques used in this work

The non-synchronous fibre development between cultivars was also reflected in their monosaccharide, linkage and glycan developmental profiles. Cultivar-dependent profiles were altered by differences in cellulose content in the secondary cell wall. Cellulose increased sample dry weight, which in turn diluted the amount of other polysaccharides per weight unit. For example, JFW15 extra-thickened secondary cell walls accounted to some extent for the earlier disappearance of glycans during development compared to other lines when analysed by glycan microarrays, monosaccharide and linkage analyses. A solution to this dilution effect would have been digesting cellulose with, for example, the fungal enzyme mixture Driselase (Sigma) after treatment of cell walls with 2 M TFA during the preparation of the alditol acetates. This would have allowed us to compare more accurately the veracity of time-dependent dynamics of sugars and linkages during development between lines that could have guided in the design of the glycan microarray experiments and data analysis.

On the other hand, secondary cell wall measurements demonstrated that cell wall thickness is only significant in JFW15 from 17 dpa onwards when compared to the commercial line FM966. In addition, glycan arrays and sugar linkage analysis showed that some epitopes such as AX1, JIM20, BS400-2 (also supported by the callose linkage analysis) are not yet affected by the amount of secondary cell wall and peaked at 17 dpa even in the extra matured JFW15 line. This suggests that the results up to 17 dpa reflect the actual relative content of monosaccharide, linkages and epitopes in cotton fibres. On the other hand, the uncoupling of the dynamics of these epitopes with the start of secondary cell wall deposition raises important biological questions at how the synthesis of this epitopes is regulated.

Additionally, it is important to take into account that a percentage of the total amount of the polysaccharides analysed through these techniques were lost during the processing of the samples material. Some soluble polysaccharides lightly embedded in the cell wall were released during the ethanol boiling step and, therefore, are not represented in the glycan array profile, as only the CDTA and NaOH extractions were analysed.

As regards to the linkage analysis results, highly variation between technical replicates were found mainly for the 30834 line, unfortunately these experiments could not be repeated due to the limiting amounts of material.

Finally, the exploratory statistical correlation analysis showed very similar correlations between properties and epitopes, this was expected as fibre properties are highly associated with each other. Nevertheless, this analysis pointed at possible interesting targets to be considered for fibre quality improvement. For example, the JIM20 and LM28 epitopes were negatively correlated to good quality parameters. Extensins and glucuronoxylan are involved in cessation of cell elongation. An approach to extend in time the elongation phase targeting this cell wall components could be useful in order to improve fibre quality.

Chapter IV

4 Immunochemical characterization of glycans present in developing and mature cotton fibre cell walls

4.1 Introduction

The synthesis of cell wall components and their remodelling in the cotton fibre are finely regulated processes that allow extensive cell elongation and cell wall maturation. In the previous chapter, the fibre tissue morphology of six cultivars from four different species using Calcofluor White staining on fibre sections and the overall developmental changes of several cell wall epitopes by glycan microarrays were described. This chapter focuses on the analysis of these cell wall glycan epitopes during fibre development, looking into the details of their immunolocalization and their possible roles in fibre development.

The first 4.2.1 section is dedicated to the cotton fibre middle lamella (CFML) with detailed data on its morphology during development and composition. Sections 4.2.2 to 4.2.7 focus on the immunolocalization of pectin, xyloglucan, arabinogalactan-proteins, heteromannan, heteroxylan and callose epitopes. The last section 4.2.8 explores the use of epitope detection chromatography, a newly developed technique (Cornuault et al., 2014), to study the biochemical changes occurring in the cell wall polysaccharides during fibre development.

The discussion section intends to bring together the results and the known concepts relating to the possible role of each polysaccharide in cell wall formation and remodelling during cotton fibre development. Suggestions for future work are also addressed through the discussion.

4.2 Results

4.2.1 Characterization of the cotton fibre middle lamella (CFML)

In the previous chapter, Calcofluor White staining of fibre sections revealed two different structures in the fibre tissue as part of the fibre middle lamella. One of these structures has been referred to as enlarged regions of the CFML and the other as paired CFML bulges. Although similar enlarged regions of the CFML were present in all cotton species and cultivars analysed here, *G. arboreum* had much fewer of them. Paired CFML bulges were only evident in *G. hirsutum* and while *G. barbadense* showed some single CFML bulges randomly distributed around the fibre tissue, *G. arboreum* did not display similar CFML bulges between fibre cell walls.

4.2.1.1 CFML morphology in the fibre tissue

Any CFML area bigger than 2 µm in diameter is referred to as an enlarged CFML region. These regions in sections are oval-shaped intercellular spaces filled with particles stained by Calcofluor White. During fast elongation the fibre tissue sometimes presented disrupted areas filled with CFML material as indicated in yellow in Figure 4-1A. The size of enlarged CFML regions was very variable within the same tissue and its major axis usually ranged between 2 and 10 µm in transverse sections (arrowheads in Figure 4-1B). The second structure mainly observed in *G. hirsutum* cultivars and referred as CFML bulges consisted of a remarkably repetitive pattern of two highly Calcofluor White fluorescent spots between two adjacent fibre cell walls throughout the fibre tissue (arrows in Figure 4-1B). These bulges were small, 1 µm or less, and their morphology resembled the CFML as previously described in Singh et al. (2009) although their paired pattern has never been addressed. Enlarged CFML regions could be seen in both longitudinal and transversal fibre sections, suggesting large three dimensional structures (arrowheads Figure 4-1) whereas CFML bulges were found in serial cross sections leading to the idea that each spot is indicative of an actual stripe

along the fibre and this was observed in longitudinal sections (arrow in Figure 4-1C).

The CFML was also present in fibres grown from cultured ovules of FM966 (Figure 4-1D) suggesting that the formation of the CFML does not require the fibres to be inside the locule and that is created from material exocytosed by the fibre cell. Moreover, the arrangement of the CFML in pairs must be defined by the adjacent fibre cells and not by other vegetative parts of the boll.
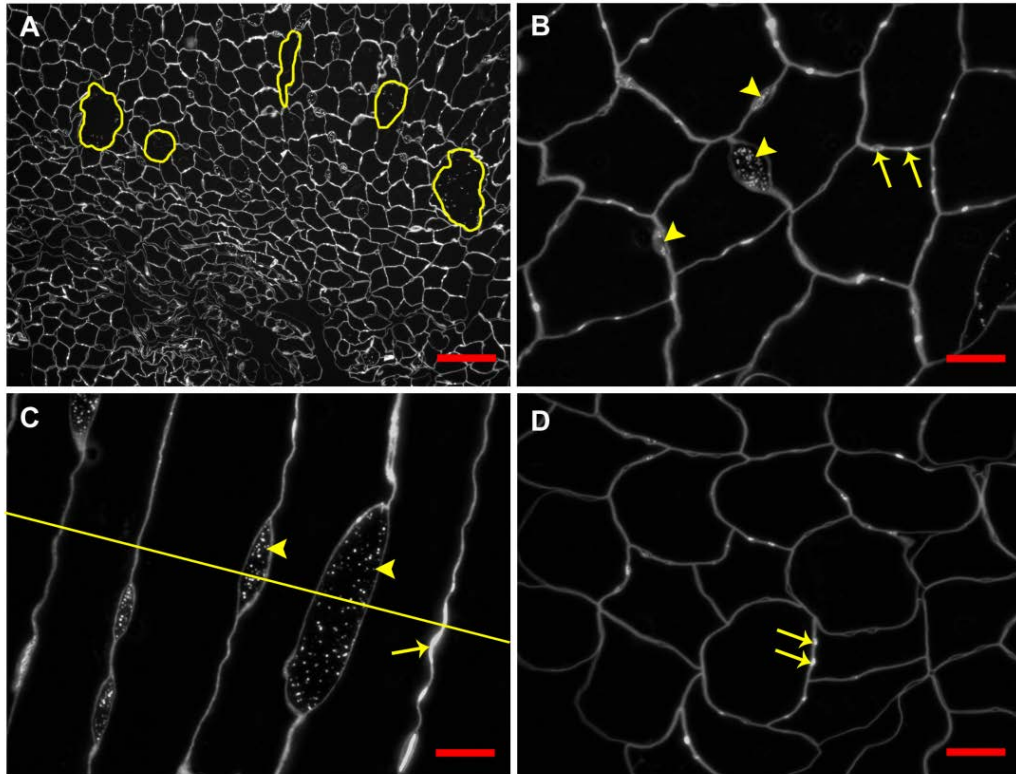
Figure 4-1. Cotton fibre middle lamella (CFML) structures. A. Fibre tissue of 15 dpa FM966 fibres (Batch1). Disrupted areas are outlined in yellow. B. Transversal section of 15 dpa FM966 fibres (Batch 1). Enlarged CFML regions (arrowheads) displayed variable sizes whereas the CFML paired bulges (arrows) were smaller than 1 μm. C. Longitudinal section of 15 dpa FM966 fibres (Batch1) showing the three dimensional structure of the enlarged CFML regions (arrowheads) and a longitudinal stripe along the fibre in the case of the CFML bulges (arrow). An indicated cross section of these fibres following the yellow line would show the image equivalent to B. D. 14 dpa cultured fibres from FM966 ovules. Fibres were completely adhered paired CFML bulges were also observed in the fibre tissue. Scale bar panel A: 50 μm. Scale bar panels B, C and D: 10 μm.

4.2.1.2 CFML dynamics during fibre development

The changes of the CFML during fibre development in FM966 (*G. hirsutum*) fibres from Batch 2 labelled with the xyloglucan LM15 probe is shown in Figure 4-2. Abundant enlarged CFML regions were observed as soon as fibre cells start adhering and they were present in the fibre tissue throughout fibre elongation (arrowhead in Figure 4-2A). Similarly, CFML bulges appeared with cell adhesion sporadically as single or paired bulges (arrows in Figure 4-2A). At the onset of secondary cell wall deposition fewer enlarged CFML regions were observed in favour of abundant CFML bulges between most cells and mostly paired (Figure 4-2B). CFML was degraded after cell adhesion as it is no longer needed during secondary cell wall deposition (Figure 4-2C), nevertheless, remnants of the CFML bulges were still visible at an advanced secondary cell wall phase (arrows in Figure 4-2D). The CFML changes with fibre development and consequently the timing of the event differs between cultivars and also depends on growing conditions, as previously discussed in Chapter 4. Although at a different pace, the same CFML dynamics were found in the other FM966 batches and in the also *G. hirsutum* line Coker (shown by LM25 labelling in Figure 4-14). On the other hand, the paired CFML bulges were not obvious in the PimaS7 and China10 (*G. barbadense*), Krasnyj (*G. herbaceum*) and JFW15 (*G. arboreum*) lines which suggests that this arrangement of the CFML in pairs is specific of the *G. hirsutum* species and questions any key biological role for fibre development of this specific CFML arrangement.

4.2.1.3 CFML composition

A wide set of antibodies and CBMs were tested to determine the composition of the CFML. As the LM15 probe, the xyloglucan LM25 probe labelled the particles inside the large CFML regions as well as in the CFML bulges in all cotton species. The images regarding LM25 labelling of the CFML can be found in section 4.2.3 Figure 4-13.
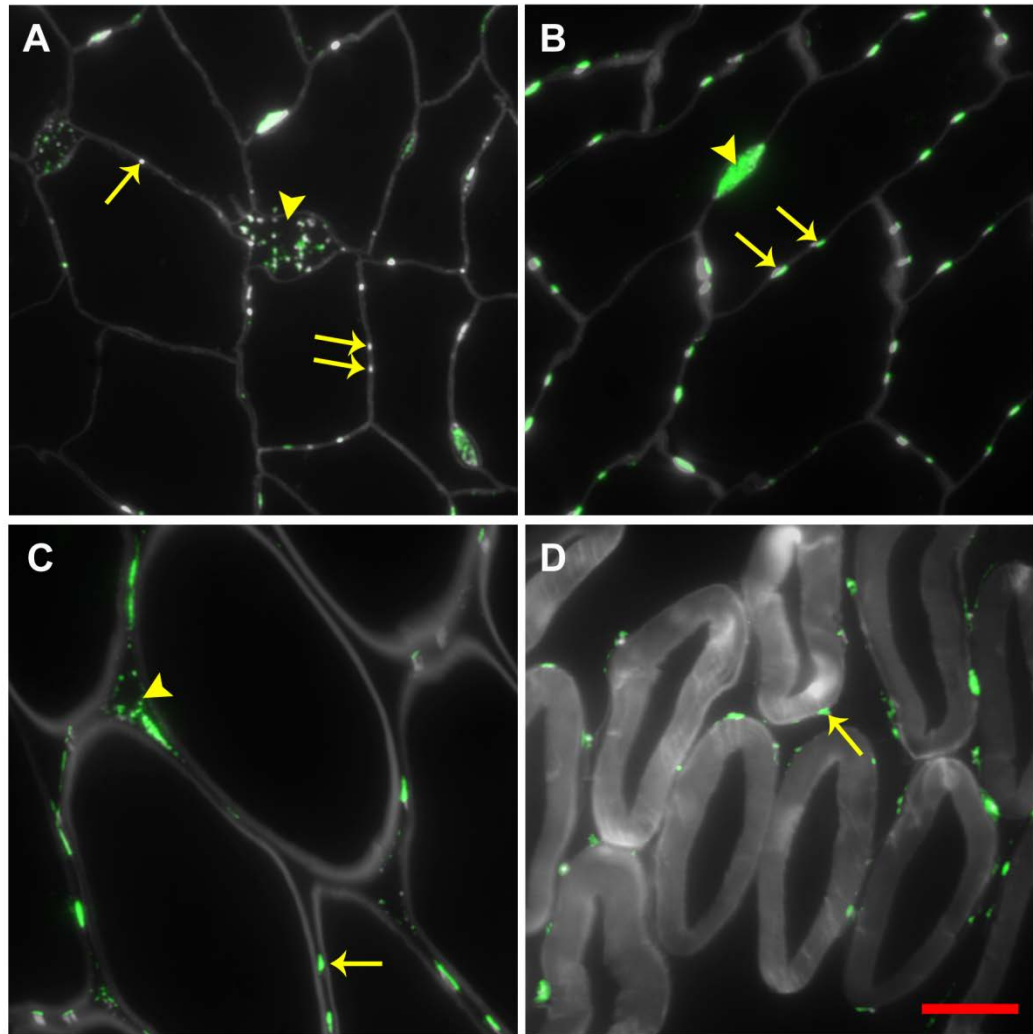
Figure 4-2. CFML evolution during fibre development. Cross sections of developing fibres from FM966 (Batch 3). Calcofluor is shown in greyscale and LM15 labelling in green. A. 5 dpa fibres from FM966. Both CFML structures, the paired bulges (arrows) and enlarged regions (arrowheads) can be observed. B. 13 dpa fibres from FM966. Paired CFML bulges (arrows) were more abundant in the fibre tissue than the enlarged regions (arrowheads). C. 17 dpa fibres from FM966. The CFML started to degrade (arrowhead) during fibre detachment and the paired bulges were still observed throughout the tissue. D. 28 dpa fibres from FM966. Remnants of the CFML bulges were visible around the fibre cell wall during the secondary cell wall deposition stage. Scale bar: 10 μm.

In addition, the occurrence of fucosylated xyloglucan in these structures in *G. barbadense* as well as in *G. hirsutum* cultivars was corroborated by the CCRC-M1 probe that specifically binds to fucose containing xyloglucan (Puhlmann et al., 1994). The de-esterified homogalacturonan LM19 probe also bound to the particles inside the CFML enlarged regions (4.2.2 Figure 4-6 and Figure 4-7). Similarly to the LM19 epitope, the arabinan LM6 epitope bound not only to the fibre cell walls but also to the particles inside the enlarged CFML regions. Images corresponding to the CCRC-M1 and LM6 labelling of the CFML can be found in Figure 4-3A.

Moreover, treatment of fibre sections with xyloglucanase efficiently removed the xyloglucan LM15 epitope, however it did not abolish Calcofluor White staining (Figure 4-3B), suggesting that other β-glucans are present in the CFML currently not detected by any of the available β-glucan probes. A xyloglucan endotransglycosylase (anti-PttXET16A) antibody (Agrisera) produced against one of the most abundant poplar XET isoforms (Bourquin et al., 2002) was able to recognise the particles inside the CFML (arrowheads Figure 4-3C) in Coker (*G. hirsutum*) fibres at 15 dpa of both non-transgenic and CslC4/XT1 transgenic lines (details of these lines are in section 4.2.3.2).

In general, the HG LM19 probe showed a more homogenous labelling inside the enlarged CFML regions compared to the xyloglucan probes. A dual labelling experiment was carried out to analyse the co-localization of these two epitopes in the particles of the enlarged CFML regions. A representative image of the dual labelling of the CFML using LM19 directly coupled to FITC and the LM15 probe is shown in Figure 4-4. The LM19 epitope was more abundant than LM15 and more homogenously distributed, suggesting that the xyloglucan particles could be held in a pectic-based suspension.
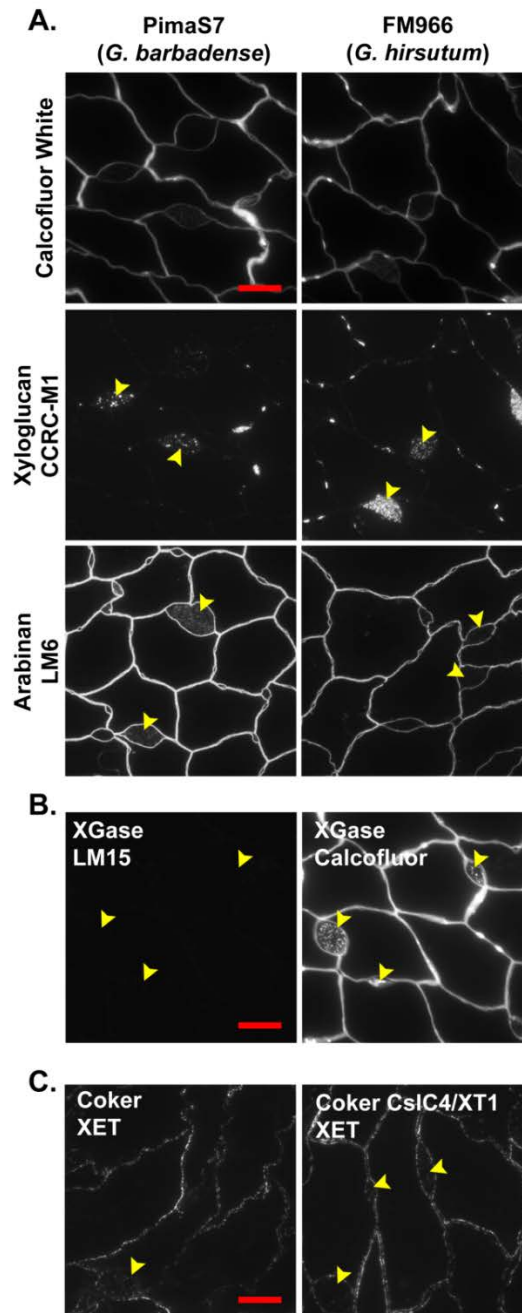
Figure 4-3. The CFML contains arabinan and fucosylated xyloglucan.
A. The fucosylated xyloglucan CCRC-M1 epitope was found in both the *G. hirsutum* and *G. barbadense* species. The arabinan LM6 epitope was also a component of the CFML. B. Treatment of resin sections with xyloglucanase removed the LM15 labelling but did not affect the staining of the CFML with Calcofluor White. C. Immunolocalization of the xyloglucan xyloxyl transferase in *G. hirsutum* wt Coker line and transgenic CslC4/XT1 Coker line. Scale bar: 10 μm.
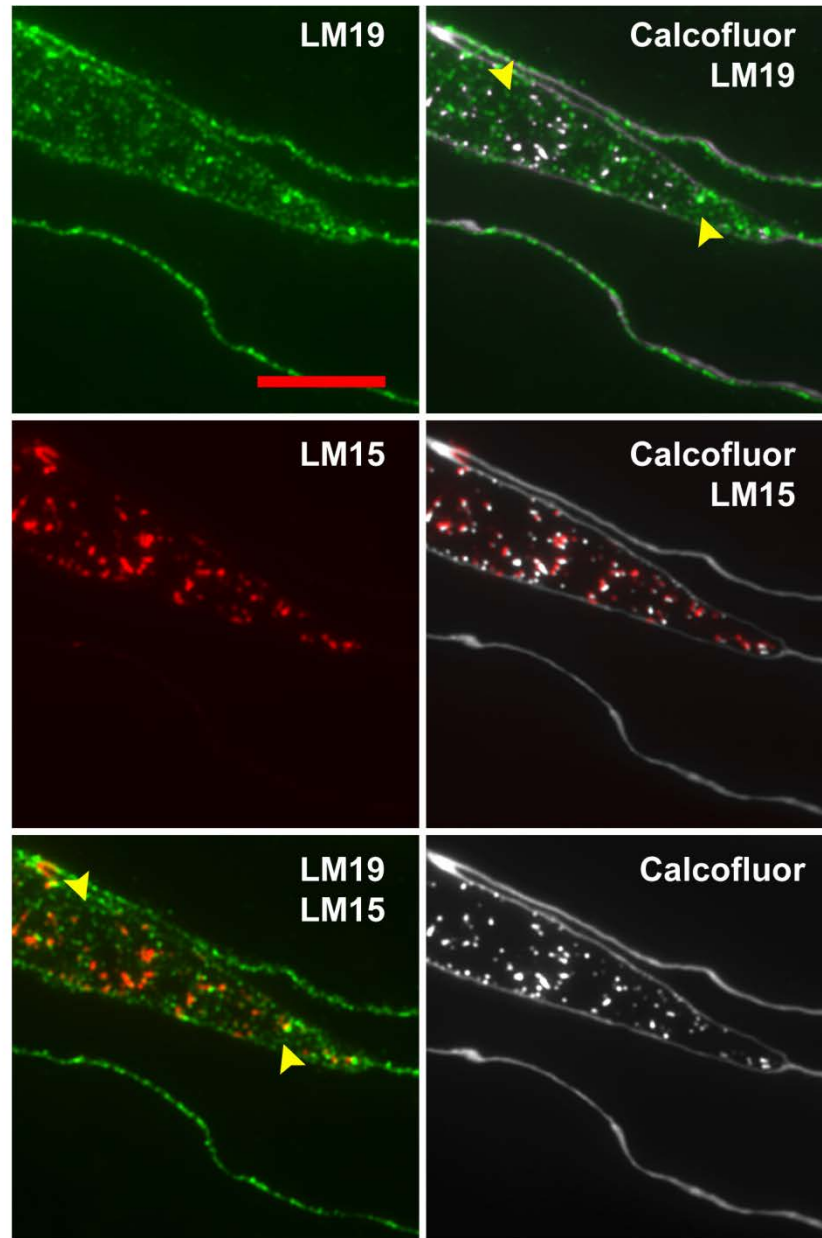
Figure 4-4. LM19 and LM15 dual labelling of CFML particles. The CFML particles labelled with the HG LM19 probe appeared more spread inside the CFML region compared to the particles labelled with LM15 and Calcofluor White, which highly co-localized. Arrowheads point to region with less abundant LM15. Scale bar: 10 µm.

4.2.2 Pectin degradation depends on cell wall context and fibre developmental stage

The primary cell wall of cotton fibres is rich in de-esterified homogalacturonan pectin at all developmental stages as shown by immunolocalization using the LM19 probe in Figure 4-5. The de-esterified HG LM19 epitope appeared around the cell wall and also in the enlarged regions of the CFML as previously described, not only in *G. hirsutum* but also in the *G. barbadense* and *G. arboreum* cultivars studied here (arrowheads in Figure 4-5). The HG LM19 epitope labelling was punctate possibly indicating pectin degradation in PimaS7 and FM966 samples during the elongation phase up to 25 dpa (arrows in Figure 4-5) but not in the JFW15 line. In order to know if this degradation was biologically relevant or simply an artefact of sample handling, labelling with the LM19 probe was examined in developing fibres of FM966 grown at different diurnal temperatures from "Batch1" (20-25°C) and "Batch2" (28-32°C) in Figure 4-6A. The LM19 epitope was found to be less degraded in Batch1 and Batch2 samples of FM966 and mainly in those grown at lower temperatures. This showed that the LM19 epitope can be found homogenously distributed around the fibre cell wall in the FM966 cultivar showing few signs of degradation and, therefore, it is likely that pectin degradation is due to sample storage differences as well as being influenced by growth temperatures. Nevertheless, HG pectin in the JFW15 samples appeared consistently less degraded than in PimaS7 and FM966 and more resistant to the action of pectate lyase (data not shown) suggesting that the pectin in the JFW15 cultivar could be in a more protective cell wall environment that preserves this epitope better. In addition, pectin degradation was more noticeable during the elongation phase (see FM966 5 to 17 dpa panels Figure 4-6 compared to 21 and 22 dpa panels in Figure 4-6 and 25 dpa in Figure 4-5) suggesting than pectin in elongating fibres might be more readably degradable than in older fibres.
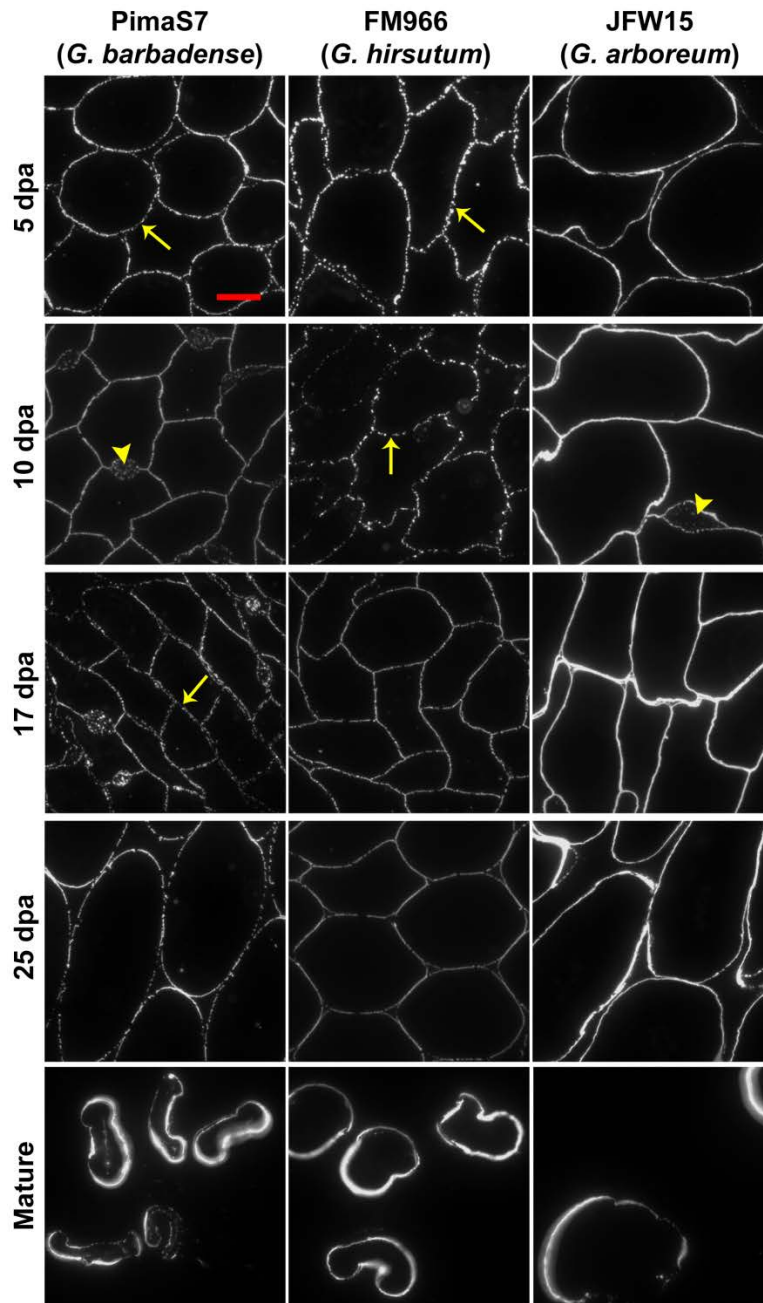
Figure 4-5. Immunolocalization of the LM19 de-esterified HG epitope in cross sections of developing and mature cotton fibres of PimaS7 (*G. barbadense*), FM966 (*G. hirsutum*) and JFW15 (*G. arboreum*). LM19 labelling was found around the fibre primary cell wall in all cultivars at all time-points. Particles of de-esterified HG were found inside CFML regions (arrowheads in PimaS7 and JFW15 lines panels). De-esterified HG degradation was visible in the PimaS7 and FM966 lines during fibre elongation (arrows). Scale bar: 10 μm.
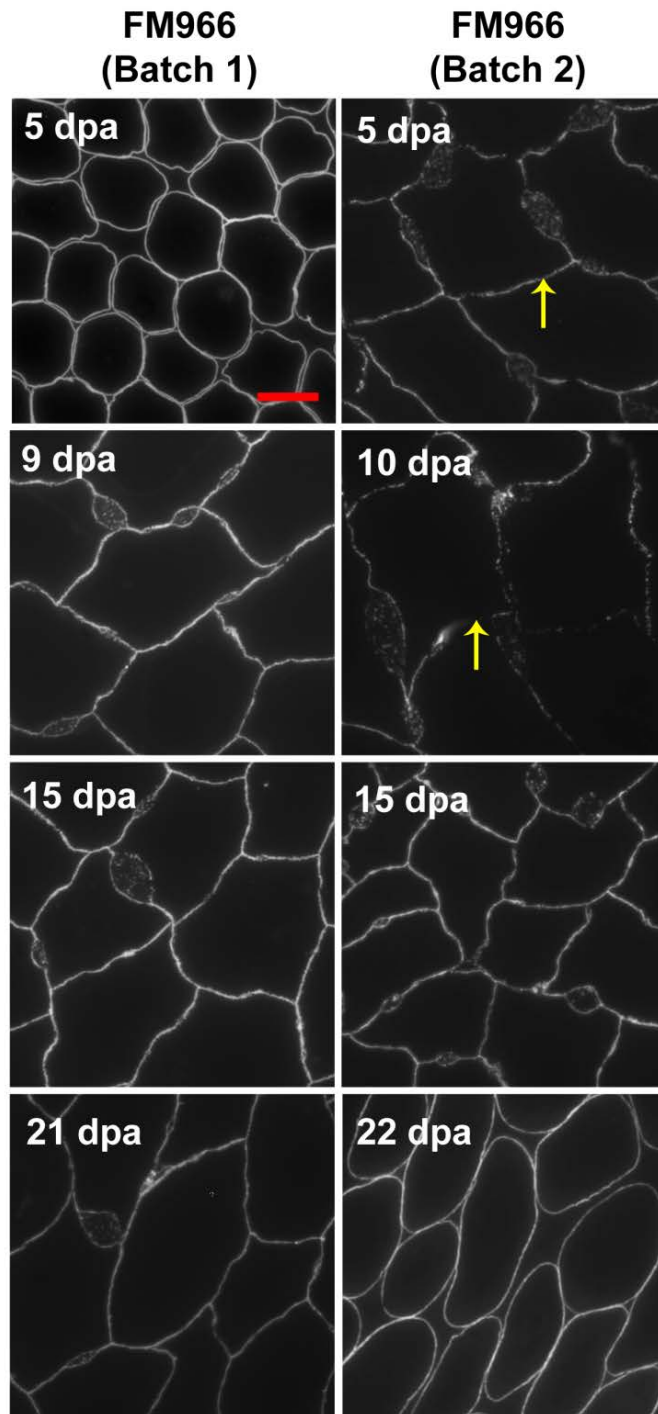
Figure 4-6. Immunolocalization of the LM19 de-esterified HG epitope in cross sections of developing fibres from FM966 (*G. hirsutum*) grown at different temperature conditions. Fewer signs of pectin degradation (arrows) were observed in fibres from Batch 1 and Batch 2 in FM966. Pectin was well preserved mainly in fibres grown at lower temperatures (Batch 1).. Scale: 10 µm.

Regarding the highly methyl esterified HG LM20 epitope, a comparative analysis between three species of cotton showed that the LM20 epitope disappeared earlier in the China10 (*G. barbadense*) and FM966 (*G. hirsutum*) lines than in the JFW15 (*G. arboreum*) line (Figure 4-7). Additional work on other batches of the FM966 line (data not shown) repeatedly showed that the highly esterified HG LM20 epitope was abundant around the fibre cell wall during the elongating phase and disappeared by the end of fibre elongation. This is supported by bibliography (Singh et al., 2009; Avci et al., 2013) and previous work done in this laboratory (Benians, 2012). The earlier disappearance (ca. 5 dpa) of the LM20 epitope as presented in Figure 4-7 compared to the glycan microarray data (ca. 20 dpa) can be explained by certain degree of degradation (as with the LM19 epitope) during sample ethanol storage and points again to highly labile pectins. These data indicate that both biological and non-biological factors are associated with HG pectin degradation in these samples and this is discussed further in 4.3.1.

The LM5 antibody binds to a chain of galactan residues (Jones et al., 1997) which are commonly found as side chain in the RG-I pectin molecule in many types of tissues. Similarly to the LM20 epitope, the galactan LM5 epitope was only present during the early stages of fibre development. Figure 4-8 depicts the punctated labelling by the LM5 probe in the cotton fibre cell wall which is similarly detected in China10 (*G. barbadense*), FM966 (*G. hirsutum*) and JFW15 (*G. arboreum*) cultivars at 5 and 10 dpa. The LM5 epitope disappeared by 17 dpa in all lines.

Masking of cell wall epitopes by other polysaccharides has been previously reported (Marcus et al., 2008; Marcus et al., 2010; Xue et al., 2013). Removal of HG pectin by pre-treatment with sodium carbonate and pectate lyase see (Materials and Methods 2.11.3) generally increase fluorescence intensity of LM5 labelling suggesting partial masking of galactan by HG.
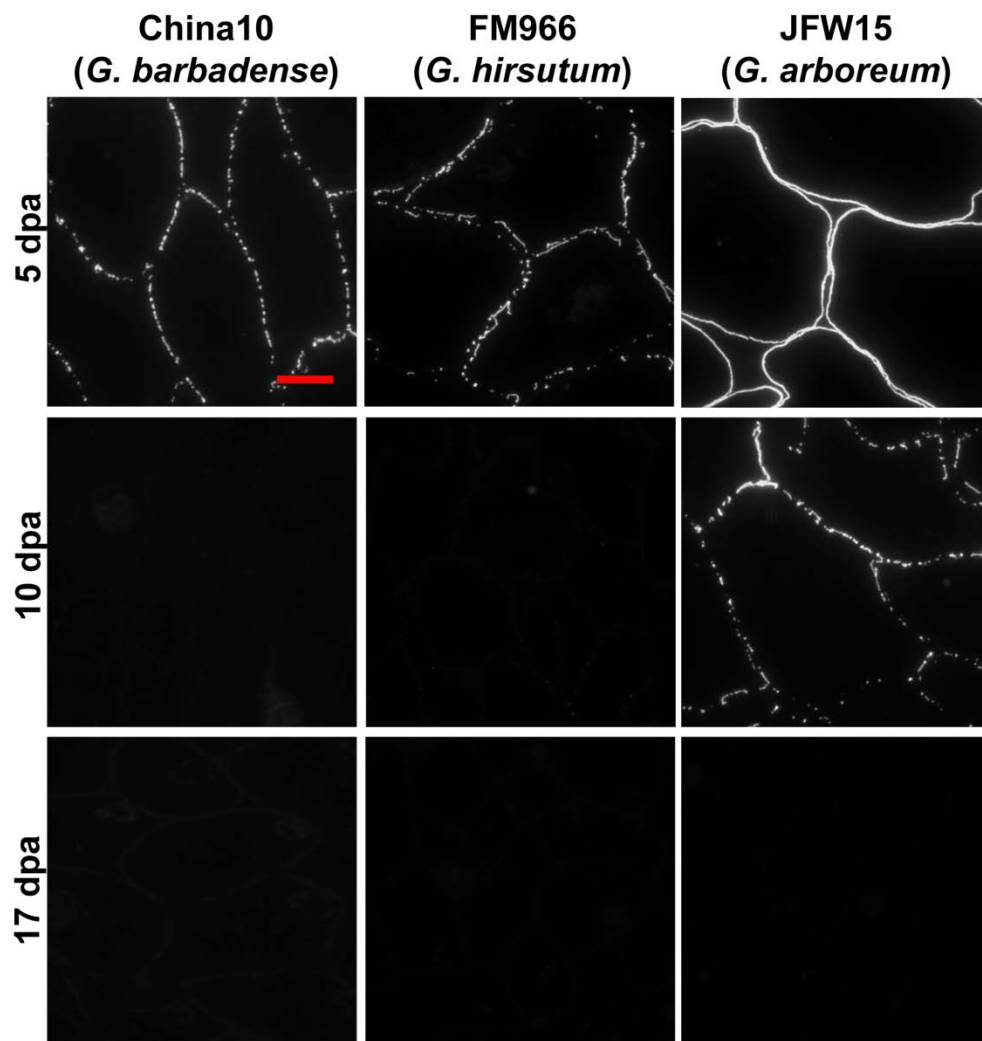
Figure 4-7. Immunolocalization of the LM20 highly esterified HG epitope. Cross sections of developing cotton fibres of China10 (*G. barbadense*), FM966 (*G. hirsutum*) and JFW15 (*G. arboreum*). Scale bar: 10 µm.
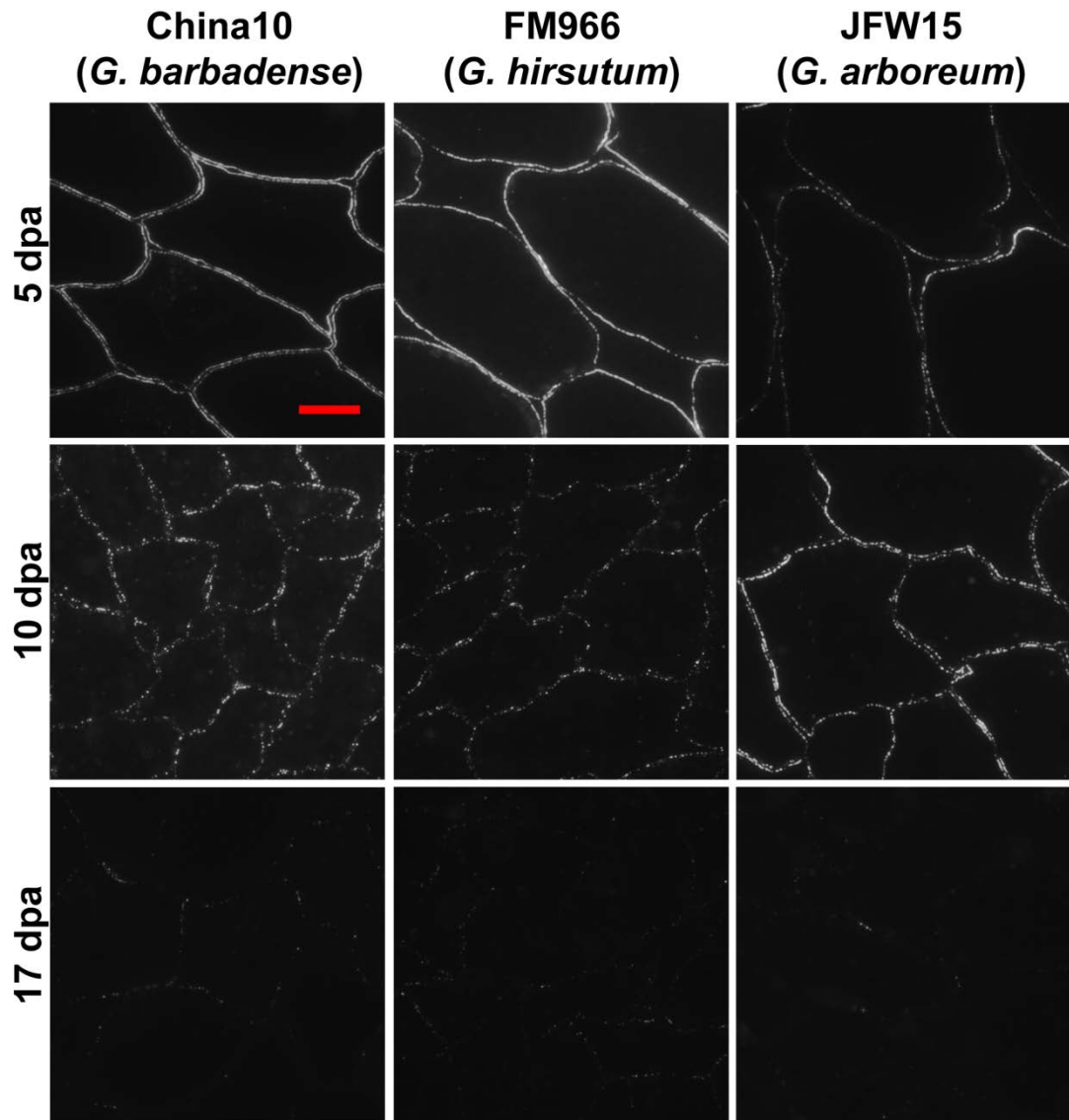
Figure 4-8. Immunolocalization of the LM5 galactan epitope. Cross sections of developing cotton fibres of China10 (*G. barbadense*), FM966 (*G. hirsutum*) and JFW15 (*G. arboreum*). All sections were pre-treated with sodium carbonate and pectate lyase. Scale bar: 10 μm.

The INRA-RU2 monoclonal antibody recognises stretches of the RG-I backbone with >2 repeats of the rhamnose-galacturonic acid disaccharide (Ralet et al., 2010). INRA-RU2 labelled the cell wall of cotton fibres in all cultivars and at all the time points analysed here (Figure 4-9). The INRA-RU2 signal was detected homogenously around the fibre cell wall at 5 dpa in all cultivars and with particularly high intensity in the PimaS7 line (5 dpa top panels). Signs of RG-I backbone degradation (arrowheads in Figure 4-9) were detected in the JFW15 (*G. arboreum*) line as early as 10 dpa and more intensely at 25 dpa. However, in FM966 (*G. hirsutum*) and PimaS7 (*G. barbadense*) lines, signs of RU-II epitope degradation were only observed at 25 dpa.

The arabinan LM6 probe can recognise chains of 5 to 7 α-1,5-linked arabinosyl residues (Willats et al., 1998) present as side chains in the RG-I molecule and as part of some AGPs (Lee et al., 2005). LM6 labelled strongly the fibre cell wall of all cultivars and was also found as part of the CFML (arrowheads in Figure 4-10A). The LM6 signal was regularly detected intracellularly in the cotton fibre (arrows in FM966 5 dpa and PimaS7 17 dpa panels in Figure 4-10A). Another atypical labelling pattern for pectin probes was also found in the inner layers of the secondary cell wall in mature fibres (arrows in all mature fibre panels in Figure 4-10A and Figure 4-10B) which may relate to AGPs. The linear arabinan LM13 antibody binds to longer arabinan chains compared to the LM6 epitope (Verhertbruggen et al., 2009). LM13 labelled the fibre cell wall very strongly in FM966 and PimaS7 until the end of fibre elongation (17 dpa) and during secondary cell wall deposition in the JFW15 (25 dpa) (Figure 4-11).
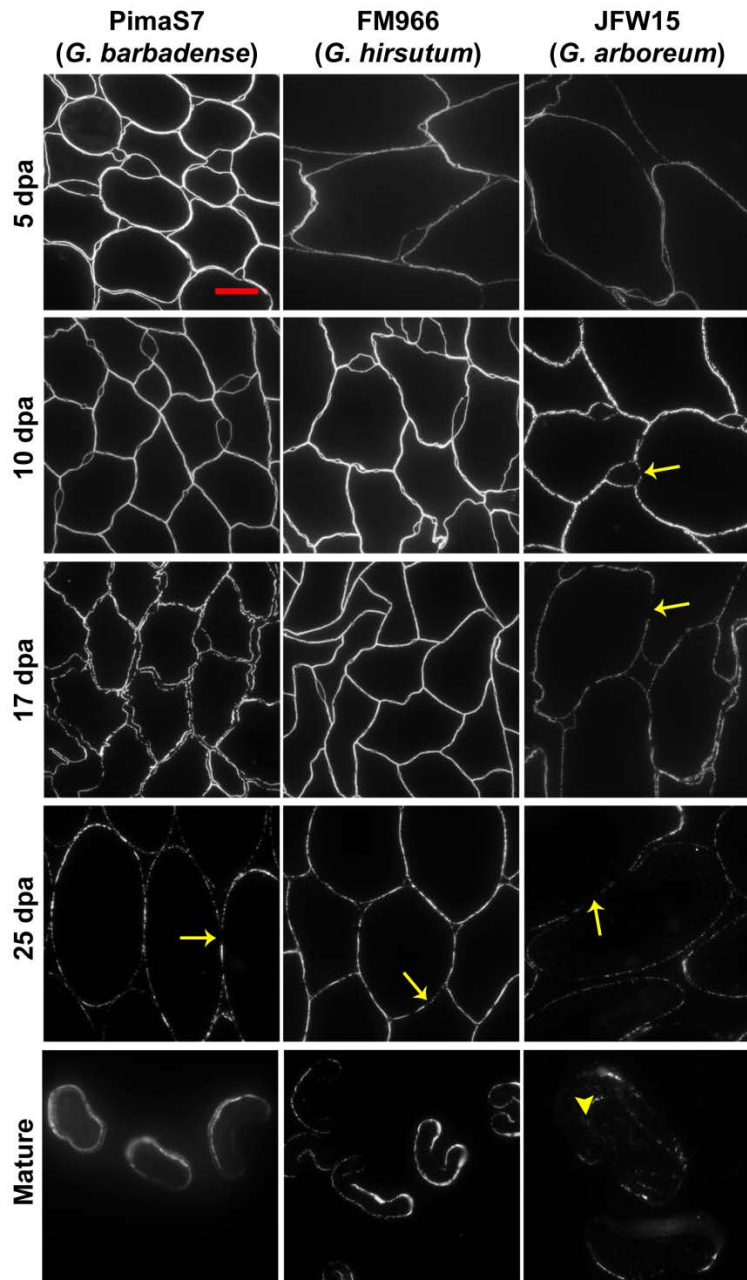
Figure 4-9. Immunolocalization of the INRA-RU2 RG-I backbone epitope. Cross sections of developing and mature cotton fibres of PimaS7 (*G. barbadense*), FM966 (*G. hirsutum*) and JFW15 (*G. arboreum*). The RG-I backbone epitope was abundant in the fibre primary cell wall of all cultivars at all timepoints. Unlike the de-esterified HG, the HG RG-I backbone degradation was mainly detected in the JFW15 line (arrowheads). Also, the FM966 and PimaS7 lines showed similar signs of degradation only at 25 dpa. Scale bar: 10 µm.
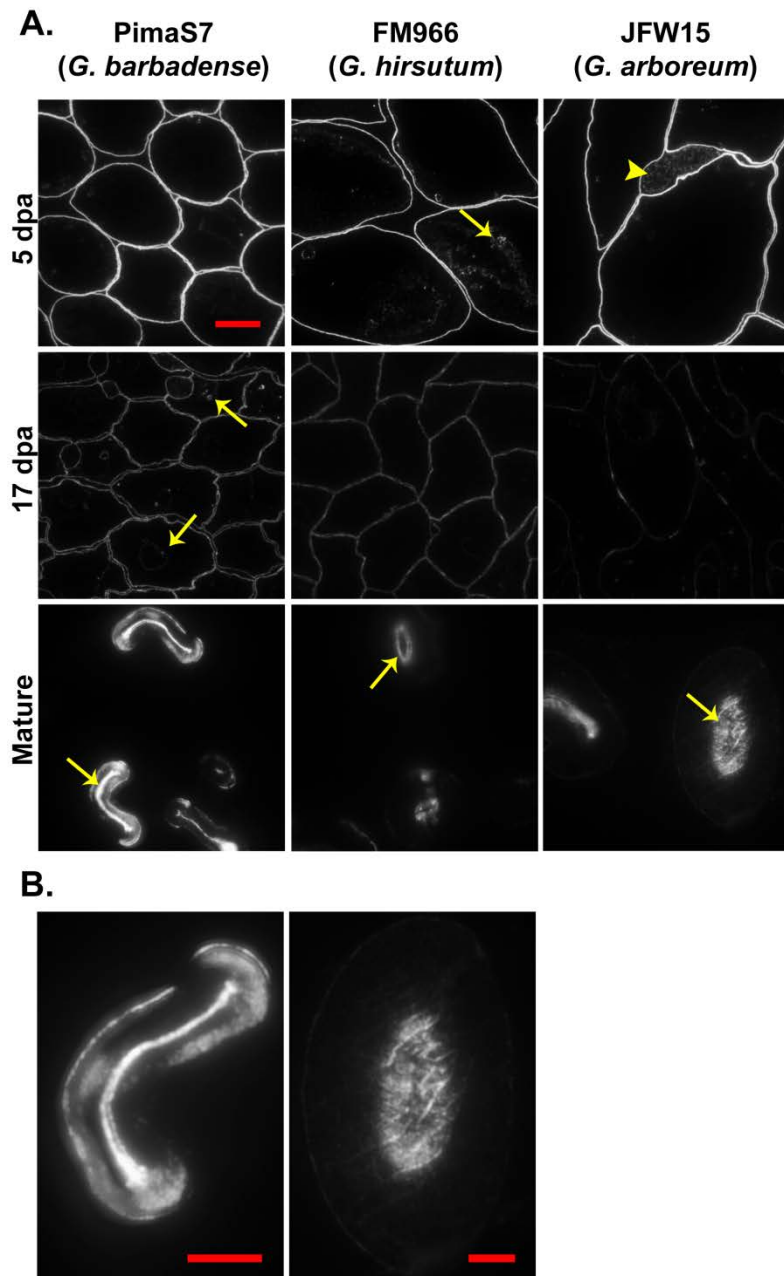
Figure 4-10. Immunolocalization of the LM6 arabinan epitope. A. Cross sections of developing and mature cotton fibres of PimaS7 (*G. barbadense*), FM966 (*G. hirsutum*) and JFW15 (*G. arboreum*). The LM6 arabinan epitope was found intracellularly LM6 (arrow in FM966 5 dpa panel) and was part of the CFML (arrowhead in the JFW15 5 dpa panel). LM6 labelled the inner part of the secondary cell wall in mature fibres. Scale bar: 10 µm. B. Close up view of LM6 epitope localization in the mature fibres from PimaS7 (left panel) and JFW15 (right panel). Arrows point to the fibre edge. Scale bars: 5 µm.
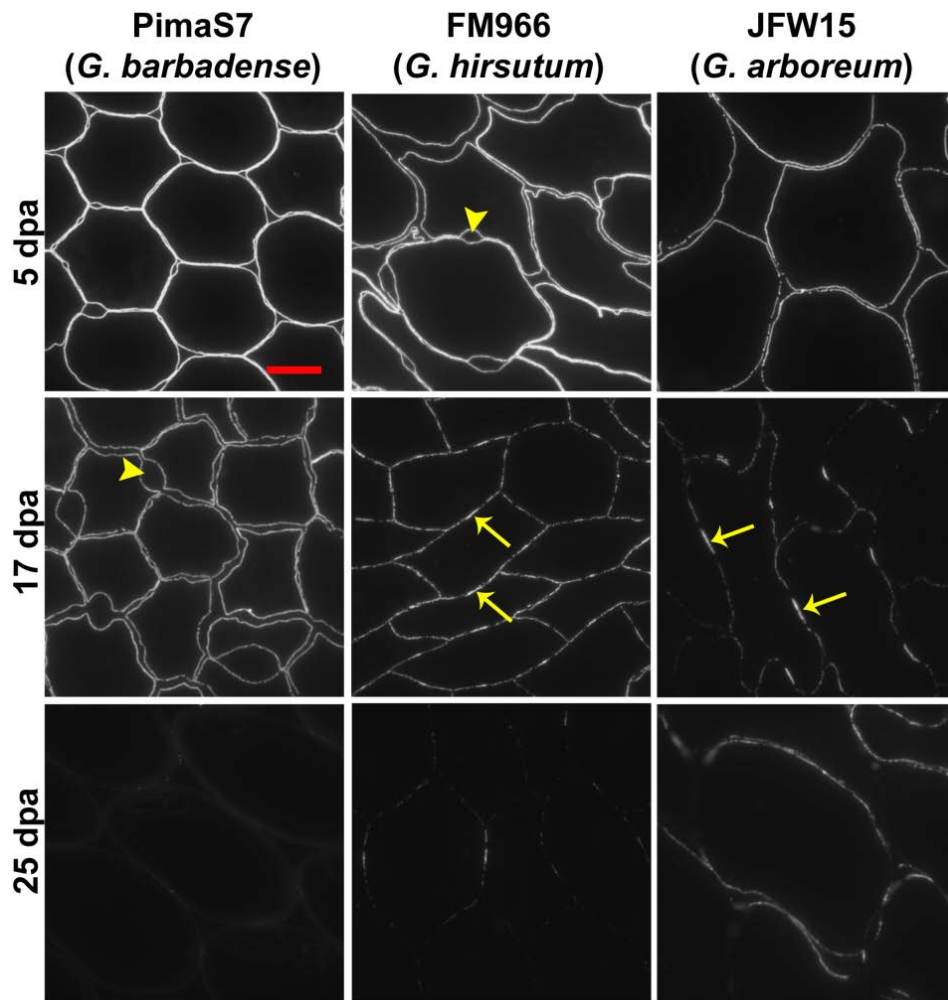
Figure 4-11. Immunolocalization of the linear arabinan LM13 epitope. Cross sections of developing and mature cotton fibres of PimaS7 (*G. barbadense*), FM966 (*G. hirsutum*) and JFW15 (*G. arboreum*). While the arabinan LM6 epitope bound to the particles of the CFML the LM13 linear arabinan epitope did not (arrowheads). A zone of stronger labelling between neighbouring cell walls were observed at 17 dpa in FM966 and JFW15 (arrows). Scale bar: 10 µm.

4.2.3 Xyloglucan is an abundant cell wall component of the cotton fibre

4.2.3.1 Immunolocalization of cell wall xyloglucan during fibre development

Further analysis of the localization of the xyloglucan LM25 epitope in the fibres of two other lines, PimaS7 and JFW15 (Figure 4-12), revealed abundant xyloglucan not only in the enlarged and paired CFML structures of the *G. barbadense, G. hirsutum* and *G. arboreum* lines (Figure 4-12 arrows) but also around the primary cell wall of developing cotton fibres and mature fibres where xyloglucan was found to be highly masked by pectin. Therefore, all sections used to produce Figure 4-12 were pre-treated with sodium carbonate and pectate lyase to uncover xyloglucan. The unmasking effect of the pectate lyase treatment was very important in the primary cell wall of mature cotton fibres.

Intracellular binding by LM15 was also observed (arrowhead in FM966 5 dpa panel) which possibly corresponded to newly formed xyloglucan. The lumen of mature fibres of China10 and FM966 lines was labelled by the LM25 probe (arrowheads in China10 and FM966 mature panels). Also, xyloglucan was weakly detected on the extra thickened secondary cell wall of the JFW15 line (arrowheads JFW15 25 dpa panel). In the next section the presence of xyloglucan in the secondary cell wall is explored further in an xyloglucan-overproducing transgenic cotton line.
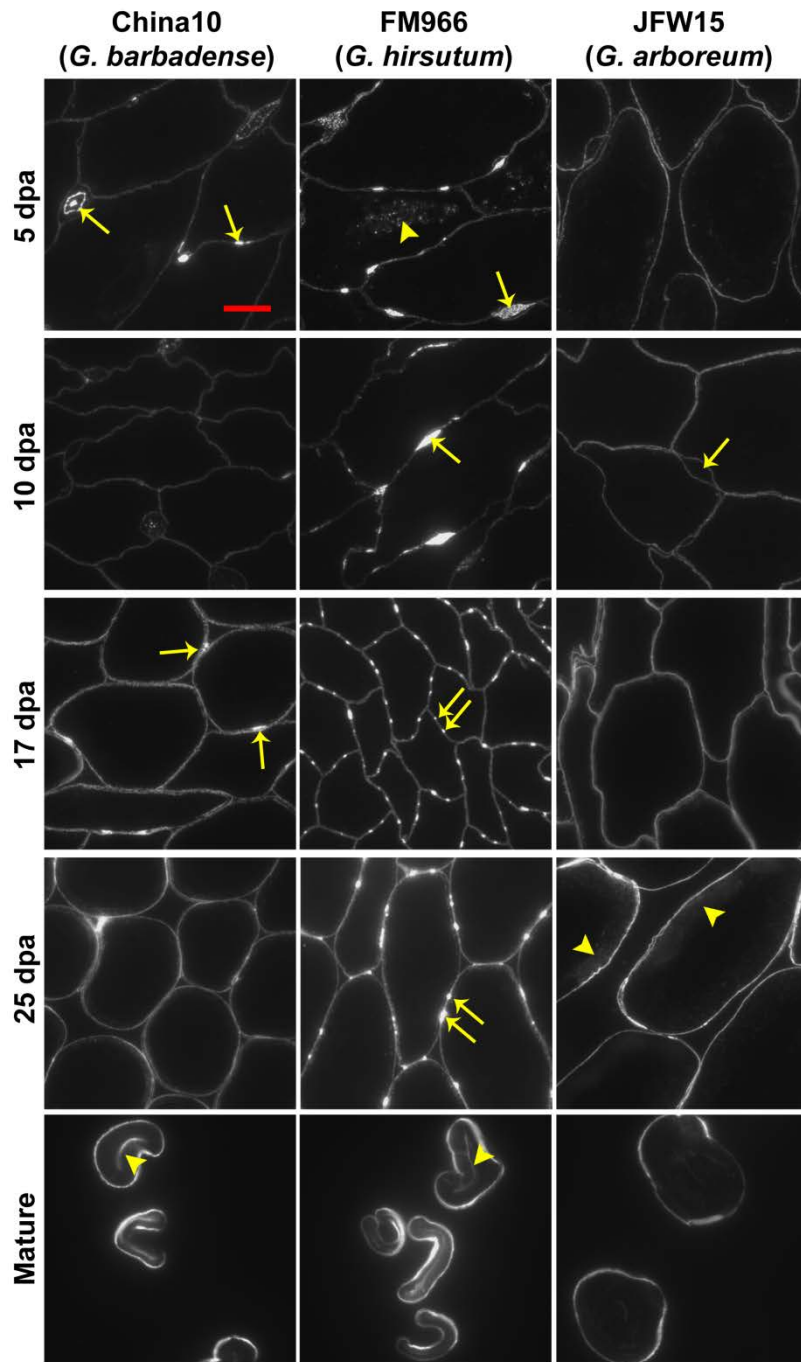
Figure 4-12. Immunolocalization of the LM25 xyloglucan epitope. Cross sections of developing and mature cotton fibres of China10 (*G. barbadense*), FM966 (*G. hirsutum*) and JFW15 (*G. arboreum*). Arrows point to xyloglucan in CFML structures and arrowheads point to xyloglucan localized intracellularly (FM996 5 dpa), in the secondary cell wall (JFW15 25 dpa) and fibre lumen (China10 and FM966 mature). All sections were pretreated with sodium carbonate and pectate lyase. Scale bar: 10 µm.

4.2.3.2 Xyloglucan as target polysaccharide for cotton fibre improvement. Immunohistochemical analysis of xyloglucan overproducing CslC4/XT1 transgenic lines

Cotton plants overproducing xyloglucan in the fibre secondary cell wall were generated by Bayer Cropscience in Ghent. Briefly, the transgenic line was created by the introduction of two genes encoding the cellulose synthase-like C protein *CSLC4* from *A. thaliana* and a xyloglucan 6-xylosyltransferaseprotein (XXT) from *A. thaliana* under a fibre specific F286 promoter whose activity is restricted to lint fibre at the secondary cell wall deposition phase The constructs were inserted in a Coker (*G. hirsutum*) background. Additional data and information regarding the invention of these transgenic plants can be found in the patent filed under the application number WO2014198885 (Meulewaeter et al., 2014). These transgenic plants, here named as CslC4/XT1, produced cotton fibres with 20-fold increased levels of xylose (mainly terminal xylose) compared to null segregrants (non-transgenic) fibres due to increased levels of xyloglucan in the secondary cell wall (Meulewaeter et al., 2014). The transgenic fibres showed better dyeability with direct dyes and fibre-reactive dyes as well as a higher capacity to uptake other compounds like flame retardants, medical compounds and softeners. The increased levels of xyloglucan also affected fibre micronaire which was reduced from values of 5.4-6 in the non-transgenic line to 3.0-4.2 in the CslC4/XT1 lines (Meulewaeter et al., 2014).

In this work, fibre samples at four dpa (15, 20, 25 and 30) from a CslC4/XT1 expressing line were collected for immunohistochemistry analyses.

Figure 4-13 shows that the CslC4/XT1 expressing line produced much more xyloglucan (labelled by the LM15 probe) in the secondary cell wall at 20, 25 and 30 dpa (arrowheads in Figure 4-13) compared to the non-transgenic line. No differences were found in their pectin content as shown by the de-esterified HG LM19 epitope (Figure 4-13) and the arabinan LM6 epitope (data not shown). The highly-esterified probe LM20 was used as a marker of fibre development which showed no difference between the wild type and the transgenic lines (data not shown). This suggests that the role of the

introduced cellulose synthase-like C protein (CSLC4) and a xyloglucan 6-xylosyltransferaseprotein (XXT) did not affect the pectin biosynthetic and turnover processes. The recognition of broader range of xyloglucan by the LM25 probe showed accumulation of xyloglucan in the secondary cell wall of non-transgenic fibres (arrows in Figure 4-14), although to a much less extent compared to the transgenic lines. The fucosylated xyloglucan CCRC-M1 epitope was only observed as part of the cell wall and CFML structures but not in the thickening secondary cell wall (arrowheads in Figure 4-14) indicating that the genes introduced did not produce fucosylation of xyloglucan as expected.

The detection of xyloglucan in mature transgenic fibres was also analysed with and without xyloglucanase treatment (Figure 4-15). As observed in developing fibres, xyloglucan accumulated in the secondary cell wall of mature transgenic fibres. However, xyloglucanase failed to digest the LM15 and LM25 epitopes suggesting that these epitopes must be chemically protected from the action of the xyloglucanase in the secondary cell wall of the CslC4/XT1 expressing line.

Increased dyeability can be associated with lower cellulose crystallinity in the transgenic fibres which can be explained by the high amounts of xyloglucan in the secondary cell wall. The fibre crystallinity was analysed (Figure 4-16) using carbohydrate-binding modules CBM3a and CBM28 as reported before in Kljun et al. (2011). CBM3a binds to crystalline cellulose and CBM28 to amorphous cellulose. As CBM3a is also able to bind to xyloglucan as well as to crystalline cellulose (see Chapter 5 section 5.2.1), sections were analysed with and without xyloglucanase treatment. The CslC4/XT1 expressing line showed similar binding of CBM3a (crystalline cellulose) and CBM28 (amorphous cellulose). Not much difference was found in sections treated with xyloglucanase however, CBM binding to xyloglucan as well as cellulose cannot be discarded as xyloglucanase failed to remove the LM15 epitope from the secondary cell wall.

The mature transgenic lines seemed generally thinner than the non-transgenic fibres on cross sections which correlates with the transgenic lines

having a lower micronaire (micronaire value depends on fibre perimeter). Also, the enlarged regions of the CFML and paired CFML bulges were still present in the transgenic lines with no difference in their xyloglucan content or localization suggesting that overexpression of xyloglucan during the secondary cell wall stage did not affect the CFML structures even if xyloglucan is one of its major components.
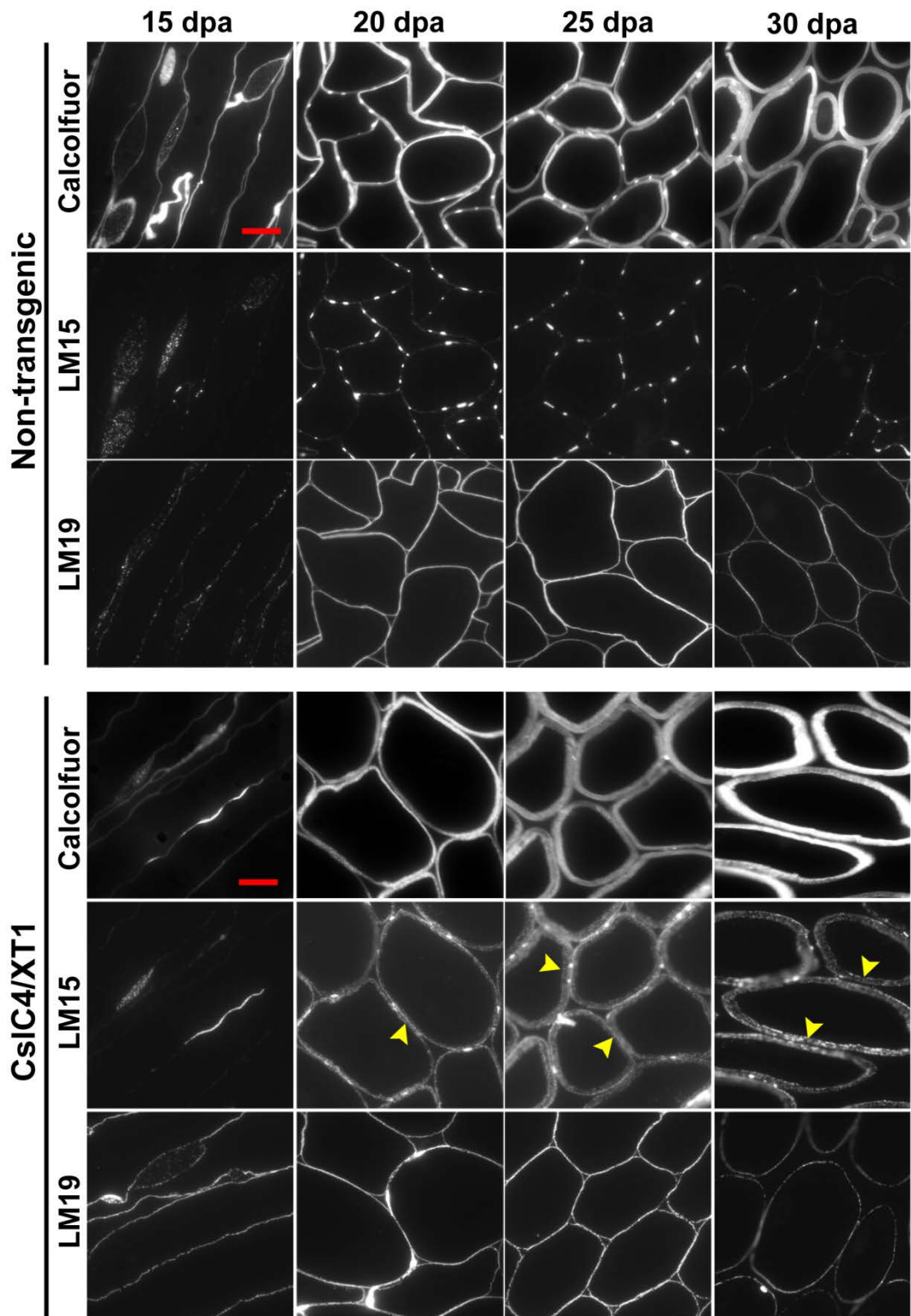
Figure 4-13. Calcofluor images and immunolocalization of the LM15 xyloglucan and the LM19 de-esterified HG epitopes. Cross sections of developing cotton fibres of non-transgenic and CslC4/XT1 expressing lines. Scale bar: 10 µm.
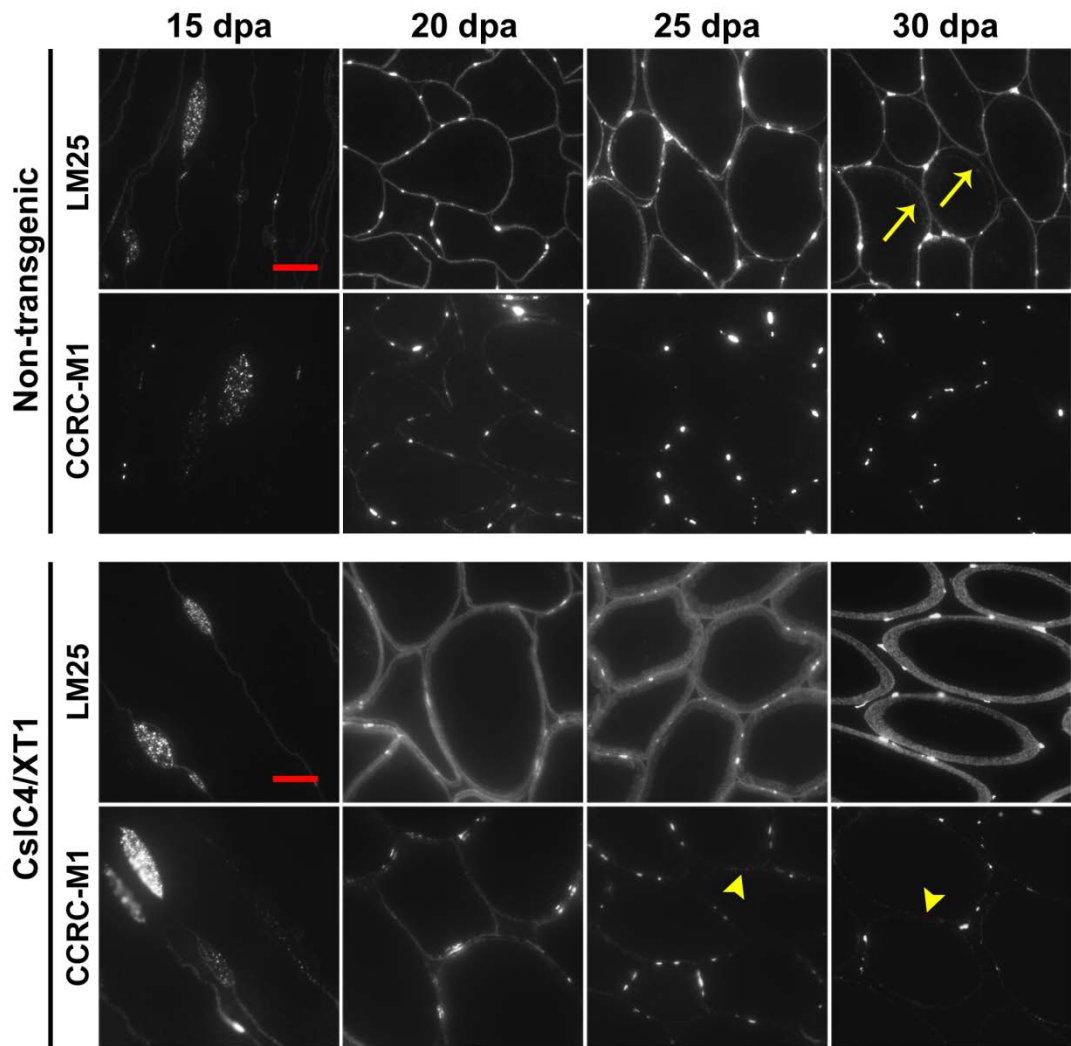
Figure 4-14. Immunolocalization of the LM25 xyloglucan and CCRC-M1 fucosylated xyloglucan epitopes. Cross sections of developing cotton fibres of non-transgenic and CslC4/XT1 expressing lines. Scale bar: 10 μm.
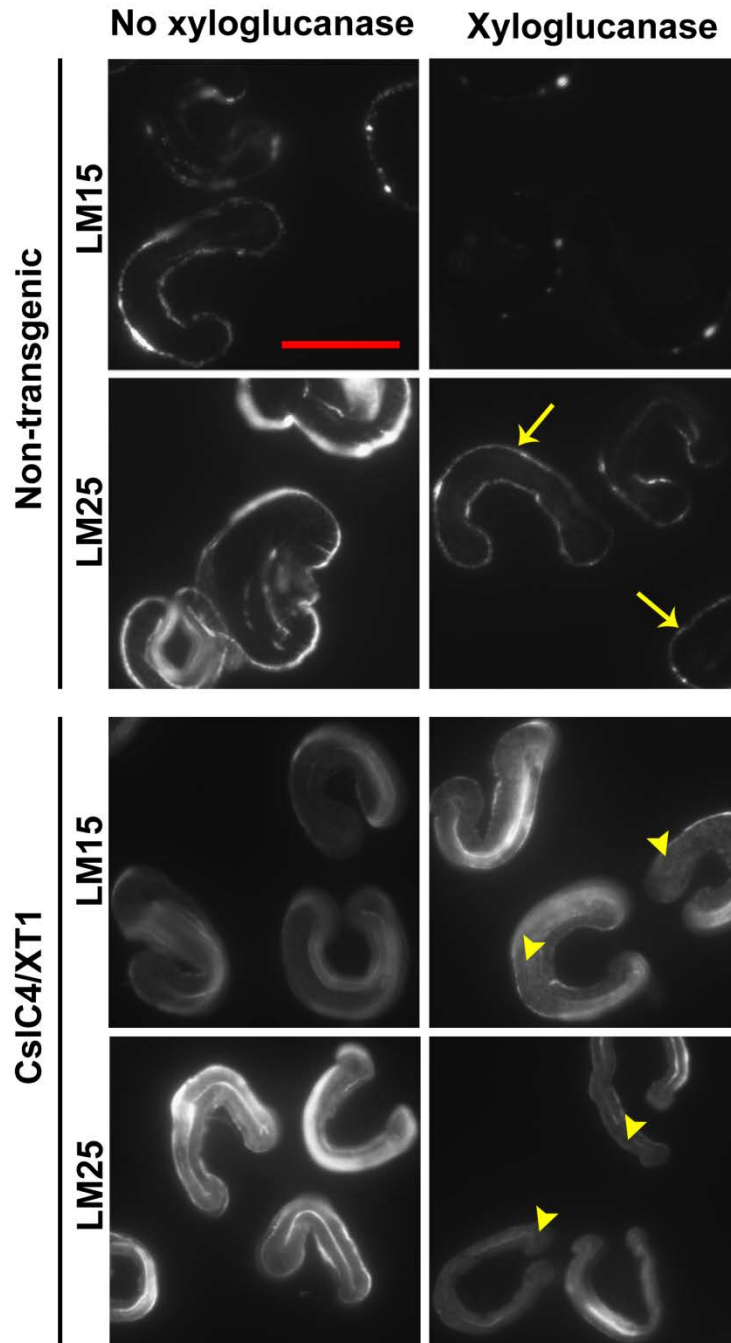
Figure 4-15. Immunolocalization of the xyloglucan LM15 and LM25 epitopes. Cross sections of mature cotton fibres of non-transgenic and CslC4/XT1 expressing lines. No xyloglucanase: 0.1 M sodium acetate pH 5.5 buffer only. Xyloglucanase: 20 µg/ml xyloglucanase in 0.1 M sodium acetate pH 5.5. Time exposure: 1 s all non-transgenic panels, 300 ms LM15 CslC4/XT1, 200 ms LM25 CslC4/XT1. Scale bar: 10 µm.
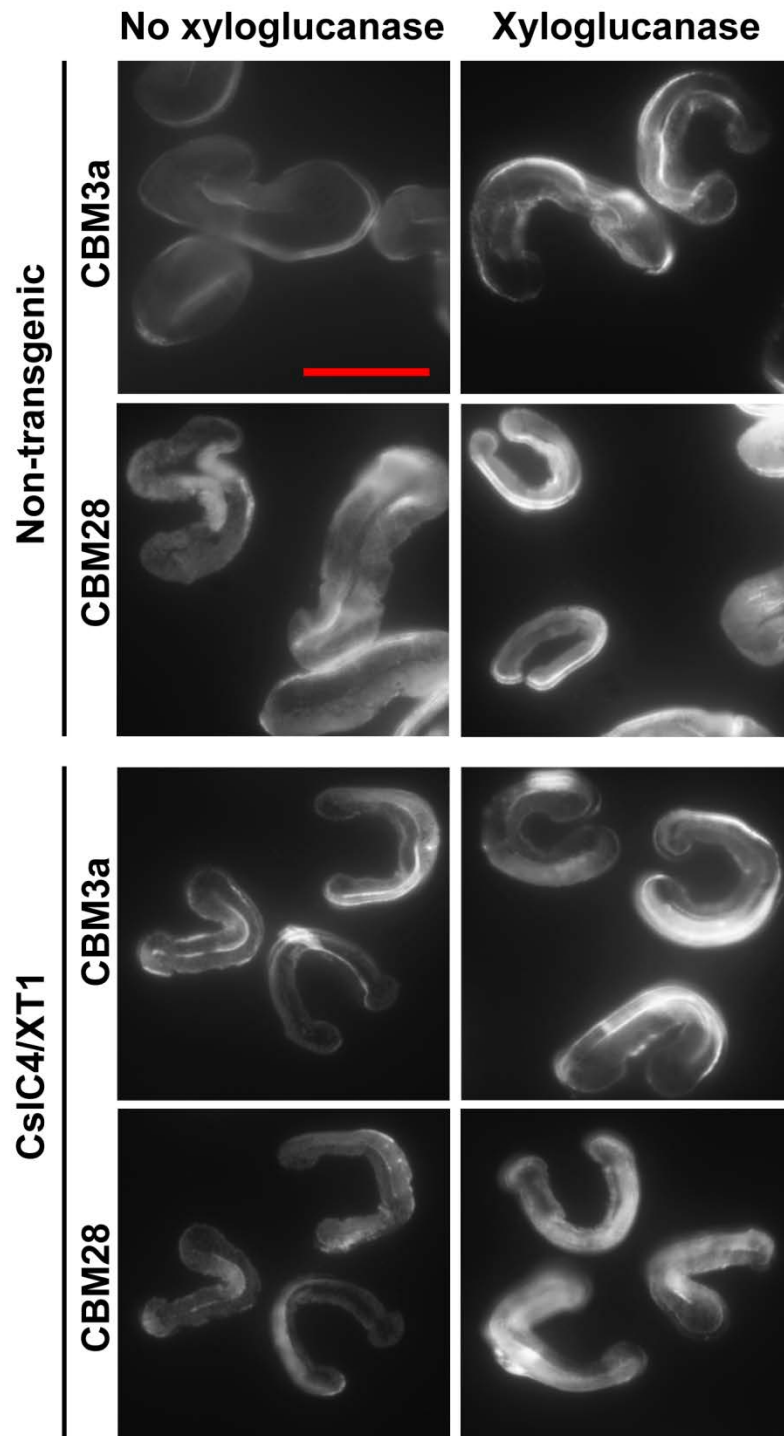
Figure 4-16. Immulabelling with CBM3a and CBM28. Cross sections of mature cotton fibres of non-transgenic and CslC4/XT1 expressing lines. No xyloglucanase: 0.1 M sodium acetate pH 5.5 buffer only. Xyloglucanase: 20 µg/ml xyloglucanase in 0.1 M sodium acetate pH 5.5. Scale bar: 10 µm.

135

4.2.4 The AGP JIM13 epitope and the arabinan LM6 epitope occur intracellularly as well as in the cell wall.

The JIM13 probe was obtained after immunization with an AGP rich-preparation from culture carrot cells (Knox et al., 1991) and it is known to bind to the acidic trisaccharide GlcA-β(1$\rightarrow$3)-GalAα(1$\rightarrow$2)Rha isolated from a partial acid hydrolysate of gum karaya (Yates et al., 1996). The JIM13 epitope has been previously observed at the cell wall as well as plasma membrane (Knox et al., 1991). In this work, the JIM13 probe was found to bind to the plasma membrane and vesicles of 5 DPA fibres (Figure 4-17). Similar binding was observed with the LM6 antibody (arrows in Figure 4-10), suggesting that the LM6 arabinan epitope is not only present in the cell wall (indicated by the cell wall labelling with LM6 but not with JIM13) but also in the glycan part of AGPs (Lee et al., 2005). This was explored further by sequential extractions of 9, 15, 21 and 30 fibre cell walls from FM966 with water, CDTA, sodium carbonate and potassium hydroxide. All extractions were run in SDS-PAGE and transferred to nitrocellulose membranes for blotting (Figure 4-18). The water extraction in early developmental stages (9 and 15 DPA mainly) showed an equivalent protein band pattern for both LM6 and JIM13 in the water extraction. These bands would presumably correspond to AGPs whose molecular weight ranged between 50 and 75 KDa (annotated bands in Figure 4-18). This finding agrees with the above immunolabelling results in which LM6 bound to intracellular structures that were also recognized by JIM13. Therefore, LM6 can detect AGPs as well as pectic arabinan in the cotton fibre.

Other hydroxyproline-rich proteins such as extensins (JIM20) were weakly detected in the JFW15 line at the onset of the secondary cell wall phase (data not shown) as it was also shown in the glycan microarray data in Chapter 3.
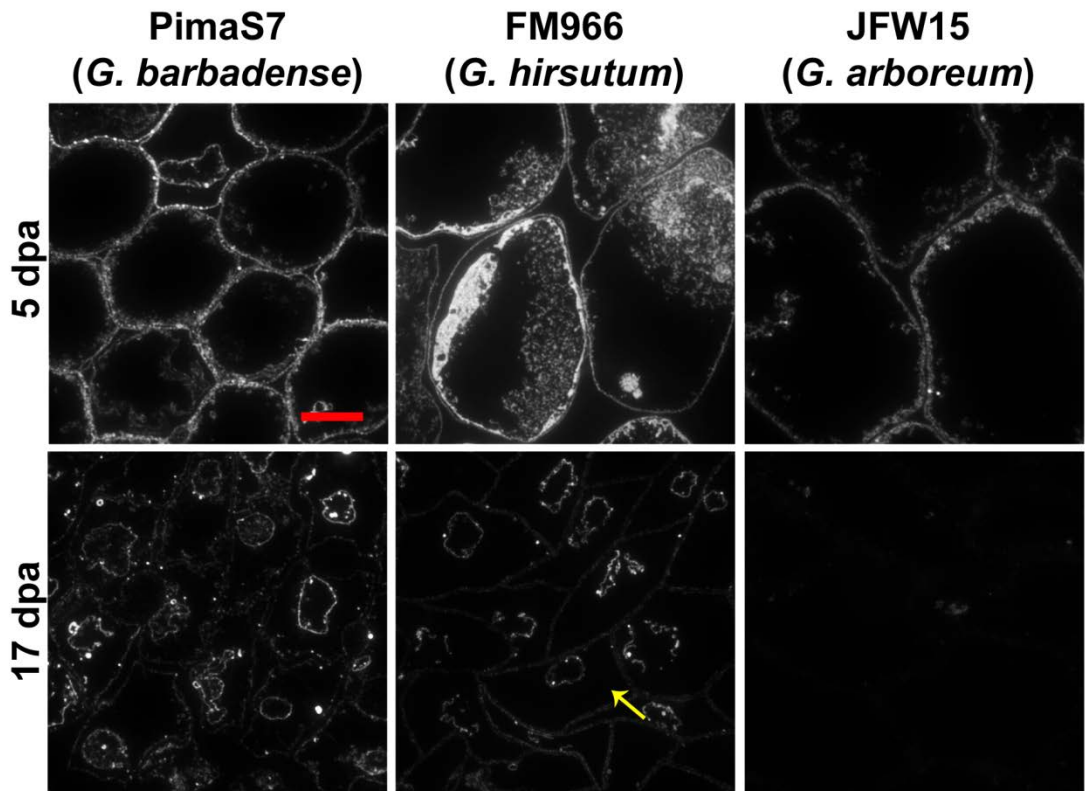
Figure 4-17. Immunolocalization of the JIM13 AGP epitope. Cross sections of developing and mature cotton fibres of PimaS7 (*G. barbadense*), FM966 (*G. hirsutum*) and JFW15 (*G. arboreum*). JIM13 labelled the fibre plasma membrane (arrows). Similar binding was found for LM6 (see arrows) which also binds to the fibre cell wall. Scale bar: 10 μm.

**A.** Arabinan – LM6
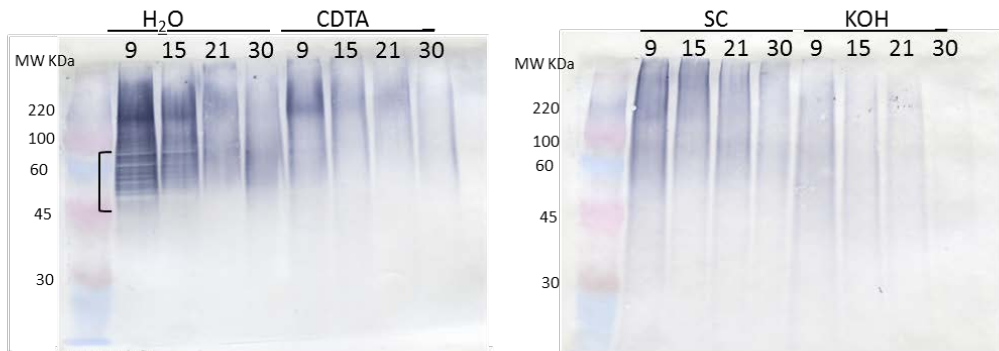
B. AGP – JIM13
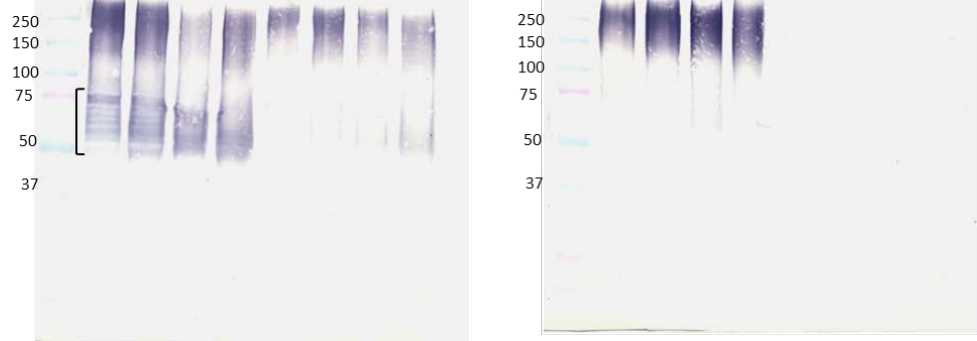
Figure 4-18. Western blot analysis of sequential fibre cell wall extractions from developing cotton fibres. Cell wall polysaccharides from 9, 15, 21 and 30 dpa fibre of FM966 Batch1 were extracted in water, sodium carbonate (SC) and potassium hydroxide and loaded on a gel. A. Immunoblotted with LM6. B. Immunoblotted with JIM13

4.2.5 Heteromannan is present in cotton fibre cell walls

The immunolocalization of heteromannan LM21 and BS400-4 epitopes in the cotton fibres was also compared using cross-sections of resin-embedded fibre at several developmental stages. On resin sections of mature cotton fibres, pre-treatment with sodium carbonate and pectate lyase uncovered heteromannan epitopes in the primary cell walls (Figure 4-19A). Both the LM21 and BS400-4 heteromannan epitopes were found in the primary cell wall of mature fibres from all cotton lines and were highly masked by pectic HG (Figure 4-19AB). The BS400-4 probe showed higher signal than the LM21 probe (Figure 4-19A) and PimaS7 (*G. barbadense*) had the highest fluorescence intensity at equivalent time exposures when compared to FM966 (*G. hirsutum*), Krasnyj (*G. herbaceum*) and JFW15 (*G. arboreum*) (Figure 4-19B). This correlates well with the glycan microarray data in which the LM21 epitope in mature fibres was detected at 40% of maximum signal observed earlier in development in PimaS7 while it was below the detection limit in other lines. *In-situ* labelling of developing PimaS7 fibre cross sections Figure 4-20) showed that the BS400-4 epitope is weakly detected in the secondary cell wall of 25 dpa fibres only and pectate lyase treatment did not unmask the epitope in developing fibres.
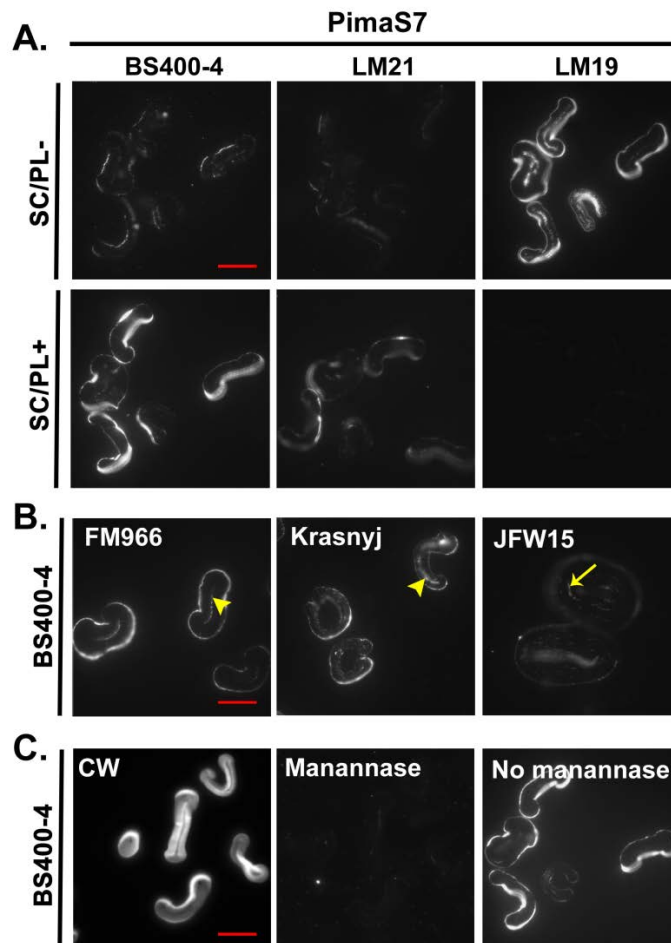
Figure 4-19. Immunolocalization of heteromannan in cross sections of mature cotton fibres. A. Unmasking of the BS400-4 and LM21heteromannan epitopes in equivalent sections of PimaS7 (*G. barbadense*) mature fibres after removal of pectic HG with pectate lyase. LM19 antibody is shown as control of the pectate lyase enzymatic action. SC: sodium carbonate. PL-: no pectate lyase treatment (only buffer). PL+: pectate lyase treated. B. The heteromannan BS400-4 epitope was found in all cotton species. Heteromannnans localized mainly at the primary cell wall and weakly in restricted regions of the secondary cell wall (arroheads) and in the lumen (arrows) in FM966 (*G. hirsutum*), Krasnyj (*G. herbaceum*) and JFW15 (*G. arboreum*). All sections were SC/PL+ treated. C. Mannanase treatment of PimaS7 mature fibres efficiently removed the heteromannan epitope BS400-4. All sections were SC/PL+ treated. All images in this figure were taken at the same time exposure (expect for Calcofluor White image in C). Time exposure in all BS400-4 and LM21 images: 1 s. Scale: 10 μm.
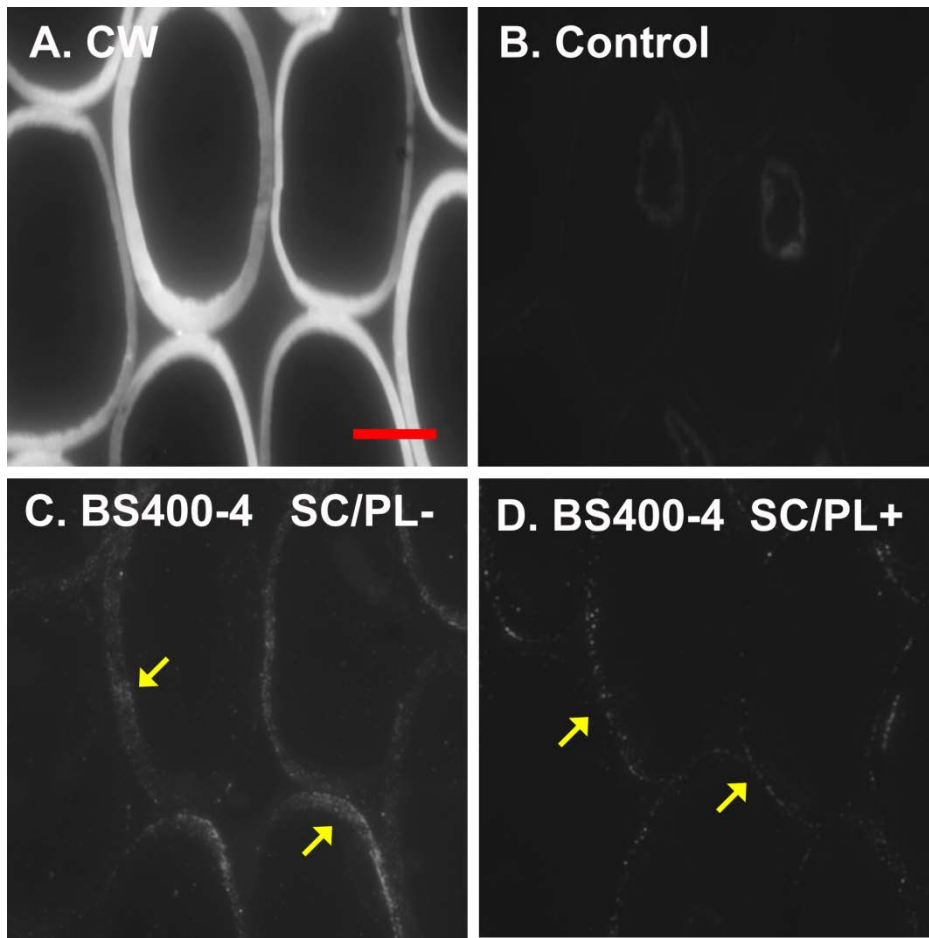
Figure 4-20. Immunolocalization of the BS400-4 heteromannan epitope in cross sections of 25 dpa from PimaS7 (*G. barbadense*) fibres. A. Representative Calcofluor White-stained cross section of 25 dpa fibres in PimaS7. B. Secondary antibody control image (SC/PL+), only autofluorescence of shrined cytoplasm cells can be seen. C. Heteromannan were weakly detected in a punctuated pattern in the growing secondary cell wall (arrows) without pectate lyase treatment. D. Pectate lyase treatment did not unmask the BS400-4 epitope. CW: Calcofluor White. SC: sodium carbonate. PL-: no pectate lyase treatment (only buffer). PL+: pectate lyase treated. Scale bar: 10 μm.

4.2.6 Heteroxylan is detected at the transition phase and during cellulose deposition in the cotton fibre secondary cell wall.

To study the presence of heteroxylan in the cotton fibre, several heteroxylan probes were screened on two cotton lines, FM966 and JFW15, at sequential developmental stages. The most abundant epitope detected was the AX1 arabinoxylan epitope which appeared in a punctuated pattern around the primary cell wall of 17 dpa fibres of FM966 and JFW15 (Figure 4-21). The already thickened secondary cell wall of JFW15 displayed AX1 labelling around the inner cell wall region (Figure 4-21AF). This double localization of the AX1 epitope was also visible in FM966 at 25 dpa (Figure 4-21C). In mature fibres, removal of pectin by pectate lyase uncovered the AX1 epitope in the primary cell wall (arrows in Figure 4-21DEIJ). Additionally, mature JFW15 fibres showed the AX1 epitope localized in concentric rings in the secondary cell wall (Figure 4-21IJ). Similar detection of heteroxylan in the secondary cell wall of mature fibres was observed when using xylan-directed carbohydrate-binding modules CBM2b-1-2 and CBM22 (Figure 4-22). The LM11 xylan antibody bound in a similar way but the signal was weaker and the UX1 glucuronoxylan (Koutaniemi et al., 2012) antibody bound mainly to the primary cell wall after pectin removal. The binding pattern in concentric rings was specific to the heteroxylan epitopes as verified by the LM19 HG antibody whose location was restricted to the primary cell wall of cotton fibres.
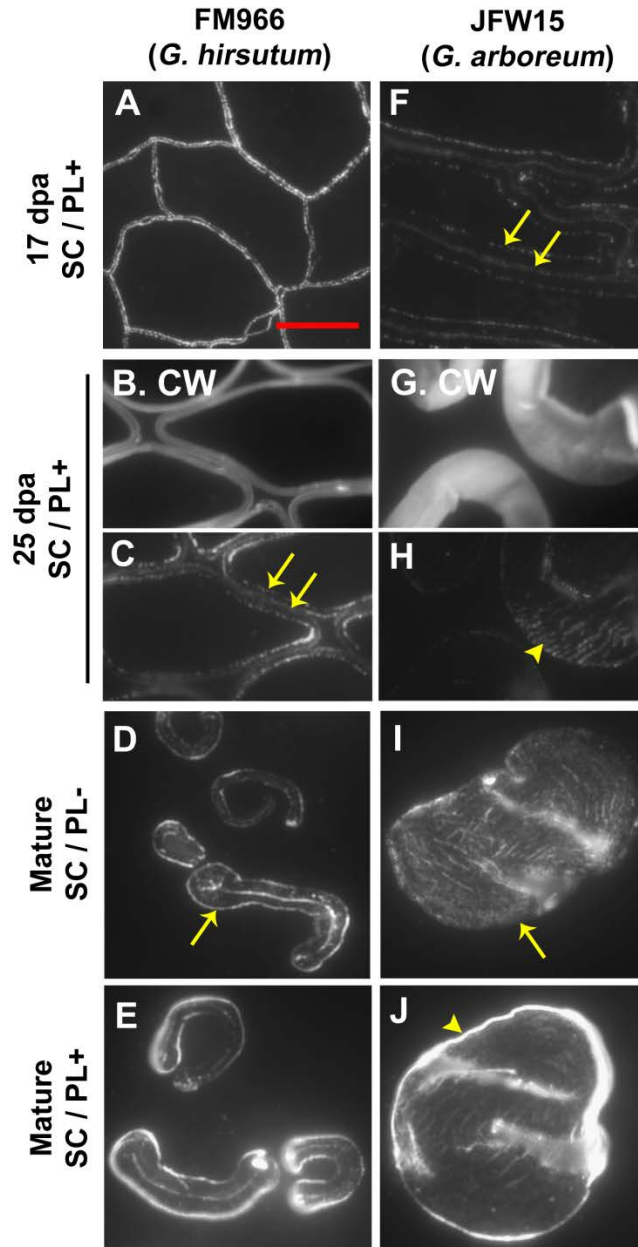
Figure 4-21. Immunolocalization of the AX1 heteroxylan epitope. Cross sections of developing and mature cotton fibres of FM966 (*G. hirsutum*) and JFW15 (*G. arboreum*). The AX1 epitope is detected at the inner and outer part of the cell wall is indicated by arrows in C and F. Unmasking of the AX1 epitope in the primary cell wall of mature fibres is shown by arrows in D, E, I and J. Striations of AX1 labelling can be seen in secondary cell walls in H, I and J. SC: sodium carbonate. PL-: no pectate lyase treatment (only buffer). PL+: pectate lyase treated. CW: Calcofluor White stained sections. Scale bar: 10 μm.
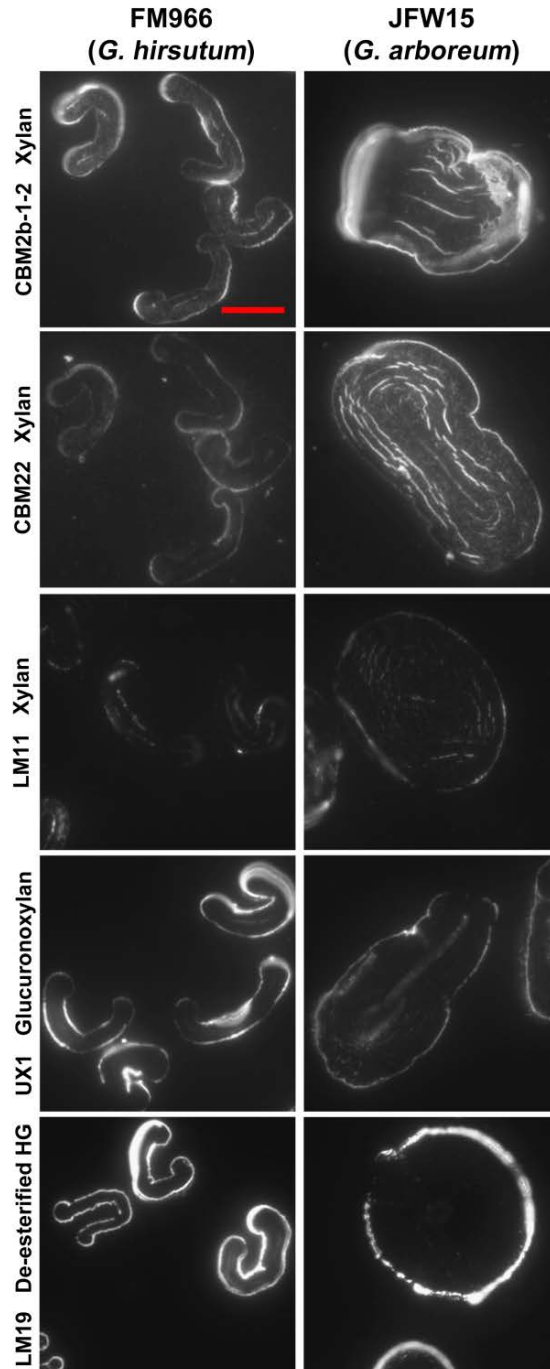
Figure 4-22. Immunodetection of an extended set of xylan epitopes/ligands. Cross sections of mature fibres of FM966 (*G. hirsutum*) and JFW15 (*G. arboreum*) using CBM2b-1-2, CBM22, LM11 and UX1 probes. LM19 (de-esterified homogalacturonan) labelling is shown as a comparative epitope specific to the primary cell wall. In all cases for the xylan probes sections were pre-treated with sodium carbonate and pectate lyase. Scale bar: 10 µm.

4.2.7 Callose detected at the innermost part of the thickening secondary cell wall

The callose BS400-2 epitope was abundant in the cotton fibre with a particular cell wall localization at the newly formed inner cell wall layer (Figure 4-23). BS400-2 labelled the cell wall of young fibres at 5 dpa in PimaS7 in a punctuated manner but a signal was not detected at the same time point in any of the other lines. BS400-2 labelling of the cell wall was strongly detected at 10 dpa in FM966 and with less intensity in the other two lines. At 17 dpa the already thickening secondary cell wall of the JFW15 line showed a gradient distribution of callose with a very strong signal at the innermost secondary cell wall layer (arrows in Figure 4-23) and decreasing towards the outside primary cell wall. This pattern became more obvious at 25 dpa in PimaS7 and the extra thickened JFW15 line and suggests that the BS400-2 callose epitope is being produced at the newly deposited cell wall layers and gets incorporated in the cell wall mainly at the end of the elongation phase and during secondary cell wall deposition. The BS400-2 epitope appeared to be distributed homogeneously throughout the cell wall of mature fibres in all cultivars.
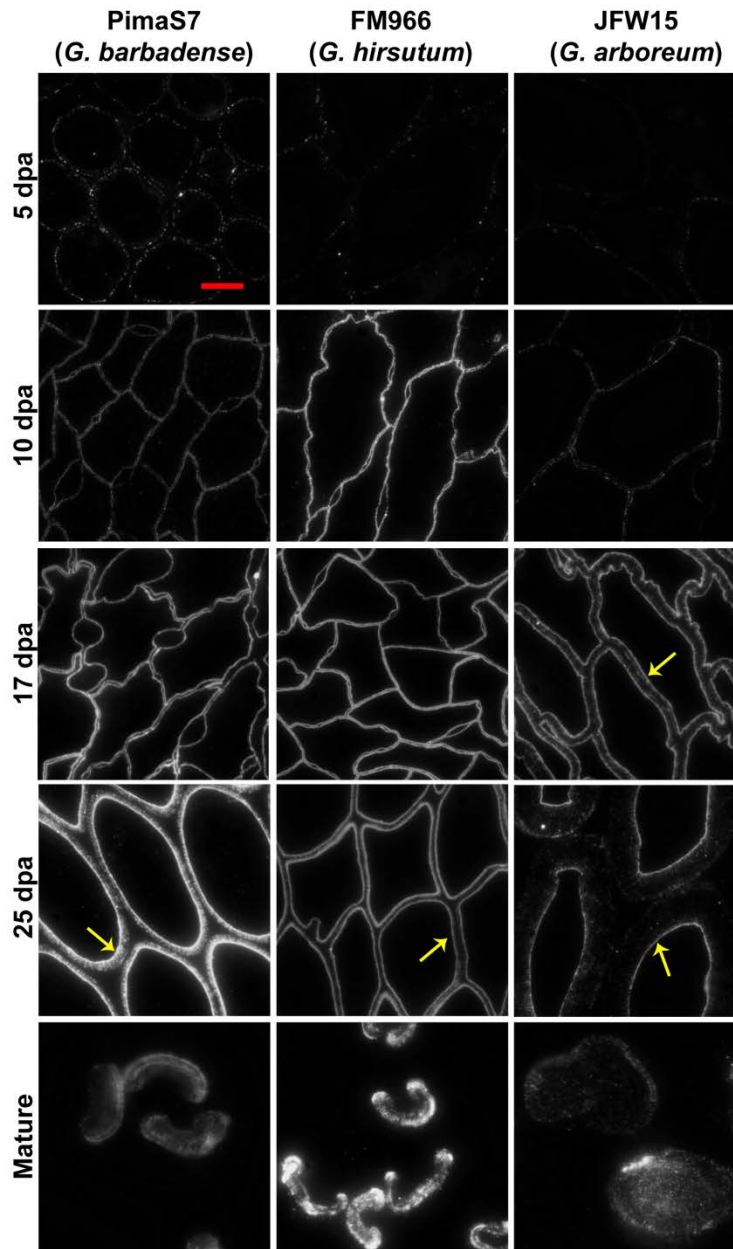
Figure 4-23. Immunolocalization of the BS400-2 callose epitope. Cross sections of developing and mature cotton fibres of PimaS7 (*G. barbadense*), FM966 (*G. hirsutum*) and JFW15 (*G. arboreum*). The BS400-2 callose epitope localised around the cotton fibre cell wall. Detection of the epitope increased during fibre development from 5 to 17 dpa. At 25 dpa, the callose epitope was highly abundant in the innermost secondary cell wall layer, decreasing gradually towards the outer secondary cell wall layers and primary cell wall. Callose was also present in fully developed fibres. Scale bar: 10 μm.

4.2.8   EDC profiling of cotton fibre glycans

Epitope detection chromatography (EDC) is a highly sensitive technique able to profile any glycan based material by separating its components through anion-exchange chromatography and identifying them by enzyme–linked immunoassay (ELISA) using cell wall directed probes (Cornuault et al., 2014). EDC can provide data on the glycan heterogeneity of a sample indicating subpopulations of a given epitope and pointing to unique glycan interactions. This technique is very useful to study the single celled cotton fibre tissue cell walls as they undergo extensive remodelling with a very active glycan synthesis and turnover.

The end of elongation was chosen for these EDC analysis as the beginning of secondary cell wall deposition is a very important phase in fibre development where cell wall glycans are modified to stop elongation and to prepare the cell for a phase of extensive cellulose deposition. Therefore, CDTA and NaOH cell wall extractions from 13, 15, 17 and 20 dpa fibres of FM966 were used which cover the transition phase (end of cell elongation and start of secondary cell wall). The samples used here were extracted as in Material and Methods section 2.16 and they belong to the same sample set used for the glycan microarray experiment in Chapter 3.

This data should be considered as an exploratory study that would benefit from replicates and from an extended antibody screening which due to time constrictions could not be done during the timeframe of this work.

Figure 4-26 shows the EDC profile of the HG (LM19 and LM20) and xyloglucan (LM15 and LM25) related epitopes in the CDTA extraction of FM966 fibre cell walls at 13, 15, 17 and 20 dpa. The broader peaks show the heterogeneity or complexity of the pectic HG population as identified by the LM19 and LM20 probes. This complexity is higher at the end of elongation (13 and 15 dpa) than at the onset of secondary cell wall (17 and 20 dpa). This possibly due to the presence of HG molecules esterified with neutral domains (possibly RG-I molecules highly branched with neutral chains) during elongation. At the end of elongation, the HG population becomes

simpler with less neutral domains covalently linked and, therefore, more acidic. The LM20 signal is very reduced by 20 dpa, this agrees with previous data and suggests that pectin is de-esterified at the end of cell elongation to promote pectin cross-linkages and cell wall stiffness.

CDTA-extracted xyloglucan detected by LM25 co-eluted with LM19 but only at 15 and 17 dpa suggesting that these two dpa in the FM966 line are relevant during the transition phase and that this acidic xyloglucan population might be produced only at this specific time.

The abundance of the RG-I related molecules (Figure 4-25) were significantly higher at these two intermediate dpa, 15 and 17 dpa. The RG-I backbone INRA-RU2 epitope co-eluted with LM19 and LM20 and the carrying molecules of INRA-RU2 epitope only appeared more acidic at the onset of cell wall deposition (20 dpa) but not earlier.

Interestingly, the LM5 and LM13 corresponding peaks are displaced to a more neutral position compared to the INRA-RU2 epitope suggesting the existence of two independent subpopulations of RG-I, one more neutral with highly substituted galactan (LM5) and arabinan (LM13) chains and one more acidic more related to HG acidic pectin core molecules. At 15 and 17 dpa co-elution of galactan and arabinan with the RG-I backbone suggests cell wall remodelling of the RG-I fraction during the transition phase. Both the LM5 and LM13 epitope signals disappeared at 20 dpa suggesting degradation of galactan (LM5) and arabinan (LM13) after fibre elongation. This correlated well with previous finding through immunolabelling and glycan microarrays.

Finally, the AGP JIM13 epitope carrying molecules showed lower acidity, and very similar peaks at all dpa, expect for 15 and 17 dpa which also showed slight co-elution with the INRA-RU2 epitope.

Neutral xyloglucan and heteromannan were not detected on the CDTA extraction but in the NaOH extraction. Figure 4-26 shows the EDC profile of NaOH cell wall extracts of 10 and 17 dpa from two cotton cultivars (FM966– *G. hirsutum* and JFW15– *G. arboreum*). The population of xyloglucan molecules at 10 dpa (LM25) had a slightly acidic subset of molecules which

is more abundant at 10 dpa than at 17 dpa. In addition, the JFW15 line showed greatly diminished xyloglucan content compared to FM966 mainly at 17 dpa, which correlates well with the higher secondary cell wall deposition.
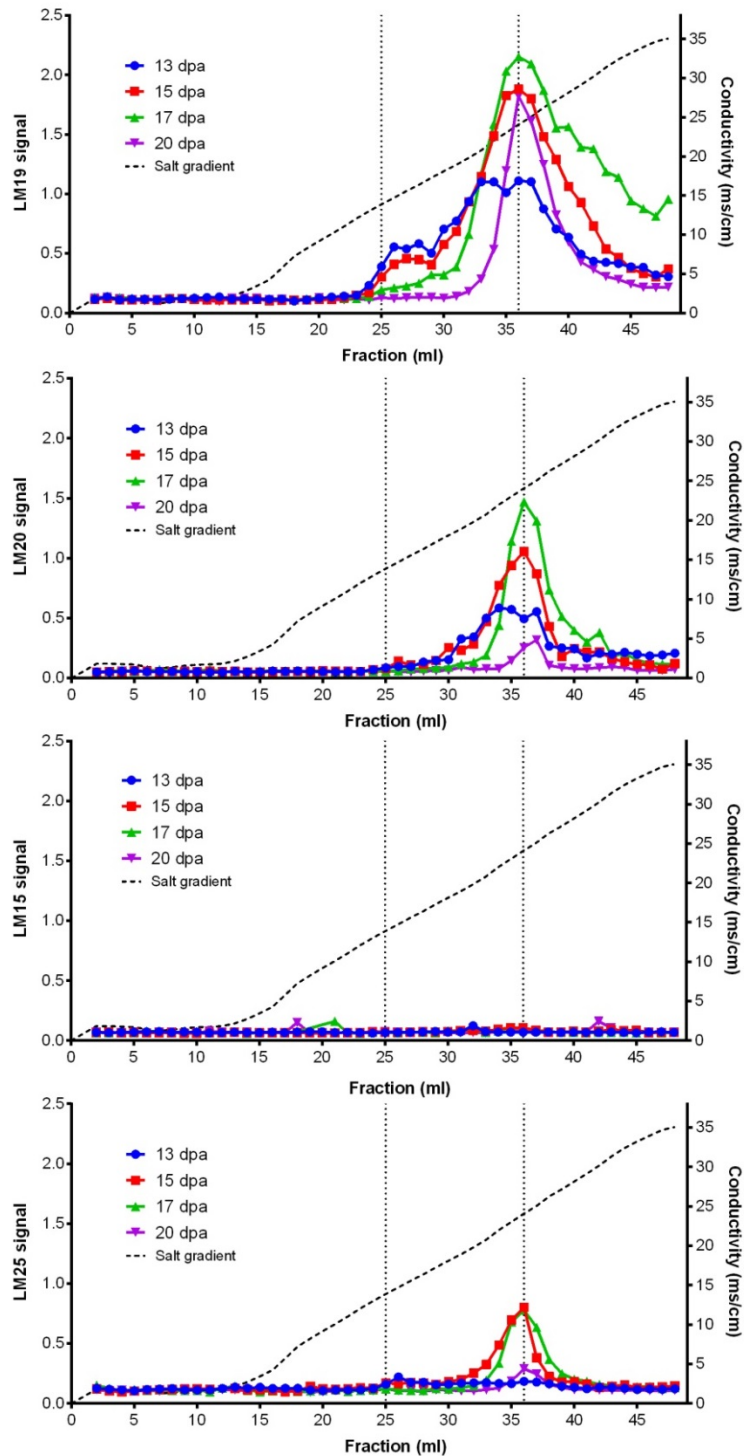
Figure 4-24. EDC profile of HG and xyloglucan related epitopes. CDTA extraction of cell wall fibres from FM966 at 13, 15, 17 and 20 dpa using de-esterified HG (LM19), highly-esterified HG (LM20), xyloglucan (LM15 and LM25) probes. Dotted line represents salt gradient measured by conductivity (ms/cm) in the right axis.
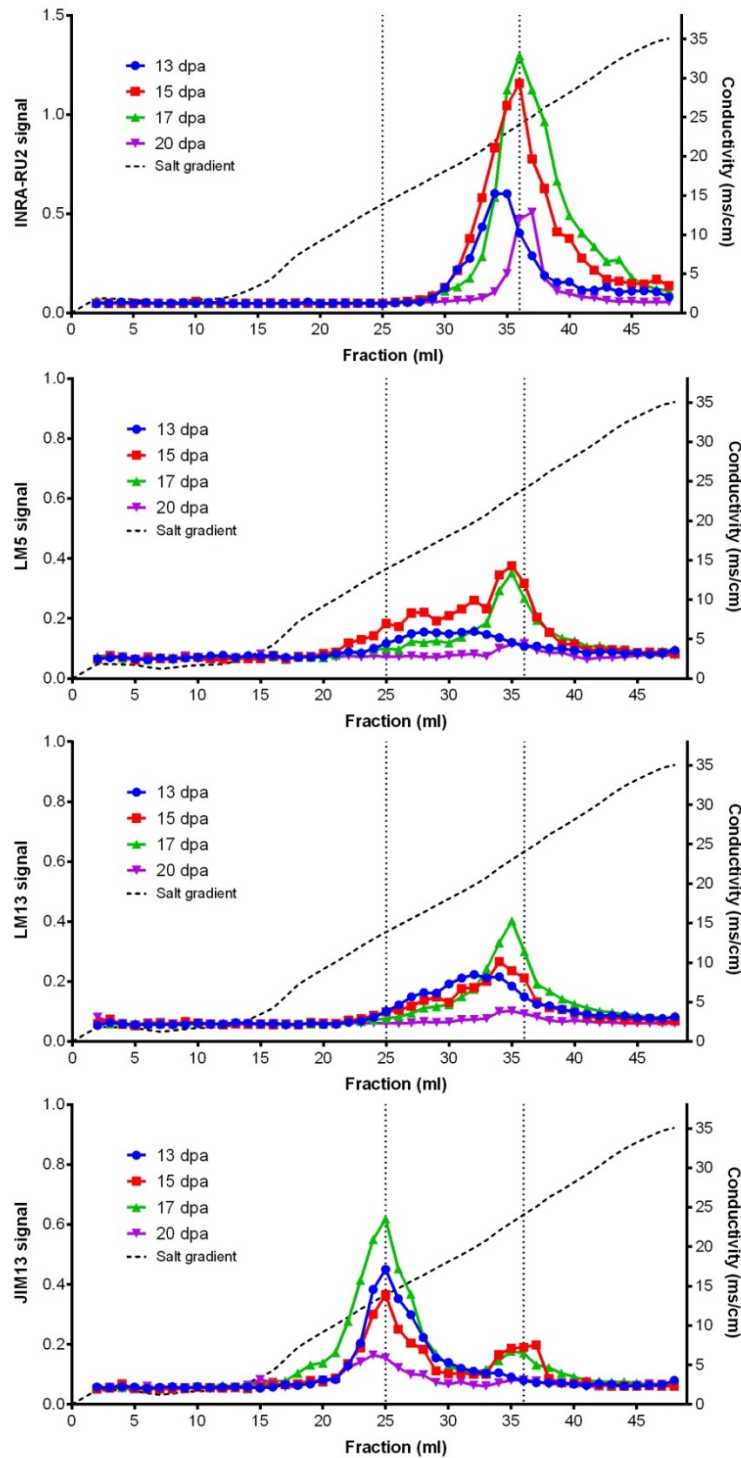
Figure 4-25. EDC profile of RG-I and AGP related epitopes. CDTA extraction of cell wall fibres from FM966 at 13, 15, 17 and 20 dpa using RG-I backbone (INRA-RU2), galactan (LM5), arabinan (LM6) and JIM13 (AGP) probes. Note the different Y axis ranges. Dotted line represents salt gradient measured by conductivity (ms/cm) in the right axis.
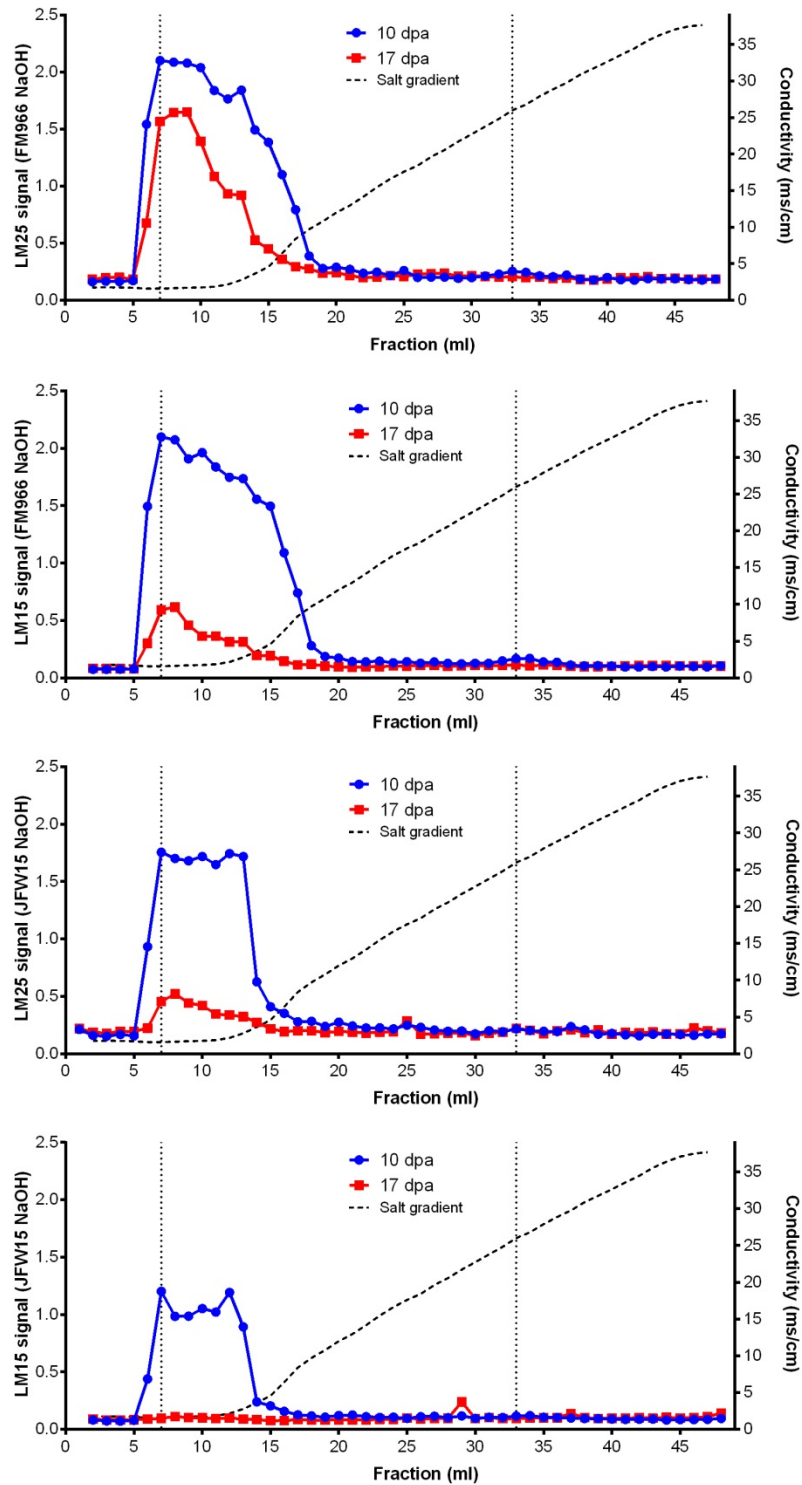
Figure 4-26. EDC profile of xyloglucan LM25 and LM15 epitopes. NaOH extraction of cell wall fibres from FM966 and JFW15 lines at 10 and 17 dpa using the xyloglucan LM25 and LM15 probes. Dotted line represents salt gradient measured by conductivity (ms/cm) in the right axis.

4.3 Discussion

Three main subjects and suggested future work are discussed below following the stages of cotton fibre development. In sections 4.3.1 and 4.3.2 the importance of the different pectin profiles and the CFML structure and composition during elongation and at the transition phase are discussed. Sections 4.3.3 and 4.3.4 are related to the novel detection of heteromannan in the cotton fibre and the importance of heteromannan, callose, and arabinoxylans during the transition phase and secondary cell wall thickening phases. Finally, section 4.3.5 discusses the genetic improvement of cotton with regards to the studied transgenic lines in this work. Section 4.3.6 refers to the arabinan-related epitopes and introduces Chapter 5 that focuses on the AGP epitope detected with the JIM13 probe.

4.3.1 Pectin is developmentally regulated in the cotton fibre

The mechanism of how HG pectin esterification modulates cell wall growth is complex. As in the pollen tube, pectin de-esterification and degradation seems to be developmentally regulated in cotton to allow extreme cell expansion by a well-tuned set of pectin modifying enzymes (see Intro section 1.1.2.7.2).

Results in 3.2.6.1 and 4.2.2 showed that de-esterified pectin is very abundant throughout the fibre cell wall, from the beginning of the elongation process until the fibre is fully matured. This contrasts with the highly extensible developing fibre cell and is in apparent contradiction with the usual correlation between de-esterified HG and cell wall rigidity. However, cell wall extensibility depends on a complex interplay of factors that modulate the final cell wall physical characteristics such as calcium availability and pectin degradation. Cell wall softening in the Arabidopsis shoot apical meristem tissue is known to be attained by HG de-esterification which in turn induces organ initiation (Peaucelle et al., 2011). In this case, HG de-esterification by PME action generates less protected pectin that can be more readily degraded by the enzymatic action of pectate lyases and

polygalacturonases which has been recently proved to induce cell elongation and flower development (Wolf and Greiner, 2012; Xiao et al., 2014). These observations agree with the results obtained by Wang et al. (2010) in which the action of a cotton pectate lyase (GhPEL) was needed to allow fibre elongation by degradation of de-esterified pectin. It follows then, that the high abundance of de-esterified HG in the elongating cotton fibre cell wall and its partial degradation creates a soft extensible cell wall that allows rapid elongation.

Another important factor to be considered for HG crosslinking is Ca^{2+} availability (Ralet et al., 2003). It has been reported that changing the subcellular calcium homeostasis in meristematic tissues by calcium accumulation in the chloroplast induce early flowering (Wang et al., 2003). Limiting calcium availability might reduce pectin cell wall crosslinking which promotes cell wall softening via pectin degradation. In relation to this, the recent idea of AGPs as Ca^{2+} capacitors is a very interesting concept on how the high Ca^{2+} binding capacity of the AGP glucuronic acid pairs can be involved in Ca^{2+} signalling (Lamport and Várnai, 2013; Pickard, 2013; Lamport et al., 2014). It is plausible that AGP might be able to take part in cotton fibre development by sequestering available Ca^{2+} and therefore reducing crosslinking of de-esterified HG molecules. Here, it was observed that AGPs are highly abundant in the cotton fibre during elongation and it would be interesting to explore the cytosolic availability of Ca^{2+} ions in the cotton fibre at different developmental phases in cultivars such as the ones used in this study.

Immunochemistry analysis in this work using probes that can discriminate between different degrees of HG esterification revealed that highly methyl-esterified HG (LM20) coexisted with de-esterified HG in the fibre primary cell wall during fibre elongation and highly-esterified HG disappeared thereafter. Pectin crosslinking through calcium ions via PME methyl de-esterification only occurs at the onset of secondary cell wall deposition (when cell elongation ceases) as shown by PME expression profiles studies in developing cotton (Liu et al., 2013). Immunohistochemistry detection of the

highly-esterified pectin (LM20) repeatedly disappeared during fibre development depeding on germoplasm and correlating with the end of elongation. Nonetheless, the presence of the LM20 epitope analysed by immunolabelling was extended in time in the JFW15 (*G. arboreum*) line compared to FM966 (*G. hirsutum*) and China10 (*G. barbadense*) lines. This contrasts with the glycan microarray data where highly methyl-esterified pectin in the *G. arboreum* lines occurs earlier than in other lines. Two factors could be influencing the apparent contradictory results. One is the dilution effect by cellulose in the glycan microarrays in JFW15 (explained in Chapter 2 discussion), another is pectin degradation in the *G. barbadense* and *G. hirsutum* lines due to handling. Pectin degradation due to handling is a manifestation of the labile nature of pectin and suggests that it might be dependent on cultivar as it mainly occurred in the *G. barbadense* and *G. hirsutum* lines.

The complexity and composition of the RG-I molecules are also important modulators of cell wall extensibility and cell elongation. The galactan LM5 epitope has been correlated with the onset of cell elongation (McCartney et al., 2003) as well as end of elongation (Willats et al., 1999; Gorshkova et al., 2004). Here, immunohistochemistry using the pectic RG-I side chain galactan epitope (LM5) on fibre sections showed that $(1\rightarrow4)$-β-galactan disappearance preceded highly-esterified disappearance (LM20) at the end of fibre elongation and that this epitope is masked by HG. Preliminary EDC experiments also showed that the galactan (LM5) epitope disappeared at the transition phase. The galactan carrying molecules (in the CDTA extraction) became less substituted and more acidic at the end of cell elongation and disappeared later on, suggesting that degradation of galactan neutral chains of initially highly branched RG-I molecules is required at the end of cell elongation. Galactan (LM5) co-elution with de-esterified pectin (LM19) is observed at elongation, while co-elution with the RG-I backbone (INRA-RU2) and highly-esterified pectin (LM20) was restricted to a short period of time at the transition phase (15 and 17 dpa) just between elongation and secondary cell wall deposition. This suggests that galactan degradation can act as a

signal of the end of cell elongation. A study on pectin composition of transgenic potato expressing a fungal endo-1,4-β-d-galactanase supports the idea that degradation of the galactan side chain facilitate the action of the PME to de-esterify pectin (Oxenbøll Sørensen et al., 2000). In this sense, as RG-I becomes less hairy, de-esterified HG stretches are more likely to interact and crosslink which stiffens the cell wall.

An extended EDC analysis together with a comparative analysis of the temporal expression and transcript levels of PME galactanases, PME, pectate lyase and polygalacturonase-related transcripts in these particular cultivars at different developmental stages could give some clues on the role of (1→4)-β-galactan in cell elongation and whether pursuing genetic approaches to delay galactan degradation is worthy in order to achieve longer fibres. Such comparative developmental analysis of the transcriptome in these particular cultivars would also shed some light on the genetic regulation of the timing of the transition phase between these lines and the reason behind the earlier transition phase and reduced fibre length in the JFW15 cultivar.

4.3.2 Fibre cell adhesion and detachment is mediated by the CFML.

Pectic HG is not only involved in cell wall extensibility and cell elongation but also in cell-cell adhesion through the middle lamella (Orfila et al., 2001; Willats et al., 2001; Jarvis et al., 2003; Marry et al., 2006; Ordaz-Ortiz et al., 2009). Cotton fibres possess a middle lamella that does not originate from cytokinesis after cell plate formation but after cell to cell contact of elongating cotton fibres. The CFML brings fibre cells together and helps them to turn and fold for an optimised packing of cells in the very restrictive volume of the cotton locule at fast elongation (Paiziev and Krakhmalev, 2004). Singh et al. (2009) showed in diverse TEM and SEM images the existence of "material-filled bulges" (see Singh el al. (2009) Figure 1-F,G and supplementary data figure S3). Those material-filled bulges were considered as evidence of the presence of a cell fibre middle lamella (CFML), and xyloglucan and non-esterified homogalacturonan were described as components of the CFML

156

(Singh et al., 2009). More recently, bigger areas named as "loosely bound xyloglucan" were also considered part of the CFML (Avci et al., 2013).

The developmental studies carried out in this work provides a novel unified description of the presence of two distinctive structures of the CFML, particle-filled enlarged regions and paired CFML bulges, the first more related to the previously described CFML in Avci et al. (2013) and the second to that in Singh et al. (2009). Screening with polysaccharide antibodies and CBMs revealed the presence of fucosylated xyloglucan (CCRC-M1) in *G. hirsutum* and *G. barbadense* in opposition to the claimed lack of fucosylated xyloglucan in *G. barbadense* by Avci et al. (2013). In addition to the reported xyloglucan and de-esterified HG (LM19) components, arabinan (LM6) and XET proteins (anti-PttXET16A) were also found in the enlarged regions of the CFML, while the bulges were mostly made of xyloglucan.

The origin of the particles in the enlarged CFML regions could be the result of the combined action of several cell wall loosening enzymes like expansins, endoglucanases and endotransglycosylases that release fragments of the cell wall allowing the cell to expand. A great number of publications review the role of these enzymes during elongation by loosening the cell wall in different systems (Fry et al., 1992; Cosgrove, 2000). The degradation of XG-cellulose tethers is essential in cell wall loosening. This degradation can take place via polysaccharide hydrolysis and addition of XG oligomers by xyloglucanases and xyloglucan endotransglucosylases/hydrolases (XTH) (Hayashi and Kaida, 2011). Literature in cotton fibres has repeatedly reported gene upregulation and peak activities of cell wall remodelling enzymes during fibre elongation - see introduction and Shimizu et al. (1997); Orford and Timmis (1998); Michailidis et al. (2009). In cotton fibres, it has been described that xyloglucan endotransglycosylase (XET) activity is particularly high during the elongation phase and then declines during the transition phase (Shao et al., 2011). CFML particles could be the result of this extensive enzymatic activity over the cell wall that digest and release polymers into the intercellular spaces.

157

Xyloglucan have been related to cell adhesion and detected in patterns around the cell wall of isolated tomato fruit pericarp parenchyma cells (Ordaz-Ortiz et al., 2009). The CFML in cotton fibres might originate then from the release of xyloglucan and pectins polymers which keeps fibre cohesiveness after the activity of cell wall remodelling enzymes.

Here, the paired pattern of CFML bulges was only prominent at the transition phase in FM966 and Coker cultivars (*G. hirsutum*), suggesting that the CFML organization into a paired pattern is specific of the *G. hirsutum* and that is not an essential feature for general fibre development. How the cell regulates the formation of this specific pattern and for what purpose is an intriguing question difficult to answer. It is worth mentioning that the linear arabinan LM13 epitope localized specifically in the region between the paired bulges and nearly no signal was detected in the cell wall region surrounding the CFML bulges. Absence of arabinan chains in the pectic polysaccharides have been commonly associated with cell-cell detachment (Iwai et al., 2001; Peña and Carpita, 2004). It is possible that the paired bulges are the starting points of cell detachment by the degradation of cell wall arabinan in the surroundings of the CFML bulges.

4.3.3   Heteromannan is present in the cotton fibre cell walls.

The presence of heteromannan was been shown here for the first time to occur in developing and mature cotton fibres of tetraploids *G. hirsutum* and *G. barbadense* as well as the diploids *G. herbaceum* and *G. arboreum* (by immunohistochemical analysis presented in this chapter and linkage analysis in Chapter 3). Heteromannan polysaccharides were only detected in 25 dpa and mature fibres by *in situ* labelling, however, it was present in all lines at earlier developmental stages in the NaOH extract as shown by glycan microarrays. This suggests that the heteromannan spatial or chemical association to other cell wall molecules (or perhaps O-acetylation of the mannosyl residues) may block the immuno-detection of heteromannan in the intact cotton fibre cell walls at early developmental stages unless extracted.

Despite the extraordinary capacity of secondary cell wall formation of the cotton fibre, mannan polysaccharides were only detected in the primary cell walls of mature fibres and linkage analysis showed that they occur at very low levels relative to cellulose. This suggests that a structural role of mannan in secondary cell wall of the cotton fibre cell walls is unlikely to be significant and another function of mannan in cell signalling and the regulation of cell elongation or secondary cell wall deposition (Liepman et al., 2007; Zhao et al., 2013) is more likely.

4.3.4 Functional significance of heteroxylan and callose production at the transition phase

4.3.4.1 Heteroxylan

Heteroxylan was abundant in the cotton fibre at later developmental stages and the arabinoxylan AX1 epitope showed a clear time-dependent developmental profile. *In situ* labelling with AX1 showed the strongest and clearest signal at 17 dpa with an AX1-rich layer in the innermost part of the forming secondary cell wall as well as the primary cell wall. This is in agreement with the glycan microarray data where the AX1 epitope showed a peak at 17 dpa for all lines suggesting a later synthesis of this epitope compared to the heteromannan epitope and pointing to a role of this epitope during the transition phase. In contrast, the LM11 antibody only bound weakly to mature fibres after pectin removal suggesting the recognition of different xylan epitopes by these probes. AX1 antibody was produced after immunization with arabinoxylan oligo-conjugates (Guillon et al., 2004), whereas LM11 was produced after immunization with a xylopentaose-BSA conjugate (McCartney et al., 2005). Although both AX1 and LM11 antibodies are expected to recognize to some extent arabinosyl-substituted xylan, LM11 in some instances does preferentially bind to unsubstituted xylan (Lovegrove et al., 2013). This differential binding of the two probes suggests that most of the cotton fibre cell wall heteroxylan is highly substituted. Interestingly, AX1 bound to the secondary cell wall of mature fibres identifying concentric layers around the fibre elongation axis. Concentric layers of cellulose have been previously observed in *G. hirsutum* cross

sections after swelling with NaOH (Balls, 1919; Haigler et al., 1991; Roberts et al., 1992). These layers have been described as daily growth-rings occurring due to a diurnal cycling of cellulose deposition that depends on day and night temperatures and can only be seen at the microscopic scale after fibre swelling. It is unclear whether the observed concentric layers in the JFW15 line are over pronounced growth rings of the same nature as the ones discussed above. It is possible that the cotton cell wall heteroxylan has a specific role in controlling aspects of this cyclic temperature-controlled cellulose microfibril deposition. In this regard, it has been recently observed that overexpression of *PtxtXyn10A*, a cell wall xylan endotransglycosylase, impacts cellulose microfibril angle in wood fibres (Derba-Maceluch et al., 2014), although the underlying cellular mechanism is unclear. A role of heteroxylan in cellulose microfibril deposition would also be consistent with the AX1-rich inner layer of secondary cell wall next to the plasma membrane.

In addition to the AX1 arabinoxylan epitope, the UX1 glucuronoxylan epitope was also present in mature fibres. Recently, it has been reported that two glucuronoxylan glycosyltransferases, GhGT43A1 and GhGT43C1, are preferentially expressed in 15 dpa and 20 dpa cotton fibres (Li et al., 2014). Although glucuronoxylans are known to be a major component of secondary cell walls and only found in minor quantities in the primary cell walls of dicotyledonous plants (Zablackis et al., 1995), in our study UX1 bound mainly to the primary cell walls of both FM966 (*G. hirsutum*) and JFW15 (*G. arboreum*) cotton fibres upon removal of pectic HG.

The function of heteroxylan is commonly related to the strengthening of cell walls and a load-bearing role as revealed by xylan mutants (Turner and Somerville, 1997; Hao and Mohnen, 2014). Cotton fibres have little need to cope with gravity or external forces during their development, but the strength of the fibre cell wall is crucial for its suitability for textile processing. The synchronicity between cellulose and heteroxylan in the cotton fibre cell wall points to a potential connection between these polysaccharides that modulates the construction (and perhaps the final fibre strengh) of

secondary cell wall in cotton fibres. As reported here, such a connection is also evidenced by the fluorescence imaging of heteroxylan epitopes striations in layers reflecting cellulose deposition in secondary cell walls.

4.3.4.2 Callose

Callose is commonly observed during wound responses in most plant tissues and in plasmodesmata gating. In the cotton fibres, callose deposits around the fibre cell wall and it also controls symplastic transport between the fibre and the seed epidermal cells at the fibre base plasmodesmata (Ruan et al., 2004). Glycan arrays and linkage analysis presented in Chapter 3 demonstrate that callose production peaks at the transition phase (around 17 dpa) which agrees with the immunohistochemical analysis in 4.2.7. and extensive literature on callose in developing cotton fibres carried out in the 70s and 80s (Meinert and Delmer, 1977; Maltby et al., 1979; Waterkeyn, 1981; Jaquet et al., 1982).

Callose immunolabelling during fibre development can be detected in fibres as early as 5 dpa in *G. barbadense* and *G. hirsutum*. Similar labelling was found at later stages as the one reported by Avci et al. (2013). Callose labelling appeared to be in the innermost cell wall layer in a similar fashion as the arabinoxylan AX1 epitope at 17 dpa. At later developmental stages callose was dispersed into the secondary cell wall in a gradient less abundantly in the older layers of cellulose whereas the arabinoxylan AX1 epitope appeared in concentric layers from the primary to the innermost secondary cell wall layer as discussed earlier.

There are several putative genes identified as callose synthases (named as CalS or GSL and belonging to the GT48 family) in Arabidopsis, *Nicotiana alata*, barley (Hong et al., 2001; Verma and Hong, 2001; Li et al., 2003; Brownfield et al., 2007) and cotton fibres (Cui et al., 2001) whose catalytic activity at the plasma membrane seems to be independent of cellulose synthases (CESAs) although both complexes are likely to interact with each other (Li et al., 2013). The higher intensity of labelling in the innermost cell wall layer might be simply a cause of the higher callose production in the proximity of the plasma membrane where is synthesised. In fact callose has

been shown to co-localise with the membrane sucrose synthase (SUS) (Amor et al., 1995; Salnikov et al., 2003) that feeds glucose into the cell wall to produce high amounts of cellulose during secondary cell wall deposition.

The role of callose at the transition phase and during the thickening fibre cell wall has been a topic of discussion since it was first detected and still not fully understood. It has been proposed that callose could form a hydrated layer outside the plasma membrane where the crystallization of cellulose microfibrils takes place (Waterkeyn, 1981) and in pollen tubes it is thought to serve as a robust layer that prevents radial cell expansion (Parre and Geitmann, 2005). The thinning of the primary cell wall during elongation might promote the production of callose at the onset of secondary cell wall to produce a stronger cell wall layer that can cope with turgor while the fibre microfibrils re-orientate into less longitudinal angle during deposition of subsequent wall layers of cellulose . The analysis of cellulose crystallinity and fibre properties after knocking-down callose synthases would provide very valuable information in our understanding of callose in the context of secondary cell wall deposition and their possible interaction with newly forming cellulose microfibrils and other glycans.

Both callose and arabinoxylans are very important polysaccharides during the transition phase and during secondary cell wall deposition in the cotton fibre and, although their roles in this system are not well understood, they both are possibly part of the cellulose deposition mechanism.

4.3.5   Genetic improvement of cotton

The immunohistochemical analysis of the CslC4/XT1 transgenic lines corroborated that the genetic approach to increase the xyloglucan content in the secondary cell wall was successful. Labelling with several xyloglucan probes indicated that the genetic modifications inserted produced xyloglucan with no fucose or galactose residues in the secondary cell wall. This increase in xyloglucan content provided the fibre with improved capacity to take up dyes.

It is worth mentioning that while in the non-transgenic lines there was nearly no binding of the LM15 antibody after xyloglucanase treatment, in the CslC4/XT1 transgenic lines the LM15 and LM25 binding to the secondary cell wall could not be removed after xyloglucanase treatment. A possible explanation is that xyloglucan in the secondary cell wall of these fibres tightly integrated with cellulose microfibrils in domains different from those in the primary cell wall (Park and Cosgrove, 2012) and that are not accessible by xyloglucanase.

4.3.6 Recognition of arabinan-related epitopes by LM6, LM13 and JIM13 probes.

The arabinan antibody LM6 labelled not only the cell wall but also was found to identify AGPs that were also detected by the AGP antibody JIM13. Western blots showed that the AGP detection is higher during the fibre elongation phase and bands with specific molecular weights could be recognized both by JIM13 and LM6 probes. These results agree with the previously reported data of LM6 binding to some AGPs (Lee et al., 2005)(Lee et al., 2005)(Lee et al., 2005)(Lee et al., 2005)(Lee et al., 2005)(Lee et al., 2005)(Lee et al., 2005)(Lee et al., 2005).

The LM13 antibody binds preferentially to a larger chains of unbranched arabinan or linearized arabinan, while LM6 would bind to a shorter and therefore more abundantly distributed arabinan epitope. LM13 is usually considered in literature as a subset of the pectic arabinan (Verhertbruggen et al., 2009), however the results presented here showed a more extensive occurrence of the LM13 epitope over the LM6 one during development, indicating that the LM13 epitope is not a subset epitope but somehow differs from the LM6 one.

4.4 Summary

The main findings of this chapter are summarised below and in Figure 4-27:

- Pectic HG has a very labile nature and HG degradation depends on environmental and handling conditions as well as the cell wall context in each cultivar.

- The CFML is present after cell adhesion during fibre elongation and might lead cell wall detachment at the onset of secondary cell wall. The CFML is composed of fucosylated xyloglucan, de-esterified HG, xyloglucan endotransglycosylase enzymes and arabinogalactan proteins not only in *G. hirsutum* cultivars but also in two lines belonging to *G. barbadense* and *G. arboreum* contradicting previously published data.

- At the onset of secondary cell wall deposition, HG is methyl de-esterified and galactan and arabinan polysaccharides are degraded promoting pectic HG crosslinking and cell wall stiffening.

- Heteromannan localization in the cotton fibre was demonstrated by two heteromannan directed probes and was mainly detected in the primary cell wall at maturation.

- The transition phase is marked by a peak of callose and arabinoxylan production. This last one was observed between secondary cell wall layers possibly correlated with the cyclic deposition of cellulose in the cotton fibre secondary cell wall.

- The arabinan LM6 epitope is also part of the molecule recognised by the AGP JIM13 probe.

- The LM13 epitope is shown here for the first time to recognise a different range of molecules compared to the LM6 epitope.

- Overproduction of xyloglucan in the secondary cell wall synthesis was confirmed by immunohistochemistry in the transgenic cotton line CslC4/XT1.
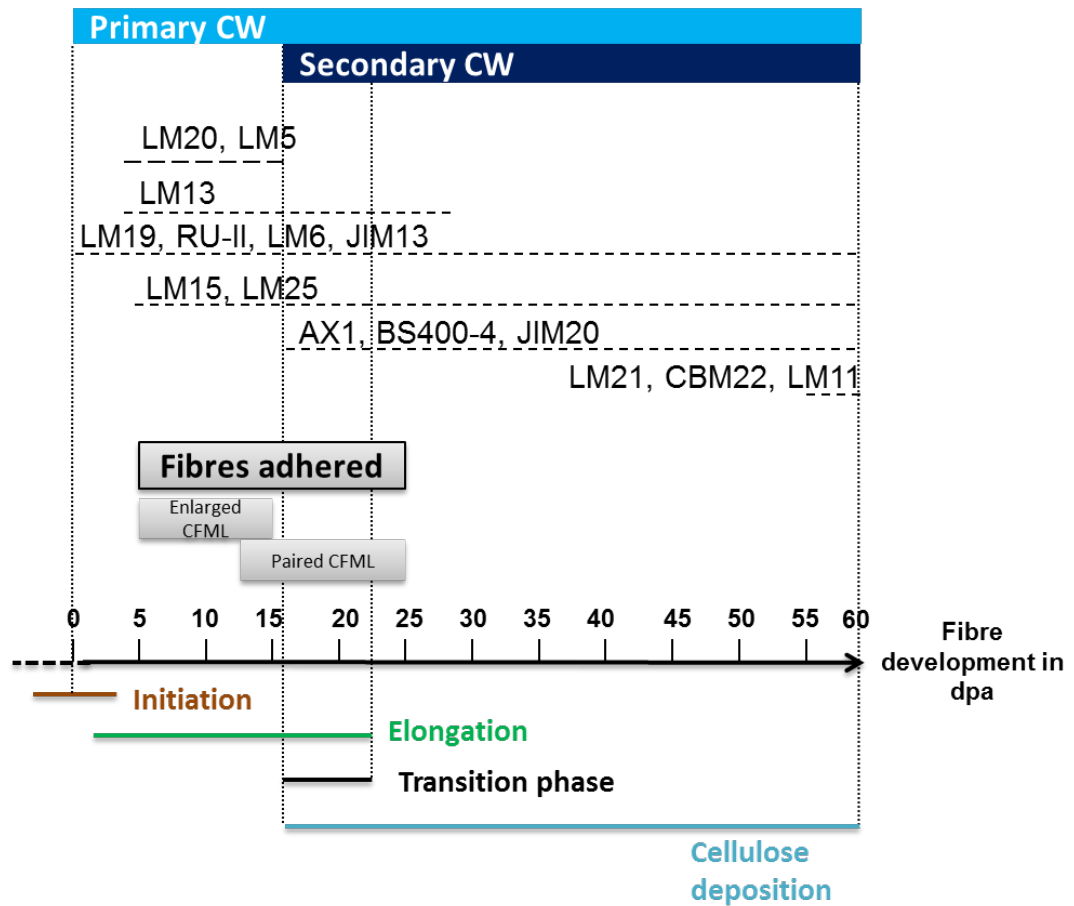
Figure 4-27. Fibre development summary diagram. Presence of the CFML and cell wall polysaccharide epitopes relative to fibre development as observed by immunochemistry analysis in the FM966 (*G. hirsutum*) cultivar.

Chapter V

5 Further aspects of mAb/CBM-based approaches to understanding cotton fibre development

5.1 Introduction

This chapter focuses on two topics: the binding specificity of the carbohydrate binding module *Ct*CBM3a a widely used probe for the detection of crystalline cellulose (see 5.2.1 and 5.2.2) and the use of an AGP-binding mAb (JIM13) to study possible novel mannan-AGP interactions in the developing cotton fibre (see 5.2.2 and 5.3.2).

5.1.1 The carbohydrate binding module *Ct*CBM3a

A wide range of microbial species and systems contribute to the degradation of the insoluble and often intractable plant structural polysaccharides using glycoside hydrolase enzymes (Gilbert, 2010). A feature of these microbial glycoside hydrolase enzymes is their modular architecture in which non-catalytic carbohydrate binding modules (CBMs) are appended via flexible linker sequences to the catalytic modules. CBMs have been extensively characterised and now grouped into 71 sequence-based families in the Carbohydrate Active Enzymes database (http://www.cazy.org/; (Lombard et al., 2014)). CBMs can also be classed as one of three binding types: type A bind to the surface of crystalline polysaccharides, type B interact with internal regions of single glycan chains (*endo*-type) and type C recognise the termini of glycan chains (*exo*-type) (Boraston et al., 2004; Gilbert et al., 2013).

The binding site of family 3a CBM, from the scaffolding subunit of *Clostridium thermocellum* (*Ct*CBM3a) is a type A module that presents a hydrophobic planar surface comprised of predominantly aromatic residues, which interact with the crystalline cellulose of microfibrils (Tormo et al., 1996). The opposite surface to the cellulose binding site forms a shallow grove containing conserved residues although the function is unknown (Tormo et al., 1996).

CBMs have been widely used as molecular probes for the *in situ* analyses of plant cell wall polysaccharides (McCartney et al., 2004; McCartney et al., 2006) and *Ct*CBM3a has been used to study the presence of crystalline cellulose in plant materials (Blake et al., 2006; Kljun et al., 2011).

This chapter's section 5.2.1 focuses on the binding specificity of the *Ct*CBM3a and it is demonstrated that in addition to binding crystalline cellulose, *Ct*CBM3a can also interact with xyloglucan *in situ* and *in vitro* at the site that binds to crystalline cellulose.

5.1.2   Arabinogalactan proteins (AGPs)

Arabinogalactan proteins (AGPs) are part of the wide group of hydroxyproline-rich glycoproteins (HRGPs) that contain glycosylated motifs O-linked to the hydroxyproline residues of the protein backbone. The carbohydrates attached are type II arabinogalactans and form up to 90 to 95% (w/w) of the molecule. AGPs and many can be found in the cell wall as well as in intercellular spaces and secretions. AGPs are incredibly heterogeneous and complex in their glycan and protein composition and profuse literature can be found regarding AGP roles in wide variety of biological processes as summarised by Ellis et al. (2010), Seifert and Roberts (2007) and briefly in the introduction of this work.

The purification of AGPs from other components to study their composition and interaction with other glycans, such as the recently discovered AGP-xylan complex (Tan et al., 2013), is a major challenge in order to relate compositional heterogeneity with functionality. The β-glucosyl Yariv reagent (β-D-Glc Yariv reagent) binds to AGPs and has been used since it was first described by Yariv et al. (1967) to isolate, detect and to disturb functionality of AGPs in plant tissues (Popper, 2011). However this β-D-Glc Yariv reagent cannot be used to isolate a unique AGP population sample and several isolation steps through chromatography and other techniques are needed. The β-D-Glc Yariv reagent has been recently shown to bind to β-1,3-galactan chains longer than five residues (Kitazawa et al., 2013; Paulsen et al., 2014).

This chapter focuses on preliminary data obtained during the isolation and initial characterization of the molecules recognised by the AGP antibody JIM13. AGPs were found to be very abundant in the water soluble substance (named fibre exudate) released by dissected developing seed/fibres during soaking in distilled water or PBS. This chapter explores the composition of the developing fibre exudate in section 5.2.2.1 and the isolation of the major AGP (JIM13) and xyloglucan (LM15) epitopes from the exudate in section 5.2.2.2. Initial experiments with a batch of the LM21 antibody (LM21*) showed labelling of fibre intracellular components in a very similar way to JIM13 at early developmental stages, binding to intracellular vesicles in all cotton cultivars. These pieces of evidence and further EDC experiments suggested a possible connection between these two epitopes, although later experiments with a new batch of the LM21 antibody did not confirm this.

5.2 Results

5.2.1 *Ct*CBM3a binding specificity

5.2.1.1 *Ct*CBM3a binds to xyloglucan in addition to crystalline cellulose intact plant cell walls

During the characterization of the CFML composition, labelling with the *Ct*CBM3a to the CFML particles was observed and the binding was removed after xyloglucanase treatment (data not shown). This initial experiments led to the hypothesis that *Ct*CBM3a protein module was not only binding to crystalline cellulose but also to xyloglucan. This was demonstrated by the fluorescence labelling of thin sections of xyloglucan-rich tamarind seed cotyledon parenchyma and crystalline cellulose-rich cotton fibres (Figure 5-1). The binding of *Ct*CBM3a to tamarind seed parenchyma cell walls is abrogated by prior treatment with xyloglucanase, whereas the binding to secondary cell walls of cotton fibres is not affected by this enzyme, demonstrating dual recognition of cell wall glucans by this molecular probe. In contrast the xyloglucan monoclonal antibody LM15 labels both sections (specifically to the primary cell walls in the case of cotton fibres) and its binding to tamarind seeds and cotton fibres was abolished by the enzyme treatment.

To determine the recognition site of xyloglucan by *Ct*CBM3a, a mutant of the protein (provided by Prof. Harry Gilbert, University of Newcastle) was used in which the five amino acids that comprise the hydrophobic cellulose binding surface were substituted with alanine (D56A,H57A,Y67A,R112A,W118A). This mutated form of *Ct*CBM3a, *Ct*CBM3a-*m*5, did not bind to either cell walls of tamarind cotyledon parenchyma or to cotton fibres (Figure 5-1), indicating that the same binding site recognises both polysaccharides.
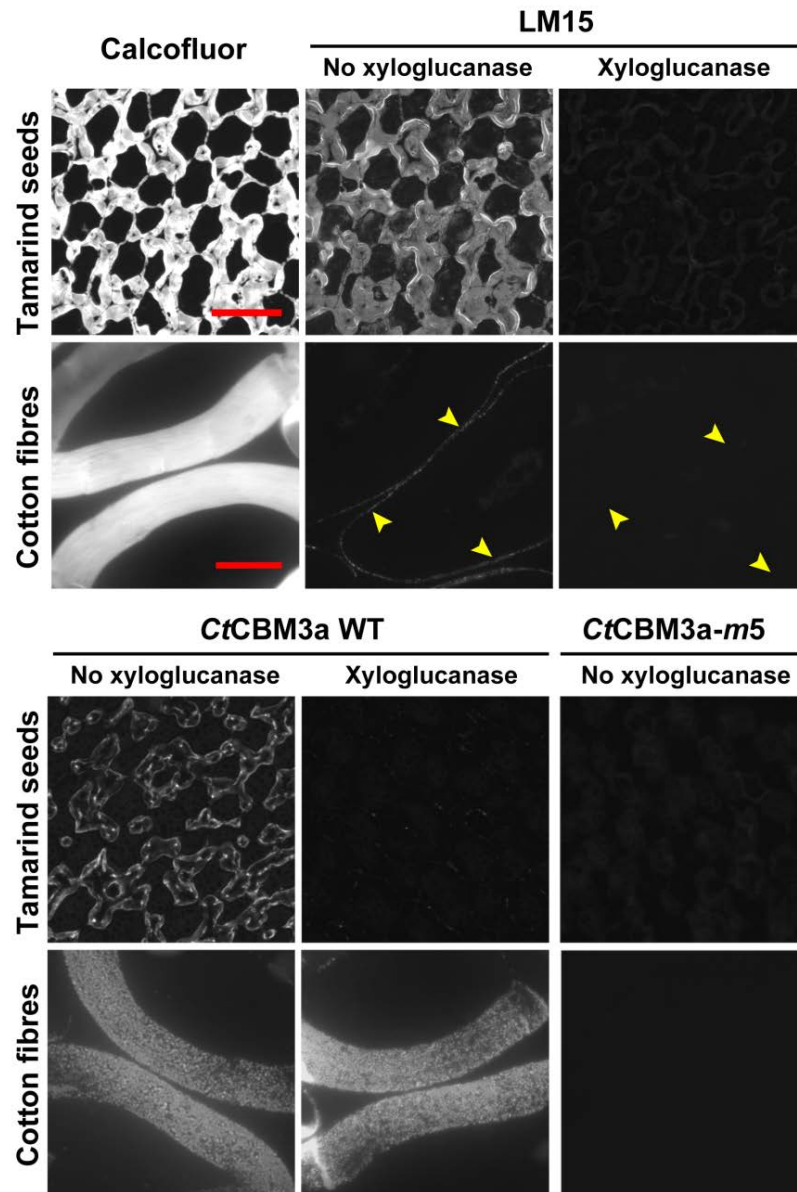
Figure 5-1. Indirect immunofluorescence detection of crystalline cellulose and xyloglucan in sections of xyloglucan-rich tamarind seed cotyledon parenchyma and cellulose-rich cotton fibres, respectively. Calcofluor White staining indicates location of all cell walls. LM15 binding to cell walls of tamarind cotyledon parenchyma cells and primary cell walls of cotton fibres (arrows) is abolished after a xyloglucanase pre-treatment. CtCBM3a WT binding to cell walls of tamarind cotyledon parenchyma cells is abolished by xyloglucanase pre-treatment however its binding to the secondary cell wall of cotton fibres is not. CtCBM3a*m*5 did not bind to cell walls of tamarind cotyledon parenchyma cells nor to cotton fibre secondary cell walls.

5.2.1.2 The crystalline cellulose-binding site of the carbohydrate binding module CBM3a can also accommodate xyloglucan

The binding capacity of wild type *Ct*CBM3a to xyloglucan was studied further by *in vitro* microtitre plate-based assays. Wild type *Ct*CBM3a (20 µg/ml) was as effective at detecting tamarind xyloglucan immobilised on microtitre plates as a 10-fold dilution of LM15 hybridoma cell culture supernatant (Figure 5-2A). There was no *in vitro* recognition of xyloglucan by *Ct*CBM3a*m*5 (Figure 5-2A) confirming the *in situ* observations. In competitive inhibition ELISA assays, the binding of both *Ct*CBM3a and LM15 to tamarind xyloglucan was reduced by ~50% by the presence of 25 µg/ml xyloglucan polysaccharide (Figure 5-2B). In contrast, while LM15 binding to tamarind XG is largely abolished by the presence of 25 µg/ml of xyloglucan-derived XXXG heptasaccharide, *Ct*CBM3a was unaffected (Figure 5-2B). Non-binding polysaccharide (galactomannan) and oligosaccharide cellohexaose were also shown for these assays (Figure 5-2B).

In summary, these observations indicate, firstly, that *Ct*CBM3a can bind to xyloglucan in solution in addition to binding to xyloglucan immobilised on substrates or as a component of cell wall composites. Secondly, the observations indicate that a large stretch of xyloglucan polysaccharide is required for recognition and not the structural features present in the xyloglucan heptasaccharide. This suggests recognition of other features of xyloglucan polysaccharides or a specific conformational form of the polymer that may be optimised when the polysaccharide is bound to the surface of cellulose microfibrils.
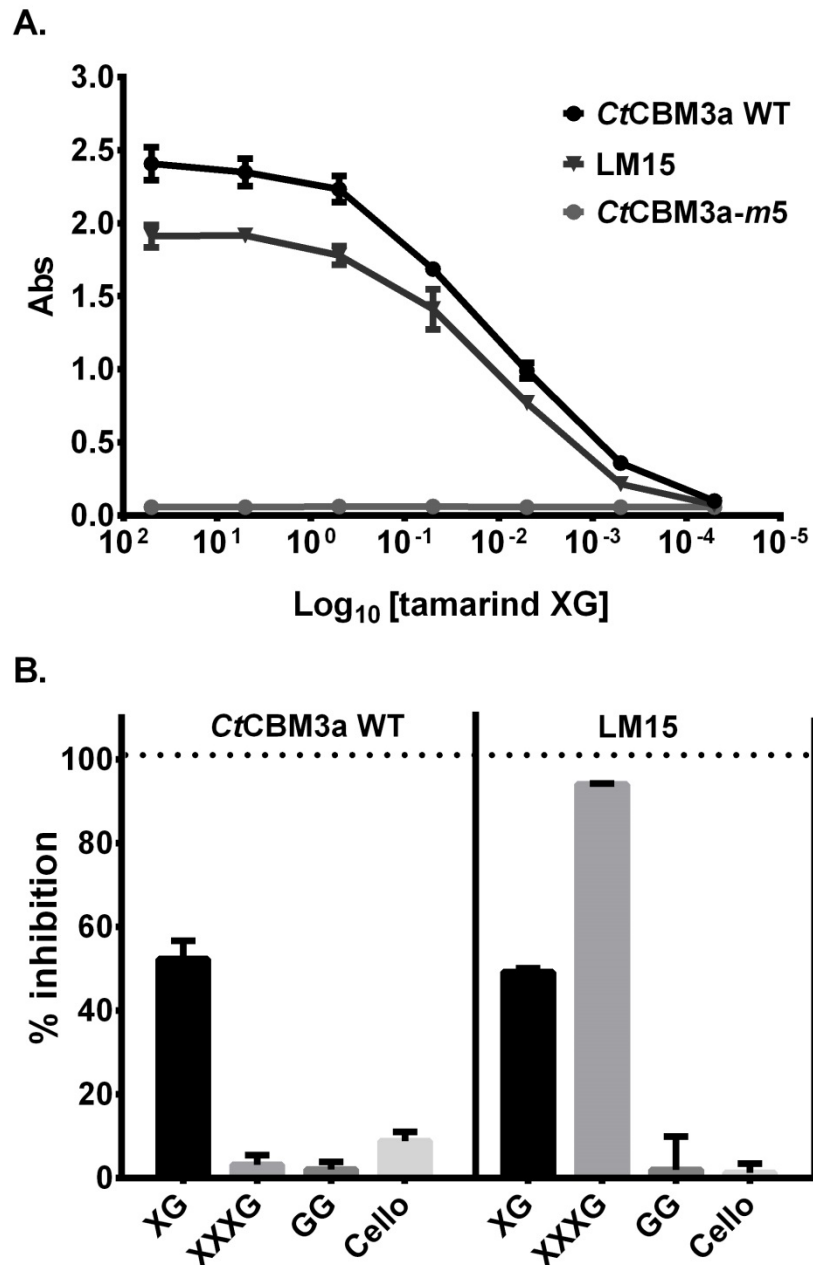
Figure 5-2. *In-vitro* **recognition of xyloglucan by *Ct*CBM3a.** A. ELISA analysis of CtCBM3a WT, CtCBM3a*m*5 and LM15 binding to tamarind xyloglucan. B. Competitive-inhibition ELISAs of LM15 and CtCBM3a WT binding to immobilised xyloglucan with xyloglucan (XG), xyloglucan heptasaccharide (XXXG), guar galactomannan (GG) and cellohexaose (Cello) in the soluble phase at 25 µg/ml. Y axis represents the percentage of inhibition achieved by the polysaccharides/haptens. Error bars: SD (n=3).

5.2.2 Study of the cotton fibre exudate and the possible existence of an AGP-mannan complex.

5.2.2.1 The cotton fibre exudate is rich in xyloglucan, AGPs and heteromannan.

The developing fibre exudate was obtained by soaking bolls (dissected at 7 and 10 dpa) in water or PBS as described in Materials and Methods section 2.3. The fibre exudate glycan composition was screened using several antibodies (Figure 5-3) and found to be very rich in xyloglucan (LM15), AGPs (JIM13, LM2 and LM14) and heteromannan (LM21*). De-esterified HG (LM19) and arabinan (LM6) were also detected as well as low amounts of galactan (LM5) and linearized arabinan (LM13), although no RG-I backbone (INRA-RU2) was detected.

To study the possible subpopulations of glycans carrying these epitopes in the cotton fibre exudate, the same materials from the fibre exudate of 7 and 10 dpa from FM966 were analysed by EDC. The more abundant polysaccharides (ie. LM15, JIM13, LM21* and LM6 epitopes) in the cotton fibre exudate were screened (Figure 5-3). The EDC profile showed that only neutral xyloglucan is present in the exudate and suggests that acidic molecules carrying xyloglucans, as those extracted in CDTA (4.2.8), are not present in the water soluble fibre exudate. Two populations of molecules carrying the LM6 epitope were observed in both water and PBS exudate, one population was neutral and another slightly acidic (asterisks in 7 dpa exudate). The AGP (JIM13) and heteromannan (LM21*) molecules co-eluted (23-33 fractions), suggesting a possible interaction of these two epitopes.
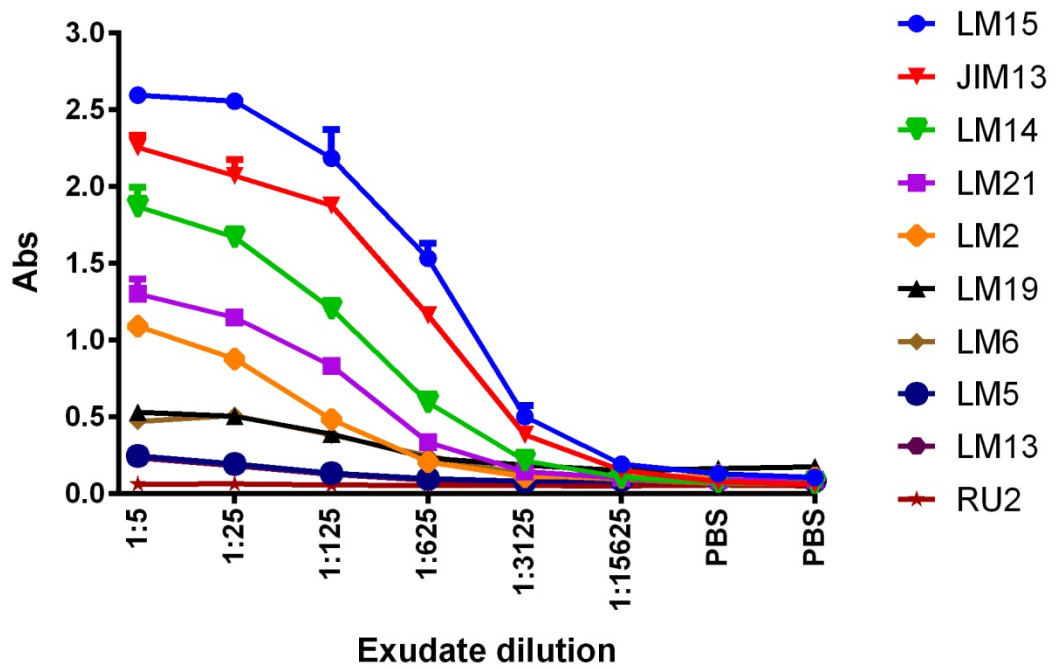
Figure 5-3. Detection of glycan epitopes in the cotton fibre exudate.
Exudate from FM966 10 dpa cotton fibres after o/n soaking in water.
Error bars: SD (n=3).
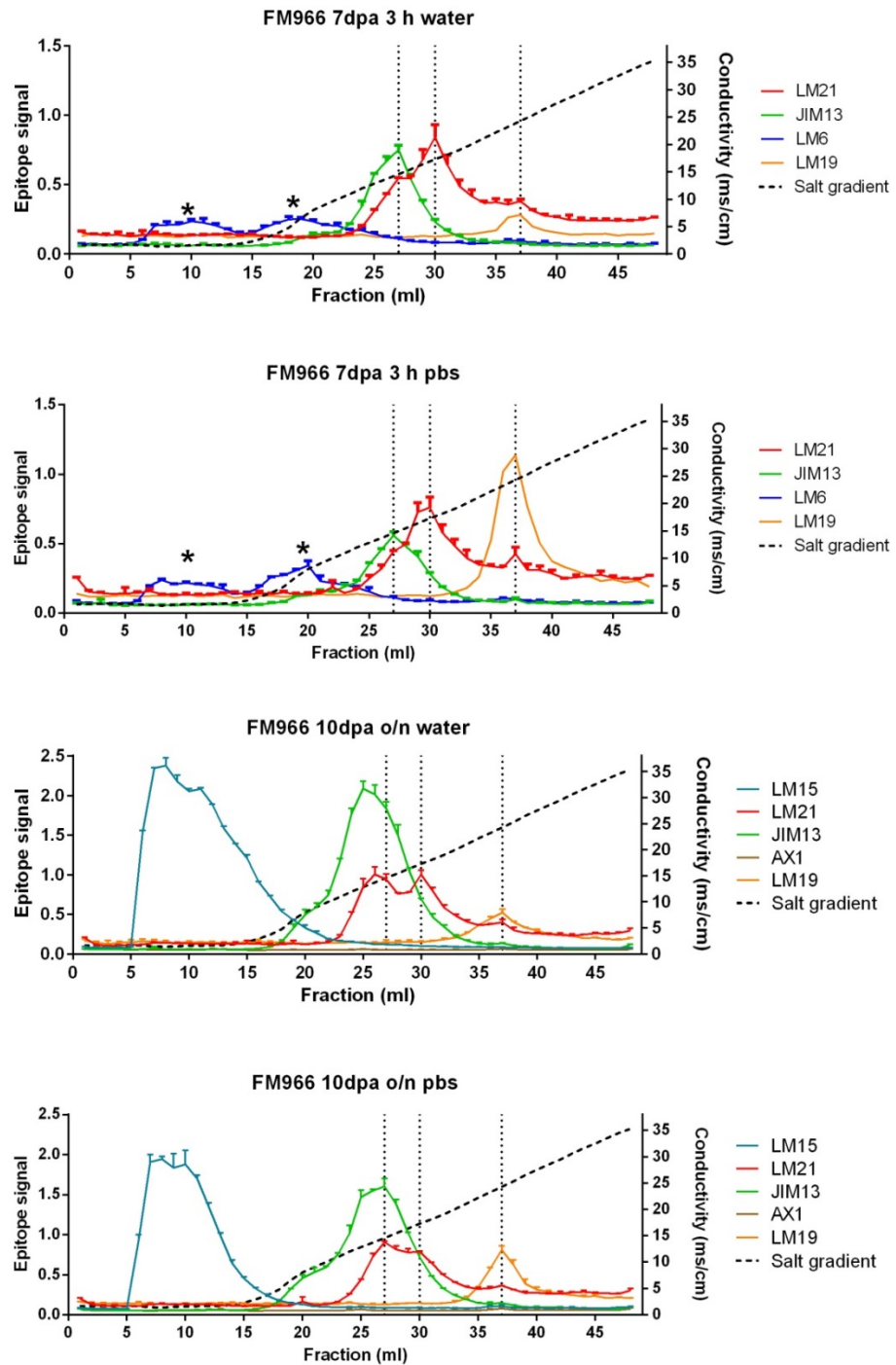
Figure 5-4. EDC profiles of water and PBS cotton fibre washes of FM966 7 dpa and 10 dpa bolls. De-esterified (LM19) was more soluble in PBS buffer than in deionised water. Asterisks highlight two LM6 subpopulations, none co-eluting with JIM13. Dotted line represents salt gradient measured by conductivity (ms/cm) in the right axis. Error bars: SD (n=2).

Moreover, immunolabelling experiments with the JIM13 and LM21* probes on fibre sections at an early developmental stage (5 dpa) suggested co-localization of these two epitopes. Figure 5-5 A shows similar binding of the AGP JIM13 and the heteromannan LM21* probes to the fibre cell wall in 5 dpa FM966 (arrows in Figure 5-5 A). JIM13 and LM21* labelled cell membrane and cytoplasmatic content (arrowheads in Figure 5-5 A) which could possibly correspond with intracellular vesicles and at plasma membrane (FM966 panel). To investigate further the intracellular location of the JIM13 and LM21* labelling, an exploratory side project with tobacco seedling expressing markers of the Golgi and trans Golgi network (TGN), ST-YFP and Syp61a-YFP respectively, were prepared for immunolocalization of the JIM13 and LM21 epitopes. The identification of the organelles labelled by JIM13 and LM21* and its possible co-localization of these epitopes at the Golgi and/or trans-Golgi network (TGN) has important implications to the characterization and biosynthesis of the heteromannan LM21 epitope and its relation to the AGP JIM13 epitope. It is possible that the heteromannan is attached to an AGP core forming an AGP polysaccharide complex that is synthesised together with the AGP in the TGN (Dupree and Sherrier, 1998). YFP-based markers have been reported to maintain fluorescence after resin embedding, however GFP could not be detected over sample autofluorescence (data not shown) and marker localization with the use of anti-GFP antibody only retrieved very faint signal (arrowheads in Figure 5-5 BC anti-GFP panel) possibly unspecific. More interestingly, LM21* and JIM13 did not co-localize but labelled different cells of the root tip. While LM21* localized mostly at the cells in the root cap (arrows Figure 5-5 B LM21* panel), JIM13 labelled cells nearer the apical meristem showing abundant intracellular labelling (arrowhead and very intensively at the cell in the epidermal layer of the root cap (arrows in Figure 5-5 B JIM13 panel). Similar labelling pattern of JIM13 and LM21* was found in the ST marker line.
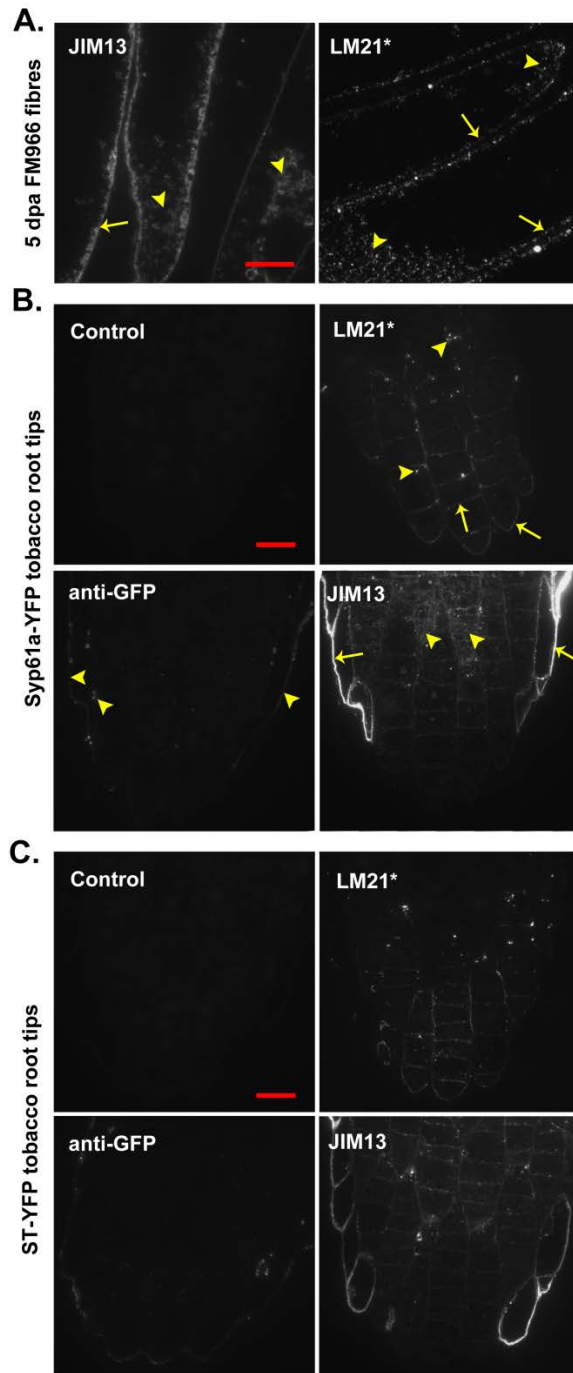
Figure 5-5. Immunolocalization of the JIM13 and LM21* epitopes.
Labelling of 5 dpa of FM966 fibre cross sections with JIM13 and LM21*.
Both probes labelled intracellular vesicles and particles (arrowheads)
as well as the fibre cell wall (arrows). B. Labelling of tobacco seedling
root tips with JIM13, LM21* and anti-GFP to label Syp61. C. Labelling
of tobacco seedling root tips with JIM13 and LM21* and anti-GFP to
label ST. All scales bars: 10 µm.

The final aim of this project was to transiently transform cotton fibres with this ST and Syp61a marker constructs to study this novel intracellular localization of the heteromannan LM21 epitope in the elongating cotton fibre, but the project was stopped upon realization of the faulty LM21* batch and unsuccessful GFP localization using resin sections.

The LM21* probe was found faulty since it showed binding to PBS-only coated ELISA plates (Figure 5-6 A) and a tail in buffer-only EDC runs (Figure 5-6 B). This faulty batch was replaced by a new one and the intracellular labelling of cotton fibres was no longer detected (Figure 5-7). A possible explanation is that some sort of denaturation of the immunoglobulin molecule had occurred and that salt (PBS buffer and salt gradient in EDC) facilitated antibody precipitation and non-specific binding to intracellular components of the fibre cell.
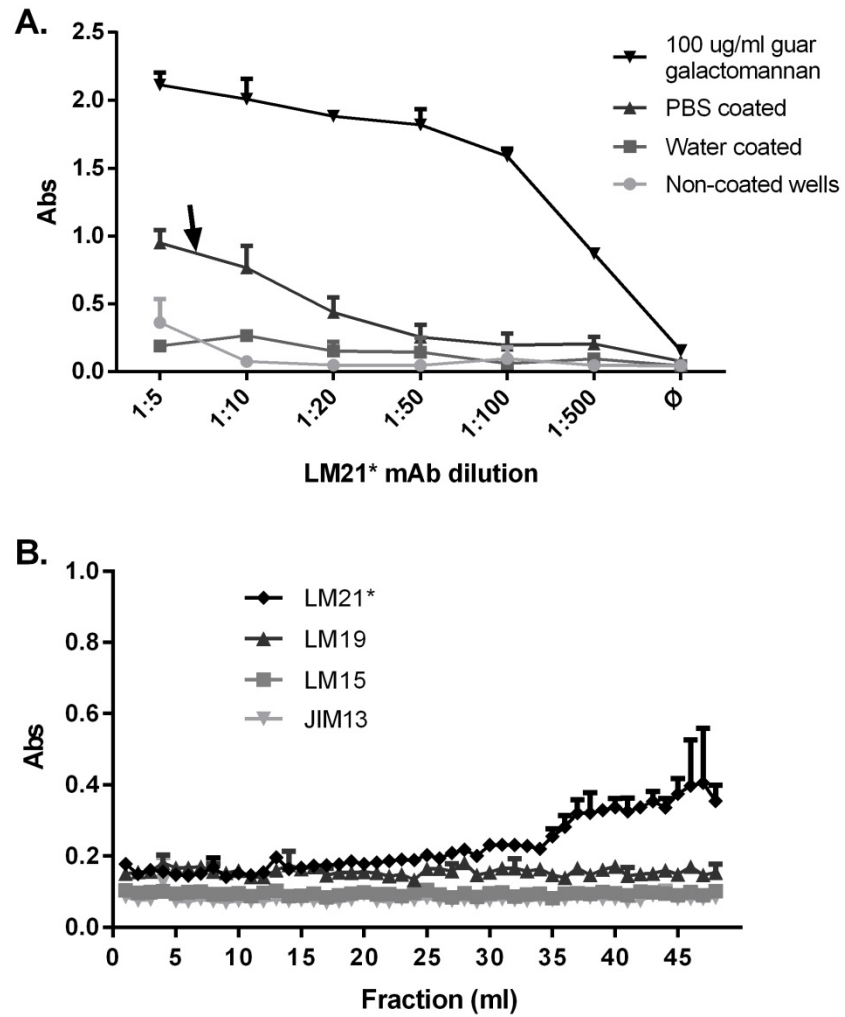
Figure 5-6. Unspecific binding of LM21* to ELISA plates. A. LM21*
binding to PBS coated ELISA plates. LM21 gave signal against guar
galactomannan and also on PBS only coated wells (arrow). Error bar:
SD (n=3). B. LM21* tail in fractions with higher salt content analysed by
EDC. Error bar: SD (n=2).
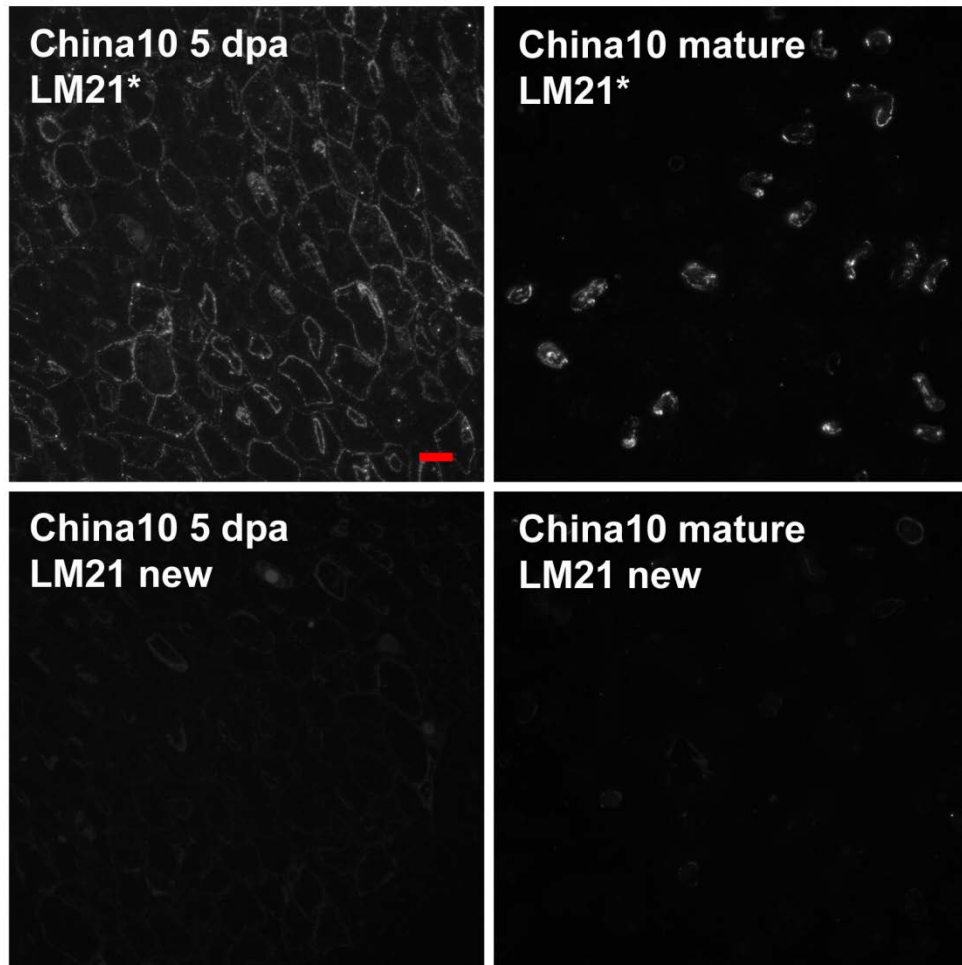
Figure 5-7. Intracellular labelling is lost in the new LM21 antibody batch. Immunolabelling of cross sections from China10 at 5 dpa and mature comparing the labelling signal from LM21* antibody batch with the new LM21 batch on developing cotton fibres. Scale bar: 20 µm.

5.2.2.2 Successful isolation of the JIM13 and LM15 epitopes from the cotton fibre exudate.

In order to characterise the AGP JIM13 and xyloglucan LM15 epitopes in the cotton fibre exudate and their possible interactions with other glycans, these probes were covalently linked to magnetic beads (Dynabeads® Life Technologies) to facilitate the isolation of JIM13 and LM15 epitopes and any other possible associated molecules. Figure 5-8A showed successful isolation of both the JIM13 and LM15 epitope. The exudate before mixing with antibody coupled beads was rich in the JIM13 and LM15 epitopes, after incubation, the JIM13 signal disappears indicating that the beads capacity is enough to bind all the JIM13 epitope present in the exudate sample. However, the signal with the LM15 epitope was still high after binding indicating excess amounts of xyloglucan in the exudate in relation to the beads capacity. Serial washes removed any excess of epitope not bound to the antibody-coupled beads. Elution with 1 M Gly recovered both JIM13 and LM15 epitopes. A subsequent wash of the beads with PBS only showed a signal in the LM15 elute.

The analysis of the elute of JIM13- and LM15-coupled beads (Figure 5-8B) showed efficient isolation of these two epitopes and that the heteromannan LM21 and AGP LM2 probes did not show any affinity for any of the immunoprecipitated molecules. In the previous section, EDC analyses of the fibre exudate showed co-elution of the JIM13 and LM21 epitopes, here ELISA experiments of the JIM13 isolated epitope concluded that these two epitopes are not associated. Interestingly, the isolated molecules with the JIM13 probe were not bound by the LM2 probe which was one the other major AGP component indicating that the LM2 epitope is not found in the isolated molecules with the JIM13 probe and suggesting two possible subpopulations of AGPs in the cotton fibre exudate. Regarding the LM15 elute, the LM25 probe bound to the xyloglucan molecules isolated with the LM15 as expected.
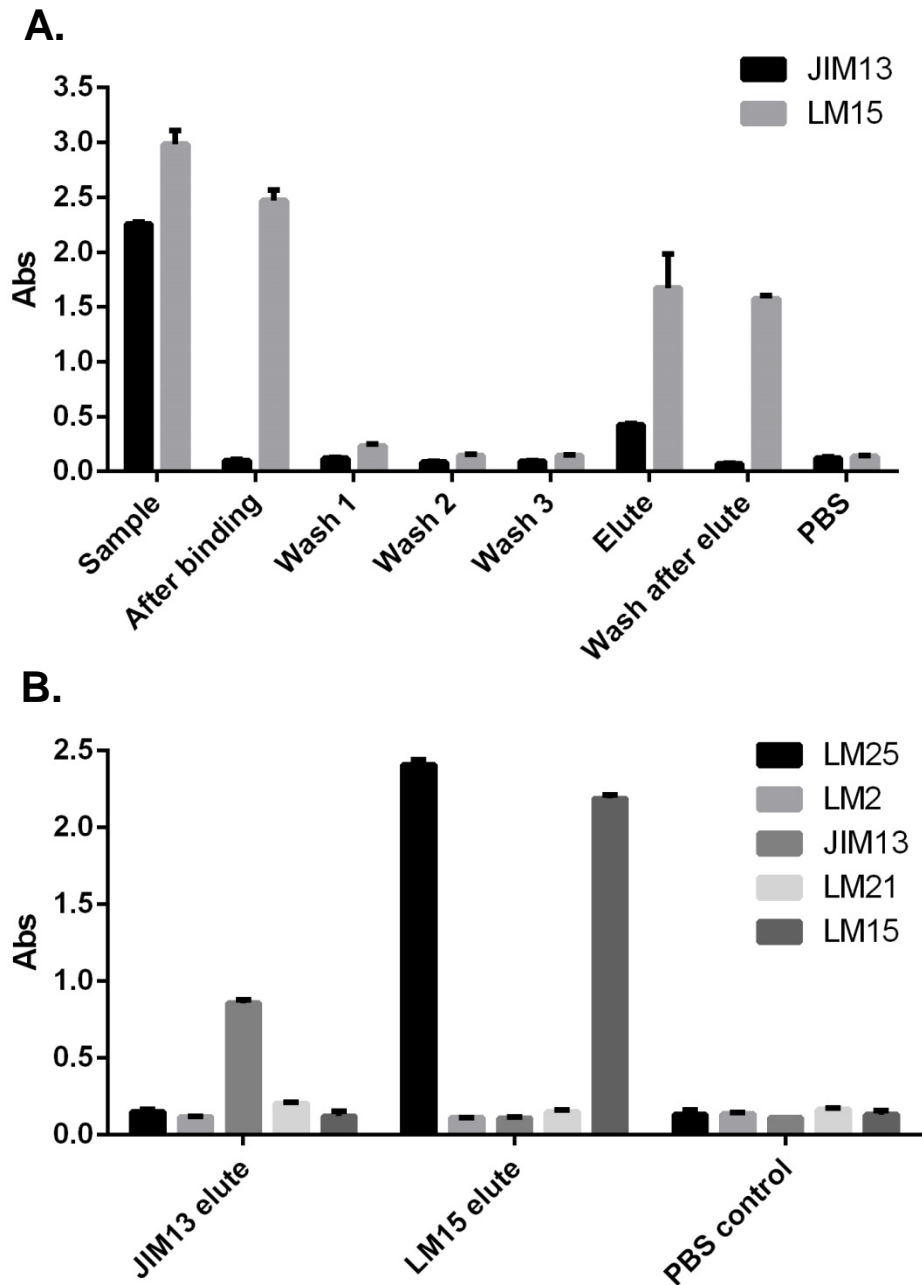
Figure 5-8. Purification of the JIM13 and LM15 epitopes. A. ELISA of the JIM13 and LM15 epitope purification process step by step probed with JIM13 and LM15 respectively. Error bars: SD (n=3). PBS: well coated with PBS. Exudate: wells coated with the exudate sample before mixing with magnetic beads. After binding: exudate sample after incubation with magnetic beads. Wash 1-3: PBS washes of magnetic beads with bound epitope. Elute: elution of bound polysaccharides with 1 M Gly. Wash after elute: PBS wash of beads after elution. Error bars: SD (n=3). B. ELISA screening of the JIM13 and LM15 elute. Error bars: SD (n=3).

5.3 Discussion and future work

5.3.1   The dual recognition of cellulose and xyloglucan by the *Ct*CBM3a binding site

*Ct*CBM3a can bind to both crystalline cellulose and xyloglucan. Although the primary sequence and three-dimensional structure of the type A CBM families are different, the structure of the recognition site is conserved presenting a flat surface of aromatic residues that interact with the multiple planar cellulose chains found in crystalline cellulose, making few if any polar interactions with their ligands (Blake et al., 2006). The binding of crystalline cellulose by the type A CBM family is based on entropic forces resulting from the release of water molecules from protein and ligand with a fixed conformation, which contrasts with the affinity of type B and C CBMs for their soluble ligands driven by changes in enthalpy (Xie et al., 2001; Boraston, 2005; Najmudin et al., 2006). Given the important role that entropy plays in ligand recognition by type A CBMs, it was thought that the loss of thermodynamic freedom when a soluble ligand binds to these proteins offsets any increase in the randomness of the system through the release of water molecules, leading to no net affinity for these glycans (Creagh et al., 1996; Boraston et al., 2004). The data reported contradicts this assumption and shows that *Ct*CBM3a binds to soluble xyloglucan. It is possible that the type A CBMs bind to xyloglucan polysaccharides but not to xyloglucan oligosaccharides because the conformational flexibility of the oligosaccharides in solution is too great for binding to occur. Another possibility is that the xylose side chains in the xyloglucan polysaccharide make interactions with the surface of the type A CBMs contributing to ligand binding.

From a biological perspective, these results indicate that *Ct*CBM3a and the other type A CBMs not only direct enzymes onto highly crystalline cellulose that is recalcitrant to attack by typical endoglucanases, but also targets xyloglucan which, in contrast, is a highly accessible glycan that is hydrolyzed by β-glucanases with a range of different specificities (Gloster et al., 2007).

184

Thus, the targeting role of type A CBMs may be broader than previously believed, explaining why these modules are appended to a range of different enzymes.

Finally, these results raise issues concerning the use of these CBMs as molecular probes for crystalline cellulose, showing the importance of comparing data before and after treatment with a highly specific xyloglucanase when using type A CBMs to study plant cell wall architecture.

5.3.2 Understanding the role of AGPs in the developing cotton fibre

AGPs are involved in a wide range of biological processes. Some of the latest studies evidenced their ability to modulate pollen development (Nguema-Ona et al., 2012), somatic embryogenesis (Poon et al., 2012), and hormonal interaction during root growth (Seifert et al., 2014). AGPs are known to participate in signalling transduction pathways during development (e.g. modulating Ca^{2+} availability), pathogen defence or mechanical and environmental stresses (Majewska-Sawka and Nothnagel, 2000; Mashiguchi et al., 2008; Zhang et al., 2011).

It is fascinating that AGPs can modulate so many different biological processes and to understand how the AGP glycan composition relates to specific functions is an important aspect for future AGP research. The recent discovery and characterization of an AGP-RG-I-xylan complex, named as arabinoxylan pectin arabinogalactan protein 1 or APAP1 (Tan et al., 2013) has brought to the cell wall community a new conception on how cell wall glycans can interact and are biosynthesised. The existence of covalently linked AGPs with other cell wall components shows that cell wall polymers interact in a more complex manner than traditionally thought and it is possible that many other AGP polysaccharide complexes (APCs) remain to be discovered. More research is needed to focus on (1) the specific functions of AGPs and APCs depending on their composition and (2) the biosynthetic pathways of their glycan motifs and other linked polysaccharides.

185

The isolation of AGP molecules from an AGP-rich and easily extractable source material is an important start point. Commonly AGP-rich sources are gum exudates (Defaye and Wong, 1986), roots and seeds mucilages (Moody et al., 1988) or media from cultured cells such as carrot cells (Knox et al., 1991; Baldwin et al., 1993) or Arabidopsis cells (Tan et al., 2013). The cotton fibre exudate has not been investigated before in this context and was found to be a source of abundant soluble AGPs, very easily extractable with a simple soaking overnight.

Yariv reagent-precipitation, anion exchange and size exclusion chromatography, lectin and immuno-affinity chromatography are some of the most used current methods to extract and purify AGP complexes. From all, immunoaffinity using antibodies recognising AGPs is the one that can provide easily extracted material with few polysaccharide contaminants. In this work, magnetic bead-assisted immunoprecipitation using the JIM13 probe was used to isolate soluble AGPs from developing fibres. ELISA and anion-exchange chromatography analysis of the immunoprecipitated molecules indicated the efficient isolation of the JIM13 epitope carrying antigen. The existence of possible AGP-mannan complex suggested by immunolabelling experiments and co-elution of related peaks by EDC was not backed up by ELISA on the isolated JIM13 epitope. The magnetic bead-assisted immunoprecipation approach chosen in this work was very effective, however the rather small quantities of isolated material is a major drawback of this methodology. JIM13 was coupled through primary amino and sulfhydryl groups to the beads without losing epitope recognition capacity and a low pH glycine buffer was effective as an elutant. This knowledge could be used to produce affinity columns so that bigger volumes can be handled.

The characterization of single AGP molecules (or even APCs) is very interesting not only from the biological point of view but also for their industrial use. Plant products based on AGs like gum Arabic are very well established products widely used for example as emulsifiers in food technology and important immunomodulatory and anti-tumorigenic

properties have been described from type II arabinogalactans in larch tree (Kelly, 1999), wolfberry fruit (Peng et al., 2014), *Astragalus* (Kiyohara et al., 2010) and ginseng (Fan et al., 2010; Gao et al., 2013) among other sources as reviewed by (Aboughe-Angone et al., 2006). Future development of affinity purification of AGs molecules and isolation of subpopulations by EDC can be of extreme importance to exploit the pharmaceutical and industrial uses of AGs as well as to characterize the biochemical structure needed for bioactivity. Moreover, the availability of several AGP probes, can be used to efficiently isolate different AGP populations, such as the LM2 and JIM13 antibodies used here, that will help advance our understanding of AGP and AGP-glycan complexes and their biological role during glycan biosynthesis and cell wall remodelling.

Chapter VI

6 General discussion and conclusions

Cotton fibres form a particular single cell tissue where individual fibres start elongating as separate entities but come together and adhere soon after. They maintain adhesion via the cotton fibre middle lamella (CFML) during cell elongation, until the secondary cell wall deposition phase starts and fibres separate again. Fibre cell machinery activity then focuses on rapidly synthesising cellulose that will accumulate in an extra developed secondary cell wall. The sequence of these events is finely regulated and is determined by genotype and temperature growth, which this work supports providing novel biochemical evidence regarding sugar composition, fibre morphological analysis and relative abundance and *in-situ* localization of glycan epitopes during several stages of fibre development in several cotton cultivars of despaired fibre quality. The main novel findings were the following:

- Extra-long high quality fibres belonging to the tetraploid species *G. barbadense* showed a time-extended presence of highly methyl-esterified HG, xyloglucan and heteromannan polysaccharides compared to other lines, pointing to a positive correlation of these cell wall glycans with an extended fibre elongation phase or a delayed transition phase.

- Earlier disappearance of highly methyl-esterified HG, galactan and arabinan pectic glycans in the *G. arboreum* JFW15 cultivar is due to an earlier start of secondary cell wall deposition and higher rate of cellulose deposition which correlates with their very low quality fibre.

- Exploratory correlation analysis between developmental glycan epitope dynamics and fibre quality pointed at extensins and glucuronoxylan as interesting targets to be considered for fibre quality improvement.

- The relationship between dpa and developmental events was proven inefficient to describe cotton fibre development. It is proposed to the

- cotton-research community the use of an standardise glycan epitope developmental profile (along with the dpa system).

- The CFML conspicuous paired cell wall bulges is likely to be a characteristic of the *G. hirsutum* cultivar only.

- The CFML is composed of arabinan, AGPs and XET in *G. hirsutum, G. barbadense, G. herbaceum* and *G. arboreum* species in addition to the known xyloglucan and pectin polysaccharides. Fucosylated xyloglucan is also part of the CFML in the *G. barbadense* cultivars in contradiction to previous reported data.

- The CslC4/XT1-expressing line produced abundant xyloglucan in the secondary cell wall compared to the non-transgenic line, confirming the transgenic approach carried out in this plant.

- Novel identification of the presence of heteromannan in cotton fibres by several approaches.

- Heteroxylan specifically localized between secondary cell wall layers of cellulose pointing to a role in the cyclic regulation of cellulose deposition.

- The LM13 epitope was more abundant during fibre development than the LM6 epitope suggesting for the first time a broader pattern of recognition of the LM13 probe in comparison to the LM6 probe.

- *Ct*CBM3a can bind to both crystalline cellulose and xyloglucan (both immobilized and soluble xyloglucan).

- AGP proteins and xyloglucan polysaccharides can be efficiently isolated by affinity purification techniques through covalent binding of JIM13 and LM15 to matrix/magnetic beads without losing epitope recognition capacity.

In a broad and simplified manner, the sequence of events that take place in the cell walls of developing cotton fibres based on these results and bibliography on the related topic can be summarised as follows:

The first phase of fibre elongation takes place from anthesis to the closure of plasmodesmata at the base of the cotton fibre (Ruan et al., 2003; Ruan et al., 2004; Ruan, 2007). The continuous polysaccharide deposition allows the

accumulation of solutes (increasing turgor pressure) without cell bursting. Also, cell wall polymer secretion provides material to create the CFML and to keep the elongating fibre bundles together (Singh et al., 2009; Avci et al., 2013). It is possible that the fibre cell wall firmness is maintained during this stage by RG-I galactan protection of highly methyl esterified HG from being degraded by PMEs. Thus, only when galactan starts being degraded by galactanases (Oxenbøll Sørensen et al., 2000) the fibre can enter a phase two of rapid elongation during plasmodesmata closure (Ruan, 2007; Stiff and Haigler, 2012). This fast elongation is aided by the previously built up turgor pressure and extensive degradation of pectin. Upon degradation of galactan, PMEs can degrade highly methyl-esterified HG and PEL enzymes (Wang et al., 2010) can then degrade pectin so that the rapid entrance of water in the fibre is assimilated by an increased capacity of cell wall loosening after pectin degradation.

The thinning process of the primary cell wall, involving changes of pH and Ca^{2+} ions might lead to the deposition of a layer of callose to seal and reinforce the thinned primary cell wall. As in the pollen tube (Parre and Geitmann, 2005), callose deposition in the fibre tip might be avoided so the cell wall can expand more in the last part of the fibre elongation phase (Haigler, 2010). This could allow fibres to uptake some more water that finally balances out osmotic pressures. The cell wall is then reinforced by the deposition of several cell wall layers of cellulose, which is controlled by temperature cycles which perhaps involves arabinoxylan deposition to modify the angle in which cellulose microfibril are laid into the cell wall (Derba-Maceluch et al., 2015).

Some of the questions that have arisen from this work and that can be considered for future projects are:

- Is galactan degradation required to enter the transition phase? Can fibre elongation phase be extended to obtain longer fibres by delaying galactan degradation (through a genetic approach involving for example galactanases)?

- Do AGPs promote the start of fibre secondary cell wall deposition by controlling the concentration of free available Ca^{2+} ions?
- What is the biological significance, if any, of the CFML paired bulges arrangement in the *G. hirsutum* lines?
- Are arabinoxylans involved in the cyclic lay down of cellulose deposition in the secondary cell wall of cotton fibres? How?
- What is the cellular mechanism behind the extraordinary higher rate of cellulose deposition in the JFW15 cultivar?

The analysis of the transcriptome developing fibres from these same cultivars specifically would help answering some of the above questions and can provide very useful information to develop genetic intervention approaches in order to obtain fibres with improved quality.

In conclusion, the cotton fibre follows an intricate system of cell elongation and secondary cell wall deposition which can be altered depending on germplasm as well as environmental conditions. Considerable information is available about the cell wall-related gene expression and actual cell wall changes occurring during fibre development. This work has contributed to the understanding of fibre cell wall development from a biochemical point of view comparing a wide range of cultivars as never done before. Future work needs to address how these changes are integrated in the cotton fibre system and the cellular machinery behind them.

Bibliography

Aboughe-Angone S, Nguema-Ona E, Boudjeko T, Driouich A (2006) Plant cell wall polysaccharides: Immunomodulators of the immune system and source of natural fibers. Phytochemistry **1**

Akita K, Ishimizu T, Tsukamoto T, Ando T, Hase S (2002) Successive Glycosyltransfer Activity and Enzymatic Characterization of Pectic Polygalacturonate 4-α-Galacturonosyltransferase Solubilized from Pollen Tubes of Petunia axillaris Using Pyridylaminated Oligogalacturonates as Substrates. Plant Physiology **130:** 374-379

Al-Ghazi Y, Bourot S, Arioli T, Dennis ES, Llewellyn DJ (2009) Transcript profiling during fiber development identifies pathways in secondary metabolism and cell wall structure that may contribute to cotton fiber quality. Plant Cell Physiology **50:** 1364-1381

Albersheim P, Darvill A, Roberts K, Sederoff R, Staehelin A (2011) Plant cell walls. Garland Sciences

Albersheim P, Nevins DJ, English PD, Karr A (1967) A method for the analysis of sugars in plant cell-wall polysaccharides by gas-liquid chromatography. Carbohydrate Research **5:** 340-345

Allen S, Richardson JM, Mehlert A, Ferguson MAJ (2013) Structure of a Complex Phosphoglycan Epitope from gp72 of Trypanosoma cruzi. Journal of Biological Chemistry **288:** 11093-11105

Alsteens D, Dupres V, Mc Evoy K, Wildling L, Gruber HJ, Dufrêne YF (2008) Structure, cell wall elasticity and polysaccharide properties of living yeast cells, as probed by AFM. Nanotechnology **19:** 384005

Amor Y, Haigler CH, Johnson S, Wainscott M, Delmer DP (1995) A membrane-associated form of sucrose synthase and its potential role in synthesis of cellulose and callose in plants. Proceedings of the National Academy of Sciences **92:** 9353-9357

Anders N, Wilkinson MD, Lovegrove A, Freeman J, Tryfona T, Pellny TK, Weimar T, Mortimer JC, Stott K, Baker JM, Defoin-Platel M, Shewry PR, Dupree P, Mitchell RAC (2012) Glycosyl transferases in family 61 mediate arabinofuranosyl transfer onto xylan in grasses. Proceedings of the National Academy of Sciences **109:** 989-993

Anderson CT, Wallace IS (2012) Illuminating the wall: using click chemistry to image pectins in Arabidopsis cell walls. Plant Signal Behaviour **7:** 661-663

Arioli T (2005) Genetic engineering for cotton fiber improvement. Pflanzenschut-Nachrichten Bayer **58:** 140-150

Arioli T, Peng L, Betzner AS, Burn J, Wittke W, Herth W, Camilleri C, Höfte H, Plazinski J, Birch R, Cork A, Glover J, Redmond J, Williamson RE (1998) Molecular Analysis of Cellulose Biosynthesis in Arabidopsis. Science **279:** 717-720

Atalla RH, Vanderhart DL (1984) Native Cellulose: A Composite of Two Distinct Crystalline Forms. Science **223:** 283-285

Atmodjo MA, Hao Z, Mohnen D (2013) Evolving Views of Pectin Biosynthesis. Annual Review of Plant Biology **64:** 747-779

Atmodjo MA, Sakuragi Y, Zhu X, Burrell AJ, Mohanty SS, Atwood JA, 3rd, Orlando R, Scheller HV, Mohnen D (2011) Galacturonosyltransferase (GAUT)1 and GAUT7 are the core of a plant cell wall pectin biosynthetic homogalacturonan:galacturonosyltransferase complex. Proceedings of the National Academy of Sciences **108:** 20225-20230

Avci U, Pattathil S, Singh B, Brown VL, Hahn MG, Haigler CH (2013) Cotton fiber cell walls of Gossypium hirsutum and Gossypium barbadense have differences related to loosely-bound xyloglucan. PLoS One **8:** 14

Babu BR, Parande A, Raghu S, Kumar TP (2007) Cotton textile processing: waste generation and effluent treatment. Journal of cotton science

Baldwin TC, McCann MC, Roberts K (1993) A Novel Hydroxyproline-Deficient Arabinogalactan Protein Secreted by Suspension-Cultured Cells of Daucus carota (Purification and Partial Characterization). Plant Physiology **103:** 115-123

Balls WL (1919) The existence of daily growth-rings in the cell wall of cotton hairs. Proceedings of the Royal Society of London. Series B, Containing Papers of a Biological Character **90:** 542-555

Baluska F, Liners F, Hlavacka A, Schlicht M, Van Cutsem P, McCurdy DW, Menzel D (2005) Cell wall pectins and xyloglucans are internalized into dividing root cells and accumulate within cell plates during cytokinesis. Protoplasma **225:** 141-155

Bashline L, Li S, Anderson CT, Lei L, Gu Y (2013) The endocytosis of cellulose synthase in Arabidopsis is dependent on mu2, a clathrin-mediated endocytosis adaptin. Plant Physiology **163:** 150-160

Baskin JM, Prescher JA, Laughlin ST, Agard NJ, Chang PV, Miller IA, Lo A, Codelli JA, Bertozzi CR (2007) Copper-free click chemistry for dynamic in vivo imaging. Proceedings of the National Academy of Sciences **104:** 16793-16797

Basra AS, ed (2000) Cotton fibers: developmental biology, quality improvement and textile processing. Food Products Press

Beasley CA, Ting IP (1973) The effects of plant growth substances on in vitro fiber development from fertilized cotton ovules. American Journal of Botany **60:** 130-139

Benians TA (2012) In situ analysis of cotton fibre cell wall polysaccharides. PhD thesis. University of Leeds

Benitez-Alfonso Y, Faulkner C, Pendle A, Miyashima S, Helariutta Y, Maule A (2013) Symplastic Intercellular Connectivity Regulates Lateral Root Patterning. Developmental Cell **26:** 136-147

Beňová-Kákošová A, Digonnet C, Goubet F, Ranocha P, Jauneau A, Pesquet E, Barbier O, Zhang Z, Capek P, Dupree P, Lišková D, Goffner D (2006) Galactoglucomannans Increase Cell Population Density and Alter the Protoxylem/Metaxylem Tracheary Element Ratio in Xylogenic Cultures of Zinnia. Plant Physiology **142:** 696-709

Blackburn RS (2004) Natural Polysaccharides and Their Interactions with Dye Molecules: Applications in Effluent Treatment†. Environmental Science & Technology **38:** 4905-4909

Blackburn RS, Burkinshaw SM (2003) Treatment of cellulose with cationic, nucleophilic polymers to enable reactive dyeing at neutral pH without electrolyte addition. Journal of Applied Polymer Science **89:** 1026-1031

Blackburn RS, Harvey A (2004) Green chemistry methods in sulfur dyeing: application of various reducing D-sugars and analysis of the importance of optimum redox potential. Environment Science Technology **38:** 4034-4039

Blake AW, McCartney L, Flint JE, Bolam DN, Boraston AB, Gilbert HJ, Knox JP (2006) Understanding the biological rationale for the diversity of cellulose-directed carbohydrate-binding modules in prokaryotic enzymes. Journal of Biological Chemistry **281:** 29321-29329

Blakeney AB, Harris PJ, Henry RJ, Stone BA (1983) A simple and rapid preparation of alditol acetates for monosaccharide analysis. Carbohydrate Research **113:** 291-299

Boraston AB (2005) The interaction of carbohydrate-binding modules with insoluble non-crystalline cellulose is enthalpically driven. Biochem J **385:** 479-484

Boraston Alisdair B, Bolam David N, Gilbert Harry J, Davies Gideon J (2004) Carbohydrate-binding modules: fine-tuning polysaccharide recognition. Biochemical Journal **382:** 769-781

Boraston AB, Nurizzo D, Notenboom V, Ducros V, Rose DR, Kilburn DG, Davies GJ (2002) Differential oligosaccharide recognition by evolutionarily-related β-1,4 and β-1,3 Glucan-binding modules. Journal of Molecular Biology **319:** 1143-1156

Boraston AB, Revett TJ, Boraston CM, Nurizzo D, Davies GJ (2003) Structural and thermodynamic dissection of specific mannan recognition by a Carbohydrate Binding Module, TmCBM27. Structure **11:** 665-675

Bosch M, Cheung AY, Hepler PK (2005) Pectin Methylesterase, a Regulator of Pollen Tube Growth. Plant Physiology **138:** 1334-1346

Bourquin V, Nishikubo N, Abe H, Brumer H, Denman S, Eklund M, Christiernin M, Teeri TT, Sundberg B, Mellerowicz EJ (2002) Xyloglucan endotransglycosylases have a function during the formation of secondary cell walls of vascular tissues. Plant Cell **14:** 3073-3088

Bowling AJ, Vaughn KC, Turley RB (2011) Polysaccharide and glycoprotein distribution in the epidermis of cotton ovules during early fiber initiation and growth. Protoplasma **248:** 579-590

Bowman DT, Van ESbroeck GA, Van't Hof J, Jividen GM (2001) Ovule fiber cell numbers in modern upland cottons. Journal of cotton science **5**

Bradow J, Davidonis G (2010) Effects of Environment on Fiber Quality. *In* J Stewart, D Oosterhuis, J Heitholt, J Mauney, eds, Physiology of Cotton. Springer Netherlands, pp 229-245

Bradow JM, Davidonis GH (2000) Quantitation of fiber quality and the cotton production-processing interface: A physiologist's perspective. Journal of Cotton Science **4:** 34-64

Braybrook SA, Hofte H, Peaucelle A (2012) Probing the mechanical contributions of the pectin matrix: insights for cell growth. Plant signaling & behavior **7:** 1037-1041

Bringmann M, Landrein B, Schudoma C, Hamant O, Hauser MT, Persson S (2012) Cracking the elusive alignment hypothesis: the microtubule-cellulose synthase nexus unraveled. Trends Plant Science **17:** 666-674

Bringmann M, Li E, Sampathkumar A, Kocabek T, Hauser M-T, Persson S (2012) POM-POM2/CELLULOSE SYNTHASE INTERACTING1 Is Essential for the Functional Association of Cellulose Synthase and Microtubules in Arabidopsis. The Plant Cell **24:** 163-177

Brown DM, Goubet F, Wong VW, Goodacre R, Stephens E, Dupree P, Turner SR (2007) Comparison of five xylan synthesis mutants reveals new insight into the mechanisms of xylan synthesis. The Plant Journal **52:** 1154-1168

Brown DM, Zhang Z, Stephens E, Dupree P, Turner SR (2009) Characterization of IRX10 and IRX10-like reveals an essential role in glucuronoxylan biosynthesis in Arabidopsis. The Plant Journal **57:** 732-746

Brown RM (2004) Cellulose structure and biosynthesis: What is in store for the 21st century? Journal of Polymer Science Part A: Polymer Chemistry **42:** 487-495

Brownfield L, Ford K, Doblin MS, Newbigin E, Read S, Bacic A (2007) Proteomic and biochemical evidence links the callose synthase in Nicotiana alata pollen tubes to the product of the NaGSL1 gene. The Plant Journal **52:** 147-156

Buchala AJ, Meier H (1985) Biosynthesis of β-glucans in growing cotton (Gossypium arboreum L. and Gossypium hirsutum L.) fibres. *In* Biochemistry of Plant Cell Walls. C.T. Brett & J.R. Hillman, Cambridge University Press, Society of Experimental Biology Seminar Series, pp 221-241

Bunterngsook B, Eurwilaichitr L, Thamchaipenet A, Champreda V (2015) Binding characteristics and synergistic effects of bacterial expansins on cellulosic and hemicellulosic substrates. Bioresource Technology **176:** 129-135

Burton RA, Gidley MJ, Fincher GB (2010) Heterogeneity in the chemistry, structure and function of plant cell walls. Nature Chemical Biology **6:** 724-732

Caffall KH, Mohnen D (2009) The structure, function, and biosynthesis of plant cell wall pectic polysaccharides. Carbohydrate Research **344:** 1879-1900

Cannon MC, Terneus K, Hall Q, Tan L, Wang Y, Wegenhart BL, Chen L, Lamport DT, Chen Y, Kieliszewski MJ (2008) Self-assembly of the plant cell wall requires an extensin scaffold. Proceedings of the National Academy of Sciences **105:** 2226-2231

Carpita NC (1996) Structure and biogenesis of the cell walls of grasses. Annual Review of Plant Physiology and Plant Molecular Biology **47:** 445-476

Carpita NC, Gibeaut DM (1993) Structural models of primary cell walls in flowering plants: consistency of molecular structure with the physical properties of the walls during growth. The Plant Journal **3:** 1-30

Cavalier DM, Lerouxel O, Neumetzler L, Yamauchi K, Reinecke A, Freshour G, Zabotina OA, Hahn MG, Burgert I, Pauly M, Raikhel NV, Keegstra K (2008) Disrupting two arabidopsis thaliana xylosyltransferase genes results in plants deficient in xyloglucan, a major primary cell wall component. The Plant Cell Online **20:** 1519-1537

Ceylan Ö, Van Landuyt L, Goubet F, De Clerck K (2013) The sensitivity and impact of dye structure and fibre micronaire on the increased dyeability of bioengineered cotton fibres. Coloration Technology **129:** 239-245

Chandra M, Sreenivasan S (2011) Studies on improved Gossypium arboreum cotton: Part I—Fibre quality parameters. Indian Journal Fibre Textile **36:** 24

Chebli Y, Kaneda M, Zerzour R, Geitmann A (2012) The Cell Wall of the Arabidopsis Pollen Tube—Spatial Distribution, Recycling, and Network Formation of Polysaccharides. Plant Physiology **160:** 1940-1955

Chen S, Ehrhardt DW, Somerville CR (2010) Mutations of cellulose synthase (CESA1) phosphorylation sites modulate anisotropic cell expansion and bidirectional mobility of cellulose synthase. Proceedings of the National Academy of Sciences **107:** 17188-17193

Chen X-Y, Kim J-Y (2009) Callose synthesis in higher plants. Plant signaling & behavior **4:** 489-492

Chen X, Guo W, Liu B, Zhang Y, Song X, Cheng Y, Zhang L, Zhang T (2012) Molecular Mechanisms of Fiber Differential Development between G. barbadense and G. hirsutum Revealed by Genetical Genomics. PLoS One **7:** e30056

Chiniquy D, Sharma V, Schultink A, Baidoo EE, Rautengarten C, Cheng K, Carroll A, Ulvskov P, Harholt J, Keasling JD, Pauly M, Scheller HV, Ronald PC (2012) XAX1 from glycosyltransferase family 61 mediates xylosyltransfer to rice xylan. Proceedings of the National Academy of Sciences **109:** 17117-17122

Cid M, Pedersen HL, Kaneko S, Coutinho PM, Henrissat B, Willats WGT, Boraston AB (2010) Recognition of the helical structure of β-1,4-galactan by a new family of carbohydrate-binding modules. Journal of Biological Chemistry **285:** 35999-36009

Ciucanu I, Kerek F (1984) A simple and rapid method for the permethylation of carbohydrates. Carbohydrate Research **131:** 209-217

Clausen MH, Willats WGT, Knox JP (2003) Synthetic methyl hexagalacturonate hapten inhibitors of anti-homogalacturonan monoclonal antibodies LM7, JIM5 and JIM7. Carbohydrate Research **338:** 1797-1800

Cornuault V, Manfield IW, Ralet MC, Knox JP (2014) Epitope detection chromatography: a method to dissect the structural heterogeneity and inter-connections of plant cell-wall matrix glycans. The Plant Journal **78:** 715-722

Cosgrove DJ (2000) Loosening of plant cell walls by expansins. Nature **407:** 321-326

Cosgrove DJ (2005) Growth of the plant cell wall. Nature Reviews Molecular Cell Biology **6:** 850-861

Cosgrove DJ (2014) Re-constructing our models of cellulose and primary cell wall assembly. Current Opinion Plant Biology. 2014 Nov 16;22C:122-131. doi: 10.1016/j.pbi.2014.11.001.

Cosgrove DJ, Li LC, Cho H-T, Hoffmann-Benning S, Moore RC, Blecker D (2002) The Growing World of Expansins. Plant and Cell Physiology **43:** 1436-1444

Creagh AL, Ong E, Jervis E, Kilburn DG, Haynes CA (1996) Binding of the cellulose-binding domain of exoglucanase Cex from Cellulomonas fimi to insoluble microcrystalline cellulose is entropically driven. Proceedings of the National Academy of Sciences **93:** 12229-12234

Cui X, Shin H, Song C, Laosinchai W, Amano Y, Brown RM, Jr. (2001) A putative plant homolog of the yeast beta-1,3-glucan synthase subunit FKS1 from cotton (Gossypium hirsutum L.) fibers. Planta **213:** 223-230

Defaye J, Wong E (1986) Structural studies of gum arabic, the exudate polysaccharide from Acacia senegal. Carbohydrate Research **150:** 221-231

Derba-Maceluch M, Awano T, Takahashi J, Lucenius J, Ratke C, Kontro I, Busse-Wicher M, Kosik O, Tanaka R, Winzell A, Kallas A, Lesniewska J, Berthold F, Immerzeel P, Teeri TT, Ezcurra I, Dupree P, Serimaa R, Mellerowicz EJ (2015) Suppression of xylan endotransglycosylase PtxtXyn10A affects cellulose microfibril angle in secondary wall in aspen wood. New Phytologist **205:** 666-681

Derba-Maceluch M, Awano T, Takahashi J, Lucenius J, Ratke C, Kontro I, Busse-Wicher M, Kosik O, Tanaka R, Winzéll A, Kallas Å, Leśniewska J, Berthold F, Immerzeel P, Teeri TT, Ezcurra I, Dupree P, Serimaa R, Mellerowicz EJ (2014) Suppression of xylan endotransglycosylase PtxtXyn10A affects cellulose microfibril angle in secondary wall in aspen wood. New Phytologist**:** n/a-n/a

Derbyshire P, McCann M, Roberts K (2007) Restricted cell elongation in Arabidopsis hypocotyls is associated with a reduced average pectin esterification level. BMC Plant Biology **7:** 31

Dhindsa R (1978) Hormonal regulation of cotton ovule and fiber growth: Effects of bromodeoxyuridine, AMO-1618 and p-chlorophenoxyisobutyric acid. Planta **141:** 269-272

Dhugga KS, Barreiro R, Whitten B, Stecca K, Hazebroek J, Randhawa GS, Dolan M, Kinney AJ, Tomes D, Nichols S, Anderson P (2004) Guar seed β-mannan synthase is a member of the cellulose synthase super gene family. Science **303:** 363-366

Dick-Perez M, Zhang Y, Hayes J, Salazar A, Zabotina OA, Hong M (2011) Structure and interactions of plant cell-wall polysaccharides by

two- and three-dimensional magic-angle-spinning solid-state NMR. Biochemistry **50:** 989-1000

Doblin MS, Pettolino F, Bacic A (2010) Plant cell walls: the skeleton of the plant world. Functional Plant Biology **37:** 357-381

Domozych DS, Sørensen I, Willats WGT (2009) The distribution of cell wall polymers during antheridium development and spermatogenesis in the Charophycean green alga, Chara corallina. Annals of Botany **104:** 1045-1056

Driouich A, Follet-Gueye M-L, Bernard S, Kousar S, Chevalier L, Vicré-Gibouin M, Lerouxel O (2012) Golgi-Mediated Synthesis and Secretion of Matrix Polysaccharides of the Primary Cell Wall of Higher Plants. Frontiers in plant science **3:** 79

Duchesne LC, Larson DW (1989) Cellulose and the Evolution of Plant Life. BioScience **39:** 238-241

Dupree P, Sherrier DJ (1998) The plant Golgi apparatus. Biochimica et Biophysica Acta (BBA) - Molecular Cell Research **1404:** 259-270

Ebringerova A, Heinze T (2000) Xylan and xylan derivatives–biopolymers with valuable properties, 1. Naturally occurring xylans structures, isolation procedures and properties. Macromolecular rapid communications**:** 542-556

Ebringerová A, Hromádková Z, Heinze T (2005) Hemicellulose. *In* T Heinze, ed, Polysaccharides I, Vol 186. Springer Berlin Heidelberg, pp 1-67

Egelund J, Petersen BL, Motawia MS, Damager I, Faik A, Olsen CE, Ishii T, Clausen H, Ulvskov P, Geshi N (2006) Arabidopsis thaliana RGXT1 and RGXT2 encode Golgi-localized (1, 3)-α-d-xylosyltransferases involved in the synthesis of pectic rhamnogalacturonan-II. The Plant Cell Online **18:** 2593-2607

Eklöf JM, Shojania S, Okon M, McIntosh LP, Brumer H (2013) Structure-Function Analysis of a Broad Specificity Populus trichocarpa Endo-β-glucanase Reveals an Evolutionary Link between Bacterial Licheninases and Plant XTH Gene Products. Journal of Biological Chemistry **288:** 15786-15799

Ellinger D, Voigt CA (2014) Callose biosynthesis in arabidopsis with a focus on pathogen response: what we have learned within the last decade. Annals of Botany **114:** 1349-1358

Ellis M, Egelund J, Schultz CJ, Bacic A (2010) Arabinogalactan-proteins: key regulators at the cell surface? Plant Physiology **153:** 403-419

Fan Y, Cheng H, Liu D, Zhang X, Wang B, Sun L, Tai G, Zhou Y (2010) The inhibitory effect of ginseng pectin on L-929 cell migration. Archives of pharmacal research **33:** 681-689

Fangel J, Pedersen H, Vidal-Melgosa S, Ahl L, Salmean A, Egelund J, Rydahl M, Clausen M, Willats WT (2012) Carbohydrate Microarrays in Plant Science. *In* J Normanly, ed, High-Throughput Phenotyping in Plants, Vol 918. Humana Press, pp 351-362

Fernandes AN, Thomas LH, Altaner CM, Callow P, Forsyth VT, Apperley DC, Kennedy CJ, Jarvis MC (2011) Nanostructure of cellulose microfibrils in spruce wood. Proceedings of the National Academy of Sciences **108:** E1195-E1203

Festucci-Buselli RA, Otoni WC, Joshi CP (2007) Structure, organization, and functions of cellulose synthase complexes in higher plants. Brazilian Journal of Plant Physiology **19:** 1-13

Fleming K, Gray DG, Matthews S (2001) Cellulose Crystallites. Chemistry – A European Journal **7:** 1831-1836

Flint EA (1950) The structure and development of the cotton fibre. Biological Reviews **25:** 414-434

Fry SC (2011) Cell wall polysaccharide composition and covalent crosslinking. Annual plant reviews: plant polysaccharides, biosynthesis and bioengineering **41:** 1-42

Fry SC, Smith RC, Renwick KF, Martin DJ, Hodge SK, Matthews KJ (1992) Xyloglucan endotransglycosylase, a new wall-loosening enzyme activity from plants. Biochemical Journal **282:** 821-828

Gao X, Zhi Y, Sun L, Peng X, Zhang T, Xue H, Tai G, Zhou Y (2013) The Inhibitory Effects of a Rhamnogalacturonan I (RG-I) Domain from Ginseng Pectin on Galectin-3 and Its Structure-Activity Relationship. Journal of Biological Chemistry **288:** 33953-33965

Gialvalis S, Seagull RW (2001) Plant hormones alter fiber initiation in unfertilized, cultured ovules of Gossypium hirsutum. Journal of Cotton Science **5:** 252-258

Giannoutsou E, Sotiriou P, Apostolakos P, Galatis B (2013) Early local differentiation of the cell wall matrix defines the contact sites in lobed mesophyll cells of Zea mays. Annals of Botany **22:** 22

Gilbert HJ (2010) The Biochemistry and Structural Biology of Plant Cell Wall Deconstruction. Plant Physiology **153:** 444-455

Gilbert HJ, Knox JP, Boraston AB (2013) Advances in understanding the molecular basis of plant cell wall polysaccharide recognition by carbohydrate-binding modules. Current Opinion Structural Biology **23:** 669-677

Gipson JR (1986) Temperature effects on growth, development, and fiber properties. Cotton physiology. The cotton foundation, Memphis**:** 47-56

Gloster TM, Ibatullin FM, Macauley K, Eklof JM, Roberts S, Turkenburg JP, Bjornvad ME, Jorgensen PL, Danielsen S, Johansen KS, Borchert TV, Wilson KS, Brumer H, Davies GJ (2007) Characterization and three-dimensional structures of two distinct bacterial xyloglucanases from families GH5 and GH12. J Biol Chem **282:** 19177-19189

Gordon S, Hsieh Y-I (2006) Cotton: science and technology. Woodhead Publishing

Gorshkova TA, Chemikosova SB, Sal'nikov VV, Pavlencheva NV, Gur'janov OP, Stolle-Smits T, van Dam JEG (2004) Occurrence of cell-specific galactan is coinciding with bast fiber developmental transition in flax. Industrial Crops and Products **19:** 217-224

Gou JY, Miller LM, Hou G, Yu XH, Chen XY, Liu CJ (2012) Acetylesterase-mediated deacetylation of pectin impairs cell elongation, pollen germination, and plant reproduction. The Plant Cell **24:** 50-65

Gou JY, Wang LJ, Chen SP, Hu WL, Chen XY (2007) Gene expression and metabolite profiles of cotton fiber during cell elongation and secondary cell wall synthesis. Cell Research **17:** 422-434

Goubet F, Barton CJ, Mortimer JC, Yu X, Zhang Z, Miles GP, Richens J, Liepman AH, Seffen K, Dupree P (2009) Cell wall glucomannan in Arabidopsis is synthesised by CSLA glycosyltransferases, and influences the progression of embryogenesis. The Plant Journal **60:** 527-538

Goubet F, Jackson P, Deery MJ, Dupree P (2002) Polysaccharide analysis using carbohydrate gel electrophoresis: a method to study plant cell wall polysaccharides and polysaccharide hydrolases. Anal Biochemistry **300:** 53-68

Gould P, Seagull RW (2002) Increasing reversal frequency in Gossypium hirsutum L. 'MD51' through exogenous application of plant hormones. Journal of Cotton Science **6:** 52-59

Gu S, Evers JB, Zhang L, Mao L, Zhang S, Zhao X, Liu S, van der Werf W, Li Z (2014) Modelling the structural response of cotton plants to mepiquat chloride and population density. Annals of Botany **114:** 877-887

Guillon F, Tranquet O, Quillien L, Utille J-P, Ordaz Ortiz JJ, Saulnier L (2004) Generation of polyclonal and monoclonal antibodies against arabinoxylans and their use for immunocytochemical location of arabinoxylans in cell walls of endosperm of wheat. Journal of Cereal Science **40:** 167-182

Haigler C (2010) Physiological and anatomical factors determining fiber structure and utility. *In* Physiology of cotton. Springer, pp 33-47

Haigler CH, Betancur L, Stiff MR, Tuttle JR (2012) Cotton fiber: a powerful single-cell model for cell wall and cellulose research. Frontiers in Plant Science **3**

Haigler CH, Rao NR, Roberts EM, Huang JY, Upchurch DR, Trolinder NL (1991) Cultured ovules as models for cotton fiber development under low temperatures. Plant Physiology **95:** 88-96

Haigler CH, Zhang D, Wilkerson CG (2005) Biotechnological improvement of cotton fibre maturity. Physiologia Plantarum **124:** 285-294

Handford M, Baldwin T, Goubet F, Prime T, Miles J, Yu X, Dupree P (2003) Localisation and characterisation of cell wall mannan polysaccharides in Arabidopsis thaliana. Planta **218:** 27-36

Hao Z, Mohnen D (2014) A review of xylan and lignin biosynthesis: Foundation for studying Arabidopsis irregular xylem mutants with pleiotropic phenotypes. Critical Review Biochemistry Molecular Biology **24:** 24

Harholt J, Jensen JK, Sorensen SO, Orfila C, Pauly M, Scheller HV (2006) ARABINAN DEFICIENT 1 is a putative arabinosyltransferase involved in biosynthesis of pectic arabinan in Arabidopsis. Plant Physiology **140:** 49-58

Harholt J, Jensen JK, Verhertbruggen Y, Sogaard C, Bernard S, Nafisi M, Poulsen CP, Geshi N, Sakuragi Y, Driouich A, Knox JP, Scheller HV (2012) ARAD proteins associated with pectic Arabinan

biosynthesis form complexes when transiently overexpressed in planta. Planta **236:** 115-128

Harholt J, Suttangkakul A, Vibe Scheller H (2010) Biosynthesis of pectin. Plant Physiology **153:** 384-395

Harmer SE, Orford SJ, Timmis JN (2002) Characterisation of six alpha-expansin genes in Gossypium hirsutum (upland cotton). Molecular Genetics and Genomics **268:** 1-9

Harzallah O, Drean J-Y (2011) Macro and micro characterization of biopolymers: case of cotton fibre, biotechnology of biopolymers. . Prof. Magdy Elnashar (Ed.), ISBN: 978-953-307-179-4, InTech.

Hayashi T, Kaida R (2011) Functions of xyloglucan in plant cells. Molecular Plant **4:** 17-24

Held MA, Be E, Zemelis S, Withers S, Wilkerson C, Brandizzi F (2011) CGR3: A Golgi-Localized Protein Influencing Homogalacturonan Methylesterification. Molecular Plant **4:** 832-844

Herve C, Rogowski A, Gilbert HJ, Paul Knox J (2009) Enzymatic treatments reveal differential capacities for xylan recognition and degradation in primary and secondary plant cell walls. The Plant Journal **58:** 413-422

Him JL, Pelosi L, Chanzy H, Putaux JL, Bulone V (2001) Biosynthesis of (1-->3)-beta-D-glucan (callose) by detergent extracts of a microsomal fraction from Arabidopsis thaliana. European Journal of Biochemistry **268:** 4628-4638

Hong Z, Delauney AJ, Verma DPS (2001) A Cell Plate–Specific Callose Synthase and Its Interaction with Phragmoplastin. The Plant Cell **13:** 755-768

Huang Q-S, Wang H-Y, Gao P, Wang G-Y, Xia G-X (2008) Cloning and characterization of a calcium dependent protein kinase gene associated with cotton fiber development. Plant Cell Reports **27:** 1869-1875

Hughs S, Gamble G, Armijo C, Tristao D (2011) Long-term storage of polyethylene film wrapped cotton bales and effects on fiber and textile quality. Journal of cotton science **15:** 127-136

Incorporated C (2013) Classification of cotton. *In*, Vol 2015. Cotton Incorporated, Classic booklet

Iqbal S, Bashir A, Naseer HM, Ahmed M, Malik KA (2008) Identification of differentially expressed genes in developing cotton fibers (*Gossypium hirsutum* L) through differential display. Electronic Journal of Biotechnology **11:** 50-59

Iwai H, Ishii T, Satoh S (2001) Absence of arabinan in the side chains of the pectic polysaccharides strongly associated with cell walls of Nicotiana plumbaginifolia non-organogenic callus with loosely attached constituent cells. Planta **213:** 907-915

Iwai H, Masaoka N, Ishii T, Satoh S (2002) A pectin glucuronyltransferase gene is essential for intercellular attachment in the plant meristem. Proceedings of the National Academy of Sciences **99:** 16319-16324

Jaquet J-P, Buchala A, Meier H (1982) Changes in the non-structural carbohydrate content of cotton (Gossypium spp.) fibres at different stages of development. Planta **156:** 481-486

Jarvis MC, Briggs SPH, Knox JP (2003) Intercellular adhesion and cell separation in plants. Plant, Cell & Environment **26:** 977-989

John ME, Keller G (1996) Metabolic pathway engineering in cotton: biosynthesis of polyhydroxybutyrate in fiber cells. Proceedings of the National Academy of Sciences **93:** 12768-12773

Johnson KL, Jones BJ, Bacic A, Schultz CJ (2003) The Fasciclin-Like Arabinogalactan Proteins of Arabidopsis. A Multigene Family of Putative Cell Adhesion Molecules. Plant Physiology **133:** 1911-1925

Jones L, Seymour GB, Knox JP (1997) Localization of pectic galactan in tomato cell walls using a monoclonal antibody specific to (1[->]4)-[beta]-D-Galactan. Plant Physiology **113:** 1405-1412

Kelly CM, Hequet EF, Dever JK (2012) Interpretation of AFIS and HVI fiber property measurements in breeding for cotton fiber quality improvement. The Journal of Cotton Science **16:** 1-16

Kelly GS (1999) Larch arabinogalactan: clinical relevance of a novel immune-enhancing polysaccharide. Alternative medicine review : a journal of clinical therapeutic **4:** 96-103

Kieliszewski M, Lamport DT (1987) Purification and Partial Characterization of a Hydroxyproline-Rich Glycoprotein in a Graminaceous Monocot, Zea mays. Plant Physiology **85:** 823-827

Kim H, Ralph J (2014) A gel-state 2D-NMR method for plant cell wall profiling and analysis: a model study with the amorphous cellulose and xylan from ball-milled cotton linters. RSC Advances **4:** 7549-7560

Kim HJ, Triplett BA (2001) Cotton fiber growth in planta and in vitro. Models for plant cell elongation and cell wall biogenesis. Plant Physiology **127:** 1361-1366

Kim S-J, Held MA, Zemelis S, Wilkerson C, Brandizzi F (2015) CGR2 and CGR3 have critical overlapping roles in pectin methylesterification and plant growth in Arabidopsis thaliana. The Plant Journal **82:** 208-220

Kitazawa K, Tryfona T, Yoshimi Y, Hayashi Y, Kawauchi S, Antonov L, Tanaka H, Takahashi T, Kaneko S, Dupree P, Tsumuraya Y, Kotake T (2013) β-Galactosyl Yariv Reagent Binds to the β-1,3-Galactan of Arabinogalactan Proteins. Plant Physiology **161:** 1117-1126

Kiyohara H, Uchida T, Takakiwa M, Matsuzaki T, Hada N, Takeda T, Shibata T, Yamada H (2010) Different contributions of side-chains in β-d-(1→ 3, 6)-galactans on intestinal Peyer's patch-immunomodulation by polysaccharides from Astragalus mongholics Bunge. Phytochemistry **71:** 280-293

Kljun A, Benians TA, Goubet F, Meulewaeter F, Knox JP, Blackburn RS (2011) Comparative analysis of crystallinity changes in cellulose I polymers using ATR-FTIR, X-ray diffraction, and carbohydrate-binding module probes. Biomacromolecules **12:** 4121-4126

Knox JP, Linstead P, King J, Cooper C, Roberts K (1990) Pectin esterification is spatially regulated both within cell walls and between developing tissues of root apices. Planta **181:** 512-521

Knox JP, Linstead PJ, Peart J, Cooper C, Roberts K (1991) Developmentally regulated epitopes of cell surface arabinogalactan

proteins and their relation to root tissue pattern formation. Plant J **1:** 317-326

Kosmidou-Dimitropoulou K, Board HC (1986) Hormonal influences on fiber development. Cotton physiology**:** 361-373

Koutaniemi S, Guillon F, Tranquet O, Bouchet B, Tuomainen P, Virkki L, Petersen H, Willats WT, Saulnier L, Tenkanen M (2012) Substituent-specific antibody against glucuronoxylan reveals close association of glucuronic acid and acetyl substituents and distinct labeling patterns in tree species. Planta **236:** 739-751

Krichevsky A, Kozlovsky SV, Tian G-W, Chen M-H, Zaltsman A, Citovsky V (2007) How pollen tubes grow. Developmental biology **303:** 405-420

Kumar M, Turner S (2015) Plant cellulose synthesis: CESA proteins crossing kingdoms. Phytochemistry **112:** 91-99

Lamport DTA, Kieliszewski MJ, Chen Y, Cannon MC (2011) Role of the extensin superfamily in primary cell wall architecture. Plant Physiology

Lamport DTA, Northcote DH (1960) Hydroxyproline in Primary Cell Walls of Higher Plants. Nature **188:** 665-666

Lamport DTA, Várnai P (2013) Periplasmic arabinogalactan glycoproteins act as a calcium capacitor that regulates plant growth and development. New Phytologist **197:** 58-64

Lamport DTA, Varnai P, Seal CE (2014) Back to the future with the AGP–Ca2+ flux capacitor. Annals of Botany **114:** 1069-1085

Laurenzi M, Tipping AJ, Marcus SE, Knox JP, Federico R, Angelini R, McPherson MJ (2001) Analysis of the distribution of copper amine oxidase in cell walls of legume seedlings. Planta **214:** 37-45

Lee J, Burns TH, Light G, Sun Y, Fokar M, Kasukabe Y, Fujisawa K, Maekawa Y, Allen RD (2010) Xyloglucan endotransglycosylase/hydrolase genes in cotton and their role in fiber elongation. Planta **232:** 1191-1205

Lee JJ, Woodward AW, Chen ZJ (2007) Gene expression changes and early events in cotton fibre development. Annals of Botany **100:** 1391-1401

Lee KD, Knox JP (2014) Resin embedding, sectioning, and immunocytochemical analyses of plant cell walls in hard tissues. *In* V Žárský, F Cvrčková, eds, Plant Cell Morphogenesis, Vol 1080. Humana Press, pp 41-52

Lee KJD, Sakata Y, Mau S-L, Pettolino F, Bacic A, Quatrano RS, Knight CD, Knox JP (2005) Arabinogalactan proteins are required for apical cell extension in the moss *Physcomitrella patens*. The Plant Cell Online **17:** 3051-3065

Lei L, Li S, Du J, Bashline L, Gu Y (2013) Cellulose synthase INTERACTIVE3 regulates cellulose biosynthesis in both a microtubule-dependent and microtubule-independent manner in Arabidopsis. Plant Cell **25:** 4912-4923

Lei L, Li S, Gu Y (2012) Cellulose Synthase Complexes: Composition and Regulation. Frontiers in Plant Science **3:** 75

Lei L, Li S, Gu Y (2012) Cellulose synthase complexes: structure and regulation. Frontiers in Plant Science **3**

Leroux O, Sørensen I, Marcus SE, Viane RL, Willats WG, Knox JP (2015) Antibody-based screening of cell wall matrix glycans in ferns reveals taxon, tissue and cell-type specific distribution patterns. BMC Plant Biology **15:** 56

Levigne SV, Ralet M-CJ, Quéméner BC, Pollet BNL, Lapierre C, Thibault J-FJ (2004) Isolation from Sugar Beet Cell Walls of Arabinan Oligosaccharides Esterified by Two Ferulic Acid Monomers. Plant Physiology **134:** 1173-1180

Li A, Xia T, Xu W, Chen T, Li X, Fan J, Wang R, Feng S, Wang Y, Wang B, Peng L (2013) An integrative analysis of four CESA isoforms specific for fiber cellulose production between Gossypium hirsutum and Gossypium barbadense. Planta **237:** 1585-1597

Li F, Fan G, Wang K, Sun F, Yuan Y, Song G, Li Q, Ma Z, Lu C, Zou C, Chen W, Liang X, Shang H, Liu W, Shi C, Xiao G, Gou C, Ye W, Xu X, Zhang X, Wei H, Li Z, Zhang G, Wang J, Liu K, Kohel RJ, Percy RG, Yu JZ, Zhu YX, Wang J, Yu S (2014) Genome sequence of the cultivated cotton Gossypium arboreum. Nature Genetics **46:** 567-572

Li J, Burton R, Harvey A, Hrmova M, Wardak A, Stone B, Fincher G (2003) Biochemical evidence linking a putative callose synthase gene with (1→3)-β-d-glucan biosynthesis in barley. Plant Molecular Biology **53:** 213-225

Li L, Huang J, Qin L, Huang Y, Zeng W, Rao Y, Li J, Li X, Xu W (2014) Two cotton fiber-associated glycosyltransferases, GhGT43A1 and GhGT43C1, function in hemicellulose glucuronoxylan biosynthesis during plant development. Plant Physiology **18:** 12190

Li S, Bashline L, Lei L, Gu Y (2014) Cellulose Synthesis and Its Regulation. The Arabidopsis Book / American Society of Plant Biologists **12:** e0169

Li S, Lei L, Somerville CR, Gu Y (2012) Cellulose synthase interactive protein 1 (CSI1) links microtubules and cellulose synthase complexes. Proceedings of the National Academy of Sciences **109:** 185-190

Li Y, Darley CP, Ongaro V, Fleming A, Schipper O, Baldauf SL, McQueen-Mason SJ (2002) Plant Expansins Are a Complex Multigene Family with an Ancient Evolutionary Origin. Plant Physiology **128:** 854-864

Li Y, Jones L, McQueen-Mason S (2003) Expansins and cell growth. Current Opinion in Plant Biology **6:** 603-610

Li Y, Liu D, Tu L, Zhang X, Wang L, Zhu L, Tan J, Deng F (2010) Suppression of GhAGP4 gene expression repressed the initiation and elongation of cotton fiber. Plant Cell Reports **29:** 193-202

Li Y, Tu L, Pettolino FA, Ji S, Hao J, Yuan D, Deng F, Tan J, Hu H, Wang Q, Llewellyn DJ, Zhang X (2015) GbEXPATR, a species-specific expansin, enhances cotton fibre elongation through cell wall restructuring. Plant Biotechnology Journal**:** n/a-n/a

Liakatas A, Roussopoulos D, Whittington W (1998) Controlled-temperature effects on cotton yield and fibre properties. Journal of Agronomy and Crop Science **130:** 463-471

Liepman AH, Nairn CJ, Willats WGT, Sørensen I, Roberts AW, Keegstra K (2007) Functional genomic analysis supports conservation of function among cellulose synthase-like a gene family members and suggests diverse roles of mannans in plants. Plant Physiology **143:** 1881-1893

Liu Q, Talbot M, Llewellyn DJ (2013) Pectin methylesterase and pectin remodelling differ in the fibre walls of two gossypium species with very different fibre properties. PLoS One **8**

Liwanag AJM, Ebert B, Verhertbruggen Y, Rennie EA, Rautengarten C, Oikawa A, Andersen MCF, Clausen MH, Scheller HV (2012) Pectin Biosynthesis: GALS1 in Arabidopsis thaliana Is a β-1,4-Galactan β-1,4-Galactosyltransferase. The Plant Cell Online

Lokhande S, Reddy KR (2014) Quantifying temperature effects on cotton reproductive efficiency and fiber quality. Agronomy Journal **106:** 1275-1282

Lombard V, Golaconda Ramulu H, Drula E, Coutinho PM, Henrissat B (2014) The carbohydrate-active enzymes database (CAZy) in 2013. Nucleic Acids Research **42:** D490-D495

Longland JM, Fry SC, Trewavas AJ (1989) Developmental Control of Apiogalacturonan Biosynthesis and UDP-Apiose Production in a Duckweed. Plant Physiology **90:** 972-976

Lovegrove A, Wilkinson MD, Freeman J, Pellny TK, Tosi P, Saulnier L, Shewry PR, Mitchell RAC (2013) RNA interference suppression of genes in glycosyl transferase families 43 and 47 in wheat starchy endosperm causes large decreases in arabinoxylan content. Plant Physiology **163:** 95-107

MacMillan CP, Mansfield SD, Stachurski ZH, Evans R, Southerton SG (2010) Fasciclin-like arabinogalactan proteins: specialization for stem biomechanics and cell wall architecture in Arabidopsis and Eucalyptus. The Plant Journal **62:** 689-703

Majewska-Sawka A, Nothnagel EA (2000) The Multiple Roles of Arabinogalactan Proteins in Plant Development. Plant Physiology **122:** 3-10

Majumdar A, Majumdar PK, Sarkar B (2005) Determination of the technological value of cotton fiber: A comparative study of the traditional and multiple-criteria decision-making approaches. Autex Research Journal **5:** 71-80

Maltby D, Carpita NC, Montezinos D, Kulow C, Delmer DP (1979) beta-1,3-Glucan in developing cotton fibers: structure, localization, and relationship of synthesis to that of secondary wall cellulose. Plant Physiology **63:** 1158-1164

Manfield IW, Orfila C, McCartney L, Harholt J, Bernal AJ, Scheller HV, Gilmartin PM, Mikkelsen JD, Paul Knox J, Willats WGT (2004) Novel cell wall architecture of isoxaben-habituated Arabidopsis suspension-cultured cells: global transcript profiling and cellular analysis. The Plant Journal **40:** 260-275

Marcus S, Verhertbruggen Y, Hervé C, Ordaz-Ortiz J, Farkas V, Pedersen H, Willats W, Knox J (2008) Pectic homogalacturonan masks abundant sets of xyloglucan epitopes in plant cell walls. BMC Plant Biology **8:** 1-12

Marcus SE, Blake AW, Benians TA, Lee KJ, Poyser C, Donaldson L, Leroux O, Rogowski A, Petersen HL, Boraston A, Gilbert HJ, Willats WG, Knox JP (2010) Restricted access of proteins to mannan polysaccharides in intact plant cell walls. The Plant Journal **64:** 191-203

Marry M, Roberts K, Jopson SJ, Huxham IM, Jarvis MC, Corsar J, Robertson E, McCann MC (2006) Cell-cell adhesion in fresh sugar-beet root parenchyma requires both pectin esters and calcium cross-links. Physiologia Plantarum **126:** 243-256

Mashiguchi K, Urakami E, Hasegawa M, Sanmiya K, Matsumoto I, Yamaguchi I, Asami T, Suzuki Y (2008) Defense-related signaling by interaction of arabinogalactan proteins and beta-glucosyl Yariv reagent inhibits gibberellin signaling in barley aleurone cells. Plant Cell Physiol **49:** 178-190

McCartney L, Blake AW, Flint J, Bolam DN, Boraston AB, Gilbert HJ, Knox JP (2006) Differential recognition of plant cell walls by microbial xylan-specific carbohydrate-binding modules. Proceedings of the National Academy of Sciences **103:** 4765-4770

McCartney L, Gilbert HJ, Bolam DN, Boraston AB, Knox JP (2004) Glycoside hydrolase carbohydrate-binding modules as molecular probes for the analysis of plant cell wall polymers. Analytical Biochemistry **326:** 49-54

McCartney L, Marcus SE, Knox JP (2005) Monoclonal antibodies to plant cell wall xylans and arabinoxylans. Journal of Histochemistry and Cytochemistry **53:** 543-546

McCartney L, Steele-King CG, Jordan E, Knox JP (2003) Cell wall pectic (1-->4)-beta-d-galactan marks the acceleration of cell elongation in the Arabidopsis seedling root meristem. The Plant Journal **33:** 447-454

McFarlane HE, Döring A, Persson S (2014) The Cell Biology of Cellulose Synthesis. Annual Review of Plant Biology **65:** 69-94

McLean BW, Bray MR, Boraston AB, Gilkes NR, Haynes CA, Kilburn DG (2000) Analysis of binding of the family 2a carbohydrate-binding module from Cellulomonas fimi xylanase 10A to cellulose: specificity and identification of functionally important amino acid residues. Protein Engineering **13:** 801-809

Mei W, Qin Y, Song W, Li J, Zhu Y (2009) Cotton GhPOX1 encoding plant class III peroxidase may be responsible for the high level of reactive oxygen species production that is related to cotton fiber elongation. Journal of Genetics and Genomics **36:** 141-150

Meikle PJ, Bonig I, Hoogenraad NJ, Clarke AE, Stone BA (1991) The location of (1→3)-β-glucans in the walls of pollen tubes of <i>Nicotiana alata using a (1→3)-β-glucan-specific monoclonal antibody. Planta **185:** 1-8

Meikle PJ, Hoogenraad NJ, Bonig I, Clarke AE, Stone BA (1994) A (1→3,1→4)-β-glucan-specific monoclonal antibody and its use in the quantitation and immunocytochemical location of (1→3,1→4)-β-glucans. The Plant Journal **5:** 1-9

Meinert MC, Delmer DP (1977) Changes in biochemical composition of the cell wall of the cotton fiber during development. Plant Physiology **59:** 1088-1097

Meulewaeter F, Jansseune K, Clerck KD, Landuyt LV, Henniger G (2014) Plant fibers with improved dyeing properties. *In* B Cropscience, ed, Ed C12N15/82; C12N9/10 Belgium

Michailidis G, Argiriou A, Darzentas N, Tsaftaris A (2009) Analysis of xyloglucan endotransglycosylase/hydrolase (XTH) genes from allotetraploid (*Gossypium hirsutum*) cotton and its diploid progenitors expressed during fiber elongation. Journal of Plant Physiology **166:** 403-416

Mihranyan A (2011) Cellulose from cladophorales green algae: From environmental problem to high-tech composite materials. Journal of Applied Polymer Science **119:** 2449-2460

Miller DH, Lamport DTA, Miller M (1972) Hydroxyproline Heterooligosaccharides in Chlamydomonas. Science **176:** 918-920

Mohnen D (2008) Pectin structure and biosynthesis. Current Opinion in Plant Biology **11:** 266-277

Moller I, Marcus SE, Haeger A, Verhertbruggen Y, Verhoef R, Schols H, Ulvskov P, Mikkelsen JD, Knox JP, Willats W (2008) High-throughput screening of monoclonal antibodies against plant cell wall glycans by hierarchical clustering of their carbohydrate microarray binding profiles. Glycoconjugate Journal **25:** 37-48

Moller I, Sorensen I, Bernal AJ, Blaukopf C, Lee K, Obro J, Pettolino F, Roberts A, Mikkelsen JD, Knox JP, Bacic A, Willats WG (2007) High-throughput mapping of cell-wall polymers within and between plants using novel microarrays. The Plant Journal **50:** 1118-1128

Montalvo JG (2005) Relationships between micronaire, fineness and maturity. part 1. fundamentals. Journal of Cotton Science **9:** 81-88

Montalvo JG, Davidonis GH, Von Hoven TM (2006) Relations between micronaire, fineness and maturity. part II. experimental. Journal of Cotton Science **9:** 89-96

Moody SF, Clarke AE, Bacic A (1988) Structural analysis of secreted slime from wheat and cowpea roots. Phytochemistry **27:** 2857-2861

Moreira LRS, Filho EXF (2008) An overview of mannan structure and mannan-degrading enzyme systems. Applied Microbiology and Biotechnology **79:** 165-178

Mort AJ, Qiu F, Maness NO (1993) Determination of the pattern of methyl esterification in pectin. Distribution of contiguous nonesterified residues. Carbohydrate Research **247:** 21-35

Mouille G, Ralet M-C, Cavelier C, Eland C, Effroy D, Hématy K, McCartney L, Truong HN, Gaudon V, Thibault J-F, Marchant A, Höfte H (2007) Homogalacturonan synthesis in Arabidopsis thaliana requires a Golgi-localized protein with a putative methyltransferase domain. The Plant Journal **50:** 605-614

Munger P, Bleiholder H, Hack H, Hess M, Stauß R, van den Boom T, Weber E (1998) Phenological growth stages of the cotton plant (*Gossypium hirsutum* L.): codification and description according to the BBCH Scale1. Journal of Agronomy and Crop Science **180:** 143-149

Najmudin S, Guerreiro CI, Carvalho AL, Prates JA, Correia MA, Alves VD, Ferreira LM, Romao MJ, Gilbert HJ, Bolam DN, Fontes CM (2006) Xyloglucan is recognized by carbohydrate-binding modules that interact with beta-glucan chains. J Biol Chem **281:** 8815-8828

Nakashima K, Yamada L, Satou Y, Azuma J, Satoh N (2004) The evolutionary origin of animal cellulose synthase. Development Genes and Evolution **214:** 81-88

Newman RH, Hill SJ, Harris PJ (2013) Wide-Angle X-Ray Scattering and Solid-State Nuclear Magnetic Resonance Data Combined to Test Models for Cellulose Microfibrils in Mung Bean Cell Walls. Plant Physiology **163:** 1558-1567

Nguema-Ona E, Coimbra S, Vicré-Gibouin M, Mollet J-C, Driouich A (2012) Arabinogalactan proteins in root and pollen-tube cells: distribution and functional aspects. Annals of Botany **110:** 383-404

Nikolaidis N, Doran N, Cosgrove DJ (2014) Plant Expansins in Bacteria and Fungi: Evolution by Horizontal Gene Transfer and Independent Domain Fusion. Molecular Biology and Evolution **31:** 376-386

Nishikubo N, Awano T, Banasiak A, Bourquin V, Ibatullin F, Funada R, Brumer H, Teeri TT, Hayashi T, Sundberg B, Mellerowicz EJ (2007) Xyloglucan Endo-transglycosylase (XET) Functions in Gelatinous Layers of Tension Wood Fibers in Poplar—A Glimpse into the Mechanism of the Balancing Act of Trees. Plant and Cell Physiology **48:** 843-855

Nishitani K, Tominaga R (1992) Endo-xyloglucan transferase, a novel class of glycosyltransferase that catalyzes transfer of a segment of xyloglucan molecule to another xyloglucan molecule. Journal of Biology Chemistry **267:** 21058-21064

Nothnagel AL, Nothnagel EA (2007) Primary cell wall structure in the evolution of land plants. Journal of Integrative Plant Biology **49:** 1271-1278

O'Donoghue EM, Somerfield SD, Sinclair BK, Coupe SA (2001) Xyloglucan endotransglycosylase: a role after growth cessation in harvested asparagus. Functional Plant Biology **28:** 349-361

Ordaz-Ortiz JJ, Marcus SE, Knox JP (2009) Cell wall microstructure analysis implicates hemicellulose polysaccharides in cell adhesion in tomato fruit pericarp parenchyma. Molecular Plant **2:** 910-921

Orfila C, Seymour GB, Willats WGT, Huxham IM, Jarvis MC, Dover CJ, Thompson AJ, Knox JP (2001) Altered Middle Lamella Homogalacturonan and Disrupted Deposition of (1→5)-α-l-Arabinan in the Pericarp ofCnr, a Ripening Mutant of Tomato. Plant Physiology **126:** 210-221

Orford SJ, Timmis JN (1998) Specific expression of an expansin gene during elongation of cotton fibres. Biochimica et Biophysica Acta (BBA) - Gene Structure and Expression **1398:** 342-346

Oxenbøll Sørensen S, Pauly M, Bush M, Skjøt M, McCann MC, Borkhardt B, Ulvskov P (2000) Pectin engineering: Modification of potato pectin by in vivo expression of an endo-1,4-β-d-galactanase. Proceedings of the National Academy of Sciences **97:** 7639-7644

Paiziev AA, Krakhmalev VA (2004) Self-organization phenomena during developing of cotton fibers. Current Opinion Solid State and Materials Science **8:** 127-133

Palmer SJ, Davies WJ (1996) An analysis of relative elemental growth rate, epidermal cell size and xyloglucan endotransglycosylase activity through the growing zone of ageing maize leaves. Journal of Experimental Botany **47:** 339-347

Paniagua C, Posé S, Morris VJ, Kirby AR, Quesada MA, Mercado JA (2014) Fruit softening and pectin disassembly: an overview of nanostructural pectin modifications assessed by atomic force microscopy. Annals of Botany **114:** 1375-1383

Park E, Díaz-Moreno SM, Davis DJ, Wilkop TE, Bulone V, Drakakaki G (2014) Endosidin 7 Specifically Arrests Late Cytokinesis and Inhibits Callose Biosynthesis, Revealing Distinct Trafficking Events during Cell Plate Maturation. Plant Physiology **165:** 1019-1034

Park YB, Cosgrove DJ (2012) Changes in cell wall biomechanical properties in the xyloglucan-deficient xxt1/xxt2 mutant of Arabidopsis. Plant Physiology **158:** 465-475

Park YB, Cosgrove DJ (2012) A revised architecture of primary cell walls based on biomechanical changes induced by substrate-specific endoglucanases. Plant Physiology **158:** 1933-1943

Park YB, Cosgrove DJ (2015) Xyloglucan and its Interactions with Other Components of the Growing Cell Wall. Plant and Cell Physiology **56:** 180-194

Parre E, Geitmann A (2005) More Than a Leak Sealant. The Mechanical Properties of Callose in Pollen Tubes. Plant Physiology **137:** 274-286

Paulsen BS, Craik DJ, Dunstan DE, Stone BA, Bacic A (2014) The Yariv reagent: Behaviour in different solvents and interaction with a gum arabic arabinogalactanprotein. Carbohydrate Polymers **106:** 460-468

Pauly M, Gille S, Liu L, Mansoori N, de Souza A, Schultink A, Xiong G (2013) Hemicellulose biosynthesis. Planta **26:** 26

Pear JR, Kawagoe Y, Schreckengost WE, Delmer DP, Stalker DM (1996) Higher plants contain homologs of the bacterial celA genes encoding the catalytic subunit of cellulose synthase. Proceedings of the National Academy of Sciences **93:** 12637-12642

Peaucelle A, Braybrook Siobhan A, Le Guillou L, Bron E, Kuhlemeier C, Höfte H (2011) Pectin-Induced Changes in Cell Wall Mechanics Underlie Organ Initiation in Arabidopsis. Current Biology **21:** 1720-1726

Pedersen HL, Fangel JU, McCleary B, Ruzanski C, Rydahl MG, Ralet M-C, Farkas V, von Schantz L, Marcus SE, Andersen MCF, Field R, Ohlin M, Knox JP, Clausen MH, Willats WGT (2012) Versatile high resolution oligosaccharide microarrays for plant glycobiology and cell wall research. Journal of Biological Chemistry **287:** 39429-39438

Peña MJ, Carpita NC (2004) Loss of Highly Branched Arabinans and Debranching of Rhamnogalacturonan I Accompany Loss of Firm Texture and Cell Separation during Prolonged Storage of Apple. Plant Physiology **135:** 1305-1313

Peng Q, Xu Q, Yin H, Huang L, Du Y (2014) Characterization of an immunologically active pectin from the fruits of Lycium ruthenicum. International journal of biological macromolecules **64:** 69-75

Pettigrew W (2001) Environmental effects on cotton fiber carbohydrate concentration and quality. Crop science **41:** 1108-1113

Pettolino FA, Hoogenraad NJ, Ferguson C, Bacic A, Johnson E, Stone BA (2001) A (1-->4)-beta-mannan-specific monoclonal antibody and its use in the immunocytochemical location of galactomannans. Planta **214:** 235-242

Pettolino FA, Walsh C, Fincher GB, Bacic A (2012) Determining the polysaccharide composition of plant cell walls. Nature Protocols **7:** 1590-1607

Pickard BG (2013) Arabinogalactan proteins – becoming less mysterious. New Phytologist **197:** 3-5

Poon S, Heath RL, Clarke AE (2012) A Chimeric Arabinogalactan Protein Promotes Somatic Embryogenesis in Cotton Cell Culture. Plant Physiology **160:** 684-695

Popper Z (2011) Extraction and Detection of Arabinogalactan Proteins. *In* ZA Popper, ed, The Plant Cell Wall, Vol 715. Humana Press, pp 245-254

Popper Z, Fry S (2008) Xyloglucan−pectin linkages are formed intra-protoplasmically, contribute to wall-assembly, and remain stable in the cell wall. Planta **227:** 781-794

Popper ZA, Michel G, Herve C, Domozych DS, Willats WG, Tuohy MG, Kloareg B, Stengel DB (2011) Evolution and diversity of plant cell walls: from algae to flowering plants. Annual Reviews Plant Biology **62:** 567-590

Puhlmann J, Bucheli E, Swain MJ, Dunning N, Albersheim P, Darvill AG, Hahn MG (1994) Generation of monoclonal antibodies against plant cell-wall polysaccharides. I. Characterization of a monoclonal antibody to a terminal alpha-(1-->2)-linked fucosyl-containing epitope. Plant Physiology **104:** 699-710

Qin Y-M, Zhu Y-X (2011) How cotton fibers elongate: a tale of linear cell-growth mode. Current Opinion in Plant Biology **14:** 106-111

Raes G, Fransen T, Verschraege L (1968) Study of the reversal phenomenon in the fibrillar structure of the cotton fiber: reversal distance distribution as origin of an extended hypothesis in the cotton fiber development. Textile Research Journal **38:** 182-195

Ralet M-C, Crépeau M-J, Buchholt H-C, Thibault J-F (2003) Polyelectrolyte behaviour and calcium binding properties of sugar beet pectins differing in their degrees of methylation and acetylation. Biochemical Engineering Journal **16:** 191-201

Ralet MC, Tranquet O, Poulain D, Moïse A, Guillon F (2010) Monoclonal antibodies to rhamnogalacturonan I backbone. Planta **231:** 1373-1383

Raven J (1997) Miniview: multiple origins of plasmodesmata. European Journal of Phycology **32:** 95-101

Reid JS, Edwards ME, Dickson CA, Scott C, Gidley MJ (2003) Tobacco transgenic lines that express fenugreek galactomannan galactosyltransferase constitutively have structurally altered galactomannans in their seed endosperm cell walls. Plant Physiology **131:** 1487-1495

Ren Y, Hansen SF, Ebert B, Lau J, Scheller HV (2014) Site-Directed Mutagenesis of IRX9, IRX9L and IRX14 Proteins Involved in Xylan Biosynthesis: Glycosyltransferase Activity Is Not Required for IRX9 Function in Arabidopsis. PLoS ONE **9:** e105014

Rennie EA, Scheller HV (2014) Xylan biosynthesis. Current Opinion Biotechnology**:** 100-107

Ridley BL, O'Neill MA, Mohnen D (2001) Pectins: structure, biosynthesis, and oligogalacturonide-related signaling. Phytochemistry **57:** 929-967

Rieter (2015) The Rieter Manual of Spinning. *In* The Rieter Manual of Spinning, Vol 3. Rieter, RIKIPEDIA

Roberts EM, Rao NR, Huang JY, Trolinder NL, Haigler CH (1992) Effects of cycling temperatures on fiber metabolism in cultured cotton ovules. Plant Physiology **100:** 979-986

Roberts K, Shirsat A (2006) Increased extensin levels in Arabidopsis affect inflorescence stem thickening and height. Journal of Experimental Botany **57:** 537-545

Rodriguez-Gacio Mdel C, Iglesias-Fernandez R, Carbonero P, Matilla AJ (2012) Softening-up mannan-rich cell walls. Journal of Experimental Botany **63:** 3976-3988

Rose JK, Braam J, Fry SC, Nishitani K (2002) The XTH family of enzymes involved in xyloglucan endotransglucosylation and endohydrolysis: current perspectives and a new unifying nomenclature. Plant and Cell Physiology **43:** 1421-1435

Rose JKC, Lee HH, Bennett AB (1997) Expression of a divergent expansin gene is fruit-specific and ripening-regulated. Proceedings of the National Academy of Sciences **94:** 5955-5960

Ruan Y-L, Xu S-M, White R, Furbank RT (2004) Genotypic and developmental evidence for the role of plasmodesmatal regulation in cotton fiber elongation mediated by callose turnover. Plant Physiology **136:** 4104-4113

Ruan YL (2007) Goldacre paper: Rapid cell expansion and cellulose synthesis regulated by plasmodesmata and sugar: insights from the single-celled cotton fibre. Functional Plant Biology **34:** 1-10

Ruan YL, Llewellyn DJ, Furbank RT (2001) The control of single-celled cotton fiber elongation by developmentally reversible gating of plasmodesmata and coordinated expression of sucrose and K+ transporters and expansin. The Plant Cell **13:** 47-60

Ruan YL, Llewellyn DJ, Furbank RT (2003) Suppression of sucrose synthase gene expression represses cotton fiber cell initiation, elongation, and seed development. The Plant Cell **15:** 952-964

Runavot JL, Guo X, Willats WG, Knox JP, Goubet F, Meulewaeter F (2014) Non-Cellulosic polysaccharides from cotton fibre are differently impacted by textile processing. PLoS One **9**

Sadava D, Chrispeels MJ (1973) Hydroxyproline-rich cell wall protein (extensin): role in the cessation of elongation in excised pea epicotyls. Developmental biology **30:** 49-55

Salnikov VV, Grimson MJ, Seagull RW, Haigler CH (2003) Localization of sucrose synthase and callose in freeze-substituted secondary-wall-stage cotton fibers. Protoplasma **221:** 175-184

Saloheimo M, Paloheimo M, Hakola S, Pere J, Swanson B, Nyyssonen E, Bhatia A, Ward M, Penttila M (2002) Swollenin, a Trichoderma reesei protein with sequence similarity to the plant expansins, exhibits disruption activity on cellulosic materials. European Journal of Biochemistry **269:** 4202-4211

Sampedro J, Cosgrove DJ (2005) The expansin superfamily. Genome Biology **6:** 242

Sampedro J, Guttman M, Li L-C, Cosgrove DJ (2015) Evolutionary divergence of β–expansin structure and function in grasses parallels emergence of distinctive primary cell wall traits. The Plant Journal **81:** 108-120

Samuel Yang S, Cheung F, Lee JJ, Ha M, Wei NE, Sze S-H, Stelly DM, Thaxton P, Triplett B, Town CD, Jeffrey Chen Z (2006) Accumulation of genome-specific transcripts, transcription factors and phytohormonal regulators during early stages of fiber cell development in allotetraploid cotton. The Plant Journal **47:** 761-775

Scheible W-R, Pauly M (2004) Glycosyltransferases and cell wall biosynthesis: novel players and insights. Current Opinion in Plant Biology **7:** 285-295

Scheller HV, Ulvskov P (2010) Hemicelluloses. Annual Reviews Plant Biology **61:** 263-289

Schröder R, Atkinson RG, Redgwell RJ (2009) Re-interpreting the role of endo-β-mannanases as mannan endotransglycosylase/hydrolases in the plant cell wall. Annals of Botany

Schubert AM, Benedict CR, Gates CE, Kohel RJ (1976) Growth and Development of the Lint Fibers of Pima S-4 Cotton. Crop science **16:** 539-543

Schultz CJ, Johnson KL, Currie G, Bacic A (2000) The Classical Arabinogalactan Protein Gene Family of Arabidopsis. The Plant Cell **12:** 1751-1768

Seagull R (1992) A quantitative electron microscopic study of changes in microtubule arrays and wall microfibril orientation during in vitro cotton fiber development. Journal of Cell Science **101:** 561-577

Seagull RW (1986) Changes in microtubule organization and wall microfibril orientation during in vitro cotton fiber development: an immunofluorescent study. Canadian Journal of Botany **64:** 1373-1381

Seagull RW, Oliveri V, Murphy K, Binder A, Kothari S (2000) Cotton fiber growth and development 2. Changes in cell diameter and wall birefringence. Journal of Cotton Science **4:** 97-104

Seifert GJ, Roberts K (2007) The biology of arabinogalactan proteins. Annual Review of Plant Biology

Seifert GJ, Xue H, Acet T (2014) The Arabidopsis thaliana FASCICLIN LIKE ARABINOGALACTAN PROTEIN 4 gene acts synergistically with abscisic acid signalling to control root growth. Annals of Botany

Seki Y, Kikuchi Y, Yoshimoto R, Aburai K, Kanai Y, Ruike T, Iwabata K, Goitsuka R, Sugawara F, Abe M, Sakaguchi K (2015) Promotion of crystalline cellulose degradation by expansins from Oryza sativa. Planta **241:** 83-93

Seveno M, Seveno-Carpentier E, Voxeur A, Menu-Bouaouiche L, Rihouey C, Delmas F, Chevalier C, Driouich A, Lerouge P (2010) Characterization of a putative 3-deoxy-D-manno-2-octulosonic acid (Kdo) transferase gene from Arabidopsis thaliana. Glycobiology **20:** 617-628

Shao M, Wang X, Ni M, Bibi N, Yuan S, Malik W, Zhang H, Liu Y, Hua S (2011) Regulation of cotton fiber elongation by xyloglucan endotransglycosylase/hydrolase genes. Genetics and Molecular Research **10:** 3771-3782

Shao MY, Wang XD, Ni M, Bibi N, Yuan SN, Malik W, Zhang HP, Liu YX, Hua SJ (2011) Regulation of cotton fiber elongation by xyloglucan endotransglycosylase/hydrolase genes. Genetics and Molecular Research **10:** 3771-3782

Shimizu Y, Aotsuka S, Hasegawa O, Kawada T, Sakuno T, Sakai F, Hayashi T (1997) Changes in levels of mRNAs for cell wall-related enzymes in growing cotton fiber cells. Plant and Cell Physiology **38:** 375-378

Shpak E, Barbar E, Leykam JF, Kieliszewski MJ (2001) Contiguous Hydroxyproline Residues Direct Hydroxyproline Arabinosylation in Nicotiana tabacum. Journal of Biological Chemistry **276:** 11272-11278

Singh B, Avci U, Eichler Inwood SE, Grimson MJ, Landgraf J, Mohnen D, Sorensen I, Wilkerson CG, Willats WG, Haigler CH (2009) A specialized outer layer of the primary cell wall joins elongating cotton fibers into tissue-like bundles. Plant Physiology **150:** 684-699

Smallwood M, Beven A, Donovan N, Neill SJ, Peart J, Roberts K, Knox JP (1994) Localization of cell wall proteins in relation to the developmental anatomy of the carrot root apex. The Plant Journal **5:** 237-246

Smallwood M, Martin H, Knox JP (1995) An epitope of rice threonine- and hydroxyproline-rich glycoprotein is common to cell wall and hydrophobic plasma-membrane glycoproteins. Planta **196:** 510-522

Smallwood M, Yates EA, Willats WGT, Martin H, Knox JP (1996) Immunochemical comparison of membrane-associated and secreted arabinogalactan-proteins in rice and carrot. Planta **198:** 452-459

Somerville C, Bauer S, Brininstool G, Facette M, Hamann T, Milne J, Osborne E, Paredez A, Persson S, Raab T, Vorwerk S, Youngs H (2004) Toward a systems approach to understanding plant cell walls. Science **306:** 2206-2211

Soriano Del Amo D, Wang W, Jiang H, Besanceney C, Yan AC, Levy M, Liu Y, Marlow FL, Wu P (2010) Biocompatible copper(I) catalysts for in vivo imaging of glycans. Journal of American Chemistry Society **132:** 16893-16899

Stewart JM (1975) Fiber initiation on the cotton ovule (*Gossypium hirsutum*). American Journal of Botany **62:** 723-730

Stewart JM, Oosterhuis DM, Heitholt JJ, Mauney JR (2010) Physiology of Cotton.

Stiff M, Haigler C (2012) Recent advances in cotton fiber development, In Cotton Flowering and Fruiting, Cotton Physiology Book Series. Edited by Oosterhuis D., Cothren T. (Cordova TN: The Cotton Foundation).

Šturcová A, His I, Apperley DC, Sugiyama J, Jarvis MC (2004) Structural Details of Crystalline Cellulose from Higher Plants. Biomacromolecules **5:** 1333-1339

Suh MW, Sasser PE (1996) The technological and economic impact of high volume instrument (HVI) systems on the cotton and cotton textile industries. Journal of Textile Industry **87:** 43-59

Tabashnik BE, Brevault T, Carriere Y (2013) Insect resistance to Bt crops: lessons from the first billion acres. Nature Biotechnology **31:** 510-521

Tabuchi A, Li LC, Cosgrove DJ (2011) Matrix solubilization and cell wall weakening by beta-expansin (group-1 allergen) from maize pollen. The Plant Journal **68:** 546-559

Tan L, Eberhard S, Pattathil S, Warder C, Glushka J, Yuan C, Hao Z, Zhu X, Avci U, Miller JS, Baldwin D, Pham C, Orlando R, Darvill A, Hahn MG, Kieliszewski MJ, Mohnen D (2013) An Arabidopsis Cell Wall Proteoglycan Consists of Pectin and Arabinoxylan Covalently Linked to an Arabinogalactan Protein. The Plant Cell **25:** 270-287

Thaker VS, Saroop S, Vaishnav PP, Singh YD (1989) Genotypic variations and influence of diurnal temperature on cotton fibre development. Field Crops Research **22:** 129-141

Thomas LH, Forsyth VT, Šturcová A, Kennedy CJ, May RP, Altaner CM, Apperley DC, Wess TJ, Jarvis MC (2013) Structure of Cellulose Microfibrils in Primary Cell Walls from Collenchyma. Plant Physiology **161:** 465-476

Thompson AJ, Tor M, Barry CS, Vrebalov J, Orfila C, Jarvis MC, Giovannoni JJ, Grierson D, Seymour GB (1999) Molecular and genetic characterization of a novel pleiotropic tomato-ripening mutant. Plant Physiology **120:** 383-390

Thompson JE, Fry SC (2000) Evidence for covalent linkage between xyloglucan and acidic pectins in suspension-cultured rose cells. Planta **211:** 275-286

Tian J, Hu X, Gou L, Luo H, Zhang Y, Zhang W (2014) Growing degree days is the dominant factor associated with cellulose deposition in cotton fiber. Cellulose **21:** 813-822

Timpa JD, Triplett BA (1993) Analysis of cell-wall polymers during cotton fiber development. Planta **189:** 101-108

Tobimatsu Y, Van de Wouwer D, Allen E, Kumpf R, Vanholme B, Boerjan W, Ralph J (2014) A click chemistry strategy for

visualization of plant cell wall lignification. Chemical Communications **50:** 12262-12265

Tokumoto H, Wakabayashi K, Kamisaka S, Hoson T (2002) Changes in the sugar composition and molecular mass distribution of matrix polysaccharides during cotton fiber development. Plant and Cell Physiology **43:** 411-418

Tormo J, Lamed R, Chirino AJ, Morag E, Bayer EA, Shoham Y, Steitz TA (1996) Crystal structure of a bacterial family-III cellulose-binding domain: a general mechanism for attachment to cellulose. The EMBO Journal **15:** 5739-5751

Turner SR, Somerville CR (1997) Collapsed xylem phenotype of Arabidopsis identifies mutants deficient in cellulose deposition in the secondary cell wall. The Plant Cell **9:** 689-701

Uhlin KI, Atalla RH, Thompson NS (1995) Influence of hemicelluloses on the aggregation patterns of bacterial cellulose. Cellulose **2:** 129-144

Van Sandt VST, Stieperaere H, Guisez Y, Verbelen J-P, Vissenberg K (2007) XET Activity is Found Near Sites of Growth and Cell Elongation in Bryophytes and Some Green Algae: New Insights into the Evolution of Primary Cell Wall Elongation. Annals of Botany **99:** 39-51

Vaughn KC, Hoffman JC, Hahn MG, Staehelin LA (1996) The herbicide dichlobenil disrupts cell plate formation: immunogold characterization. Protoplasma **194:** 117-132

Vaughn KC, Turley RB (1999) The primary walls of cotton fibers contain an ensheathing pectin layer. Protoplasma **209:** 226-237

Veličković D, Ropartz D, Guillon F, Saulnier L, Rogniaux H (2014) New insights into the structural and spatial variability of cell-wall polysaccharides during wheat grain development, as revealed through MALDI mass spectrometry imaging. Journal of Experimental Botany

Verhertbruggen Y, Marcus SE, Haeger A, Ordaz-Ortiz JJ, Knox JP (2009) An extended set of monoclonal antibodies to pectic homogalacturonan. Carbohydrate Research **344:** 1858-1862

Verhertbruggen Y, Marcus SE, Haeger A, Verhoef R, Schols HA, McCleary BV, McKee L, Gilbert HJ, Paul Knox J (2009) Developmental complexity of arabinan polysaccharides and their processing in plant cell walls. The Plant Journal **59:** 413-425

Verhertbruggen Y, Yin L, Oikawa A, Scheller HV (2011) Mannan synthase activity in the CSLD family. Plant Signaling and Behavior **6:** 1620-1623

Verma DP, Hong Z (2001) Plant callose synthase complexes. Plant Molecular Biology **47:** 693-701

Vissenberg K, Martinez-Vilchez IM, Verbelen J-P, Miller JG, Fry SC (2000) In vivo colocalization of xyloglucan endotransglycosylase activity and its donor substrate in the elongation zone of arabidopsis roots. The Plant Cell Online **12:** 1229-1237

Wada M, Heux L, Sugiyama J (2004) Polymorphism of cellulose I family: reinvestigation of cellulose IVI. Biomacromolecules **5:** 1385-1391

Wakeham H, Spicer N (1951) The strength and weakness of cotton fibers. Textile Research Journal **21:** 187-194

Wang D, Xu Y, Li Q, Hao X, Cui K, Sun F, Zhu Y (2003) Transgenic expression of a putative calcium transporter affects the time of Arabidopsis flowering. The Plant Journal **33:** 285-292

Wang HH, Guo Y, Lv FN, Zhu HY, Wu SJ, Jiang YJ, Li FF, Zhou BL, Guo WZ, Zhang TZ (2010) The essential role of GhPEL gene, encoding a pectate lyase, in cell wall loosening by depolymerization of the de-esterified pectin during fiber elongation in cotton. Plant Molecular Biology **72:** 397-406

Wang K, Wang Z, Li F, Ye W, Wang J, Song G, Yue Z, Cong L, Shang H, Zhu S, Zou C, Li Q, Yuan Y, Lu C, Wei H, Gou C, Zheng Z, Yin Y, Zhang X, Liu K, Wang B, Song C, Shi N, Kohel RJ, Percy RG, Yu JZ, Zhu YX, Wang J, Yu S (2012) The draft genome of a diploid cotton Gossypium raimondii. Nature Genetics **44:** 1098-1103

Wang L, Li X-R, Lian H, Ni D-A, He Y-k, Chen X-Y, Ruan Y-L (2010) Evidence that high activity of vacuolar invertase is required for cotton fiber and arabidopsis root elongation through osmotic dependent and independent pathways, respectively. Plant Physiology **154:** 744-756

Wang S, Li E, Porth I, Chen J-G, Mansfield SD, Douglas CJ (2014) Regulation of secondary cell wall biosynthesis by poplar R2R3 MYB transcription factor PtrMYB152 in Arabidopsis. Scientific Reports **4**

Wang X, Zhang L, Evers JB, Mao L, Wei S, Pan X, Zhao X, van der Werf W, Li Z (2014) Predicting the effects of environment and management on cotton fibre growth and quality: a functional–structural plant modelling approach. AoB Plants **6:** plu040

Waterkeyn L (1981) Cytochemical localization and function of the 3-linked glucan callose in the developing cotton fibre cell wall. Protoplasma **106:** 49-67

Wendel JF, Cronn RC (2002) Polyploidy and the evolutionary history of cotton. Advances in Agronomy **87:** 139-186

Wilkins TA, Arpat AB (2005) The cotton fiber transcriptome. Physiologia Plantarum **124:** 295-300

Willats WG, Marcus SE, Knox JP (1998) Generation of monoclonal antibody specific to (1-->5)-alpha-L-arabinan. Carbohydrate Research **308:** 149-152

Willats WG, Orfila C, Limberg G, Buchholt HC, van Alebeek GJ, Voragen AG, Marcus SE, Christensen TM, Mikkelsen JD, Murray BS, Knox JP (2001) Modulation of the degree and pattern of methyl-esterification of pectic homogalacturonan in plant cell walls. Implications for pectin methyl esterase action, matrix properties, and cell adhesion. Journal of Biological Chemistry **276:** 19404-19413

Willats WGT, Knox JP (1999) Immunoprofiling of pectic polysaccharides. Analytical Biochemistry **268:** 143-146

Willats WGT, Steele-King CG, Marcus SE, Knox JP (1999) Side chains of pectic polysaccharides are regulated in relation to cell proliferation and cell differentiation. The Plant Journal **20:** 619-628

Willats WGT, Steele-King CG, McCartney L, Orfila C, Marcus SE, Knox JP (2000) Making and using antibody probes to study plant cell walls. Plant Physiology and Biochemistry **38:** 27-36

Wilson LG, Fry JC (1986) Extensin—a major cell wall glycoprotein. Plant, Cell & Environment **9:** 239-260

Wolf S, Greiner S (2012) Growth control by cell wall pectins. Protoplasma **249:** 011-0371

Wolf S, Grsic-Rausch S, Rausch T, Greiner S (2003) Identification of pollen-expressed pectin methylesterase inhibitors in Arabidopsis. FEBS Letters **555:** 551-555

Xiao C, Somerville C, Anderson CT (2014) POLYGALACTURONASE INVOLVED IN EXPANSION1 functions in cell elongation and flower development in Arabidopsis. The Plant Cell **26:** 1018-1035

Xie H, Bolam DN, Nagy T, Szabo L, Cooper A, Simpson PJ, Lakey JH, Williamson MP, Gilbert HJ (2001) Role of hydrogen bonding in the interaction between a xylan binding module and xylan. Biochemistry **40:** 5700-5707

Xu SM, Brill E, Llewellyn DJ, Furbank RT, Ruan YL (2012) Overexpression of a potato sucrose synthase gene in cotton accelerates leaf expansion, reduces seed abortion, and enhances fiber production. Molecular Plant **5:** 430-441

Xu W-L, Zhang D-J, Wu Y-F, Qin L-X, Huang G-Q, Li J, Li L, Li X-B (2013) Cotton PRP5 gene encoding a proline-rich protein is involved in fiber development. Plant molecular biology **82:** 353-365

Xue J, Bosch M, Knox JP (2013) Heterogeneity and glycan masking of cell wall microstructures in the stems of Miscanthus giganteus, and its parents M. sinensis and M. sacchariflorus. PLoS One **8:** e82114

Yamamoto H, Horn F (1994) In Situ crystallization of bacterial cellulose I. Influences of polymeric additives, stirring and temperature on the formation celluloses I α and I β as revealed by cross polarization/magic angle spinning (CP/MAS) 13C NMR spectroscopy. Cellulose **1:** 57-66

Yang JL, Zhu XF, Peng YX, Zheng C, Li GX, Liu Y, Shi YZ, Zheng SJ (2011) Cell wall hemicellulose contributes significantly to aluminum adsorption and root growth in Arabidopsis. Plant Physiology **155:** 1885-1892

Yapo BM (2011) Pectic substances: from simple pectic polysaccharides to complex pectins—A new hypothetical model. Carbohydrate Polymers **86:** 373-385

Yariv J, Lis H, Katchalski E (1967) Precipitation of arabic acid and some seed polysaccharides by glycosylphenylazo dyes. Biochemical Journal **105:** 1C-2C

Yates EA, Valdor J-F, Haslam SM, Morris HR, Dell A, Mackie W, Knox JP (1996) Characterization of carbohydrate structural features recognized by anti-arabinogalactan-protein monoclonal antibodies. Glycobiology **6:** 131-139

Yatsu LY, Jacks TJ (1981) An ultrastructural study of the relationship between microtubules and microfibrils in cotton (Gossypium hirsutum L.) cell wall reversals. American Journal of Botany **68:** 771-777

Yin L, Verhertbruggen Y, Oikawa A, Manisseri C, Knierim B, Prak L, Jensen JK, Knox JP, Auer M, Willats WGT, Scheller HV (2011) The cooperative activities of CSLD2, CSLD3, and CSLD5 are required for normal arabidopsis development. Molecular Plant **4:** 1024-1037

York WS, O'Neill MA (2008) Biochemical control of xylan biosynthesis—which end is up? Current Opinion in Plant Biology **11:** 258-265

Zablackis E, Huang J, Muller B, Darvill AG, Albersheim P (1995) Characterization of the cell wall polysaccharides of Arabidopsis thaliana leaves. Plant Physiology **107:** 1129-1138

Zabotina OA (2012) Xyloglucan and its biosynthesis. Frontiers in Plant Science **3**

Zavaliev R, Ueki S, Epel B, Citovsky V (2011) Biology of callose (β-1,3-glucan) turnover at plasmodesmata. Protoplasma **248:** 117-130

Zhang M, Zheng X, Song S, Zeng Q, Hou L, Li D, Zhao J, Wei Y, Li X, Luo M, Xiao Y, Luo X, Zhang J, Xiang C, Pei Y (2011) Spatiotemporal manipulation of auxin biosynthesis in cotton ovule epidermal cells enhances fiber yield and quality. Nature Biotechnology **29:** 453-458

Zhang T, Mahgsoudy-Louyeh S, Tittmann B, Cosgrove D (2014) Visualization of the nanoscale pattern of recently-deposited cellulose microfibrils and matrix materials in never-dried primary walls of the onion epidermis. Cellulose **21:** 853-862

Zhang Y, Yang J, Showalter AM (2011) AtAGP18, a lysine-rich arabinogalactan protein in Arabidopsis thaliana, functions in plant growth and development as a putative co-receptor for signal transduction. Plant signaling & behavior **6:** 855-857

Zhao M-r, Han Y-y, Feng Y-n, Li F, Wang W (2012) Expansins are involved in cell growth mediated by abscisic acid and indole-3-acetic acid under drought stress in wheat. Plant Cell Reports **31:** 671-685

Zhao Y, Song D, Sun J, Li L (2013) Populus endo-beta-mannanase PtrMAN6 plays a role in coordinating cell wall remodeling with suppression of secondary wall thickening through generation of oligosaccharide signals. The Plant Journal **74:** 473-485

ZhiMing Y, Bo K, XiaoWei H, ShaoLei L, YouHuang B, WoNa D, Ming C, Hyung-Taeg C, Ping W (2011) Root hair-specific expansins modulate root hair elongation in rice. The Plant Journal **66:** 725-734

Zhong R, Lee C, Zhou J, McCarthy RL, Ye Z-H (2008) A Battery of Transcription Factors Involved in the Regulation of Secondary Cell Wall Biosynthesis in Arabidopsis. The Plant Cell **20:** 2763-2782

Zhong R, Ye Z-H (2014) Secondary Cell Walls: Biosynthesis, Patterned Deposition and Transcriptional Regulation. Plant and Cell Physiology

Zhu XF, Shi YZ, Lei GJ, Fry SC, Zhang BC, Zhou YH, Braam J, Jiang T, Xu XY, Mao CZ, Pan YJ, Yang JL, Wu P, Zheng SJ (2012) XTH31, encoding an in vitro XEH/XET-active enzyme, regulates aluminum sensitivity by modulating in vivo XET action, cell wall xyloglucan content, and aluminum binding capacity in Arabidopsis. The Plant Cell **24:** 4731-4747

Zhu XF, Wan JX, Sun Y, Shi YZ, Braam J, Li GX, Zheng SJ (2014) Xyloglucan Endotransglucosylase-Hydrolase17 Interacts with Xyloglucan Endotransglucosylase-Hydrolase31 to Confer Xyloglucan Endotransglucosylase Action and Affect Aluminum Sensitivity in Arabidopsis. Plant Physiology **165:** 1566-1574

Zverlov VV, Volkov IY, Velikodvorskaya GA, Schwarz WH (2001) The binding pattern of two carbohydrate-binding modules of laminarinase Lam16A from Thermotoga neapolitana: differences in beta-glucan binding within family CBM4. Microbiology **147:** 621-629

Zykwinska A, Thibault JF, Ralet MC (2007) Organization of pectic arabinan and galactan side chains in association with cellulose microfibrils in primary cell walls and related models envisaged. Journal of Experimental Botany **58:** 1795-1802

Zykwinska AW, Ralet M-CJ, Garnier CD, Thibault J-FJ (2005) Evidence for in vitro binding of pectin side chains to cellulose. Plant Physiology **139:** 397-407